



HAL
open science

Role of the NSR-ASCO ribonucleoprotein complex in the regulation of plant development

Richard Rigo

► **To cite this version:**

Richard Rigo. Role of the NSR-ASCO ribonucleoprotein complex in the regulation of plant development. Molecular biology. Université Paris-Saclay, 2021. English. NNT: 2021UPASB029 . tel-03334187

HAL Id: tel-03334187

<https://theses.hal.science/tel-03334187v1>

Submitted on 3 Sep 2021

HAL is a multi-disciplinary open access archive for the deposit and dissemination of scientific research documents, whether they are published or not. The documents may come from teaching and research institutions in France or abroad, or from public or private research centers.

L'archive ouverte pluridisciplinaire **HAL**, est destinée au dépôt et à la diffusion de documents scientifiques de niveau recherche, publiés ou non, émanant des établissements d'enseignement et de recherche français ou étrangers, des laboratoires publics ou privés.

Rôle du complexe ribonucléoprotéique
NSR-ASCO dans la régulation du
développement des plantes
*Role of the NSR-ASCO ribonucleoprotein
complex in the regulation of plant development*

Thèse de doctorat de l'université Paris-Saclay

École doctorale n° 567, Sciences du végétal : du gène à l'écosystème (SEVE)
Spécialité de doctorat : Biologie
Unité de recherche : Université Paris-Saclay, CNRS, INRAE, Univ Evry,
Institute of Plant Sciences Paris-Saclay (IPS2), 91405, Orsay, France
Réfèrent : Faculté des sciences d'Orsay

**Thèse présentée et soutenue à Paris-Saclay,
le 18/06/2021, par**

Richard RIGO

Composition du Jury

Marianne DELARUE Professeure des universités, Université Paris-Sud	Présidente
Julio SAEZ-VASQUEZ Directeur de recherche, CNRS, Université de Perpignan Via Domitia	Rapporteur
Dorothee STAIGER Professeure, Bielefeld University	Rapporteur
Antoine MARTIN Chargé de Recherche, CNRS, Université de Montpellier	Examineur

Direction de la thèse

Martin CRESPI Directeur de recherche, CNRS, IPS2	Directeur
Céline CHARON Maîtresse de conférences, Université Paris-Sud	Co-encadrante & Examinatrice

Acknowledgments

First, I would like to deeply thank Dorothee STAIGER and Julio SAEZ-VASQUEZ for accepting to read and evaluate my thesis manuscript. Similarly, I would like to express my sincere thanks to Marianne DELARUE and Antoine MARTIN for accepting to be a part of my thesis defense.

I also want to express my gratitude to my thesis committee members: Moussa BENCHAMED, Hervé VAUCHERET, Chloé ZUBIETA and Lionel NAVARRO. Thank you for your time, advice and insightful comments that allowed me to bring new ideas to my thesis.

I want to thank the Doctoral School ED 567 for giving me the opportunity to conduct this thesis, meet so many fascinating people, and add this “brick” into my career path.

I also would like to express my gratitude to all past and present Doc'en Herbe members. I learned so many things thanks to you, and had the opportunity to organize and participate to amazing meetings!

I want to thank all my colleagues from the IPS2 and from the teaching staff at Université Paris-Sud. Thank you for your kindness, generosity, good mood, and advice. The everyday life would not be the same without you. Sometimes the simplest smile or “Hello!” is enough to really brighten your day.

I profusely thank all the past and present members of the REGARN team: Thomas B, Aurélie, Jérémie, Christine, Céline S, Caroline, Olivier, Hélène, Sébastien, Jérémy, Natali, Laetitia, Gautier, Ambre, Thomas R, Andana, Yu-Ming and Agathe. Thank you all for having welcomed me in the team, always being available for my questions, providing your technical assistance, and of course sharing joyful moments and having a great time in the lab! A special thanks to all the current and former interns, who always bring their energy and good mood to the lab. I would also like also to thank all the FF Team for their kindness, good mood, sense of humor, and for being always willing to share a few drinks or snacks!

Finally, I could not write these lines without owing a tremendous sense of gratitude to Martin CRESPI and Céline CHARON, my thesis supervisors. Martin, thank you for your limitless enthusiasm and joy that were a great motivation throughout my PhD, and always pushed me to give my best for science! Céline, since my beginnings at the IPS2, you offered me kindness, trust and advice that allowed me to grow as a scientist, but also as a person. I deeply thank both of you for giving me such opportunities during this thesis, like participating in international seminars, or being able to teach at the University. I sincerely hope that I honored all the help and the knowledge you have provided me throughout these years.

A mes très chers amis,

Merci pour votre éternel soutien et votre amitié indéfectible. Vos attentions, vos conseils et vos encouragements illuminent les moments difficiles, et m'ont toujours permis de donner le meilleur de moi-même. Merci d'être là.

A mes camarades de recherche, passés et présents,

Que ce soit au cours du Master, de mes stages ou de ma thèse, un énorme merci à tous autant que vous êtes ! Grâce à votre aide, votre gentillesse, votre écoute, (votre folie !), vous avez tous contribué à faire de ma thèse ce qu'elle est aujourd'hui. C'est souvent dans les moments les plus difficiles que l'on crée les liens les plus forts, et en voilà la preuve ! Mention spéciale à MC-FF et al., pour m'avoir tant épaulé sur ces derniers instants de la thèse. Votre présence au quotidien a été un réel moteur, et m'a permis de redoubler de motivation dans les instants difficiles. Mon départ est d'autant plus difficile car je sais que je vais devoir vous quitter, mais je vous souhaite à tous réussite et bonheur dans chaque projet que vous allez entreprendre.

Je tenais tout particulièrement à remercier Agathe, collègue et amie sincère. J'ai eu la chance de pouvoir t'encadrer pendant ton M2, célébrer avec toi l'obtention de ton concours de thèse, et t'accompagner sur tes premiers pas de thésarde. Tu es une personne incroyable, pleine de talents et de ressources : n'en doute jamais ! Ton écoute et ton amitié m'ont toujours aidé à aller de l'avant, j'espère ainsi pouvoir faire de même au cours de ta propre « aventure » de thèse. Mille merci du fond du cœur !

I would also like to thank all the interns / PhD students that stayed for a while in the team and made possible to discuss and share our cultures. Wil, I wish you all the best for the end of your thesis. I am sure we will meet again and share a few drinks together! Miss you! Anna, I wish you all the best as well and I hope you will show me Poland one day! (Tęsknię za tobą !)

Para mis compañeros del EPILAB,

No hay suficientes palabras para describir la suerte que tuve de conocerlos. Fede, ("Jefe") gracias por tu ayuda incondicional. Desde mi Master 2 me enseñaste a pensar, a cuestionar mis experimentos, y a crecer como investigador. Siempre te has tomado el tiempo de ayudarme, y contestar a mis preguntas. Sos un genio, recuérdalo siempre! A mis queridos Flor L, Flor M, y Johan (Pepito), gracias por su amistad tan genuina. Trabajar con ustedes fue un enorme placer, y seguro seguiremos generando nuevos recuerdos juntos ! También gracias a todos los demás miembros del EPILAB y del IAL, por su buen humor y buena onda. Por último, quiero agradecer a Mika y Camille (Gamysh), por su ayuda y por haber compartido su departamento conmigo. Siempre recordaré esas caminatas por las calles de Santa Fe y Córdoba (Piki). Un pedazo de mí permanecerá con ustedes en Argentina (y siempre habrá un poco de mate en mi panza!) Les re quiero!

Mojej drahej rodine,

Ďakujem vám z celého srdca za všetku vašu lásku, starostlivosť a podporu. Tým kým som a aký som, je vďaka vám, vašej láske, ktorú v duši nosím ako vzácny diamant. Z malého chlapca sa stal dospelý muž, ktorý vám bude navždy vďačný za všetko čo ste spravili a obetovali pre neho a každý deň sa bude snažiť, aby ste boli na neho hrdí... Milujem vás nekonečne!

Enfin, je tenais à remercier une personne en particulier (qui se reconnaîtra !). Merci d'avoir été là à chaque instant, de m'avoir épaulé, écouté, (supporté...) jusqu'à la fin ! Merci pour tout ton amour, ton soutien, tes encouragements, ton aide et surtout ta patience à travers cette longue marche que fut la thèse. J'adresse également mes remerciements à toute ta famille, qui ont montré un soutien tout aussi infaillible, et m'ont aidé à franchir ce cap ! Merci du fond du cœur, à toi, à eux. Je vous aime.

Table of contents

Abbreviations	1
List of Figures and Tables	4
Introduction	6
1.1 LncRNAs, emergent regulators of plant development.....	7
1.1.1 Identification and classification of lncRNAs	8
1.1.2 Characteristics of lncRNAs.....	11
1.1.3 Functions of lncRNAs in plants and associated mechanisms	15
1.2 Alternative splicing, a mean to face environmental cues	24
1.2.1 The spliceosome machinery.....	25
1.2.2 Alternative splicing in the regulation of plant-microbe interactions.....	31
1.2.3 Alternative splicing regulation during abiotic stresses.....	43
1.3 LncRNAs, novel players in AS regulation	46
1.3.1 LncRNAs regulate AS at different levels.....	46
1.3.2 The lncRNA ASCO, a hijacker of splicing regulators	51
Aim of the thesis.....	56
Results	58
2.1 NSRs modulate the transcriptome to regulate cross-talks between hormones and immune responses.....	59
2.1.1 Introduction	59
2.1.2 Publication: Nuclear Speckle RNA Binding Proteins Remodel Alternative Splicing and the Non-coding Arabidopsis Transcriptome to Regulate a Cross-Talk between Auxin and Immune Responses	60
2.1.4 Complementary results	75
2.1.5 Discussion.....	78
2.1.6 Materials and Methods.....	83
2.1.7 References.....	86

2.2	The lncRNA <i>ASCO</i> interacts with highly conserved splicing factors and is involved in the plant response to stresses	89
2.2.1	Introduction	89
2.2.2	Publication: The <i>Arabidopsis</i> lncRNA <i>ASCO</i> modulates the transcriptome through interaction with splicing factors	90
2.2.3	Complementary results	127
2.2.4	Discussion.....	131
2.2.5	Material and Methods.....	132
2.2.6	References.....	133
2.3	<i>ASCO</i> , a novel actor in temperature sensing?	137
2.3.1	Introduction	137
2.3.2	Results	139
2.3.3	Discussion.....	151
2.3.4	Material and Methods.....	154
2.3.5	References.....	159
	Conclusions and Perspectives.....	163
3.1	The NSR- <i>ASCO</i> complex, a novel player in the plant response to environment ...	163
3.2	<i>ASCO</i> , a lncRNA interacting with the splicing machinery	165
3.3	The study of <i>ASCO</i> conservation, a key to understanding its role?	167
3.4	lncRNAs as a model for RNA therapeutics?	169
	References.....	170
	Résumé.....	187

Abbreviations

ABA	abscisic acid
AP2	APETALA2
APOLO	AUXIN REGULATED PROMOTER LOOP
AS	alternative splicing
ASCO	ALTERNATIVE SPLICING COMPETITOR
BiFC	bimolecular fluorescence complementation
BP	branch point
CBF	C-REPEAT/DEHYDRATION-RESPONSIVE ELEMENT BINDING FACTOR
circRNA	circular RNA
CLF	CURLY LEAF
CLK1	CDC2-Like Kinase 1
coIP	coimmunoprecipitation
COOLAIR	COLD INDUCED LONG ANTISENSE INTRAGENIC RNA
COP	convergently overlapping pair
COR	COLD REGULATED
COVID-19	coronavirus disease 2019
DAS	differentially alternatively spliced
DEG	differentially expressed gene
DNA	deoxyribonucleic acid
DRIR	DROUGHT-INDUCED LNCRNA
DZ	division zone
EdU	5-ethynyl-2'-deoxyuridine
Ef-cd	EARLY FLOWERING-COMpletely DOMINANT
ELENA1	ELF18-INDUCED LONG NONCODING RNA 1
EMT	epithelial–mesenchymal transition
ENOD40	EARLY NODULIN40
ESE	exonic splicing enhancer
ESS	exonic splicing suppressor
FC	fold-change
FIB2	FIBRILLARIN 2
FLC	FLOWERING LOCUS C
flg22	flagellin peptide 22
GRP7	GLYCINE-RICH RNA BINDING PROTEIN 7
H3K27me3	histone 3 lysine 27 trimethylation
hnRNP	heterogeneous nuclear ribonucleoprotein
HSF	heat shock factor
HSFA1D	HEAT SHOCK TRANSCRIPTION FACTOR A1D
HSP	heat shock protein
HTT	HEAT-INDUCED TAS1 TARGET
IAA	INDOLE-3-ACETIC ACID
ICE	INDUCER OF CBF EXPRESSION

iCLIP	individual-nucleotide resolution UV cross-linking and immunoprecipitation
IE	interactor element
incRNA	intronic lncRNA
IR	intron retention
IRES	internal ribosome entry site
ISE	intronic splicing enhancer
ISS	intronic splicing suppressor
JA	jasmonic acid
LDMAR	LONG-DAY SPECIFIC MALE-FERTILITY-ASSOCIATED RNA
lincRNA	long intergenic ncRNA
lncRNA	long non-coding RNA
LR	lateral root
LRFC	lateral root founder cell
LRP	lateral root primordia
MADS	MCM1-AGAMOUS-DEFICIENS-SRF
MALAT1	METASTASIS ASSOCIATED LUNG ADENOCARCINOMA TRANSCRIPT 1
MCP	MS2 coat protein
MED19a	MEDIATOR SUBUNIT 19A
miRNA	micro-RNA
mRNA	messenger RNA
MtRBP1	Medicago truncatula RNA-Binding Protein 1
NAT	natural antisense transcript
ncRNA	non-coding RNA
NEAT	NUCLEAR PARASPECKLE ASSEMBLY TRANSCRIPT 1
NLS	nuclear localization signal
NMD	nonsense mediated decay
NOX	NADPH oxidase
NSR	Nuclear Speckle RNA-binding
nt	nucleotide
NTC	nineteen complex
ORF	open reading frame
PAMP	Pathogen-associated molecular pattern
PB	pladienolide B
PIP-seq	protein interaction profile sequencing
PMS1T	PHOTOPERIOD-SENSITIVE GENIC MALE STERILITY T
Pol	polymerase
PR1	PATHOGENESIS-RELATED GENE1
pre-mRNA	precursor messenger RNA
Psm	Pseudomonas syringae pathovar maculicola
Pst	Pseudomonas syringae pathovar Tomato
PTBP1	polypyrimidine tract-binding protein
PTC	premature termination codon
PTI	PAMP-triggered immunity
QC	quiescent center
RAM	root apical meristem
RBP	RNA-binding protein
RCF1	REGULATOR OF CBF GENE EXPRESSION 1

RdDM	RNA-directed DNA methylation
RNA	ribonucleic acid
RNP	ribonucleoprotein
ROS	reactive oxygen species
RRM	RNA Recognition Motif
rRNA	ribosomal RNA
RS domain	arginine/serine-rich domain
RSA	root system architecture
R-turn	right-hand turn
SA	salicylic acid
SARS-CoV-2	Severe acute respiratory syndrome coronavirus 2
SD	structural domain
SE	structural element
SEP3	SEPALLATA3
SF	splicing factor
siRNA	small interfering RNA
SNP	single-nucleotide polymorphism
snRNA	small nuclear RNA
snRNP	small nuclear ribonucleoprotein
SPF45	SPLICING FACTOR 45
SR protein	serine/arginine-rich protein
SS	splice site
STA1	STABILIZED1
SUF	SUPPRESSOR OF FEMINIZATION
TCV	Turnip crinkle virus
TE	transposable element
TF	transcription factor
TP	time-point
TriFC	trimolecular fluorescence complementation
tRNA	transfer RNA
TSS	transcription start site
TYCLV	Tomato yellow leaf curl virus
TZ	transition zone
UTR	untranslated region
VIGS	virus-induced gene silencing
XPP	xylem-pole-pericycle
(Y)n	polypyrimidine tract

List of Figures and Tables

	Title	Page
Figure 1	Discovery and classification of lncRNAs.	10
Figure 2	The sequence and structure of lncRNAs drive their interactions with other components of the cell.	12
Figure 3	lncRNAs and their associated regulatory mechanisms.	16
Figure 4	lncRNAs fine-tune the transcriptional response to biotic (A) and abiotic (B) stresses in plants.	22
Figure 5	Pre-mRNA Splicing by the major U2-dependent spliceosome.	26
Figure 6	Spliceosomal U snRNP components conserved in <i>Arabidopsis</i> .	28
Figure 7	Alternative splicing events and their regulation by non-snRNP proteins in plants.	30
Figure 8	lncRNAs modulate alternative splicing through various mechanisms.	48
Figure 9	The ASCO lncRNA hijacks NSR splicing factors to modulate AS during lateral root formation.	52
Figure 10	<i>nsr</i> mutants exhibit an altered response to flg22.	76
Figure 11	NSRs participate in the plant response to pathogens.	79-80
Figure 12	NSRs and their involvement in plant defense responses.	82
Figure 13	ASCO expression patterns in the plant.	128
Figure 14	ASCO suppression leads to fewer cell divisions upon flg22 treatment.	130
Figure 15	ASCO suppression induces a “cold-like” response in the plant.	140
Figure 16	RNAi-ASCO lines show altered expression of cold-responsive genes.	143-144
Figure 17	Deregulation of ASCO expression leads to an altered response to cold.	147-148
Figure 18	ASCO suppressed plants present cold-induced splicing events.	150
Figure 19	The NSR-ASCO complex is regulated by heat at the transcriptional level.	152
Figure 20	Integration of the NSR-ASCO complex in the plant response to stresses.	164
Figure 21	ASCO exhibits highly variable expression among <i>Arabidopsis</i> ecotypes.	168
	Title	Page
Table 1	List of primers used for RT-qPCR in Chapter 1.	85
Table 2	List of primers used for RT-qPCR in Chapter 3.	157

Introduction

1.1 LncRNAs, emergent regulators of plant development

As sessile organisms, plants are continuously exposed to their environment, facing biotic and abiotic stresses. These require fast adaptation. Plants partially achieve this growth and developmental plasticity by modulating the repertoire of genes they express. In recent years, the extensive use of high-throughput technologies led to the discovery, apart from messenger RNAs resulting from gene transcription, of thousands of RNA molecules with low or no protein-coding potential (the so-called noncoding RNAs, ncRNAs), questioning their function. The discovery of ribosomal RNA (rRNA) and transfer RNA (tRNA) in the late 1950s were the first steps unveiling this unsuspected non-coding world. These housekeeping ncRNAs are abundantly and ubiquitously expressed in cells, regulating generic cellular functions. They notably comprise small nuclear and nucleolar RNAs, transfer RNAs, ribosomal RNAs, telomerase RNAs, tRNA-derived fragments and tRNA halves (Zhang et al., 2019a). On the other hand, the so-called regulatory ncRNAs can be divided into two main categories based on their length. Small ncRNAs are less than 50 nucleotides (nt) in length and comprise micro-RNAs (miRNAs), small interfering RNAs (siRNAs) and piwi-interacting RNAs (Brosnan and Voinnet, 2009; Zhang et al., 2019a). Long non-coding RNAs (lncRNAs) are longer than 200 nt and exhibit low or no coding potential. They also comprise antisense RNAs, transposon-derived RNAs, circular RNAs and enhancer RNAs (Fonouni-Farde et al., 2021). In this next section, I will focus on the identification, the characteristics and the roles of these specific long non-coding RNA molecules.

1.1.1 Identification and classification of lncRNAs

1.1.1.1 Pipelines for discovery of new lncRNAs

Long non-coding RNAs slowly emerged as major regulators of a plethora of cellular and molecular processes (Figure 1A). For a long time, these “behind the scenes” actors of the cell remained hidden by coding-genes and the associated dogma of molecular biology: DNA is transcribed into messenger RNA (mRNA), and mRNA is translated into a functional protein. However, the so-called “C-value paradox” representing the imbalance between developmental complexity and genome size pointed out there must be “something else” than only coding genes in the genome (Thomas, 1978; Eddy, 2012; Kung et al., 2013). The tremendous advances in next-generation sequencing have determined that almost 90% of the eukaryotic genome gets transcribed, whereas only 2% of the genome gets translated (Ariel et al., 2015; Lee et al., 2019). This remaining non-coding part of the genome contains transposons, pseudogenes, repeated sequences (Ohno, 1972), but also ncRNAs with unarguable cellular and biological functions. This latter category includes lncRNAs, RNA molecules whose size ranges between 200 nt to 100,000 nt (Derrien et al., 2012). Previous attempts for transcriptomic analyses and search for lncRNAs mostly relied on microarray data, usually lacking in coverage depth and therefore missing out a large amount of non-coding transcripts (Ben Amor et al., 2009). The extensive use of next-generation DNA and RNA sequencing made possible the discovery of hundreds and thousands of new lncRNAs in a large spectrum of plant species (Li et al., 2014b; Karakülah and Unver, 2017; Xin et al., 2011; Ma et al., 2019; Yan et al., 2020).

A growing number of pipelines and computational tools have in particular emerged for lncRNAs prediction among sequencing data. In the past, prediction tools such as CPC or PhyloCSF were usually developed based on known protein databases and relied on comparative genomics methods and sequence alignments (Kong et al., 2007; Lin et al., 2011). These tools exhibited heterogeneous efficiencies for lncRNA identification, most of them being time-consuming and dependent on prior annotations. Nowadays, more and more prediction tools rather use alignment-free methods and search for a list of intrinsic features specific to lncRNAs. These new tools notably include the Coding Potential Assessment Tool (CPAT), the Coding Potential Calculator 2 (CPC2), the predictor of long non-coding RNAs and messenger RNAs based on an improved k-mer scheme (PLEK) and the Plant lncRNA Identification Tool (PLIT) (Wang et al., 2013; Li et al., 2014a; Kang et al., 2017; Deshpande et al., 2019). For example, the Coding Potential Calculator 2 (CPC2) tool uses open reading frame (ORF) length and integrity, peptide isoelectric point and the Fickett

score to predict the coding potential of a transcript (Kang et al., 2017). At the DNA level, the Fickett score corresponds to the degree to which each base is favored in one codon position versus another, independently of ORF positions (Fickett, 1982; Wang et al., 2013). At the RNA level, ORF integrity and length provide clues about the coding potential since coding-transcripts tend to exhibit longer ORFs than non-coding ones. The isoelectric point of a peptide is the pH at which it carries zero net charge (Bjellqvist et al., 1994). This feature usually differs between peptides from non-coding and coding transcripts and helps in determining their coding potential (Kang et al., 2017).

1.1.1.2 Position classification of lncRNAs

This growing availability of computational tools and standardization of pipelines to conduct *in silico* identification allowed the discovery of a tremendous amount of new non-coding transcripts in many species (Bhatia et al., 2017). This increasing amount of data requires storage and also a way to classify these newly discovered transcripts. This led to the development of various lncRNA databases and repositories such as NONCODE v4, lncRNADB v2.0, RNAcentral, CANTATADB, PLNlncRbase and GreenC (Bhatia et al., 2017). NONCODE v4 and lncRNADB v2.0 are comprehensive databases of eukaryotic ncRNAs, including the species *Homo sapiens*, *Mus musculus*, *Gorilla gorilla*, *Drosophila melanogaster*, *Arabidopsis thaliana*, etc... For its part, RNAcentral also integrates ncRNAs from prokaryotes such as *Bacillus subtilis* or *Escherichia coli*. CANTATADB, PLNlncRbase and GreenC are plant specific databases compiling annotated lncRNAs from diverse plant and algae species. The *Arabidopsis* Information Resource 10 (TAIR10) database combines structure and organization-related information about *Arabidopsis thaliana*'s (*A. thaliana*) genome, including functional annotation of coding and non-coding transcripts (Lamesch et al., 2012). These annotations depend on various criteria that organize lncRNAs into specific categories, facilitating the study of their roles and way of function.

lncRNAs can be classified in particular into different biotypes with respect to their genomic location and the orientation of their transcription (Figure 1B). Long intergenic ncRNAs (lincRNAs) consist of independent transcriptional units present within the genomic interval between two genes. Intronic lncRNAs (incRNAs) start within an intron and do not overlap with any exon. Long non-coding sense or antisense transcripts overlap with exons respectively in the same or opposite direction of an existing coding-gene. Finally some Pol-V dependent lncRNAs are transcribed in gene promoters in both directions. A large number of lncRNAs belonging to these different biotypes were characterized, demonstrating that their genomic location can also impact their molecular role. For example, antisense or incRNAs can directly impact *in cis* the expression of their associated coding gene (Ariel et al., 2015

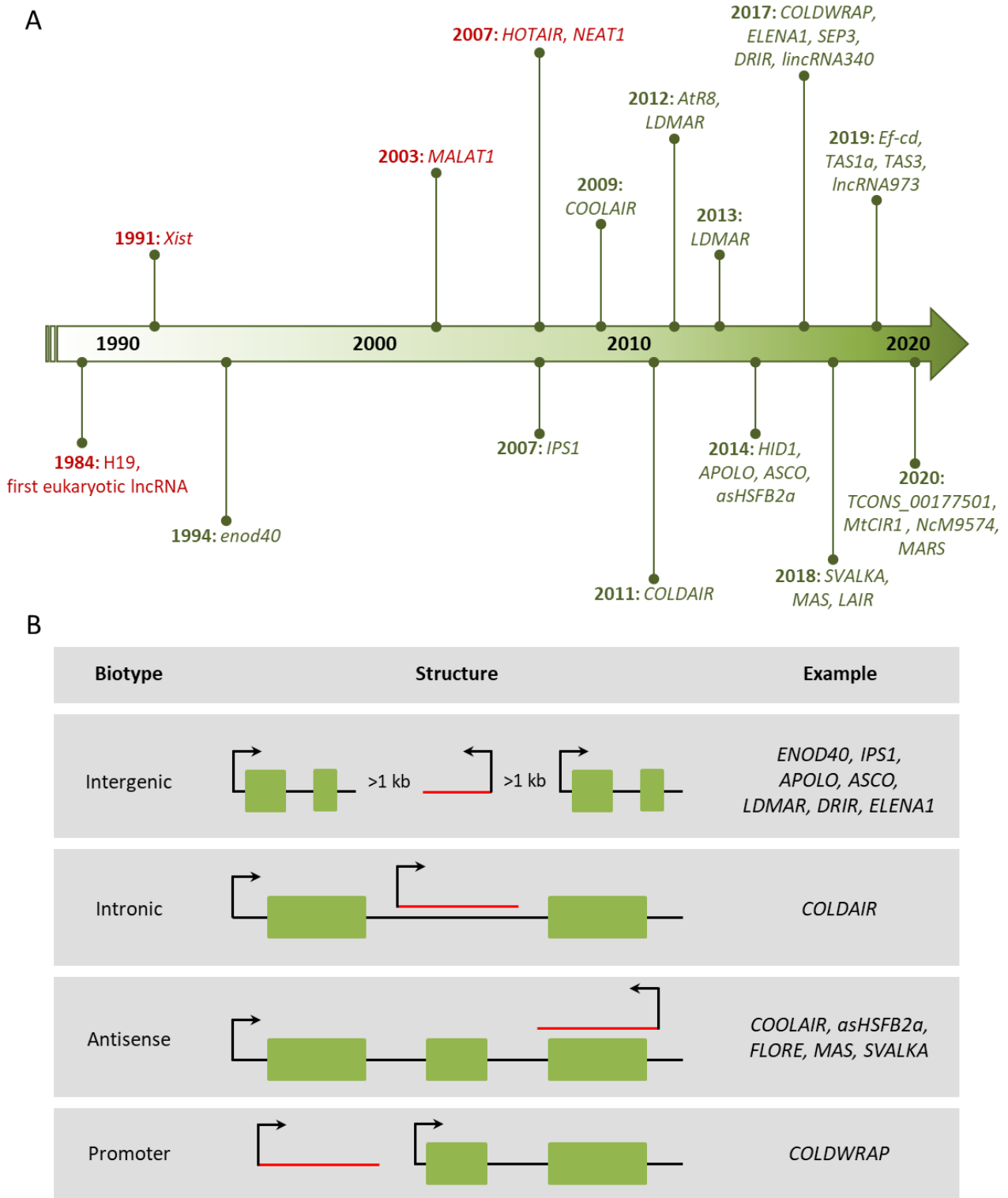


Figure 1. Discovery and classification of lncRNAs.

A. Timeline of lncRNA discovery. lncRNAs characterized in plants and animals are respectively indicated in green and red.

B. lncRNA classification. The image depicts the different characterized biotypes based on their relationship with their neighboring coding genes: intergenic, intronic, antisense and located in the promoter. Green boxes represent exons. Directions of transcription are indicated by arrows. Examples of plant lncRNAs are given for each biotype.

Adapted from Chen et al., 2020 and Jha et al., 2020. For *MARS* lncRNA, see Roulé et al., 2020.

; Rai et al., 2019). At last, the discovery of all of these lncRNAs helped to better understand how these transcripts differ from coding-ones, and describe their common characteristic features.

1.1.2 Characteristics of lncRNAs

1.1.2.1 Transcription of lncRNAs

lncRNAs were described in a large array of organisms including animals, plants, yeast (Houseley et al., 2008), and even in prokaryotes (Bernstein et al., 1993) and viruses (Reeves et al., 2007). Mammalian lncRNAs are by far the best-studied, but recent advances in the plant biology field allowed to extend the knowledge about eukaryotic lncRNAs features. First of all, lncRNAs share some similarities with mRNAs concerning their biogenesis. Indeed, most eukaryotic lncRNAs are transcribed by RNA polymerase II just like protein-coding mRNAs (Ulitsky and Bartel, 2013). However, some lncRNAs can be transcribed by other polymerases (Liu et al., 2015). For example, the *Arabidopsis* lncRNA *AtR8* involved in hypoxia is transcribed by Pol III, which usually transcribes housekeeping ncRNAs such as tRNAs and 5S rRNAs (Wu et al., 2012). In addition to this, a subset of lncRNAs can be transcribed by the plant-specific Pol IV and Pol V, involved in the RNA-directed DNA methylation (RdDM) pathway (Wierzbicki et al., 2008; Liu et al., 2015). These Pol V transcripts usually correspond to lncRNAs located in the promoter of coding-genes (Zheng et al., 2013). Besides these differences in polymerase use, recent studies in mammals described differences during lncRNA transcription itself. Indeed, Pol II displays less efficient pausing on lncRNA promoters relative to that of mRNAs, explaining the less precise transcription of some lncRNAs and earlier termination throughout gene bodies (Schlackow et al., 2017).

1.1.2.2 Post-transcriptional changes in lncRNAs

As stated earlier, most of eukaryotic lncRNAs are Pol II transcribed, meaning they harbor a 5'-cap and are polyadenylated at their 3'-end (Guttman et al., 2009; Liu et al., 2012; Liu et al., 2015). However, some lncRNAs do not possess a polyA tail such as the mammalian lncRNA *MALAT1* and instead exhibit a specialized short poly(A) tail-like moiety at its 3' end (Wilusz et al., 2008).

Another category of eukaryotic non-polyadenylated non-coding transcripts are circular RNAs (circRNAs) which join their heads with tails covalently in a process called back-splicing (Chen, 2016). For example, the *Arabidopsis* circRNA *circSEPALLATA3* (*circSEP3*) was

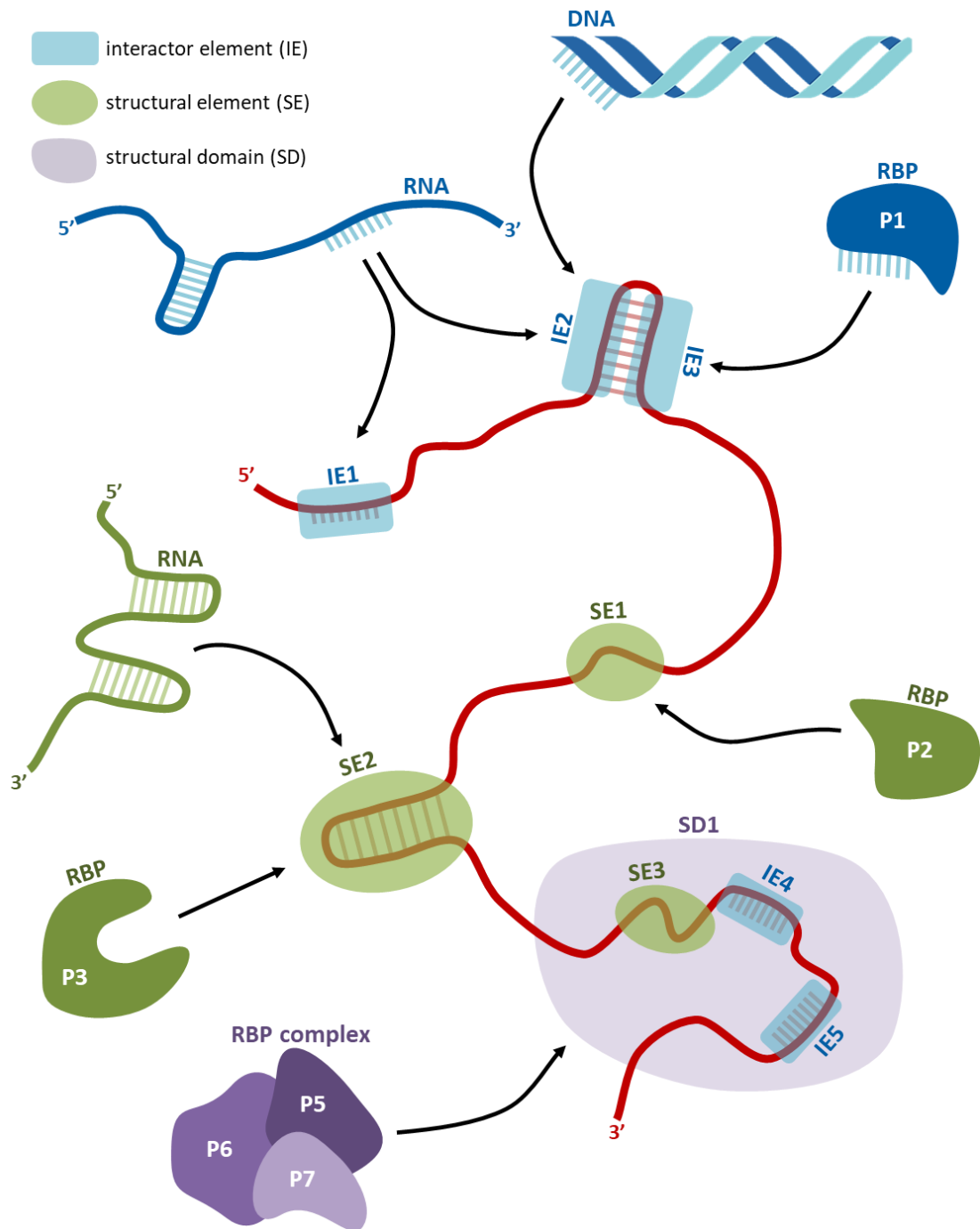


Figure 2. The sequence and structure of lncRNAs drive their interactions with other components of the cell.

Schematic view of lncRNA's sequence and structural features. Each lncRNA (in red) can contain multiple interactor elements (IEs, blue areas) and/or structural elements (SEs, green areas) along its transcript. IEs are required for physical interactions through base complementarity with RNA or DNA, and sequence-specific recognition by proteins (P). SEs govern the emergence of secondary and/or tertiary 3D RNA structures that are necessary for interaction with other cellular partners, including RNAs and proteins. The combination of specific IEs and SEs can result in structural domains (SDs, purple areas), key features for the association of the lncRNA with larger cellular complexes. Adapted from Fabbri et al., 2019.

shown to modulate flower development by impacting the splicing of its cognate mRNA *SEP3* (Conn et al., 2017).

Besides these circRNAs emerging from a backsplicing event, a large portion of lncRNAs are themselves subjected to splicing. Indeed, up to 40–50% of lncRNA genes contain introns just like protein-coding genes (Liu et al., 2012; Ulitsky and Bartel, 2013; Wang et al., 2014). Nevertheless, recent studies demonstrated that one of the main differences between mRNAs and lncRNAs is their splicing efficiency, which could be attributed to a lack of splicing factor binding. For example, the protein U2AF65 and the serine/arginine-rich (SR) proteins SRSF1,2,5,6,7,9 exhibited weaker binding to lncRNAs compared to coding transcripts (Melé et al., 2017; Krchnáková et al., 2019). As for mRNAs, splicing of lncRNAs can be modulated by the perception of external cues such as cold, which was shown to modulate the splicing of 135 lncRNA genes in *A. thaliana* (Calixto et al., 2019). Interestingly, the splicing process can also be modulated by the deposition of specific marks on the RNA, such as 6-methyladenosine (m6A). This mark was also identified among lncRNAs and was shown to play key roles in RNA subcellular distribution, stability, and structure (He et al., 2020).

1.1.2.3 Structure and subcellular localization of lncRNAs

Even if lncRNAs do not code for proteins, the modulation of their splicing can lead to transcripts with altered sequence, structure and/or stability. Rather than possessing specific domains like functional proteins, lncRNAs harbor specific sequences and secondary structures which can *in fine* shape their 3D structure and affect their interaction with other molecules (Zampetaki et al., 2018; Fabbri et al., 2019). Interactor elements (IEs) serve for physical interactions with various partners through base complementarity (with other nucleic acids) and sequence-specific recognition by RNA-binding proteins (RBPs). On the other hand, structural elements (SEs) allow the formation of secondary and/or 3D lncRNA structures, directing their functional interactions with other cellular partners. Structural domains contain both IEs and SEs in various combinations and permit interactions with RBP complexes (Fabbri et al., 2019). The association of these different elements could represent one of the languages that serve for directing lncRNAs interactions (Figure 2) (Helder et al., 2016; Zampetaki et al., 2018). As an example, the lncRNA *Xist* harbors 33 regions that form well-defined secondary structures linked by structurally variable regions, including a conserved A-repeat element. This region forms an inter-repeat structure which is essential for its control over X chromosome inactivation (Pintacuda et al., 2017).

The understanding of the RNA repertoire still requires further efforts for seizing the underlying signals that allow lncRNAs to exert their functions. Nevertheless, a few studies have tried to associate well known protein-domains with their RNA counterparts (Goff and Rinn, 2015). One of these signals consists in the information guiding their subcellular localization. Indeed, lncRNAs can either be exported to the cytosol or reside in the nucleus, contributing to various cell processes in both cases (Carlevaro-Fita and Johnson, 2019). lncRNAs are generally more enriched in the nucleus compared to mRNAs, possibly due to their less efficient splicing and their interactions with nuclear RBPs. A recent study discovered an RNA motif that recognizes the U1 small nuclear ribonucleoprotein (snRNP) and is essential for mobilizing lncRNAs to chromatin, therefore retaining them into the nucleus (Yin et al., 2020). Similarly, the lncRNA *BORG* exhibits a pentamer RNA motif which is essential for nuclear retention. The mutation of this motif to a scrambled sequence resulted in the loss of nuclear localization. Conversely, the addition of a single copy of the motif in a cytoplasmic RNA was sufficient to induce its retention in the nucleus (Zhang et al., 2014). These specific RNA domains could therefore represent the RNA counterparts of the well described nuclear localization signal (NLS) present in proteins (Goff and Rinn, 2015). The characterization of these RNA signals will be of major relevance to develop new tools for molecular biology and the study of the mechanisms of action of lncRNAs.

1.1.2.4 Tissue-specificity and stability of lncRNAs

Besides the regulation of their subcellular localization, lncRNAs expression at the tissue level is also tightly regulated. Interestingly, lncRNAs are generally more expressed in a tissue-specific manner than coding-genes in both plants and animals (Liu et al., 2012; Tsoi et al., 2015; Zou et al., 2016). For instance, more than 30% of *Arabidopsis* lncRNAs display an organ- or developmental-specific expression pattern (Liu et al., 2012). In addition, lncRNAs present lower expression levels than mRNAs, possibly due to overall lower levels of these transcripts and/or high tissue specificity among various organs (Li et al., 2016; Liu et al., 2016). These lower levels could also be due to differences in lncRNA decay and turnover rate (Szabo et al., 2020). Indeed, some studies showed that lncRNAs half-lives vary over a wide range, with some transcripts exhibiting either poor (half-life < 2h) or strong (half-life > 16h) stability. Nevertheless, lncRNAs and mRNAs display on average quite comparable decay rates among tissues (Clark et al., 2012; Tani et al., 2012). The growing number of discovered lncRNAs and their high tissue-specificity suggest that lncRNAs could serve as potent markers of tissues and developmental stages, underlining their potent role throughout development in eukaryotes.

1.1.2.5 Conservation of lncRNAs

Surprisingly, lncRNAs are quite poorly conserved at the inter-species level (Wood et al., 2013; Deng et al., 2018). Indeed, unlike protein-coding genes whose conservation directly relies on their nucleotide or amino acid sequence, the features constituting lncRNA conservation are harder to detect. Rather than having conservation only through nucleotide sequence, some studies proposed a model including 4 dimensions of lncRNA conservation: sequence, structure, function, and expression from syntenic loci (Diederichs, 2014). In some cases, lncRNAs can be conserved at nucleotide level just like protein-coding genes such as the lncRNA *MALAT1* whose sequence is conserved among mammals (Ma et al., 2015). On the other hand, the lncRNA structure can represent an alternative way of conserving information. Indeed, two distinct sequences can give rise to similar 2D and/or 3D structures. For example, the *COOLAIR* lncRNA exhibits two right-hand turn (R-turn) motifs that are evolutionarily conserved across *Brassicaceae* species (Hawkes et al., 2016). Remarkably, sequence and structure conservation are not always necessary for conservation of lncRNA function. The human *JPX* lncRNA and its mouse homolog display deep divergence in their nucleotide sequences and RNA secondary structures. Regardless of these differences, both human and murine *JPX* display robust binding to CTCF, a protein that is essential to *JPX*'s role in X chromosome inactivation. Moreover, expression of human *JPX* can functionally complement the loss of *JPX* in mouse embryonic stem cells (Karner et al., 2020). Finally, lncRNA transcription at a given genomic locus could be conserved whereas neither the sequence, structure, nor function of the transcript are conserved. This lncRNA syntenic location could impact the expression of neighboring genes in species harboring this genomic locus (Ulitsky et al., 2011; Wang et al., 2011). At last, all of the presented dimensions of lncRNA conservation are intrinsically connected and influence each other, providing another layer of complexity to be considered apart from nucleotide sequence in lncRNA evolutionary conservation. The understanding of these mechanisms represents one of the greatest challenges that the lncRNA field will have to face in coming years.

1.1.3 Functions of lncRNAs in plants and associated mechanisms

1.1.3.1 Major functions of eukaryotic lncRNAs

The previous chapter described the specificities in the biogenesis, structure, localization, expression patterns and conservation of lncRNAs compared to mRNAs. For now, mammalian lncRNAs are by far the best-studied. It was stated earlier that lncRNAs could be classified according to their genomic location and transcription orientation. Another major

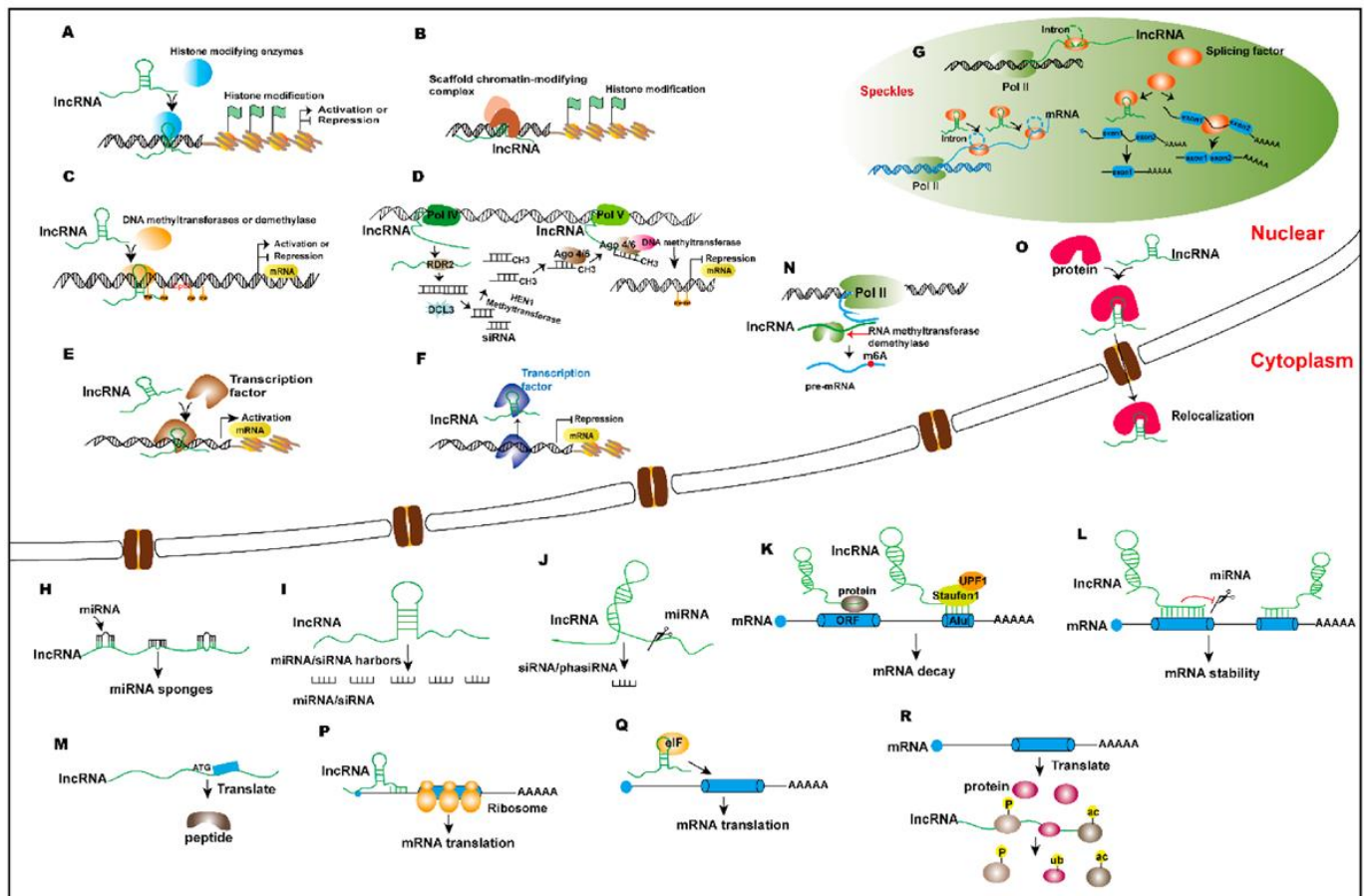


Figure 3. LncRNAs and their associated regulatory mechanisms.

- A. LncRNAs activate or repress gene transcription through interaction with histone-modifying enzymes.
- B. LncRNAs recruit histone-modifying complexes or act as scaffolds for multiple histone modifiers to regulate histone modification of genes and thereby regulate gene transcription.
- C. DNA methyltransferases or demethylases can be recruited by LncRNAs to target gene transcription.
- D. LncRNAs transcribed by Pol IV/V are involved in RNA-dependent DNA methylation, thus activating or repressing gene transcription.
- E, F. LncRNAs activate or repress gene transcription through interaction with TFs.
- G. LncRNAs regulate AS of pre-mRNAs through interaction with SFs. SFs directly regulate the LncRNA's AS in nuclear speckles.
- H. LncRNAs regulate target gene expression by acting as miRNA sponges.
- I. LncRNAs act as miRNA or siRNA precursors.
- J. LncRNAs are targeted by miRNAs to produce siRNA or phased small-interfering RNAs (phasiRNAs).
- K. LncRNAs are involved in the Staufen1-mediated mRNA decay, and LncRNAs bind to proteins and mediate mRNA decay.
- L. LncRNAs modulate mRNA stability by directly binding to mRNAs, competing with other interactors such as miRNAs.
- M. LncRNAs can be translated to peptides.
- N. LncRNAs regulate mRNA expression through interaction with RNA methyltransferases or demethylases.
- O. LncRNAs associate with proteins to regulate protein localization.
- P. LncRNAs interact with mRNAs and affect mRNA translation.
- Q. LncRNAs regulate mRNA translation through interaction with the translation initiation complex eIF (eukaryotic initiation factor).
- R. LncRNAs interact with proteins and control protein phosphorylation, acetylation, and ubiquitination at the post-translation level.

Adapted from Zhang et al., 2019b.

way to classify lncRNAs is by their role and action in the cell, and in which cellular process they intervene (Figure 3) (Zhang et al., 2019b; Statello et al., 2021). The regulation of transcription is the category where most studied lncRNAs were shown to play a role. For instance, the lncRNA *UMLILO* acts as an immune gene-priming transcript and is central to the establishment of trained immunity in mice (Fanucchi et al., 2019). In addition to this, lncRNAs can act at the post-transcriptional level, impacting either transcript stability or splicing such as *PNCTR*. This lncRNA interacts with the polypyrimidine tract-binding protein (PTBP1), an RBP regulating precursor-mRNA (pre-mRNA) processing in the nucleus and mRNA translation in the cytoplasm. *PNCTR* can sequester more than 6 PTBP1 proteins at a time, altering PTBP1 associated splicing regulation (Yap et al., 2018). Thanks to their specific structures, several lncRNAs can promote the interaction between various partners like *NEAT* which serves as a scaffold for paraspeckles, nuclear bodies that regulate multiple aspects of gene expression (Lin et al., 2018). Besides their roles in the nucleus, lncRNAs can also exert roles that affect cellular organelles. The *SAMMSON* lncRNA facilitates CARF binding to p32, a mitochondrial protein essential in the processing of mitochondrial rRNAs. This leads to enhanced mitochondrial rRNA synthesis, promoting cell growth and tumorigenic potential (Vendramin et al., 2018). Remarkably, a massive amount of these newly discovered lncRNAs function in cancer development or present deregulated expression in cancerous cells (Huarte, 2015; Schmitt and Chang, 2016, Carlevaro-Fita et al., 2020). Indeed, lncRNA transcription changes can provide signals of malignant transformation and inform about tumor progression statuses. Hence, the study of lncRNAs in animals stands out as an important necessity to monitor and understand cancer development, one of the biggest medical challenges of the modern era. Nevertheless, these are just a few examples of the lncRNAs that were found to act in many vital processes in animals.

1.1.3.2 lncRNAs involved in plant development

What about plant lncRNAs then? Even if the study of lncRNAs in plants is not as extensive as in animals, their involvement during plant development and stress responses already started to emerge. They were shown to act through very diverse mechanisms such as modulation of DNA methylation (Ariel et al., 2014), controlling histone modification (Kim et al., 2017), by acting in cis (Pang et al., 2019) or in trans (Zhang et al., 2019c, Ariel et al., 2020) of specific targets, by acting as miRNA precursors (Xin et al., 2011) or miRNA target mimics (Franco-Zorrilla et al., 2007, Unver and Tombuloglu, 2020). Interestingly, a substantial number of lncRNAs were described as regulators of major biological processes such as flowering time, development of reproductive organs or response to biotic and abiotic stresses (Chen et al., 2020).

The tight regulation of floral onset and development of sexual organs at the right moment is a crucial point for reproductive success and progeny survival. Flowering time is governed by a plethora of both external cues such as temperature and day length, and internal cues including hormonal balance and sugar content (Kim et al., 2009; Kim 2020; Izawa, 2021). The exposure to prolonged cold during winter is called vernalization and is essential to permit flowering in the upcoming growing season. The perception of this cold period downregulates the expression of the flowering repressor *FLOWERING LOCUS C* (*FLC*). This activates a complex signaling cascade and leads *in fine* to flowering during spring. Several lncRNAs were shown to impact the expression of *FLC*, including *COOLAIR* (Swiezewski et al., 2009; Marquardt et al., 2014; Hawkes et al., 2016), *COLDAIR* (Kim et al., 2017) and *COLDWRAP* (Kim and Sung, 2017).

FLC silencing is mediated by the Polycomb Repression Complex 2 (PRC2) through the deposition of histone 3 lysine 27 trimethylation (H3K27me3), a repressive chromatin modification. The *COOLAIR* transcripts are transcribed from the 3' end of the *FLC* locus and modulate the repression of *FLC* expression (Swiezewski et al., 2009). *COOLAIR* is alternatively polyadenylated and alternatively spliced, and produces a short and a long isoform with polyA tails. Its alternative splicing is notably controlled by the core spliceosome component PRP8a (Marquardt et al., 2014). This AS contributes to the usage of *COOLAIR*'s proximal poly(A) site, promoting the activity of an H3K4me2 demethylase and further leading to reduced *FLC* transcription. This constitutes a positive feedback mechanism that reinforces proximal polyadenylation and low expression of *FLC*. On the contrary, distal polyadenylation coincides with a high expression state of *FLC* (Swiezewski et al., 2009).

On the other hand, the lncRNA *COLDAIR* is transcribed from the first intron of *FLC* and is crucial for the enrichment of PRC2 at the *FLC* locus, therefore contributing to *FLC* silencing. The mutation of a specific region in *COLDAIR* disrupts its interaction with the PRC2 component CURLY LEAF (CLF), resulting in vernalization insensitivity and absence of *FLC* repression (Kim et al., 2017). At last, *COLDWRAP* is transcribed from the repressed proximal promoter of *FLC* and interacts with the CLF component of PRC2 as well. This interaction permits the formation of an intragenic chromatin loop which is essential for stable *FLC* repression upon vernalization (Kim and Sung, 2017). This set of studies underlines the importance of lncRNAs during plant development and their roles in the control of transcription and epigenetic status during major biological processes.

The tight control of flowering time is a prerequisite for proper flower development, gamete meeting and successful sexual reproduction. Once all the conditions for flowering onset are fulfilled, the vegetative meristems undergo molecular and structural changes, becoming floral meristems which in turn will produce the floral organs. Many lncRNAs were

also found to regulate the development and function of sexual organs in various species such as the *LONG-DAY SPECIFIC MALE-FERTILITY-ASSOCIATED RNA (LDMAR)* (Ding et al., 2012), *PHOTOPERIOD-SENSITIVE GENIC MALE STERILITY T (PMS1T)* (Fan et al., 2016) and *EARLY FLOWERING-COMPLETELY DOMINANT (Ef-cd)* (Fang et al., 2019) in rice, *BcMF11* (Song et al., 2013) in *Brassica campestris*, *SUPPRESSOR OF FEMINIZATION (SUF)* (Hisanaga et al., 2019) in *Marchantia polymorpha* and *LINC-AP2* (Gao et al., 2016) in *A. thaliana*. Interestingly, the lncRNA *LINC-AP2* was found to integrate both developmental status and biotic stress signals. The *Turnip crinkle virus (TCV)* can infect *A. thaliana* plants, leading to a severely distorted floral structure. *LINC-AP2* expression was shown to be upregulated in response to *TCV* infection, concomitantly with a decrease in *APETALA2 (AP2)* expression, an essential floral structure-related gene. *LINC-AP2* overexpressing plants exhibited higher sensitivity to *TCV* and higher virus content, as well as reduced *AP2* expression. Similarly, *TCV*-infected *ap2* mutants also displayed more severe viral symptoms and failed to open their floral buds (Gao et al., 2016). Hence, the upregulation of a specific lncRNA negatively correlates with the expression of a major regulator of floral development in the context of viral infection. Therefore, lncRNAs can also act as integrators of external cues during organ establishment, allowing plants to adapt to their environment.

1.1.3.3 Plant lncRNAs involved in biotic stress responses

Most identified plant lncRNAs were characterized as stress-responsive in plants, underlying the importance of studying the role of these lncRNAs during stresses (Shafiq et al., 2016; Chen et al., 2020). Since pests and diseases are an inherent part of our agricultural challenges, the understanding of the molecular mechanisms driving plant resistance to pathogens is of major importance. To this end, the study of lncRNAs in response to biotic stresses delivers new perspectives in how plants can adapt to and counteract pathogens (Zhang et al., 2020; Zaynab et al., 2021). In *A. thaliana*, a subset of lncRNAs was found to be responsive to infection by the fungal pathogen *Fusarium oxysporum*. Moreover, 10 of *F. oxysporum*-induced lncRNAs were functionally characterized using various mutated lines, and 5 of them were linked to disease development (Zhu et al., 2014). A growing number of lncRNA studies are also emerging in crops. A strand-specific RNA sequencing assay on potato stem tissues identified a total of 1113 lincRNAs, 559 of them being responsive to *Pectobacterium carotovorum subsp. Brasiliense* infection (Kwenda et al., 2016). Similarly, RNA sequencing of tomato samples infected with *Tomato yellow leaf curl virus (TYLCV)* predicted 1565 lncRNAs, including a set of lncRNAs which had their expression changing upon virus infection. The lncRNAs *slylnc0049* and *slylnc0761* were significantly up-regulated by *TYLCV* and were selected for virus-induced gene silencing (VIGS) assay. The decrease

of their expression led to higher virus accumulation inside the plants, suggesting their involvement in tomato resistance to TYLCV (Wang et al., 2015a). The comparison of two grape cultivars that are susceptible (*Cabernet Franc*) and tolerant (*Merlot*) to *Lasioidiplodia theobromae* led to the discovery of 1826 novel candidate lncRNAs, 782 of them being differentially expressed between the susceptible and resistant cultivars upon infection. 36 of these lncRNAs exhibited high homology with characterized miRNA precursors from *Vitis vinifera*, *Arabidopsis lyrata*, and *Arabidopsis thaliana*, suggesting their putative link with miRNA production (Xing et al., 2019).

One of the best characterized lncRNA involved in the response to biotic stresses is *ELF18-INDUCED LONG NONCODING RNA 1 (ELENA1)*, which was described as a positive regulator of expression of immune responsive genes in *A. thaliana* (Figure 4A). Indeed, *ELENA1* suppression leads to decreased expression of *PATHOGENESIS-RELATED GENE1 (PR1)* and enhanced susceptibility to *Pseudomonas syringae* pv *tomato* DC3000. On the other hand, *ELENA1* overexpression resulted in elevated *PR1* expression and a pathogen resistance phenotype. The regulation of *PR1* expression is permitted by *ELENA1* direct interaction with the positive regulator MEDIATOR SUBUNIT 19a (MED19a). This lncRNA-protein interaction allows the enrichment of MED19a on *PR1* promoter, leading to expression activation (Seo et al., 2017). A more recent study unveiled an additional layer of complexity in this molecular process. Besides its binding to MED19a, *ELENA1* can effectively bind to FIBRILLARIN 2 (FIB2), a negative transcriptional regulator for immune responsive genes, including *PR1*. *ELENA1* was found to disrupt the FIB2/MED19a complex, facilitating FIB2 release from the *PR1* promoter and leading to *PR1* expression (Seo et al., 2019). These studies provide examples of how lncRNAs fine-tune protein-protein interactions, modulating their function throughout gene transcription.

Other lncRNAs were shown to integrate multiple environmental cues. Recently, Muthusamy and colleagues (2019) compared various banana genotypes and identified novel lncRNAs responsive to *Mycosphaerella eumusae*, a fungi causing Eumusae leaf spot disease, and *Pratylenchus coffeae*, a root lesion nematode. The comparison of resistant and sensitive banana genotypes allowed characterizing thousands of lncRNAs, a substantial number of them being pathogen and/or genotype-specific. Interestingly, 100 of these pathogen-related lncRNAs were also regulated in drought stress in banana, suggesting a putative crosstalk between biotic and abiotic stress responses (Muthusamy et al., 2019). Hence, lncRNAs could act as integrators of multiple external signals, and modulate specific signaling pathways in plants.

1.1.3.4 Plant lncRNAs involved in abiotic stress responses

Abiotic stresses consist of environmental factors such as extreme temperatures (cold, freezing or heat), drought (water deficit) or excessive watering, salinity or toxic substances that negatively impact plant growth, development, yield, and seed quality. As for biotic stresses, a growing number of lncRNAs were shown to be responsive to these stresses and some of them participate in the establishment of plant tolerance (Jha et al., 2020; Waititu et al., 2020; Urquiaga et al., 2021). In *Populus trichocarpa*, the analysis of sequencing data comparing plants under control and drought conditions led to identify 2542 lincRNAs, where 504 of them were drought-responsive (Shuai et al., 2014). Similarly, an RNAseq assay in cassava searched for new lncRNAs in shoot apices and young leaves under drought and cold stress. 318 lncRNAs were described as responsive to drought and/or cold stress, a majority of them being co-expressed concordantly or discordantly with their neighboring genes (Li et al., 2017b).

Remarkably, some lncRNAs were positively correlated with miRNA-targeted genes such as the cold-repressed *lincRNA159*. This lncRNA was predicted to bind *miR164* and its expression is coordinated with an expression decrease of *miR164*-targeted NAC genes under cold treatment (Li et al., 2017b). These *miR164*-targeted NAC genes are conserved among plants and their decrease in expression causes drought tolerance, pinpointing their importance in plant acclimation to this stress (Fang et al., 2014). LncRNAs can therefore act as miRNA target-mimics to fine-tune the establishment of environmental responses.

A recent study described the *DROUGHT-INDUCED LNCRNA (DRIR)* in *Arabidopsis*, which positively regulates drought and salt responses. Its expression is highly induced upon drought and salt stress but also upon abscisic acid (ABA) treatment, and the overexpression of *DRIR* provides enhanced tolerance to these stresses. These overexpressing lines also display altered expression of genes involved in ABA signaling, water transport and other stress-relieving processes (Quin et al., 2017).

Another study characterized the impact of lncRNAs on cold acclimation and tolerance to freezing in *Arabidopsis*. The response to cold involves transcriptional changes of thousands of genes (Calixto et al., 2018), mainly governed by the rapid up-regulation of the C-REPEAT/DEHYDRATION-RESPONSIVE ELEMENT BINDING FACTORS (CBFs) (Medina et al., 2011). These highly conserved transcription factors (TFs) promote cold tolerance through the regulation of *COLD REGULATED (COR)* genes. This ensemble of cold-sensitive genes allows adjustment of both physiological and biochemical properties of plant cell interiors, providing freezing tolerance (Zhao et al., 2016). Kindgren and colleagues (2018) characterized a cascade of two lncRNAs regulating *CBF1* expression (Figure 4B).

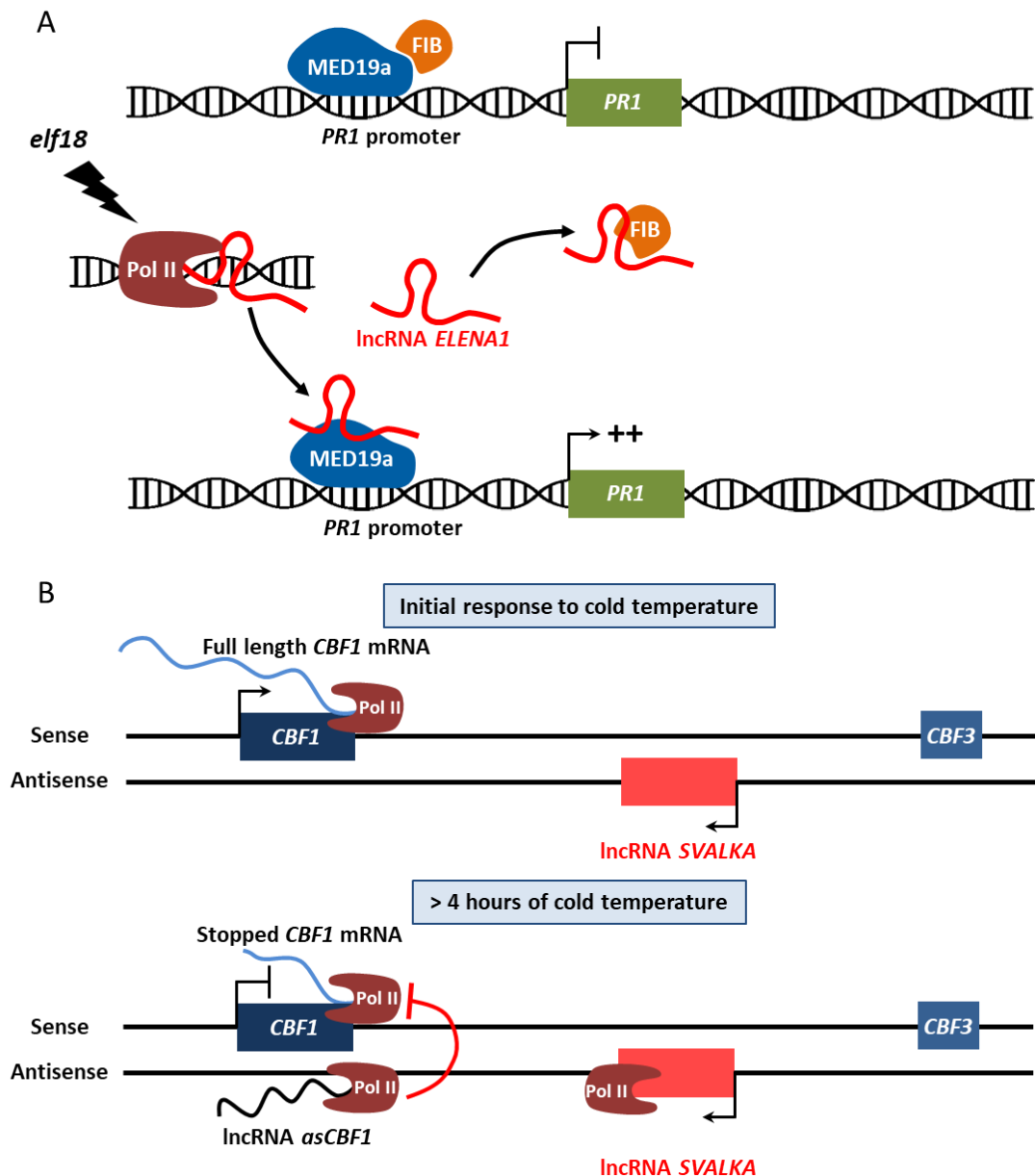


Figure 4. LncRNAs fine-tune the transcriptional response to biotic (A) and abiotic (B) stresses in plants.

A. In control conditions, the Mediator subunit 19a (MED19a) binds the *PATHOGENESIS-RELATED GENE 1 (PR1)* promoter along with FIBRILLARIN 2 (FIB2), which directly interacts with MED19a and represses *PR1* expression. A treatment with the elicitor *elf18*, a bacterial peptide derived from the translation elongation factor Tu, increases the expression levels of the lncRNA *ELF18-INDUCED LONG-NONCODING RNA 1 (ELENA1)*. This lncRNA directly binds to MED19a and FIB2, hence blocking FIB2 binding to MED19a. This promotes the release of FIB2 from the *PR1* promoter, causing *PR1* induction.

B. The lncRNA *SVALKKA* represses sense *CBF1* transcription. At the beginning of cold perception by the plant, sense *CBF1* is normally transcribed and *SVALKKA* is not expressed. However, after 4 h of cold exposure *SVALKKA* is also transcribed and some read-through transcription leads to expression of antisense *CBF1* lncRNA (*asCBF1*). The transcription of *asCBF1* increases Pol II occupancy on both strands, provoking Pol II collision and restricting the expression of full-length *CBF1*.

‘→’ indicates facilitation and activation of gene expression, ‘←’ indicates repression.

Adapted from Zhang et al., 2019.

The *SVALKA* lncRNA was shown to regulate *CBF1* expression and affects freezing tolerance of the plant. Interestingly, a cryptic lncRNA overlapping with *CBF1* on its antisense strand was identified and named *asCBF1*. This transcript results from Pol II read-through transcription of *SVALKA*, and its expression suppresses *CBF1* expression by Pol II collision (Kindgren et al., 2018). This provides evidence of how lncRNAs control the expression of major regulators of stress-response, giving the ability to appropriately acclimate to a changing environment. As previously introduced, stress perception leads to expression changes in both coding and non-coding genes, provoking major transcriptome re-shaping.

Surprisingly, some stresses such as cold are able to modulate both expression and alternative splicing (AS) of lncRNAs (Calixto et al., 2019), adding further complexity to transcriptome regulation. Indeed, AS is a mechanism that allows the production of several transcripts from one single gene by exon-intron shuffling. As for lncRNAs, the extensive use of next-generation sequencing allowed to discover thousands of new transcripts resulting from AS of coding genes, a massive amount being produced upon either abiotic (Calixto et al., 2018; Ling et al., 2018) or biotic stresses (Mandadi and Scholthof, 2015; Bedre et al., 2019; Ibrahim et al., 2021). Together with lncRNAs, AS adds “versatility” to the transcriptome and broadens the transcript repertoire of plants, notably during biotic and abiotic stresses. This amazing adaptability of the transcriptome is one of the keystones that allow plants to efficiently counteract the stresses they face, and to thrive in their proximate environment.

1.2 Alternative splicing, a mean to face environmental cues

Plants are sessile organisms that constantly need to adapt to their ever-changing environment through the fine-tuning of their cellular features, therefore impacting their tissue properties and overall growth. This is permitted by the modulation of gene expression, which shapes both transcriptome and proteome outputs. As most eukaryotic genes are interrupted by introns, an essential step in gene expression is the removal of introns through the splicing of pre-mRNA transcripts. The recognition of splicing sites on pre-mRNAs can be sometimes modulated or perturbed, giving rise to a set of mRNA sequences from a single parental gene due to retained introns or alternatively chosen splice sites. This process, termed AS, mainly exerts two major molecular functions in the cells. First, AS can enhance the proteome repertoire by the generation of two or more distinct protein isoforms, usually exhibiting different structural or functional features (Kelemen et al., 2013). Secondly, sequence changes engendered by a specific splicing event can directly impact the stability of an mRNA, leading to a decrease of its expression by nonsense mediated decay (NMD) (Lewis et al., 2003). The exponential growth of transcriptome analyses using next-generation technologies led to the discovery of a myriad of new AS events. In *Arabidopsis* for example, up to 60-83% of multi-exonic genes undergo AS (Marquez et al., 2012; Zhang et al., 2017; Zhu et al., 2017). Compared to other reigns, AS is more prevalent in plants than in *Drosophila* species (20–37% of multi-exonic genes) (Gibilisco et al., 2016), but less than in humans where virtually every multi-exonic gene can undergo AS (Pan et al., 2008; Wang et al., 2008). Eukaryotic transcriptomes constantly evolved and several studies have shown that a concomitant evolution of AS patterns occurred as well, reporting a negative correlation between the number of AS events and the size of protein families in human, *Mus musculus*, *Drosophila melanogaster*, and *Caenorhabditis elegans* (Kopelman et al., 2005; Su et al., 2006; Talavera et al., 2007; Iñiguez and Hernández, 2017). In addition to this, the domestication process of various organisms such as plant crops was also shown to dramatically affect AS patterns. For instance, sorghum and wheat domestication led to a significant decrease of AS event abundance in comparison with wild species (Ranwez et al., 2017; Yu et al., 2020). Hence, understanding how and which factors can affect AS will be a major challenge that will shed light on transcriptome complexity. In this next part, I will describe the molecular mechanisms defining AS, and discuss the role of AS in plants and in their global acclimation to stresses.

1.2.1 The spliceosome machinery

1.2.1.1 The core components of the spliceosome machinery

The discovery of the pre-mRNA splicing process occurred more than 40 years ago, thanks to the analysis of viral mRNA processing in infected mammalian cells (Berget et al., 1977; Chow et al., 1977). The critical steps of splicing consist of the recognition of intron position and its further removal through 2 trans-esterification reactions, mediated by the so-called spliceosome. This splicing machinery is a large and dynamic ribonucleoprotein (RNP) complex located in the nucleus and composed of Uridine-rich small nuclear RNAs (snRNAs) and numerous spliceosome-associated proteins (Ru et al., 2008; Shi, 2017). Two spliceosomes coexist in most eukaryotes: the major U2-dependent spliceosome, which catalyzes the removal of U2-type introns, and the minor U12-dependent spliceosome, which is less abundant and splices the rare U12-type class of introns. These 2 complexes mainly differ by their composition and the sequences they target (Patel and Steitz, 2003; Turunen et al., 2013; Olthof et al., 2020). The assembly of the spliceosome is permitted by the interactions between small nuclear ribonucleoproteins (snRNPs) and the pre-mRNA. The study of yeast spliceosomes allowed identifying 50-60 snRNP subunits and about 100 of additional splicing-related factors, a majority of them being conserved in metazoans (Fabrizio et al., 2009). In comparison, the purification of *Drosophila* and human spliceosomal complexes identified a total of 260 and 400 proteins, respectively (Rappsilber et al., 2002; Herold et al., 2009; Will and Lührmann, 2011). Comparative analyses of sequence and mass spectrometry data indicate a conservation of about 430 spliceosomal factors in *Arabidopsis* (Koncz et al., 2012).

During splicing, the spliceosome assembles at each intron in a precise order, which is conserved among eukaryotes (Figure 5). The spliceosome assembly starts with U1 snRNP binding to the 5'-splice site, followed by U2 snRNP binding to the intron branch site. Next, the U4/U6-U5 snRNPs associate to form the pre-catalytic spliceosome. This pre-catalytic complex is converted into an activated spliceosome by the dissociation of U1 and U4 snRNPs and the binding of the PRP19-CDCL5 complex (called the nineteen complex (NTC) in yeast). The NTC is required for stable association of U5 and U6 with the spliceosome after the release of U4. Finally, the branching reaction occurs where both exons are ligated and the intron lariat is removed. The complex therefore disassembles into individual snRNPs and associated proteins (Chan and Cheng, 2005; Will and Lührmann, 2011; Koncz et al., 2012; Slane et al., 2020). Remarkably, 7 common proteins are present in U1, U2, U4, and U5 snRNPs. These proteins harbor an Sm domain and were named as SmB, SmD1, SmD2,

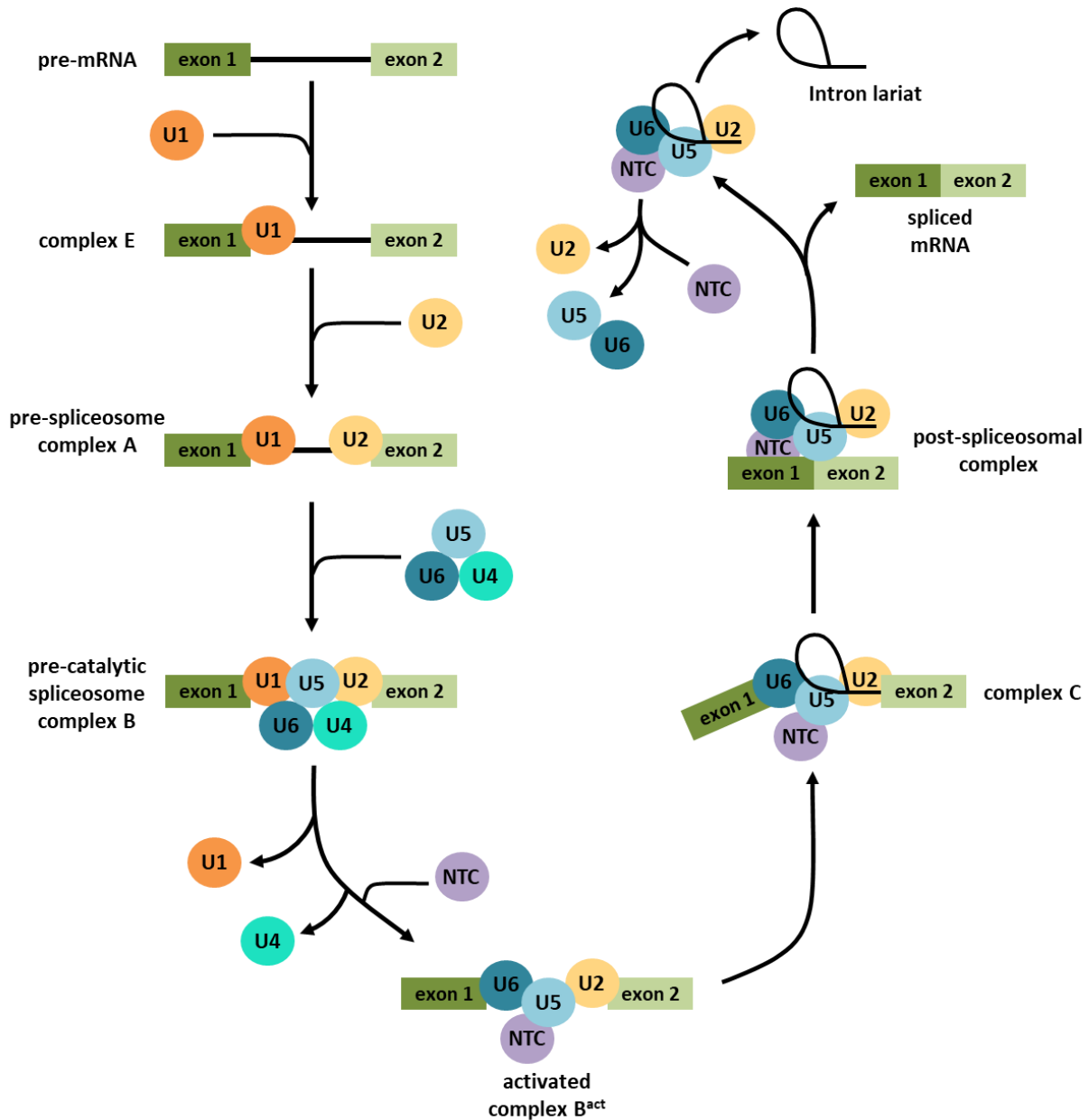


Figure 5. Pre-mRNA Splicing by the major U2-dependent spliceosome.

The spliceosome assembles at each intron in a precise order. The splicing process is initiated by the interaction of the U1 snRNP with the 5' splice site through base pairing. The U2AF (U2) subunit U2AF³⁵ binds to the intron/exon border and U2AF⁶⁵ binds to the polypyrimidine tract upstream of the intron/exon border, forming complex E. Subsequently, the U2 snRNP binds to the branch point, defining the pre-spliceosome complex A. The U4/U6-U5 snRNP is then docked onto the U2 snRNP, leading to the pre-catalytic complex B. This pre-catalytic complex is converted into the activated complex B^{act} by the dissociation of U1 and U4 snRNPs and the binding of the PRP19-CDCL5 complex (also called the nineteen complex (NTC)). The NTC is required for stable association of U5 and U6 with the spliceosome after the release of U4. The spliceosome complex then carries out the first catalytic step of splicing at 5' splice site, generating complex C, which contains the free exon 1 and the intron-exon 2 lariat intermediate. Complex C catalyzes the second step of the splicing reaction, the cleavage at the 3' splice site, the ligation of the exons, and the release of the spliced mRNA. The lariat is finally degraded and the snRNPs are recycled. Adapted from Meyer et al., 2015.

SmD3, SmE, SmF, and SmG (Ru et al., 2008). A second group comprises related “like Sm” proteins (Lsm2–8), the counterparts of Sm proteins in U6 snRNP. These Sm proteins mediate protein interactions with other core proteins of the splicing complex, forming the structural core of the snRNPs (Golisz et al., 2013). The role of some of these spliceosome components was already characterized in plants. For example, the SmD1b protein impacts the splicing of specific pre-mRNAs but also their stability (Elvira-Matelot et al., 2016). Besides Sm proteins, a few other actors such as Brr2, Snu114 and PRP8 were characterized as core components of the U4/U6-U5 tri-snRNP complex. Their interaction allows the formation of the catalytically active spliceosome (Bartels et al., 2002; Maeder et al., 2009). There are two PRP8 paralogs in *Arabidopsis*: PRP8a and PRP8b, which impact splicing to modulate ovule competence for pollen tube attraction (Kulichová et al., 2020). Moreover, a mutant defective in PRP8a resulted in an embryo lethal phenotype (Schwartz et al., 1994). Additionally, PRP8a was shown to regulate the splicing of the lncRNA *COOLAIR*, modulating the activity of the *FLC* locus (Marquardt et al., 2014).

More and more efforts are being made to identify spliceosome components in plants, and to understand their roles and specificities (Figure 6) (Koncz et al., 2012; Kanno et al., 2020). With this growing number of studies investigating splicing associated mechanisms, it became clear that the components of the spliceosome are major regulators of cellular processes and eukaryotic development.

1.2.1.2 Alternative splicing: a matter of choice

Splicing of nascent pre-mRNAs takes place in the nucleus and most of the time in a co-transcriptional fashion. The splicing machinery first recognizes splice sites, the boundaries that define exons and introns. Then it removes introns, joins the exons to finally generate a mature mRNA molecule. The so-called AS occurs when multiple splice sites can be chosen by the spliceosome machinery, resulting in the generation of multiple mRNAs from one single pre-mRNA. There are different types of AS events that can occur in eukaryotes, including exon skipping being the most frequent AS event in animals, and intron retention being predominant in plants (Figure 7A) (Wang et al., 2015b; Marquez et al., 2012). The selection of these alternative splice sites does not solely depend on core spliceosomal components, but also to a large extent on other additional RNA-binding proteins, globally designated as splicing factors (SFs). These SFs mainly fall into two categories: heterogeneous nuclear ribonucleoproteins (hnRNPs) and serine/arginine-rich (SR) proteins (Figure 7B) (Barta et al., 2008; Wachter et al., 2012; Yeap et al., 2014; Zhang et al., 2020). The selection of the splicing event is guided by the recognition of specific cis-regulatory elements on the pre-mRNA called intronic or exonic splicing enhancer (ISE and ESE respectively) or suppressor

<p>U1: Sm core U1-70K LUC7a/b (LUC7-rl) U1A U1C PRP39a/b</p> <p>PRP40a/b RBM25</p>	<p>U2: Sm core U2AF65a/b (AULP3p) U2AF35a/b URP SF1 PTB1/2/3</p> <p>U2A' U2B''a/b SF3a120_SAP114-1 (SAP114-2) (SAP114-3) (SAP114p) SF3a66_SAP62 SF3a60_SAP61 (<i>ato</i>) SF3b155_SAP155 SF3b145_SAP145 (SF3b150p) SF3b130_SAP130a/b SF3b49_SAP49a (emb2444)/b SF3b14a-1/2 SF3b_4b-1/2 SF3b10a/b tatSF1 (<i>elf9</i>)</p> <p>PRP5_1a/b (PRP5_2) SPF45 (<i>DRT111</i>) SPF30 SR140-1/2 SFb125 (<i>DDX24</i>)</p>	<p>U5: Sm core U5-220_PRP8a (sus2, emb14/33/177)/b U5-200-2_BRR2 (emb1507) (U5-200-1) (U5-200-2b) (U5-200-3) U5-116-1_SNU11a (mee5/clo1/gfa1)/b (U5-116-2) (U5-116-3) U5-102_PRP6 (<i>sta1/emb2770</i>) U5-100_PRP28 U5-40 U5-15 (YLS8) U5-52</p>
<p>Sm family: SmBa/Bb SmD1a/b SmD2a/b SmD3a/b SmEa/b SmFa/b SmGa/b</p>		<p>U4/U6: Sm/Lsm core PRP3a/b PRP4 (<i>lis, emb2776</i>) PRP31 (<i>emb1220</i>) Tri-20a/b(<i>CYP7/ROC2</i>) U4/U6-15.5_SNU13a/b/c</p>
<p>LSm family: LSm1a/b LSm2 LSm3a/b LSm4 (<i>emb1644</i>) LSm5 (<i>sad1</i>) LSm6/b LSm7 LSm8</p>		<p>U4/U6.U5 tri snRNP: Sm/LSm core Tri120_SNU66 (<i>mdf, dot2</i>) Tri65_a/b/c Tri-27_RY1 PRP38 SRL1 SNU23</p>

Figure 6. Spliceosomal U snRNP components conserved in *Arabidopsis*.

The different proteins are classified based on their association with snRNPs and to which protein family they belong. Spliceosome components encoded by two or more genes are highlighted in bold. Characterized gene mutations are indicated in red. Adapted from Koncz et al., 2012.

(ISS and ESS respectively) sequences (Witten and Ule, 2011; Staiger and Brown, 2013). Notably, SR proteins were shown to exert vital roles in both animals and plants, especially during development or response to stresses (Long and Caceres, 2009; Duque, 2011). These non-snRNP proteins share a multidomain structure characterized by the presence of one or two RNA Recognition Motifs (RRMs) at their N-terminus, and a reversibly phosphorylated arginine/serine-rich (RS) domain at their C-terminus (Graveley, 2000; Bourgeois et al., 2004). The RRM is essential for SR protein binding to pre-mRNAs through the recognition of splicing regulating sequences such as ESEs or ESSs. Moreover, the RRM provides RNA-binding specificity to the protein, where each ESE/ESS is thought to be recognized by unique sets of SR proteins (Graveley et al., 1999).

The RRM domain is one of the most abundant protein domains in eukaryotes (Marris et al., 2005). The small family of Nuclear Speckle RNA-binding (NSRs) proteins was also shown to harbor this RNA-binding motif and to exert a role during AS. NSR proteins were initially described as MtRBP1 (for *Medicago truncatula* RNA-Binding Protein 1) because of their ability to bind RNAs in this species (Campalans et al., 2004). Hereafter, the two closely MtRBP1-related proteins identified in *A. thaliana* were renamed as NSRa and NSRb due to their localization in nuclear speckles of the cell. These RBPs may participate in the AS of specific transcripts during nodule or lateral root formation. Interestingly, it was also shown that their function in AS can be modulated *in vivo* by interactions with various lncRNAs including *EARLY NODULIN40 (ENOD40)* and *ALTERNATIVE SPLICING COMPETITOR (ASCO)* (Campalans et al., 2004; Bardou et al., 2014). Recent studies analyzed the conservation of the NSR family across plant species. A phylogenetic analysis indicates that the NSR family appeared during land colonization by plants, suggested by their absence in algae and their presence in all land plants including bryophytes. This prevalence and the conservation of some motifs including the RRM suggest their involvement in splicing modulation and key adaptive processes throughout evolution (Lucero et al., 2020).

Indeed, the tight regulation of AS patterns is one of the major features that participated in the shaping of transcriptomes throughout evolution. In animals, the comparison of organ-specific transcriptomes from different vertebrate species spanning ~350 million years of evolution described dramatic differences in AS patterns and complexity among vertebrate lineages (Barbosa-Morais et al., 2012; Merkin et al., 2012). Curiously, AS evolves much faster than gene expression which leads to highly divergent AS patterns even in closely related species such as *Vigna radiata* and *Vigna angularis*, two species of mung beans that share only 2.8% of AS events (Satyawati et al., 2016).

Finally it appears that splicing determinants such as alternative splice site position as well as the size of exon-exon junctions were one of the major drivers of AS divergence (Ling

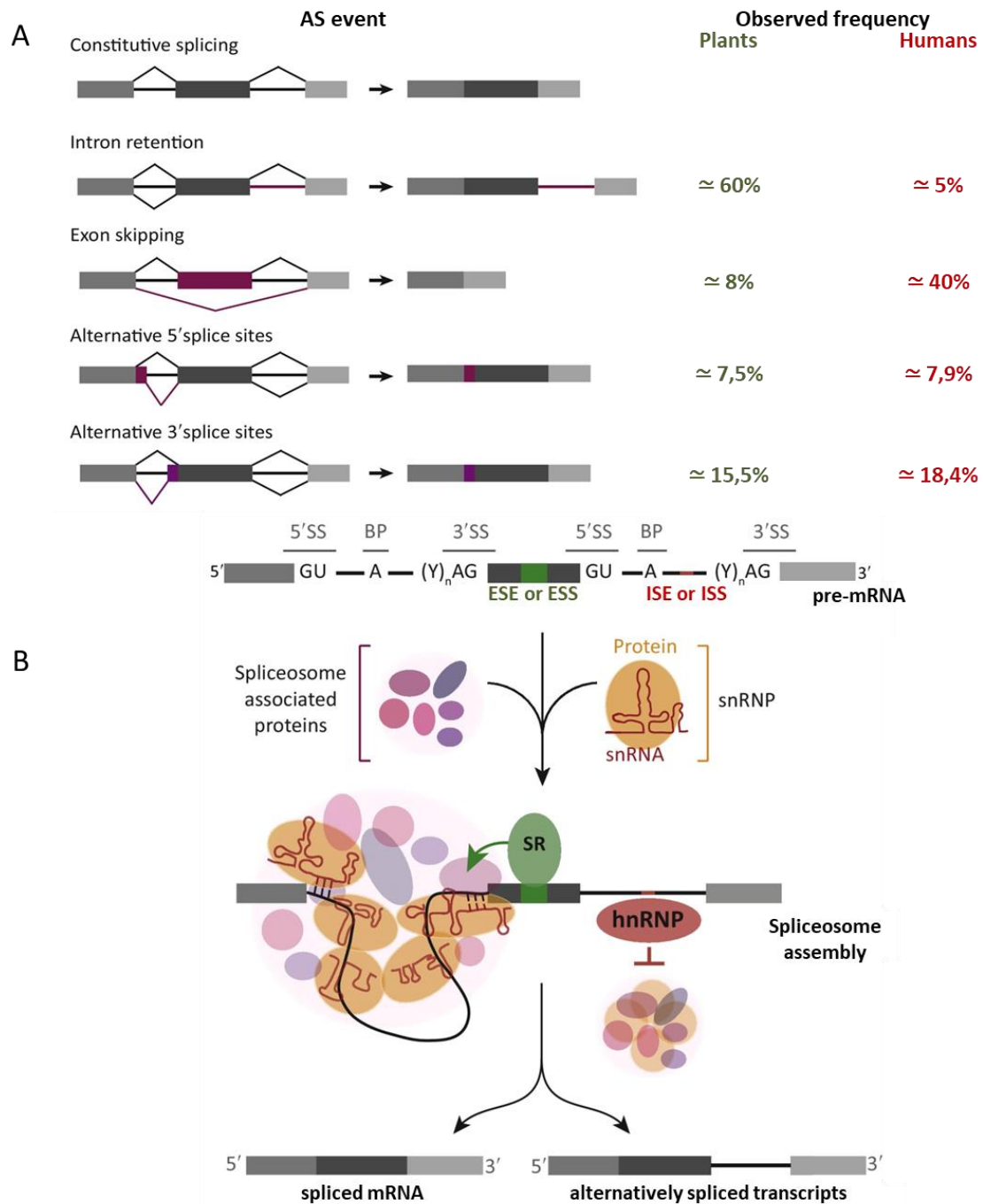


Figure 7. Alternative splicing events and their regulation by non-snRNP proteins in plants.

A. Schematic representation of different types of AS and their associated frequencies in both plants and humans.

B. Schematic representation of the splicing process and regulation of AS. Canonical sequences in the pre-mRNA define the splice sites (5' splice site, branch point, polypyrimidine tract, and 3' splice site), while additional cis-regulatory elements in exons (ESEs or ESSs) or introns (ISEs and ISSs) modulate the recognition of splice sites by the spliceosome. SR proteins and hnRNPs are non-snRNP proteins that recognize specific sets of cis-regulatory elements, therefore regulating the efficiency of splice-site recognition. Variations in the selection of splice sites result in the production of different mRNA molecules from the same pre-mRNA through AS. The example depicted here shows an hnRNP recognizing an intronic silencer sequence which leads to the retention of this intron. BP, branch point; 5' SS, 5' splice site; (Y)_n, polypyrimidine tract; 3' SS, 3' splice site; ESE or ESS: exonic splicing enhancer or suppressor; ISE or ISS: intronic splicing enhancer or suppressor.

Adapted from Laloum et al., 2018 and Chaudhary et al., 2019.

et al., 2019). Recently, it was shown that when compared to animals *A. thaliana* disproportionately uses AS for the establishment of stress responses. In contrast, animals tend to use AS for tissue-specific transcriptomic and proteomic diversification. Moreover, the regulations operated by AS in response to stresses seem not to overlap with targets of transcriptional regulation. Hence, the majority of genes regulated by AS and gene expression under various conditions do not overlap, underlying the complementarity and importance of these two layers of transcriptome regulation during stress responses (Martín et al., 2021). The next two subchapters will therefore shed light over the involvement of AS during responses to either biotic or abiotic stresses in plants.

1.2.2 Alternative splicing in the regulation of plant-microbe interactions

Plants are constantly challenged by the organisms thriving in their surroundings. The need to resist and survive external attacks exists since the dawn of life, and plants have evolved exquisite mechanisms to cope with these biotic stresses, including AS. This part will be presented under the form of a review in which I participated as first author. I mainly contributed by the generation of one figure and the writing of chapters concerning AS in the modulation of immunity receptor function and signaling, and AS in the context of hormonal pathways.

Publication: Alternative Splicing in the Regulation of Plant–Microbe Interactions

Alternative Splicing in the Regulation of Plant–Microbe Interactions

Richard Rigo, Jérémie Bazin, Martin Crespi* and Céline Charon

Institute of Plant Sciences Paris-Saclay IPS2, CNRS, INRA, Univ Paris Sud, Univ Evry, Univ Paris-Diderot, Université Paris-Saclay, 91405 Orsay Cedex, France

*Corresponding author: E-mail, martin.crespi@ips2.universite-paris-saclay.fr.

(Received January 15, 2019; Accepted April 22, 2019)

As sessile organisms, plants are continuously exposed to a wide range of biotic interactions. While some biotic interactions are beneficial or even essential for the plant (e.g. rhizobia and mycorrhiza), others such as pathogens are detrimental and require fast adaptation. Plants partially achieve this growth and developmental plasticity by modulating the repertoire of genes they express. In the past few years, high-throughput transcriptome sequencing have revealed that, in addition to transcriptional control of gene expression, post-transcriptional processes, notably alternative splicing (AS), emerged as a key mechanism for gene regulation during plant adaptation to the environment. AS not only can increase proteome diversity by generating multiple transcripts from a single gene but also can reduce gene expression by yielding isoforms degraded by mechanisms such as nonsense-mediated mRNA decay. In this review, we will summarize recent discoveries detailing the contribution of AS to the regulation of plant–microbe interactions, with an emphasis on the modulation of immunity receptor function and other components of the signaling pathways that deal with pathogen responses. We will also discuss emerging evidences that AS could contribute to dynamic reprogramming of the plant transcriptome during beneficial interactions, such as the legume–symbiotic interaction.

Keywords: Alternative splicing • Hormone signaling • Immunity • Symbiosis.

Introduction

As plants are sessile organisms, they are vulnerable to neighboring biotic interactants that potentially impact on fecundity, yield and lifespan. To counterbalance these potential fatal attacks, the plant immune system has evolved inducible and constitutive defense responses. Given the detrimental impact that pathogen and fungal infection has on crop productivity, and the failure of chemical fungicides to contain this issue as well as the need for a more sustainable agriculture, it is essential to understand how plants respond to pathogens. In addition, many microbes, notably those involved in symbiotic interactions, exert beneficial effects on plant growth and crop yield. Over the past several decades, researchers have focused on understanding the transcriptional regulators of biotic stress responses. However, post-transcriptional regulatory mechanisms, such as pre-mRNA

splicing, are also major contributors to cellular gene expression and stress responses. Recently it has been acknowledged that RNA processing and particularly pre-mRNA splicing is a key component of the plant immune response to a wide array of biotic interactions.

Here, we highlight recent works concerning the role of pre-mRNA splicing regulation in the modulation of plant defenses as well as beneficial interactions. First, we describe recent work concerning the role of the modulation of splicing factor (SF) activity by host immunity signaling pathway or directly by pathogen effector and its consequence on pre-mRNA splicing patterns. Second, we emphasize the role of alternative splicing (AS) events in modulating immune receptor function, and how hormone signaling pathways play a central role in the regulation of plant immune responses. Finally, we discuss the relevant effects of AS regulation in root symbiotic interactions.

Pre-mRNA AS in Plants

Most eukaryotic genes are interrupted by introns. Therefore, an essential step in gene expression is the removal of introns through the splicing of precursor mRNA transcripts (pre-mRNAs). Proper translation of mRNAs into functional proteins relies on accurate splicing of primary transcripts. Indeed, null mutants of the core splicing machinery are not usually viable as major misregulation of intron processing is incompatible with gene expression (Staiger and Brown 2013). Pre-mRNA splicing is carried out by the spliceosome, a large molecular complex consisting of five small nuclear ribonucleoproteins (snRNPs) and numerous spliceosome-associated proteins, which assemble at introns in a precise order (Plaschka et al. 2018, Fig. 1). During splicing, 5' and 3' splice sites, which define both ends of each intron in a pre-mRNA, together with the branch site (a consensus sequence located near the 3' splice site), are recognized by a diverse array of proteins associated with well-characterized noncoding RNAs (Uridine-rich small nuclear RNAs or snRNAs). Five distinct complexes containing snRNA (U1, U2, U4, U5 and U6) and their associated proteins (snRNP) are assembled sequentially to perform the spliceosomal splicing cycle in all eukaryotes (Plaschka et al. 2018). The recognition of splicing sites on pre-mRNAs can be sometimes modulated or perturbed, giving rise to a set of mRNA sequences from a single parental gene due to retained introns or alternatively chosen splice sites. This process, termed AS, is precisely regulated and therefore

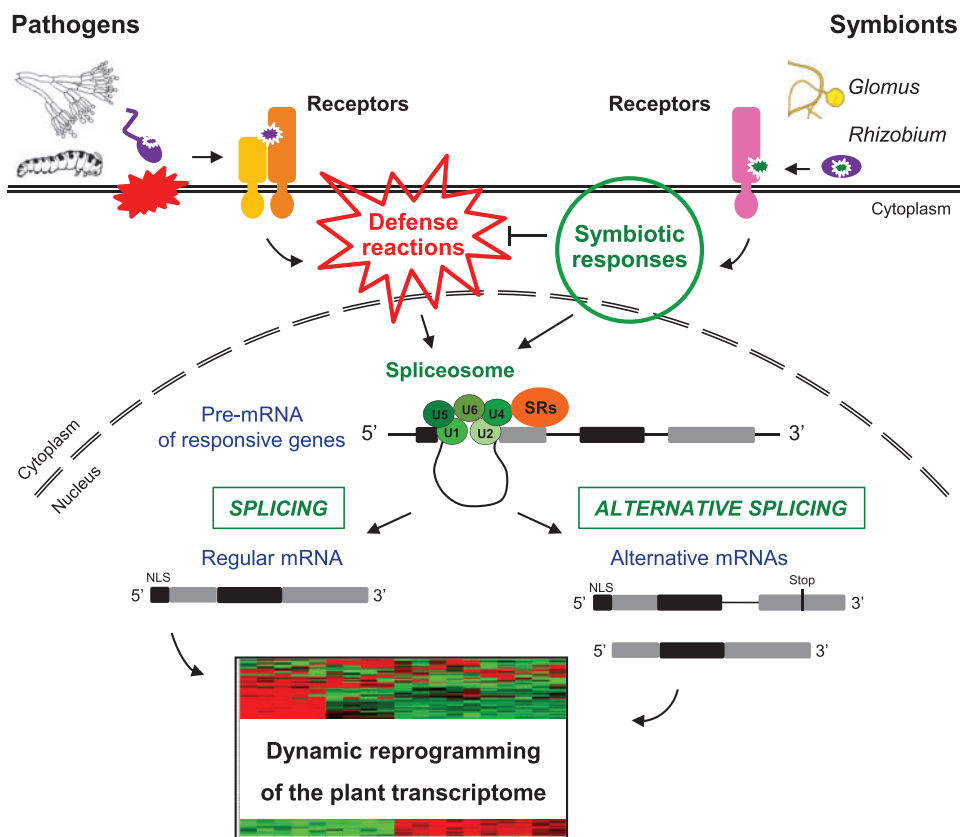


Fig. 1 Dynamic reprogramming of the plant transcriptome in response to biotic interactions. Pathogens such as bacteria, fungi or herbivores trigger plant receptors to initiate signaling cascades leading to defense reactions and expression changes of defense responsive genes. The splicing of their pre-mRNAs, i.e. the removal of introns, initiates during transcription and requires the spliceosome, a large complex consisting of a core of five small nuclear ribonucleoproteins (snRNPs), called U1, U2, U4, U5 and U6. Splicing regulators such as serine-arginine (SR) proteins can modulate the specificity of the spliceosome, and as a consequence, produce different mRNA isoforms. While most defense responsive genes have only their expression modified, others may have stable expression but modified AS, as exemplified here (intron retention generating an alternative stop codon or 5' exon skipping leading to the absence of the NLS domain), leading to truncated proteins. In the case of beneficial plant–microbe interactions (exemplified with the *Rhizobium* bacteria or the *Glomus* plant-AM fungi), analogous processes can occur. Thus both transcriptional and post-transcriptional changes participate to the dynamic reprogramming of the plant transcriptome.

boosts the coding capacity of a genome by increasing transcriptome diversity (Syed et al. 2012). The biological importance of AS is further highlighted by the large number of human diseases caused by mutations in *cis*-acting sequence elements in the pre-mRNA or in certain regulators of the splicing machinery (Scotti and Swanson 2016).

The outcome of AS depends on several factors: (i) splice site strength, (ii) *cis*-regulatory sequence in pre-mRNA that stimulates or represses exon recognition but also (iii) on the activity of *trans*-acting factors [such as RNA-binding proteins (RBPs) and SFs]. The expression levels of these *trans*-acting factors, their localization, their own splicing mRNA stability and translation efficiency have been shown to modulate AS (Baralle and Giudice 2017). Plant spliceosomes have not yet been isolated. However, *in vitro* studies with yeast and human spliceosomes have revealed the large diversity of spliceosome-associated proteins. For instance, the yeast spliceosome contains over 300 different proteins (Jurica and Moore 2003, Will and Lührmann 2011). Comparative genomics studies in *Arabidopsis* have led to the identification of twice the

number of splicing regulatory factors compared with humans (Wang and Brendel 2004, Koncz et al. 2012, Reddy et al. 2013), including large multigenic protein families such as the Serine-Rich (SR) proteins and heterogeneous nuclear ribonucleoproteins (hnRNPs). This suggests the existence of genome duplication and genomic rearrangement in the course of evolution on several spliceosomes, and raises the question of whether these diverse plant SFs have redundant roles or have acquired new functions during the course of evolution. Indeed, mutations in *trans*-acting factors of AS regulation cause various developmental and stress response phenotypes (Staiger and Brown 2013). In plants, AS-mediated regulation is a key regulator of gene expression. Indeed, 60–70 % of the intron-containing genes undergo AS. As an example, the small-sized genome of *Arabidopsis* was shown to encode 82,190 nonredundant transcripts from 34,212 genes (R. Zhang et al. 2017). AS is essential for proper plant growth and development and participates in the modulation of the response to a number of environmental stimuli, including light, temperature, nutrients or water availability (Reddy et al. 2013). In the context of a pathogen

infection, recent data have shown that SFs may represent key targets for host immunity but also for pathogen effectors to alter AS patterns in order to modulate the immune response or the host transcriptome.

SFs as Regulators of Plant Immunity

Recent progress in high-throughput sequencing of RNA and bioinformatics tools to analyze AS events at a genome-wide scale have shown that AS is an important component of host transcriptome reprogramming in response to bacterial and virus infection in several plant species (Howard et al. 2013, Mandadi and Scholthof 2015, Song et al. 2017, Zheng et al. 2017, Zhu et al. 2018). For example, a genome-wide analysis of transcription in *Arabidopsis thaliana* after treatment with *Pseudomonas syringae* pathovar tomato indicated that more than 44% of multiexon genes show evidence for AS. Moreover, certain ratios of alternative isoforms were significantly changed between treatments without significant changes in gene expression, suggesting a regulatory role for these isoforms in the pathogenic response (Howard et al. 2013). Little is known about the precise mechanism that controls AS regulation in response to these biotic factors. However, recent works have highlighted the important role of SF proteins in the plant immune response to a diverse range of biotic interactions (Fig. 1). Diverse pathogens produce elicitors such as the flagellin peptides (e.g. flg22) or lipopolysaccharides from bacteria, or chitin and heptaglucoisides from fungi. These molecules are referred to as pathogen-associated molecular patterns (PAMPs) and their perception by the cell leads to PAMP-triggered immunity (PTI) (Borrelli et al. 2018). MAPK and other signaling kinases are known to be regulated by these PAMPs. Proteomic analyses identified a considerable number of splicing-related proteins as major phosphorylation targets in plants (de la Fuente van Bentem et al. 2006), and several of these splicing proteins are phosphorylated by MAPKs in vitro (Feilner et al. 2005, de la Fuente van Bentem et al. 2008), suggesting a role for MAPKs in AS regulation. Furthermore, certain SFs are phosphorylated in response to PAMPs. These SFs carry phosphorylation motifs for CDPKs and MAPKs (Rayapuram et al. 2014) and, recently, it was shown that several phosphorylated SFs are direct targets of MAPKs. For example, MPK4 targets several phosphorylation sites in SCL30 (Rayapuram et al. 2018), a SR protein involved in AS control (Yan et al. 2017). Very recently, the *Arabidopsis* genome-wide analysis of AS in response to flg22 revealed a number of significant AS events leading to important protein modifications in critical PTI regulators such as CPK28, CRK29 and SERK4, demonstrating the importance of AS modulation in PTI. Subsequent analysis of *mpk3*, *mpk4* and *mpk6* mutants for defects in PAMP-triggered AS revealed that *mpk4* mutant plants were strongly compromised in more than 40% of these AS events, whereas no major changes in AS transcripts were observed in *mpk3* and *mpk6*, highlighting a potential role of MPK4 in AS regulation (Bazin et al. 2019). This common body of evidence is pointing toward an important role for PTI-signaling triggered protein

phosphorylation in the control of AS regulation during plant immune responses.

Evidence that AS regulation participates in plant immunity also came out from a genetic screen looking for suppressor of the *snc1 npr1* mutant phenotype, which constitutively activates defense responses and has enhanced resistance to pathogens. This screen identified *MOS14*, which encodes a transporter of SR proteins, as essential for proper splicing of *R* genes (Xu et al. 2011). Further evidence concerning the role of SR protein in AS-mediated regulation of immunity came from the demonstration that *sr45-1* mutants show major defects in AS patterning and were more resistant to the bacterial pathogen *P. syringae* PmaDG3 as well as to the oomycete pathogen *Hyaloperonospora parasitica* Noco2 (X.-N. Zhang et al. 2017).

Interestingly, several studies from independent research groups have recently shown that pathogen effectors can reprogram the host pre-mRNA splicing machinery to subvert immunity. Huang et al. (2017) demonstrated that PsAvr3c, an avirulence effector from the oomycete plant pathogen *Phytophthora sojae*, physically binds to the soybean serine/lysine/arginine-rich proteins, GmSKRPs, to prevent its proteasomal degradation. Furthermore, RNA-seq analysis of *GmSKRP1* and *PsAvr3c* overexpressing lines revealed a large number of AS events similarly modulated by the two factors, including several defense-related genes (Huang et al. 2017). Analysis of PsAvr3c effectors in other *Phytophthora* species showed that PsAvr3c family members display differences in promoting infection in an SKRP-dependent manner. Indeed ProbiAvh89, a PsAvr3c ortholog from *Phytophthora cinnamomi* var. *robiniae* but not PparvAvh214 (from *Phytophthora parvispora*) was shown to modulate AS in a similar mode to PsAvr3c (Huang et al. 2017, Zhang et al. 2018). A similar mechanism was later identified in a completely different pathosystem. Cyst nematodes use effector proteins to manipulate host cellular processes in order to establish the feeding site necessary for their parasitism. During infection with *Heterodera schachtii*, the effector protein 30D08 is delivered to plant cells and targeted to the plant nucleus where it interacts with SMU2, an auxiliary spliceosomal protein (Chung et al. 2009). Both 30D08 and SMU2 were shown to be necessary for parasitism establishment and ectopic expression of 30D08 under the SMU2 promoter led to splicing changes that affected the expression of several genes functionally linked to cellular processes known to be important for feeding site formation (Verma et al. 2018).

Another mechanism for quelling plant immunity was found during the infection of plants by *P. syringae*. The type III effector HopU1 codes for a mono-ADP-ribosyltransferase, which is injected into the plant cells by the pathogen, and was shown to target several host plant RBPs including the glycine-rich RBP, GRP7 (Fu et al. 2007, Jeong et al. 2011). GRP7 is known to respond to environmental cues and to affect the AS of certain transcripts via direct interaction with their mRNAs (Streitner et al. 2012). Further studies have shown that GRP7 overexpression leads to enhanced resistance against *P. syringae* pathovar tomato DC3000 and alters the expression of *PATHOGENESIS RELATED (PRR)* transcripts associated with salicylic acid (SA)- and jasmonic acid-dependent defenses (Hackmann et al. 2014).

In fact, HopU1 was found to modify two arginine residues within the RRM domain of GRP7, leading to a reduced ability of GRP7 to bind to its mRNA targets such as *FLS2* and *EFR*, two major components of PTI, and ultimately resulting in a reduction of *FLS2* accumulation upon infection (Nicaise et al. 2013). This virulence strategy, which targets an AS-regulating RBP rather than the pattern recognition receptor (PRR) proteins themselves, expands further the regulatory mechanisms involving AS in plant defense.

Taken together, AS regulation is a key component to reprogram the plant transcriptome during host responses to pathogen attacks. Furthermore, completely unrelated plant pathogens have evolved effectors to alter the host AS machinery, highlighting a multilevel AS regulation in plant immune responses.

AS as a Modulator of Immunity Receptor Function and Signaling

Animals and plants have both developed specific strategies to cope with pathogen infection. On the one hand, mammals possess specialized cells in the body that confer them with adaptive immunity whereas plants, on the other hand, have a large number of immune receptors in all cell types. Plant immune responses can be divided into two main types and both rely on the activation of receptors either inside the cell or at its surface (Borrelli et al. 2018). The first mechanism consists of the perception of elicitors or PAMPs, as mentioned before, which are generic signals for the presence of a pathogen and are recognized by PRRs, which include receptor-like kinases (RLKs) and receptor-like proteins (RLPs). A recent study pointed out the involvement of AS in the modulation of PRRs sensitivity in response to PAMPs. The tobacco *Nt-Sd-RLK* receptor was shown to have two possible isoforms whose expression ratio is regulated by the bacterial LPS. In the absence of PAMPs, tobacco cells produce the shorter isoform of *Nt-Sd-RLK*, which exhibits a truncated kinase domain and cannot undergo phosphorylation and activation, but is still able to bind LPS and perform a 'surveillance' function. When cells perceive the LPS and start to activate defense responses, the transcription of a longer *Nt-Sd-RLK* alternative isoform containing the kinase domain is triggered. The kinase domain is then phosphorylated to initiate signaling cascades and amplify defense responses (Sanabria and Dubery 2016). In a similar way, the RLKs *SNC4* and *CERK1* were shown to undergo AS in responses to PAMPs. Analysis of suppressor mutants of *snc4-1D* identified two SFs, *SUA* and *RSN2*, required for the proper splicing of *SNC4*, as well as of *CERK1* pre-mRNAs (Zhang et al. 2014), further underlying the importance of AS in the regulation of plant immunity.

The second defense mechanism acts through resistance (R) proteins, which are deployed to recognize corresponding pathogen effector proteins called Avirulence (Avr) proteins, leading to the so-called effector-triggered immunity (Yang et al. 2014). More than 100 R genes have been cloned from diverse species, and most of them exhibit a conserved structure

with nucleotide-binding domain (NB-ARC) and a leucine-rich repeat domain (LRR) (Yang and Wang 2016). The NB-ARC domain is highly conserved and essential for intramolecular interactions of R proteins (Rairdan and Moffett 2006). In contrast, the LRR motif confers pathogen recognition specificity for the plant (Padmanabhan et al. 2009). Many examples of AS of NBS-LRR genes were reported in diverse plant species such as *Arabidopsis*, tobacco, tomato, *Medicago truncatula* and rice (reviewed in Yang et al. 2014). In certain cases, exemplified by the tobacco *N* gene, this AS is modulated upon pathogen infection and leads to intron retention or of cryptic (nonannotated) exons, introducing premature stop-codons in these alternative transcripts. This AS event results in truncated proteins with no or fewer LRR repeats or modified C-termini, and leads to the abolition or modification of protein function (Yang et al. 2014). The expression of these alternative transcripts is often necessary to obtain at least partial resistance against the pathogen, but in certain cases it is not sufficient for full resistance. Indeed, in *M. truncatula*, both full and truncated isoforms of *RCT1* mRNA need to be expressed to confer effective resistance against *Colletotrichum trifolii*, a hemi-biotrophic fungus (Tang et al. 2013). Thus, AS represents an efficient mechanism to precisely tune the function of plant immunity receptors and allow modulating the setup of defense responses.

Besides PRRs and R genes, which are the most well-characterized targets of AS in immunity, other steps of defense signaling can be subjected to AS. WRKY transcription factors (TFs) consist of a large family of regulatory proteins involved in the response to diverse biotic and abiotic stresses. A number of WRKY genes in *Arabidopsis* and rice were predicted to have alternative open reading frames (Xie et al. 2005). A recent study provided evidence for AS of *OsWRKY62* and *OsWRKY76* pre-mRNAs, with the production of alternative shorter transcripts. The abundance of these isoforms was shown to increase upon pathogen infection as well as in *OsWRKY62/76* RNAi-lines. The resulting truncated proteins carry a partial or complete loss of the N-terminal CC domain and exhibit a reduced ability to bind the W-box motif, leading to reduced repressor activity in planta. Since these shorter isoforms can interact with each other and with full-length proteins, they are thought to exert a dominant-negative function on WRKY action, showing an example of AS-mediated feedback regulation for WRKY TFs (Liu et al. 2016).

AS of Hormonal Signaling Pathways during Biotic Stress

Phytohormones are compounds that are critical for helping the plant to adapt to adverse conditions. The intricate hormone signaling networks and their ability to crosstalk make them central nodes for mediating defense responses. The plant hormone jasmonate (JA) plays not only a significant role in the regulation of plant growth and development but also a major role in the response to biotic stresses (Campos et al. 2014). JA controls the expression of a large set of genes that coordinates various defense traits such as the production of chemical

defense compounds. The regulation of defense gene expression is permitted by the control of the abundance of jasmonate ZIM domain (JAZ) transcriptional repressors. Low JA levels lead to the accumulation of JAZ proteins in the nucleus, where they bind MYC TFs to actively repress JA-response genes. In the presence of JA, JAZ proteins are recruited to the F-box protein CORONATINE INSENSITIVE1 (COI1), which is the specificity determinant of the E3 ubiquitin ligase SCFCO11. JAZ proteins are then degraded in an ubiquitin-dependent manner, relieving their repressive action on JA-responsive genes (as reviewed in Campos et al. 2014 and Chini et al. 2016).

AS was shown to increase functional diversity of JAZ proteins and allow a feedback regulation of JA signaling (Chung and Howe 2009, Chung et al. 2010, Moreno et al. 2013). A key feature of JAZ proteins is the C-terminal Jas motif that mediates JA-dependent interaction with COI1 or MYC TFs. Most JAZ genes from evolutionarily diverse plants present a conserved intron that splits the Jas motif in two parts. In the *Arabidopsis* JAZ family, most JAZs exhibit AS events involving retention of this intron, generating proteins without the full Jas motif (Chung et al. 2010). However, some JAZs exhibit an N-terminal cryptic MYC-interaction domain (CMID) which allows MYC binding but does not recruit SCFCO11 (F. Zhang et al. 2017). For example, the AS of *JAZ10* pre-mRNA produces three splice variants that differ in their C-termini. The full-length isoform binds strongly to COI1 in the presence of JA, whereas truncated splice variants interact weakly or not at all with COI1. As a consequence, all three isoforms retain the ability to bind MYC TF and repress MYC target gene expression, but are partially or fully resistant to JA-induced degradation (Yan et al. 2007, Chung and Howe 2009, Chung et al. 2010). As those JAZs variants can accumulate in the presence of JA, they allow to re-repress MYC TFs leading to JA desensitization and a reestablishment of signal homeostasis (Fig. 2).

Another key hormone involved in the response to biotic stress is SA, which is essential for the establishment of both local and systemic-acquired resistance (SAR) in the plant (An and Mou 2011). The non-expressor of Pathogenesis-Related gene 1 (*NPR1*) plays critical roles in the SA signaling pathway and acts as a SA receptor (Loake and Grant 2007, Wu et al. 2012). At present, there is no evidence of AS events of this SA signaling component in *Arabidopsis*. However, in a recent study, eight *NPR1* homologs were identified in the apple genome and 12 different transcripts were cloned by RT-PCR, suggesting the existence of AS events (Zhang et al. 2016). The expression of the different homologs and associated isoforms was differentially regulated in two different cultivars, Pacific Rose and Qinguan, respectively, sensitive and resistant to the *Marssonina coronaria* fungus. The *MdNPR1* gene was found to be highly homologous to *AtNPR1*, which suggests it may function as a key regulator in SAR like *AtNPR1*. The AS of the *MdNPR1* pre-mRNA produces two isoforms, *MdNPR1a* and *b*, the latter lacking the NLS domain at its C-terminus. As both isoforms harbor the conserved cysteine residues, Cys82 and Cys216, thought to be critical for intermolecular disulfide bond formation between *AtNPR1* proteins (Mou et al. 2003), *MdNPR1a* and *b* may also be able to form homo- or hetero-

oligomers in the cytoplasm. Therefore, the relative abundance of the two isoforms could drive the shuttling of the complex within the cell, and fine-tune SA signaling. Since *MdNPR1a* could be only detected in the sensitive Pacific Rose cultivar, this could provide clues as to the role of AS in the sensitivity toward pathogens in apple trees (Zhang et al. 2016). However further studies will be needed to assess whether the AS of SA signaling components is widespread among other crops and plant species.

Brassinosteroids (BRs) are a class of steroid phytohormones that controls a wide range of developmental processes within the plant (Wei and Li 2016) and also act as negative regulators of plant innate immunity. BRs antagonize SA-mediated immunity (De Vleeschauwer et al. 2012) whereas the JA pathway suppresses BRs-mediated susceptibility of the plant (He et al. 2017). A recent study demonstrated that attack by a herbivore inhibits the BR pathway while it activates the SA and JA pathways. Conversely the BR pathway suppresses the SA pathway upon herbivorous infestation, and in a JA-dependent manner (Pan et al. 2018). Among BRs signaling components, the *BES1* and *BRZ1* TFs are major factors involved in the regulation of hundreds of BR-signaling genes (Yu et al. 2011). *BES1* is phosphorylated upon *flg22* perception, being a direct target of MPK6 during PTI. The phosphorylated form of *BES1* then exits the nucleus and is retained in the cytoplasm (Fig. 2). This *BES1* inactivation lowers BRs signaling and contributes to plant immunity toward *P. syringae* (Kang et al. 2015). Interestingly, another study indicated that the *BES1* pre-mRNA can undergo AS to produce two isoforms, *BES1-S*, the canonical isoform and *BES1-L*, which exhibits an extra NLS domain at its N terminus. Given the mechanism of homo-dimerization between *BES1* isoforms or hetero-dimerization of *BES1* with the TF *BRZ1*, the presence of a preferentially nuclear isoform provides a new layer of regulation in *BES1/BRZ1* shuttling and therefore in BR cell signaling (Fig. 2). *BES1-L* isoform was detected in the majority of *A. thaliana* ecotypes, but not in other species, including its *Brassicaceae* relatives, suggesting a recent appearance of this AS event in *Arabidopsis* (Jiang et al. 2015). Further studies will be needed to understand the involvement of *BES1-L* isoform in the response to biotic stresses, and also whether *BES1* splice variants occur in other species. As a modulator of the specific steps of JA, SA and BR signaling, AS intervenes at an intricate layer of regulation of this network to control plant immunity. Interestingly, steroid signaling in animals is also regulated by AS (Hirata et al. 2003). Indeed, sex steroid receptors in mammals are nuclear TFs that undergo extensive AS, most of the time alternative 5' UTRs or exons. These events tend to affect tissue distribution or expression levels of these receptors rather than its coding sequence. Also, in certain cases such as cancer cells, these AS events can result in constitutively active or dominant-negative receptors (Schreihofer et al. 2018).

Hence, AS stands out as a powerful and conserved tool to adapt and fine-tune hormonal signaling in both plants and animals, allowing the diversification of the signaling repertoire toward diseases or pathogens. By impacting protein localization, function, stability or ligand sensitivity, AS modulates

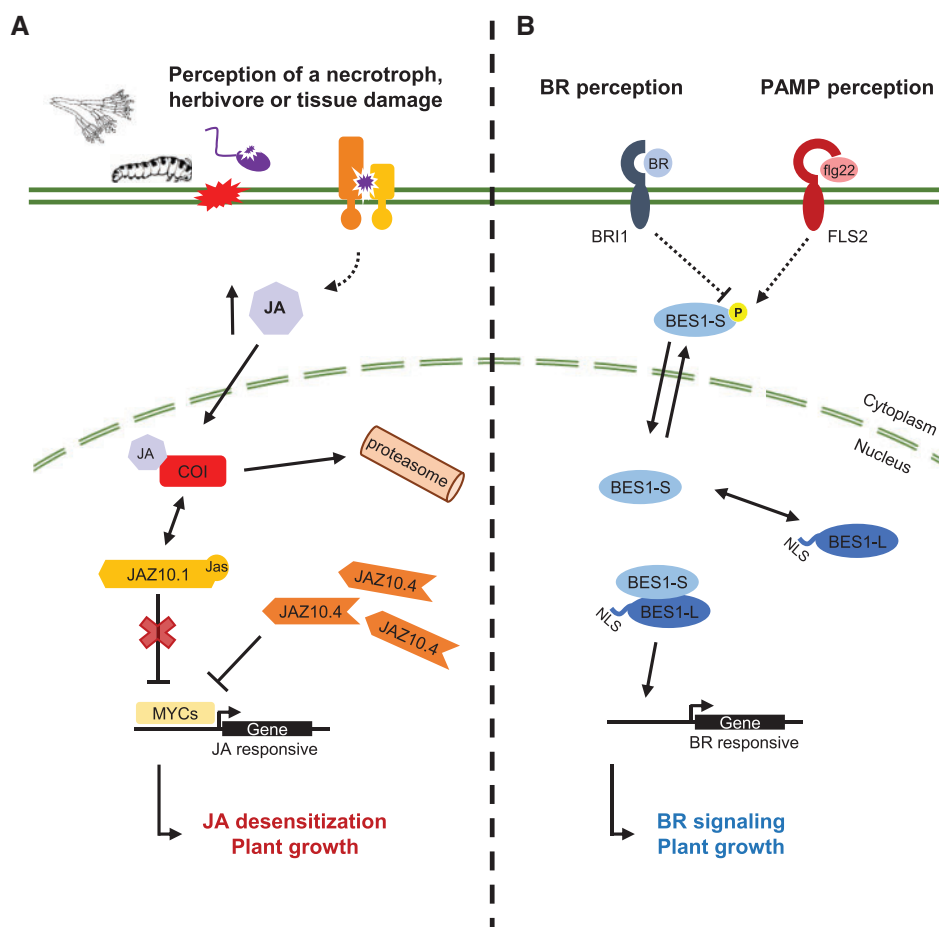


Fig. 2 AS is a powerful tool to adapt and fine-tune hormonal signaling in plants. (A) Upon perception of a necrotrophic pathogen or the attack of a herbivore, JA production is induced in the cell. Elevated JA levels lead to the recruitment of JAZ proteins such as JAZ10 to the F-box protein COI1, an interaction mediated by the presence of the Jas motif in JAZ10. The binding to COI1 leads to the ubiquitin-dependent degradation of JAZ10 via the proteasome. The degradation of JAZs repressors clears the path for MYCs TF to activate the expression of JA-responsive genes. The *JAZ10* gene can undergo AS to produce two splice variants, *JAZ10.1* and *JAZ10.4*, the latter lacking the Jas motif. The expression of *JAZ10.4* is induced upon longer exposure to JA, leading to the accumulation of JAZ10.4 proteins that cannot be targeted by COI1. This isoform still harbors a CMID, allowing the resulting protein to re-repress MYCs and JA responses and establishing a negative regulatory circuit on JAZ responses. (B) The perception of a PAMP such as flg22 by the FLS2 receptor leads to the phosphorylation of the BES1 TF. This can be counteracted by the binding of BR to the BRI1 receptor, leading to the dephosphorylation of BES1. The dephosphorylated form of BES1 is then retained in the cytoplasm and contributes to immunity against the bacterial pathogen. However, the *BES1* gene can also produce a longer isoform called *BES1-L*. The resulting BES1-L protein exhibits an additional NLS domain and is therefore constitutively nuclear, allowing retention of the canonical short BES1-S isoform in the nucleus by forming heterodimers. These different dimers and heterodimers can activate BR-signaling pathways, promoting plant growth and affecting pathogen responses.

sensing and transmission of the signal to allow the cell to set up the most adapted response.

AS of Hormonal Biosynthesis Actors

Besides hormone perception and its associated signaling, the regulation of hormone biosynthesis and degradation is another key aspect that needs to be regulated in response to stresses. As discussed above, JA is a major driver of the response to biotic stress, and its cellular levels are tightly regulated to modulate the growth/defense balance. One of the main players in this process is the *LOX* gene family involved in oxylipin synthesis, lipid-derived compounds including JA (Liavonchanka and Feussner 2006). A recent study in the tea

plant (*Camellia sinensis*), showed that out of 11 *CsLOX* genes identified, six of them underwent dynamic AS upon biotic stresses. *CsLOX1* and *CsLOX3* AS isoforms were predicted to be degraded by NMD, therefore regulating the abundance of corresponding full-length transcripts. On the other hand, *CsLOX2*, *CsLOX5*, *CsLOX9* and *CsLOX10* may encode for truncated proteins with altered activity. This led to propose a mechanism of competing or compensating regulation between isoforms in response to insect or fungi infection (Zhu et al. 2018). As these results highlight the role of AS in JA biosynthesis, searching for similar regulations in other species and/or in response to specific biotic stresses may help to understand the underlying diversity of LOX-mediated responses in biotic interactions.

Auxin is essential for embryonic and post-embryonic development, tropisms and many other processes. The mechanisms associated with its transport, perception and signal transduction have been mostly elucidated (as reviewed in Teale et al. 2006). Besides its key role in plant growth, auxin also has a major impact on microorganism–plant interactions. Indeed, auxin can be synthesized by various microorganisms, disturbing the auxin balance in the plant and interfering with its development. Therefore the downregulation of auxin signaling was shown to be a part of the defense response against bacteria (as reviewed in Spaepen and Vanderleyden 2011). The YUCCA family of flavin-dependent mono-oxygenases is one of the actors involved in auxin biosynthesis. A study revealed the involvement of AS in the control of YUCCA4 localization, both at the macroscopic and cellular level. One of the YUCCA4 splice variants was shown to be restricted to flowers and anchored to the endoplasmic reticulum via a hydrophobic C-terminal transmembrane domain whereas the other isoform is ubiquitous (Kriechbaumer et al. 2012).

Hormonal regulation by AS can be performed at different levels (biosynthesis and signaling) and may contribute to the diversification of biotic interactions responses in different plants (Fig. 2). Furthermore, this opens perspectives for the development of AS-related drugs or modulators of AS responses for the control of pathogens in the field, a major agricultural trait as actual chemical pesticides may not be able to cope with the major pressure on crop productivity.

AS in Symbiotic Interactions

In contrast to the negative effects generally provoked by pathogen and fungal interactions, there are many beneficial plant–microbe interactions that may be critical for plant growth in the field and they are emerging as a key component of a sustainable agriculture, as is well known for nitrogen-fixing symbiosis in legumes. Despite that extensive genome-wide analyses are still lacking, growing evidence suggests that AS could also contribute to the dynamics of the plant transcriptome during these interactions (Boscari et al. 2013, Handa et al. 2015; Fig. 1).

Endosymbioses such as the legume-rhizobia or the plant-arbuscular mycorrhizal (AM) fungi symbiosis involve complex cellular reprogramming, as microbes need to invade the host, requiring extensive exchange with plant cells without inducing pathogen responses. In the case of legume–rhizobia interactions, this symbiosis results in the development of a specialized organ on the root, called the nodule, in which bacteria provide fixed nitrogen to the host (Oldroyd et al. 2011). Nodule development depends on the establishment of a sophisticated molecular dialog between the bacteria and the plant. Firstly, flavonoids that are exuded by the plant roots induce the biosynthesis of specific lipo-chitooligosaccharides by the rhizobia, the Nod factors, which are recognized by SymRK RLPs. Once perceived by the root, Nod factors trigger the nodule developmental process by eliciting cell dedifferentiation and division in the cortex and pericycle to produce the nodule primordium. Concomitantly, the microsymbionts attach to and enter the root hair cells while

the plant forms a tube-like infection thread through which the bacteria move into the root cortex. They are then released by endocytosis into the cytoplasm of the nodule primordium cells to form bacteroids, in which atmospheric N₂ fixation finally takes place (Oldroyd et al. 2011). Despite the probable huge amount of genes undergoing AS during nodule organogenesis, as shown in *M. truncatula* (23,165 putative transcript isoforms from 6,587 genes; Boscari et al. 2013), only a few alternatively spliced transcripts has been analyzed in detail.

In *Lotus japonicus*, the SymRK-INTERACTING PROTEIN 1 (SIP1) TF was shown to interact with the Nod factor receptor kinase SymRK and binds to the *NIN* promoter (Zhu et al. 2008). The *SIP1* pre-mRNA can give rise to a long (*SIP1L*) and short (*SIP1S*) mRNA, both expressed in developing nodules (Wang et al. 2013). Downregulation of *SIP1* gene expression by an RNAi approach (affecting both *SIP1L* and *SIP1S* transcript levels) was shown to affect nodulation as well as AM development, pointing toward the important role of SIP1 in global symbiosis establishment. Whereas overexpression of either *SIP1L* or *SIP1S* independently increased the number of nodules formed on transgenic hairy root, indicating a positive role of each variant in nodulation, no such experiments were performed for AM symbiosis and so their precise role in this process is still lacking (Wang et al. 2013). Interestingly, only the short alternative *SIP1* transcript drives the direct interaction with SymRK but phylogenetic analysis suggests that this variant is only present in *L. japonicus*. Thus, evolution of a specific AS event allowing SIP1 to interact with SymRK may have occurred in *L. japonicus* to preserve its ability to undergo symbiosis (Wang et al. 2013). Another AS event was linked to the TF *MtHAP2-1*, a CCAAT-binding TF that plays a key role during nodule development, possibly by regulating nodule meristem function (Comber et al. 2006). Retention of an intron in the 5' leader sequence of *MtHAP2-1* was shown to increase during nodule development, exposing a new small ORF (uORF1) in the 5'UTR which is translated into a small polypeptide, uORF1p. In turn, the uORF1p peptide binds to *MtHAP2-1* mRNA, and reduces its accumulation. This novel peptide/mRNA regulatory mechanism may contribute to spatial restriction of *MtHAP2-1* expression within the nodule (Comber et al. 2008). Thus, by modulating TF isoforms, AS events may play key roles in symbiotic interactions and permit the control of the plant response to its bacterial symbiont.

During the symbiosis between *Rhizobia* and legumes, as well as in the symbiosis of plants and AM fungi, the microbes are hosted intracellularly inside specialized membrane compartments of the plant host. These membrane compartments, although morphologically different, create a symbiotic interface that controls efficient exchange of nutrients and signals. In *M. truncatula*, the *SYNTAXIN OF PLANTS 132* (*SYP132*) gene encodes a target-membrane soluble NSF-attachment protein receptor (t-SNARE) required for the maturation of symbiosomes into functional forms. The *SYP132* gene produces two transcripts, both expressed during symbiosis (Huisman et al. 2016, Pan et al. 2016), by alternative termination of transcription. Both transcripts code for full-length syntaxin proteins but differ in their SNARE domain as well as in the transmembrane domain

of their C-terminus. Subcellular localization studies have shown that the SYP132C isoform is mostly found on the plasma membrane, whereas the SYP132A isoform is located on the symbiosome membrane surrounding the bacteroids in the legume symbiosis (Pan et al. 2016), as well as on the peri-arbuscular membrane of the plant-AM fungi interface (Huisman et al. 2016). By interacting with the VAMP721d/e vesicle-SNARE proteins, SYP132A were able to label secretory vesicles specifically destined for the host-microbe interface (Pan et al. 2016).

Another gene also required for bacteroids viability and undergoing AS is *DOES NOT FIX NITROGEN 2 (DNF2)*. This gene encodes a phospholipase C-like protein required for symbiosome persistence, to prevent plant defense-like reactions and to avoid early nodule senescence (Bourcy et al. 2013). As previously mentioned, the modulation of defense response pathways must occur during symbiosis to permit the invasion of the plant host cell by the bacteria without triggering cell death. At least five mRNA splice variants exist for *DNF2* in *M. truncatula* with putative first intron retention and variations in the third exon length. All variants conserved the region coding for the phospholipase C domain. The most abundant transcript encodes an additional signal peptide in its 5' end, whereas the other *DNF2* mRNAs are predicted to generate proteins lacking this signal peptide, suggesting that they may be addressed to different compartments of the cell (Bourcy et al. 2013). Recent findings suggest that *DNF2* may modulate the ethylene signaling pathway to prevent plant defenses during intracellular accommodation of the rhizobia (Berrabah et al. 2018), although the exact role of each isoform is still undetermined. Hence, AS is critical for the regulation of the symbiotic dialog at the host-microbe interface inside cells.

As the legume-rhizobia symbiosis coopted many components related to plant pathogenesis (Deakin and Broughton 2009), not surprisingly several genes were also found to play a role in both pathogenic and symbiotic interactions. For example, the soybean TIR-NBS-LRR-type resistance gene *Rj2* was shown to restrict nodulation with specific rhizobial strains (Yang et al. 2010). Two splice variants were identified for *Rj2* with putative retention of its fourth intron (Tang et al. 2016). AS introduces a premature termination codon generating a truncated protein consisting of the entire TIR, NBS and LRR domains but missing the C-terminal domain of the full-length *Rj2* protein. The regular, but not the alternative, transcript alone appeared to be sufficient to restrict nodulation by specific *Bradyrhizobium japonicum* strains questioning the potential role of this splice variant (Tang et al. 2016).

In sum, although genome-wide analyses of AS in symbiotic interactions are generally lacking, there are several examples where AS events play critical roles at different levels of symbiotic interactions: from the initial signaling; the regulation of the host-symbiont interface; and the modulation of pathogenic responses by the symbionts.

Conclusions and Perspectives

Progress in the analysis of the transcriptome has shown that, in addition to gene expression changes, AS may also contribute to

changes in transcriptome reprogramming (Fig. 1). Indeed, several genes may show changes only in their transcript isoform ratios in response to biotic interactions without changing their global mRNA levels and hence a global view of AS is really needed to fully appreciate the significance of such induced changes in gene expression. Exon rearrangements due to changes in AS has emerged as a powerful mechanism to change key signaling components or biosynthesis regulators in signaling pathways triggered by pathogens or their effectors in plants (Fig. 2). This expansion of the signaling pathways may be critical in certain aspects of pathogen resistance and/or in beneficial biotic interactions and may need to be increasingly considered for a thorough description and understanding of regulatory networks involved in plant-microbe interactions. Furthermore, the enhanced proteome diversity generated by AS mechanisms may also be involved in the evolution of defense mechanisms and the adaptation of plants to different environments where pathogens may have diverged.

Another emerging theme is the cell specificity of AS events (Li et al. 2016, Foley et al. 2017) which also may lead to distinct cell type-specific responses to pathogens, as demonstrated for the response to environmental changes (Capovilla et al. 2015, Ling et al. 2018), reinforcing the idea that AS could be a relevant target for crop improvement in a changing climate. For example, in response to climate change, certain pathogen or beneficial interactions can be altered and may lead to new agricultural positive or negative performances in a specific geographical location. Armed with this knowledge, we could speculate that certain SNPs in genomic regions linked to stress resistance and other environmental agricultural traits are linked to AS events. In animals, there is a plethora of drugs that are known to affect splicing, as defects in splicing have been linked to several diseases, such as various types of cancer (Guigo and Valcarcel 2015). Given that the heart of the splicing machinery and its enzymatic requirements are highly conserved in eukaryotes, it is tempting to speculate that these compounds may offer interesting alternatives for the control of disease also in plants. This may open up wide prospects for developing alternative pesticides to the current ones used that are based on other mechanisms. Additional descriptions of pathogen interactions with genome-wide approaches coupled to advanced computational methods may yield new targets for pathogen control in field conditions and expand the chemical toolkit for managing plant-microbe interactions, both pathogenic and beneficial, in agriculture.

Finally, the AS landscape continues to expand offering an exceptional variation in signaling pathways including retro-feedback controls as many of the genes coding enzymes involved in splicing regulation are themselves alternatively spliced. This emerging dimension may strongly enhance the capacity to integrate multiple and diverse regulatory circuits in system biology networks to assess plant-microbe interactions.

Funding

This work was supported by grants from the 'Laboratoire d'Excellence (LABEX) Saclay Plant Sciences [SPS; ANR-10-

LABX-40], the ANR grant SPLISIL [ANR-16-CE12-0032] and the Ministère de l'Enseignement Supérieur et de la Recherche for a PhD fellowship to R.R., all three sources from France.

Disclosures

The authors have no conflicts of interest to declare.

References

- An, C. and Mou, Z. (2011) Salicylic acid and its function in plant immunity. *J. Integr. Plant Biol.* 53: 412–428.
- Baralle, F.E. and Giudice, J. (2017) Alternative splicing as a regulator of development and tissue identity. *Nat. Rev. Mol. Cell Biol.* 18: 437–451.
- Bazin, J., Mariappan, K.G., Blein, T., Volz, R., Crespi, M. and Hirt, H. (2019) Role of MPK4 in pathogen-associated molecular pattern-triggered alternative splicing in Arabidopsis. *bioRxiv* 511980. doi: <https://doi.org/10.1101/511980>.
- Berrabah, F., Balliau, T., Ait-Salem, E.H., George, J., Zivy, M., Ratet, P., et al. (2018) Control of the ethylene signaling pathway prevents plant defenses during intracellular accommodation of the rhizobia. *New Phytol.* 219: 310–323.
- Borrelli, G.M., Mazzucotelli, E., Marone, D., Crosatti, C., Michelotti, V., Vale, G., et al. (2018) Regulation and evolution of NLR genes: a close interconnection for plant immunity. *Int. J. Mol. Sci.* 19: 1662.
- Boscardi, A., Del Giudice, J., Ferrarini, A., Venturini, L., Zaffini, A.-L., Delledonne, M., et al. (2013) Expression dynamics of the *Medicago truncatula* transcriptome during the symbiotic interaction with *Sinorhizobium meliloti*: which role for nitric oxide? *Plant Physiol.* 161: 425–439.
- Bourcy, M., Brocard, L., Pislariu, C.I., Cosson, V., Mergaert, P., Tadege, M., et al. (2013) *Medicago truncatula* DNF2 is a PI-PLC-XD-containing protein required for bacteroid persistence and prevention of nodule early senescence and defense-like reactions. *New Phytol.* 197: 1250–1261.
- Campos, M.L., Kang, J.-H. and Howe, G.A. (2014) Jasmonate-triggered plant immunity. *J. Chem. Ecol.* 40: 657–675.
- Capovilla, G., Pajoro, A., Immink, R.G.H. and Schmid, M. (2015) Role of alternative pre-mRNA splicing in temperature signaling. *Curr. Opin. Plant Biol.* 27: 97–103.
- Chini, A., Gimenez-Ibanez, S., Goossens, A. and Solano, R. (2016) Redundancy and specificity in jasmonate signalling. *Curr. Opin. Plant Biol.* 33: 147–156.
- Chung, H.S., Cooke, T.F., Depew, C.L., Patel, L.C., Ogawa, N., Kobayashi, Y., et al. (2010) Alternative splicing expands the repertoire of dominant JAZ repressors of jasmonate signaling. *Plant J.* 63: 613–622.
- Chung, H.S. and Howe, G.A. (2009) A critical role for the TIFY motif in repression of jasmonate signaling by a stabilized splice variant of the JASMONATE ZIM-domain protein JAZ10 in Arabidopsis. *Plant Cell* 21: 131–145.
- Chung, T., Wang, D., Kim, C.-S., Yadegari, R. and Larkins, B.A. (2009) Plant SMU-1 and SMU-2 homologues regulate pre-mRNA splicing and multiple aspects of development. *Plant Physiol.* 151: 1498–1512.
- Combier, J.P., de Billy, F., Gamas, P., Niebel, A. and Rivas, S. (2008) Trans-regulation of the expression of the transcription factor MtHAP2-1 by a uORF controls root nodule development. *Genes Dev.* 22: 1549–1559.
- Combier, J.-P., Frugier, F., de Billy, F., Boualem, A., El-Yahyaoui, F., Moreau, S., et al. (2006) MtHAP2-1 is a key transcriptional regulator of symbiotic nodule development regulated by microRNA169 in *Medicago truncatula*. *Genes Dev.* 20: 3084–3088.
- de la Fuente van Bentem, S., Anrather, D., Dohnal, I., Roitinger, E., Csaszar, E., Joore, J., et al. (2008) Site-specific phosphorylation profiling of Arabidopsis proteins by mass spectrometry and peptide chip analysis. *J. Proteome Res.* 7: 2458–2470.
- de la Fuente van Bentem, S., Anrather, D., Roitinger, E., Djamei, A., Hufnagl, T., Barta, A., et al. (2006) Phosphoproteomics reveals extensive in vivo phosphorylation of Arabidopsis proteins involved in RNA metabolism. *Nucleic Acids Res.* 34: 3267–3278.
- De Vleeschauwer, D., Van Buyten, E., Satoh, K., Balidion, J., Mauleon, R., Choi, I.-R., et al. (2012) Brassinosteroids antagonize gibberellin- and salicylate-mediated root immunity in rice. *Plant Physiol.* 158: 1833–1846.
- Deakin, W.J. and Broughton, W.J. (2009) Symbiotic use of pathogenic strategies: rhizobial protein secretion systems. *Nat. Rev. Microbiol.* 7: 321–320.
- Feilner, T., Hultschig, C., Lee, J., Meyer, S., Immink, R.G.H., Koenig, A., et al. (2005) High throughput identification of potential Arabidopsis mitogen-activated protein kinases substrates. *Mol. Cell. Proteomics* 4: 1558–1568.
- Foley, S.W., Gosai, S.J., Wang, D., Selamoglu, N., Sollitti, A.C., Koster, T., et al. (2017) A global view of RNA-protein interactions identifies post-transcriptional regulators of root hair cell fate. *Dev. Cell* 41: 204–220.e5.
- Fu, Z.Q., Guo, M., Jeong, B., Tian, F., Elthon, T.E., Cerny, R.L., et al. (2007) A type III effector ADP-ribosylates RNA-binding proteins and quells plant immunity. *Nature* 447: 284–288.
- Guigo, R. and Valcarcel, J. (2015) RNA. Prescribing splicing. *Science* 347: 124–125.
- Hackmann, C., Korneli, C., Kutyniok, M., Koster, T., Wiedenlubbet, M., Muller, C., et al. (2014) Salicylic acid-dependent and -independent impact of an RNA-binding protein on plant immunity. *Plant. Cell Environ.* 37: 696–706.
- Handa, Y., Nishide, H., Takeda, N., Suzuki, Y., Kawaguchi, M. and Saito, K. (2015) RNA-seq transcriptional profiling of an arbuscular mycorrhiza provides insights into regulated and coordinated gene expression in *Lotus japonicus* and *Rhizophagus irregularis*. *Plant Cell Physiol.* 56: 1490–1511.
- He, Y., Zhang, H., Sun, Z., Li, J., Hong, G., Zhu, Q., et al. (2017) Jasmonic acid-mediated defense suppresses brassinosteroid-mediated susceptibility to rice black streaked dwarf virus infection in rice. *New Phytol.* 214: 388–399.
- Hirata, S., Shoda, T., Kato, J. and Hoshi, K. (2003) Isoform/variant mRNAs for sex steroid hormone receptors in humans. *Trends Endocrinol. Metab.* 14: 124–129.
- Howard, B.E., Hu, Q., Babaoglu, A.C., Chandra, M., Borghi, M., Tan, X., et al. (2013) High-throughput RNA sequencing of pseudomonas-infected Arabidopsis reveals hidden transcriptome complexity and novel splice variants. *PLoS One* 8: e74183.
- Huang, J., Gu, L., Zhang, Y., Yan, T., Kong, G., Kong, L., et al. (2017) An oomycete plant pathogen reprograms host pre-mRNA splicing to subvert immunity. *Nat. Commun.* 8: 2051.
- Huisman, R., Hontelez, J., Mysore, K.S., Wen, J., Bisseling, T. and Limpens, E. (2016) A symbiosis-dedicated SYNTAXIN OF PLANTS 13II isoform controls the formation of a stable host-microbe interface in symbiosis. *New Phytol.* 211: 1338–1351.
- Jeong, B., Lin, Y., Joe, A., Guo, M., Korneli, C., Yang, H., et al. (2011) Structure function analysis of an ADP-ribosyltransferase type III effector and its RNA-binding target in plant immunity. *J. Biol. Chem.* 286: 43272–43281.
- Jiang, J., Zhang, C. and Wang, X. (2015) A recently evolved isoform of the transcription factor BES1 promotes brassinosteroid signaling and development in *Arabidopsis thaliana*. *Plant Cell* 27: 361–374.
- Jurica, M.S. and Moore, M.J. (2003) Pre-mRNA splicing: awash in a sea of proteins. *Mol. Cell* 12: 5–14.
- Kang, S., Yang, F., Li, L., Chen, H., Chen, S. and Zhang, J. (2015) The Arabidopsis transcription factor BRASSINOSTEROID INSENSITIVE1-ETHYL METHANESULFONATE-SUPPRESSOR1 is a direct substrate of MITOGEN-ACTIVATED PROTEIN KINASE6 and regulates immunity. *Plant Physiol.* 167: 1076–1086.

- Koncz, C., Dejong, F., Villacorta, N., Szakonyi, D. and Koncz, Z. (2012) The spliceosome-activating complex: molecular mechanisms underlying the function of a pleiotropic regulator. *Front. Plant Sci.* 3: 9.
- Kriechbaumer, V., Wang, P., Hawes, C. and Abell, B.M. (2012) Alternative splicing of the auxin biosynthesis gene YUCCA4 determines its subcellular compartmentation. *Plant J.* 70: 292–302.
- Li, S., Yamada, M., Han, X., Ohler, U. and Benfey, P.N. (2016) High-resolution expression map of the Arabidopsis root reveals alternative splicing and lincRNA regulation. *Dev. Cell* 39: 508–522.
- Liavonchanka, A. and Feussner, I. (2006) Lipoxygenases: occurrence, functions and catalysis. *J. Plant Physiol.* 163: 348–357.
- Ling, Y., Serrano, N., Gao, G., Atia, M., Mokhtar, M., Woo, Y.H., et al. (2018) Thermoprimer triggers splicing memory in Arabidopsis. *J. Exp. Bot.* 69: 2659–2675.
- Liu, J., Chen, X., Liang, X., Zhou, X., Yang, F., Liu, J., et al. (2016) Alternative splicing of rice WRKY62 and WRKY76 transcription factor genes in pathogen defense. *Plant Physiol.* 171: 1427–1442.
- Loake, G. and Grant, M. (2007) Salicylic acid in plant defence—the players and protagonists. *Curr. Opin. Plant Biol.* 10: 466–472.
- Mandadi, K.K. and Scholthof, K.-B.G. (2015) Genome-wide analysis of alternative splicing landscapes modulated during plant-virus interactions in *Brachypodium distachyon*. *Plant Cell* 27: 71–85.
- Moreno, J.E., Shyu, C., Campos, M.L., Patel, L.C., Chung, H.S., Yao, J., et al. (2013) Negative feedback control of jasmonate signaling by an alternative splice variant of JAZ10. *Plant Physiol.* 162: 1006–1017.
- Mou, Z., Fan, W. and Dong, X. (2003) Inducers of plant systemic acquired resistance regulate NPR1 function through redox changes. *Cell* 113: 935–944.
- Nicaise, V., Joe, A., Jeong, B., Korneli, C., Boutrot, F., Westedt, I., et al. (2013) *Pseudomonas* HopU1 modulates plant immune receptor levels by blocking the interaction of their mRNAs with GRP7. *EMBO J.* 32: 701–712.
- Oldroyd, G.E.D., Murray, J.D., Poole, P.S. and Downie, J.A. (2011) The rules of engagement in the legume-rhizobial symbiosis. *Annu. Rev. Genet.* 45: 119–144.
- Padmanabhan, M., Cournoyer, P. and Dinesh-Kumar, S.P. (2009) The leucine-rich repeat domain in plant innate immunity: a wealth of possibilities. *Cell. Microbiol.* 11: 191–198.
- Pan, G., Liu, Y., Ji, L., Zhang, X., He, J., Huang, J., et al. (2018) Brassinosteroids mediate susceptibility to brown planthopper by integrating with the salicylic acid and jasmonic acid pathways in rice. *J. Exp. Bot.* 69: 4433–4442.
- Pan, H., Oztas, O., Zhang, X., Wu, X., Stonoha, C., Wang, E., et al. (2016) A symbiotic SNARE protein generated by alternative termination of transcription. *Nat. Plants* 2: 15197.
- Plaschka, C., Lin, P.-C., Charenton, C. and Nagai, K. (2018) Prespliceosome structure provides insights into spliceosome assembly and regulation. *Nature* 559: 419–422.
- Rairdan, G.J. and Moffett, P. (2006) Distinct domains in the ARC region of the potato resistance protein Rx mediate LRR binding and inhibition of activation. *Plant Cell* 18: 2082–2093.
- Rayapuram, N., Bigeard, J., Alhoraibi, H., Bonhomme, L., Hesse, A.-M., Vinh, J., et al. (2018) Quantitative phosphoproteomic analysis reveals shared and specific targets of Arabidopsis mitogen-activated protein kinases (MAPKs) MPK3, MPK4, and MPK6. *Mol. Cell. Proteomics* 17: 61–80.
- Rayapuram, N., Bonhomme, L., Bigeard, J., Haddadou, K., Przybylski, C., Hirt, H., et al. (2014) Identification of novel PAMP-triggered phosphorylation and dephosphorylation events in *Arabidopsis thaliana* by quantitative phosphoproteomic analysis. *J. Proteome Res.* 13: 2137–2151.
- Reddy, A.S.N., Marquez, Y., Kalyana, M. and Barta, A. (2013) Complexity of the alternative splicing landscape in plants. *Plant Cell* 25: 3657–3683.
- Sanabria, N.M. and Dubery, I.A. (2016) Alternative splicing of the receptor-like kinase Nt-Sd-RLK in tobacco cells responding to lipopolysaccharides: suggestive of a role in pathogen surveillance and perception? *FEBS Lett.* 590: 3628–3638.
- Schreihofer, D.A., Duong, P. and Cunningham, R.L. (2018) N-terminal truncations in sex steroid receptors and rapid steroid actions. *Steroids* 133: 15–20.
- Scotti, M.M. and Swanson, M.S. (2016) RNA mis-splicing in disease. *Nat. Rev. Genet.* 17: 19–32.
- Song, J., Liu, H., Zhuang, H., Zhao, C., Xu, Y., Wu, S., et al. (2017) Transcriptomics and alternative splicing analyses reveal large differences between maize lines B73 and Mo17 in response to aphid *Rhopalosiphum padi* infestation. *Front. Plant Sci.* 8: 1738.
- Spaepen, S. and Vanderleyden, J. (2011) Auxin and plant-microbe interactions. *Cold Spring Harb. Perspect. Biol.* 3: a001438.
- Staiger, D. and Brown, J.W.S. (2013) Alternative splicing at the intersection of biological timing, development, and stress responses. *Plant Cell* 25: 3640–3656.
- Streitner, C., Koster, T., Simpson, C.G., Shaw, P., Danisman, S., Brown, J.W.S., et al. (2012) An hnRNP-like RNA-binding protein affects alternative splicing by in vivo interaction with transcripts in *Arabidopsis thaliana*. *Nucleic Acids Res.* 40: 11240–11255.
- Syed, N.H., Kalyana, M., Marquez, Y., Barta, A. and Brown, J.W.S. (2012) Alternative splicing in plants—coming of age. *Trends Plant Sci.* 17: 616–623.
- Tang, F., Yang, S., Gao, M. and Zhu, H. (2013) Alternative splicing is required for RCT1-mediated disease resistance in *Medicago truncatula*. *Plant Mol. Biol.* 82: 367–374.
- Tang, F., Yang, S. and Zhu, H. (2016) Functional analysis of alternative transcripts of the soybean Rj2 gene that restricts nodulation with specific rhizobial strains. *Plant Biol. J.* 18: 537–541.
- Teale, W.D., Paponov, I.A. and Palme, K. (2006) Auxin in action: signalling, transport and the control of plant growth and development. *Nat. Rev. Mol. Cell Biol.* 7: 847–859.
- Verma, A., Lee, C., Morriss, S., Odu, F., Kenning, C., Rizzo, N., et al. (2018) The novel cyst nematode effector protein 3D08 targets host nuclear functions to alter gene expression in feeding sites. *New Phytol.* 219: 697–713.
- Wang, B.-B. and Brendel, V. (2004) The ASRG database: identification and survey of *Arabidopsis thaliana* genes involved in pre-mRNA splicing. *Genome Biol.* 5: R102.
- Wang, C., Zhu, H., Jin, L., Chen, T., Wang, L., Kang, H., et al. (2013) Splice variants of the SIP1 transcripts play a role in nodule organogenesis in *Lotus japonicus*. *Plant Mol. Biol.* 82: 97–111.
- Wei, Z. and Li, J. (2016) Brassinosteroids regulate root growth, development, and symbiosis. *Mol. Plant* 9: 86–100.
- Will, C.L. and Lührmann, R. (2011) Spliceosome structure and function. *Cold Spring Harb. Perspect. Biol.* 3: a003707.
- Wu, Y., Zhang, D., Chu, J.Y., Boyle, P., Wang, Y., Brindle, I.D., et al. (2012) The Arabidopsis NPR1 protein is a receptor for the plant defense hormone salicylic acid. *Cell Rep.* 1: 639–647.
- Xie, Z., Zhang, Z.-L., Zou, X., Huang, J., Ruas, P., Thompson, D., et al. (2005) Annotations and functional analyses of the rice WRKY gene superfamily reveal positive and negative regulators of abscisic acid signaling in aleurone cells. *Plant Physiol.* 137: 176–189.
- Xu, S., Zhang, Z., Jing, B., Gannon, P., Ding, J., Xu, F., et al. (2011) Transportin-SR is required for proper splicing of resistance genes and plant immunity. *PLoS Genet.* 7: e1002159.
- Yan, Q., Xia, X., Sun, Z. and Fang, Y. (2017) Depletion of Arabidopsis SC35 and SC35-like serine/arginine-rich proteins affects the transcription and splicing of a subset of genes. *PLoS Genet.* 13: e1006663.
- Yan, Y., Stolz, S., Chetelat, A., Reymond, P., Pagni, M., Dubugnon, L., et al. (2007) A downstream mediator in the growth repression limb of the jasmonate pathway. *Plant Cell.* 19: 2470–2483.
- Yang, S., Tang, F., Gao, M., Krishnan, H.B. and Zhu, H. (2010) R gene-controlled host specificity in the legume-rhizobia symbiosis. *Proc. Natl. Acad. Sci. USA* 107: 18735–18740.
- Yang, S., Tang, F. and Zhu, H. (2014) Alternative splicing in plant immunity. *Int. J. Mol. Sci.* 15: 10424–10445.
- Yang, X. and Wang, J. (2016) Genome-wide analysis of NBS-LRR genes in sorghum genome revealed several events contributing to

- NBS-LRR gene evolution in grass species. *Evol. Bioinform. Online* 12: 9–21.
- Yu, X., Li, L., Zola, J., Aluru, M., Ye, H., Foudree, A., et al. (2011) A brassinosteroid transcriptional network revealed by genome-wide identification of BES1 target genes in *Arabidopsis thaliana*. *Plant J.* 65: 634–646.
- Zhang, F., Ke, J., Zhang, L., Chen, R., Sugimoto, K., Howe, G.A., et al. (2017) Structural insights into alternative splicing-mediated desensitization of jasmonate signaling. *Proc. Natl. Acad. Sci. USA* 114: 1720–1725.
- Zhang, J., Jiao, P., Zhang, C., Tong, X., Wei, Q. and Xu, L. (2016) Apple NPR1 homologs and their alternative splicing forms may contribute to SA and disease responses. *Tree Genet. Genomes* 12: 92.
- Zhang, R., Calixto, C.P.G., Marquez, Y., Venhuizen, P., Tzioutziou, N.A., Guo, W., et al. (2017) A high quality *Arabidopsis* transcriptome for accurate transcript-level analysis of alternative splicing. *Nucleic Acids Res.* 45: 5061–5073.
- Zhang, X.-N., Shi, Y., Powers, J.J., Gowda, N.B., Zhang, C., Ibrahim, H.M.M., et al. (2017) Transcriptome analyses reveal SR45 to be a neutral splicing regulator and a suppressor of innate immunity in *Arabidopsis thaliana*. *BMC Genomics* 18: 772.
- Zhang, Y., Huang, J., Ochola, S.O. and Dong, S. (2018) Functional analysis of PsAvr3c effector family from phytophthora provides probes to dissect SKRP mediated plant susceptibility. *Front. Plant Sci.* 9: 1105.
- Zhang, Z., Liu, Y., Ding, P., Li, Y., Kong, Q. and Zhang, Y. (2014) Splicing of receptor-like kinase-encoding SNC4 and CERK1 is regulated by two conserved splicing factors that are required for plant immunity. *Mol. Plant* 7: 1766–1775.
- Zheng, Y., Wang, Y., Ding, B. and Fei, Z. (2017) Comprehensive transcriptome analyses reveal that potato spindle tuber viroid triggers genome-wide changes in alternative splicing, inducible trans-acting activity of phased secondary small interfering RNAs, and immune responses. *J. Virol.* 91: e00247–17. doi: 10.1128/JVI.00247-17.
- Zhu, C., Li, X. and Zheng, J. (2018) Transcriptome profiling using Illumina- and SMRT-based RNA-seq of hot pepper for in-depth understanding of genes involved in CMV infection. *Gene* 666: 123–133.
- Zhu, H., Chen, T., Zhu, M., Fang, Q., Kang, H., Hong, Z., et al. (2008) A novel ARID DNA-binding protein interacts with SymRK and is expressed during early nodule development in *Lotus japonicus*. *Plant Physiol.* 148: 337–347.

1.2.3 Alternative splicing regulation during abiotic stresses

Besides the need to deter pathogens and other organisms from altering their integrity, plants are confronted with physical and chemical characteristics of their close environment: the so-called abiotic factors. They include cold, heat, drought or salinity and many studies highlighted the importance of AS during the plant acclimation to these stresses (Staiger and Brown, 2013; Laloum et al., 2018; Punzo et al., 2020). ABA is a major phytohormone that plays crucial roles in a varied range of abiotic stresses and participates in many developmental processes such as seed dormancy, seed germination and control of stomatal closure (Jones, 2016; Vishwakarma et al., 2017). Remarkably, the use of a splicing inhibitor on plants, the pladienolide B (PB), dramatically affects ABA responses and mimics the perception of an abiotic stress (Ling et al., 2017). PB treatment perturbs AS by promoting intron retention and reducing other forms of AS, causing the accumulation of aberrantly processed mRNAs. This effect seems to be restrained to stress-related and ABA-related genes. Indeed, the use of PB induces the expression of well-known ABA markers such as *RD29A*, provoking stomatal closure and leading to a typical ABA-like response. Finally, PB also alters the function and localization of some SFs such as SR45, a negative regulator of ABA signaling (Carvalho et al., 2010). Thus, a clear link exists between splicing modulation and responses to abiotic stress mediated by ABA (Punzo et al., 2020; Zhan et al., 2015).

The phytohormone ABA notably participates in the response to heat stress, one of the most important abiotic threats affecting agricultural productivity worldwide, notably in the context of climate change. The ABA signaling pathway affects a plethora of processes in the cell including sugar metabolism, antioxidant and heat shock protein (HSP) levels (Islam et al., 2018). Plants subjected to sub-lethal heat stress develop thermotolerance, a relatively well-conserved mechanism among different organisms (Mittler et al., 2012). This process of sublethal heat stress treatment to improve thermotolerance to a lethal heat stress is known as priming. This heat-stress memory state or priming will remain active for several days. The acquisition of thermotolerance was shown to be mainly dependent on the activation of HSPs such as Hsa32 or HsfA2 (Charng et al., 2006; Charng et al., 2007; Lämke and Bäurle, 2017). Interestingly, the AS patterns of *HsfA2* are major drivers of the resilience to heat stress. At 22°C, the *HsfA2* pre-mRNA is fully spliced, producing the full-length *HsfA2* transcript. Moderate heat (37°C) leads to the generation of the splice variant *HsfA2-II* harboring a cryptic exon. This new exon presents a premature termination codon (PTC), leading to the degradation of *HsfA2-II* by NMD. Finally, when subjected to extreme heat (42–45 °C), a third splice variant *HsfA2-III* is produced through the cryptic 5' splice site in the intron. This isoform encodes for a truncated protein, S-HsfA2, which localizes to the nucleus and can bind to

HsfA2's own promoter. This results in a positive autoregulatory loop that controls *HsfA2* expression through AS (Sugio et al., 2009; Liu et al., 2013). This example underlines the potency of AS in regulating the function of major stress regulators, especially by fine-tuning the levels of specific isoforms during gradual stresses. Recently, a few studies analyzed transcriptome-wide AS patterns and showed that a reduction in core spliceosomal activity was likely behind the overall AS remodeling upon abiotic stress (Martín et al., 2021). Indeed, the comparison of heat primed and non-primed plants indicates that non-primed plants display a higher number of genes showing intron retention. Remarkably, these intron retention levels remained higher during recovery after heat stress, whereas recovering primed plants had AS patterns more alike to non-stressed control plants, suggesting that their return to a functional control-like splicing is improved (Ling et al., 2018). Thus, several abiotic stresses such as high temperatures can heavily impact splicing processes leading to the production of incorrectly spliced transcripts, resulting, *in fine*, in plant death. Priming prepares the splicing machinery to cope with this perturbation through the modulation of splicing itself.

As opposed to heat stress, low temperatures represent as well a major environmental factor that adversely impacts plant growth and development. As heat has a global inhibitory effect on splicing, one can wonder about the impact of cold on the spliceosome machinery. Thus, many studies intended to unravel transcriptome changes occurring upon cold stress and see how AS patterns respond to cold perception (Leviatan et al., 2013; Calixto et al., 2018; Li et al., 2020). Rather than blocking the splicing machinery *per se*, cold perception provokes expression and AS changes in thousands of genes. Curiously, these two effects only partially overlap, suggesting that changes in mRNA accumulation and AS target different subsets of genes. The genes presenting differential expression or AS during the early cold response are mainly TFs, RBPs, and splicing regulators (Calixto et al., 2018). For example, the GLYCINE-RICH RNA BINDING PROTEIN 7 (GRP7) is a hnRNP-like protein whose expression is upregulated by cold and confers freezing tolerance in *Arabidopsis*. This SF was shown to regulate AS of a varied range of transcripts by direct binding *in vivo* (Kim et al., 2008; Streitner et al., 2012). Similarly, the U2B"-like snRNP undergoes AS upon cold sensing and is required for proper AS of cold stress regulators, promoting cold acclimation and freezing tolerance (Calixto et al., 2018). Hence, the response to cold is mediated by rapid changes in expression and AS of either major transcription or splicing factors. These small changes impacting a limited number of genes quickly propagate through associated signaling cascades, resulting in a major reshaping of the transcriptome. Nevertheless, cold perception by the plant does not solely alter the expression or splicing of protein-coding transcripts. Calixto and colleagues (2019) identified a subset of lncRNAs exhibiting AS upon

cold stress, including *TAS1a*. The cold-induced intron retention in *TAS1a* causes a reduction in the abundance of siRNAs derived from *TAS1a*. These siRNAs target various genes including *HEAT-INDUCED TAS1 TARGET1* and *2* (*HTT1* and *HTT2*, respectively), which are upregulated during heat stress and mediate thermotolerance (Calixto et al., 2019; Li et al., 2014c). The regulation of AS in lncRNAs suggests the existence of an additional layer of complexity in the control of transcriptome content upon stresses. Thus, a growing number of studies reported the ability of lncRNAs to act as AS modulators in response to stress or diseases (Romero-Barrios et al., 2018). The next subchapter will focus on the characterization of these specific splicing-related lncRNAs and define the mechanisms they use to achieve their control over AS.

1.3 LncRNAs, novel players in AS regulation

As mentioned above, lncRNAs are emerging as versatile regulators of a myriad of processes in eukaryotes. From organ development to stress responses, these non-coding molecules act at multiple scales to exert their roles within the cell. Some of these lncRNAs were shown to greatly modulate the transcriptome content, leading to the fine-tuning of cellular properties in tissues. Similarly, AS represents a tremendous source of transcriptome and proteome diversity, adjusting the levels of isoforms exhibiting specific features. Hence, it is not surprising that some lncRNAs were found to act in AS related processes (Pisignano et al., 2021).

1.3.1 LncRNAs regulate AS at different levels

This part will describe the mechanisms through which lncRNAs regulate AS, providing clues about the potential role of lncRNAs in the control of this post-transcriptional mechanism. Four types of regulation seem to emerge (Figure 8): chromatin remodelling, formation of lncRNA-RNA hybrids, alteration of SFs and AS hijackers.

1.3.1.1 LncRNAs as chromatin remodelers

Eukaryotic genomes are tightly condensed into chromatin fibers composed of DNA wrapped around nucleosomes made of histone proteins. Post-translational modifications of histone tails define the accessibility to chromatin, ultimately reflecting the activity of gene transcription at these loci. Besides impacting gene transcription, the chromatin context of a locus was also found to affect AS. Since splicing mainly occurs cotranscriptionally, the modulation of Pol II elongation rate by the chromatin context fine-tunes the choice of alternative splice sites (Schor et al., 2009; Luco et al., 2011). Some studies already described existing relationships between chromatin states and lncRNAs (Wang et al., 2011; Flynn and Chang, 2012). In plants, a recent study uncovered the role of the non-coding circRNA *SEP3* in the AS modulation of its proper gene (Conn et al., 2017). *SEP3* is a member of the MADS (MCM1-AGAMOUS-DEFICIENS-SRF)-box superfamily and was shown to participate in flower development. Defects in *SEP3* splicing provoke floral homeotic phenotypes, underlying its importance in this developmental process (Severing et al., 2012; Conn et al., 2017). Surprisingly, the overexpression of a circRNA containing the entire exon 6 of the *SEP3* gene led to the accumulation of the AS variant *SEP3.3* lacking this exon 6. It was further shown that *SEP3* exon 6 circRNA can directly interact with its cognate DNA

locus, resulting in the formation of an RNA:DNA hybrid also called R-loop. This structure promotes transcriptional pausing, which coincides with the recruitment of SFs and AS (Wongsurawat et al., 2012). This specific mechanism suggests that circRNAs may participate in the AS regulation of their cognate exon-skipped messenger RNAs. Further genome-wide characterization of R-loops in exon-introns boundaries will be needed to assess the prevalence of this mechanism in the *Arabidopsis* genome (Ariel et al., 2017). Nevertheless, these findings strengthen the idea that chromatin conformation plays a major role in splicing pattern determination.

In animals, lncRNAs were also found to modulate AS through chromatin interactions. For example, the lncRNA *asFGFR2* is transcribed from the human *FGFR2* locus and induces epithelial-specific AS of *FGFR2* (Gonzalez et al., 2015). This AS is permitted by the recruitment of chromatin modifiers specifically to its own locus, leading to changes in the methylation status of this locus. Thus, the presence of *asFGFR2* ensures the deposition of H3K27me3 mark and the decrease of H3K36me2/3 marks, resulting in impaired recruitment of the chromatin-binding protein MRG15 and the negative splicing regulator PTBP1. The MRG15–PTBP1 complex cannot any longer inhibit the inclusion of the exon IIIb in *FGFR2*, leading to the epithelial-specific AS of this gene (Gonzalez et al., 2015). Hence, lncRNAs can change chromatin conformation either by direct binding to DNA or by recruiting specific protein partners, resulting in AS changes. Nevertheless, certain lncRNAs were shown to directly bind RNA molecules rather than DNA to modulate the AS patterns of their targets.

1.3.1.2 LncRNA-RNA hybrids as AS regulators

Natural antisense transcripts (NATs) represent a class of lncRNAs transcribed from the opposite strand of a protein-coding gene, overlapping or not with portions of exons of the coding gene (Khorkova et al., 2014). Regardless of their genomic origin, NATs can hybridize with pre-mRNAs and form RNA-RNA duplexes. These complexes were shown to impact AS during various biological processes, including apoptosis in mammalian cells. One major apoptotic pathway in animals is activated through the interaction between the Fas receptor (Fas) and the Fas ligand (FasL) (Villamizar et al., 2016). At the *FAS* locus, the antisense lncRNA *SAF* is transcribed in reverse orientation and from the opposite strand of the first intron of *FAS*. *SAF* localizes in the nucleus where it binds to the Fas receptor pre-mRNA and the human SPLICING FACTOR 45 (SPF45). This interaction facilitates the AS and exclusion of the exon 6, leading to the production of a soluble Fas protein that protects cells against FasL-induced apoptosis (Villamizar et al., 2016). Thus, NAT transcripts can facilitate interactions between pre-mRNAs and specific SFs.

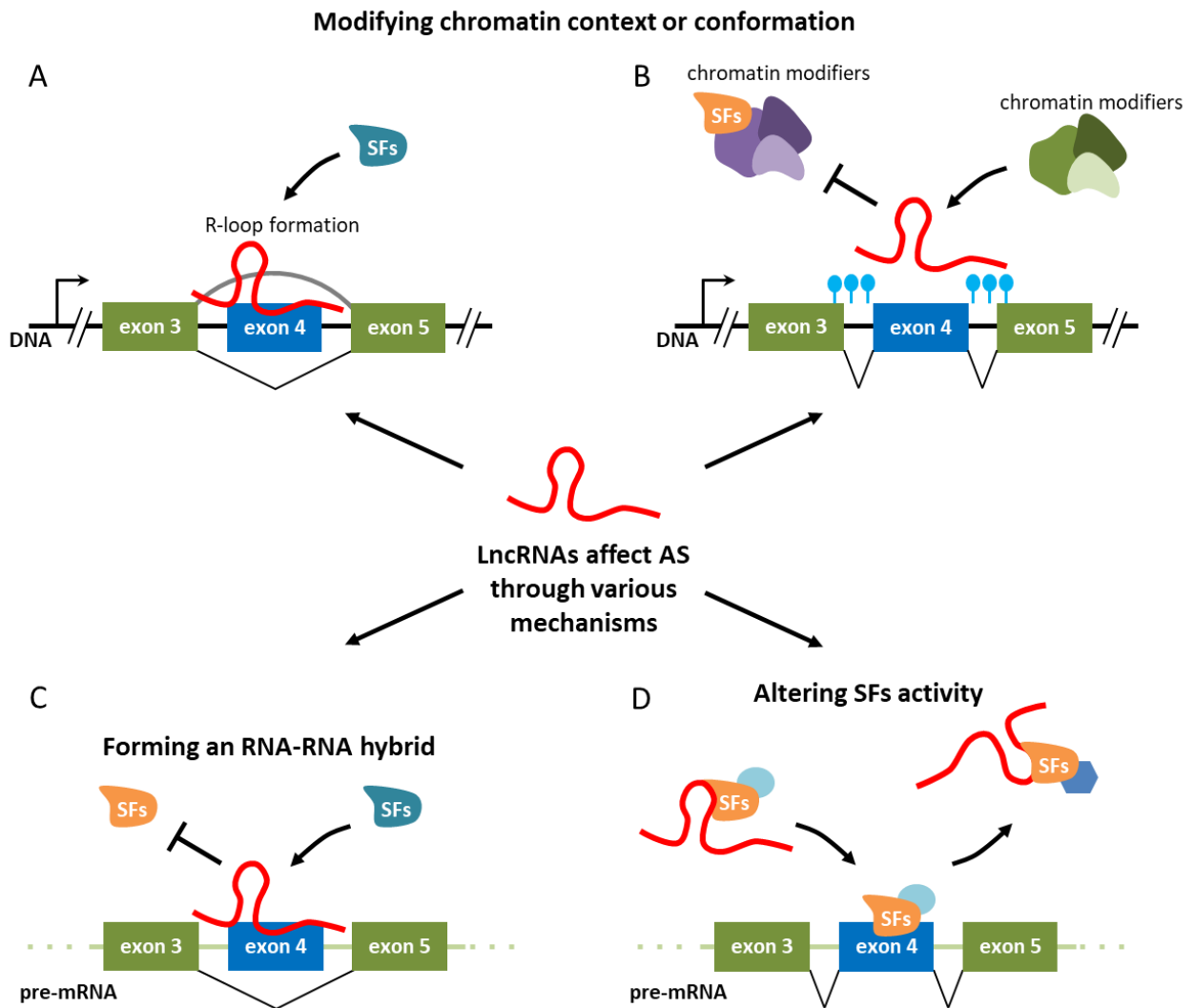


Figure 8. LncRNAs modulate alternative splicing through various mechanisms.

LncRNAs (in red) can control pre-mRNA splicing by:

A. interacting with specific DNA loci, resulting in the formation of an RNA:DNA hybrid called R-loop. This structure promotes transcriptional pausing, leading to SF recruitment and AS.

B. modifying chromatin accessibility through recruiting or blocking the access to chromatin modifying complexes at the transcribed genomic locus.

C. hybridizing with pre-mRNA molecules (light green), modulating the binding of specific SFs and therefore fine-tuning AS.

D. promoting SF recruitment, facilitating SF post-translational changes or sequestering SFs into specific subnuclear compartments, thereby interfering with SF activities.

Adapted from Pisignano et al., 2021.

Another example of NAT involvement in AS modulation was uncovered during epithelial–mesenchymal transition (EMT) in animals (Beltran et al., 2008). The expression of *Snail1* in epithelial cells triggers EMT, leading to the up-regulation of *ZEB2* synthesis, a transcriptional repressor of E-cadherin. In normal conditions, the large intron located at the 5'- untranslated region (UTR) of *ZEB2* is spliced out. This intron contains a structural intronic motif that works as an internal ribosome entry site (IRES) which serves to promote translation. When EMT is triggered, *Snail1* promotes the transcription of a NAT encoded in the opposite strand of the *Zeb2* locus, covering the 5' splice site of the *Zeb2* 5'-UTR. This further leads to the inclusion of the 5'-UTR located intron harboring the IRES, resulting in enhanced *ZEB2* translation (Beltran et al., 2008). Thus, antisense transcription can also affect pre-mRNA splicing by masking specific splice sites and preventing their processing.

In *A. thaliana*, the search for overlapping gene pairs among transcriptomic data unveiled a large proportion of convergently overlapping pairs (COPs) with the potential to form double-stranded RNAs (Jen et al., 2005). Remarkably, COPs were enriched in genes containing introns and genes with alternatively spliced transcripts. In addition, the increased frequency of alternatively spliced and variably polyadenylated transcripts when an intron overlaps with a NAT suggests that the formation of NAT lncRNA-RNA pairs may regulate the AS of protein-coding genes (Jen et al., 2005). Consistently, a genome-wide screen of trans-NATs in *A. thaliana* allowed the identification of 1,320 putative trans-NAT pairs (Wang et al., 2006). Most of them were predicted to form extended double-stranded RNA duplexes with their sense partners. Interestingly, more than 85% of trans-NATs were found in the same tissue as their sense partners. In addition, a substantial number of trans-NATs were predicted to produce siRNAs, suggesting their potential role in inducing RNA silencing of their sense target. Finally, the study showed that trans-NAT pairs have a much higher proportion of AS events compared to all transcription units in the genome, suggesting that some trans-NATs might function in regulating AS of their targets in *Arabidopsis* (Wang et al., 2006). Thus, lncRNAs can take advantage of sequence similarity to bind specific transcripts and modulate their splicing. Besides binding chromatin DNA or RNA, lncRNAs can also interact with splicing-related proteins to alter their features, resulting in changes in their activity.

1.3.1.3 LncRNAs altering splicing factors activity

The modulation of protein activity can occur through many ways: by promoting post-translational modification of the protein, changing its subcellular localization, or impacting protein binding to other partners or transcript targets. One of the most notorious and deeply characterized lncRNAs associated with AS regulation are the *NUCLEAR PARASPECKLE*

ASSEMBLY TRANSCRIPT 1 (NEAT1) and *METASTASIS ASSOCIATED LUNG ADENOCARCINOMA TRANSCRIPT 1 (MALAT1) / NUCLEAR PARASPECKLE ASSEMBLY TRANSCRIPT 2 (NEAT2)*. Both of these lncRNAs were shown to modulate the localization and phosphorylation status of SFs, and to exhibit differential expression in a wide range of human and murine tissues (Hutchinson et al., 2007; Bernard et al., 2010).

NEAT1 is a highly abundant lncRNA found in paraspeckles, nuclear domains controlling the sequestration of splicing-related proteins. During adipocyte differentiation, the abundance of *NEAT1* is dynamically regulated to modulate the relative levels of PPAR γ mRNA isoforms, the major TF driving adipogenesis. In short, *NEAT1* was shown to interact with the SR protein SRp40 (SFRS5), leading to SRp40 retention in paranuclear bodies. The *NEAT1*-SRp40 interaction enhances SRp40 phosphorylation by CDC2-LIKE KINASE 1 (CLK1), a kinase specifically targeting SFs. This change in SRp40 phosphorylation promotes PPAR γ AS, therefore fine-tuning the adipogenesis process (Jiang et al., 2009; Cooper et al., 2014).

The lncRNA *MALAT1/NEAT2* localizes in nuclear speckles and exerts oncogenic roles within the cell (Hutchinson et al., 2007). Indeed, its aberrant expression is associated with the development and progression of many types of cancers (Malakar et al., 2016; Wang et al., 2016a; Li et al., 2017a). Like *NEAT1*, *MALAT1* can effectively modulate SF distribution and phosphorylation, leading to AS changes in their target pre-mRNAs (Tripathi et al., 2010). Nevertheless, *MALAT1* was also shown to exert roles in AS through the disruption of SF complexes. The growth of cancer cells is promoted by PTBP2, whose oncogenic effects are repressed by its direct interaction with the tumor suppressor SFPQ (He et al., 2007; Meissner et al., 2000). *MALAT1* was found to directly bind to SFPQ, but not to PTBP2. Hence, the hijacking of SFPQ by *MALAT1* leads to the disruption of the splicing regulator complex SFPQ-PTBP2 and the further release of the oncogene PTPB2, triggering tumor growth and metastasis (Ji et al., 2014).

In plants, the characterization of lncRNAs directly involved in AS is still at its infancy. Nevertheless, a few examples showing lncRNAs interactions with SFs are slowly emerging. In the legume plant *Medicago truncatula*, the lncRNA *ENOD40* is rapidly induced upon interaction with symbiotic rhizobial bacteria. It is expressed in the root pericycle and in the differentiating cells of the nodule primordia (Crespi et al., 1994; Compaan et al., 2001). The overexpression of *ENOD40* leads to accelerated nodulation, mainly caused by increased initiation of primordia and an enhanced sensitivity to nodulation signals (Charon et al., 1999). *ENOD40* was found to be highly structured and did not associate with polysomes (Asad et al., 1994; Crespi et al., 1994). Yeast three-hybrid assays revealed direct interaction between *ENOD40* and the constitutive RNA Binding Protein 1 (RBP1), which localizes into nuclear

speckles where the splicing machinery is also hosted (Campalans et al., 2004). During nodulation, RBP1 is re-localized to cytoplasmic granules through its association with *ENOD40*. Therefore, the highly structured *ENOD40* lncRNA contributes to nucleocytoplasmic trafficking of RBP1, suggesting that RBP1 role in the nucleus may be perturbed during nodule development (Campalans et al., 2004). Indeed, MtRBP1 represents a close homolog of AtNSRs splicing factors which were also shown to interact with specific lncRNAs, including *ASCO* (Bardou et al., 2014; Lucero et al., 2020).

1.3.2 The lncRNA *ASCO*, a hijacker of splicing regulators

The lncRNA named *ASCO* was shown to modulate AS during lateral root development in *A. thaliana* (Bardou et al., 2014). Identified first by Ben Amor *et al.* (2009) using a genome-wide bioinformatics analysis of *Arabidopsis* full-length cDNA databases, it is encoded within an intergenic region of chromosome 1 (AT1G67105). It has a size of 786 nt and no obvious protein-coding capacity. Consistently, *ASCO* was not found to be associated with ribosomes (Bazin et al., 2017). A ClustalW and MUSCLE alignment identified at least 4 *ASCO* paralogs in *A. thaliana*, and suggested a conservation of *ASCO* and its paralogs between different Brassicaceae species. These comparisons uncovered a specific conserved region in the middle of *ASCO* RNA corresponding to a stem-loop structure (Romero-Barrios, 2016).

The *ASCO* genomic locus was found to be highly methylated, predominantly exhibiting the H3K9me2 repressive mark which is usually associated with transposons, repetitive sequences, and silent constitutive heterochromatin (Zhang et al., 2007; Margueron and Reinberg, 2011). Indeed, a 365pb retrotransposon (AT1TE82280) was identified in the promoter sequence of *ASCO*, terminating 197pb ahead of the *ASCO* transcription start site (TSS). This transposable element (TE) is a member of the class I ATLINE1_5 family, which transposes through an RNA intermediate with a “copy and paste” mechanism. This transposon is transcribed in the same direction as *ASCO*, potentially impacting its transcription through various ways.

Despite the repressive marks all over its locus, *ASCO* transcripts are well detected in *Arabidopsis* tissues. GUS expression analysis using Pro*ASCO*:GUS transgenic plants showed expression in the hypocotyl and the shoot apical meristem, in vascular tissues and guard cells of the cotyledons, and in vascular tissues of the root. Moreover, *ASCO* was found to be specifically repressed by auxin in roots (Romero-Barrios, 2016). Consistently, the overexpression of *ASCO* led to altered sensitivity to auxin with 35S-*ASCO* plants exhibiting a reduced lateral root (LR) density in presence of this hormone. Curiously, a similar phenotype was observed for plants lacking both NSRa and NSRb splicing factors, harboring even less

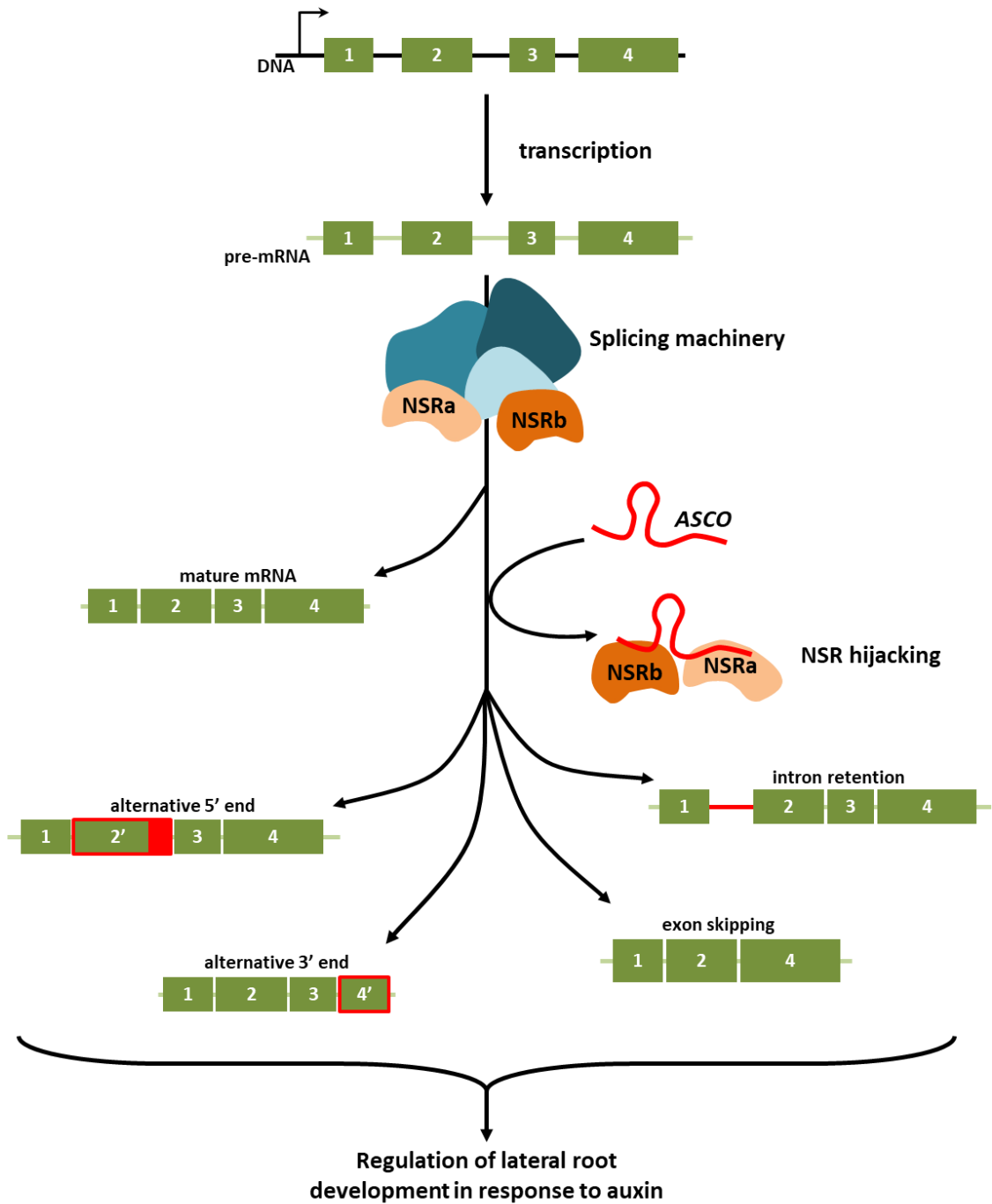


Figure 9. The ASCO lncRNA hijacks NSR splicing factors to modulate AS during lateral root formation.

The NSR splicing factors can bind to their pre-mRNA targets, but also to the ASCO lncRNA. The binding of this competitor RNA results in the AS of mature mRNAs, exhibiting events of alternative 5' or 3' ends, intron retention or exon skipping. The hijacking of NSRs by ASCO participates in the regulation of lateral root development in response to auxin.

Adapted from Romero Barrios et al., 2018.

and shorter LRs (Bardou et al., 2014). A transcriptomic analysis of this *nsra/b* double mutant uncovered an important number of AS events, notably in response to auxin (Tran et al., 2016). Some of these AS events were also identified in the *ASCO* overexpressing lines treated with auxin. Moreover, RNA immunoprecipitation assays established that NSRs bind not only with their alternatively spliced mRNA targets, but also with the *ASCO* lncRNA *in vivo*. *In vitro* experiments further suggested that *ASCO* can displace AS targets from an NSR-containing complex (Bardou et al., 2014). Hence, Bardou and colleagues (2014) proposed a model where the lncRNA *ASCO* hijacks the NSR splicing factors, modulating their function in AS during the plant response to auxin (Figure 9).

Taken together, these studies suggest that lncRNAs integrate a dynamic splicing network including many SFs and their associated pre-mRNA targets. Through these interactions with a varied range of partners, lncRNAs exert control over transcriptome reprogramming through AS in eukaryotes.

Aim of the thesis

The study of lncRNAs in plants is a fast-paced field which sheds light on these new regulators of the transcriptome. The team where I pursued my PhD focuses on the mechanisms through which lncRNAs affect plant development and explores the molecular basis of interactions between lncRNAs and specific ribonucleoproteins. Indeed, various lncRNAs were characterized in the team including the lncRNA *AUXIN REGULATED PROMOTER LOOP (APOLO)* which promotes the formation of R-loops and modulates transcription in response to auxin (Ariel et al., 2014; Ariel et al., 2020). Another one is the lncRNA *ALTERNATIVE SPLICING COMPETITOR (ASCO)* which regulates lateral root initiation through alternative splicing via direct binding to the plant specific NSR splicing factors, as mentioned above (Bardou et al., 2014). However, molecular mechanisms involved in this process still remain unclear.

Indeed, these findings raised many questions about the impact of the NSR-ASCO interaction in AS modulation. Are NSRs and ASCO only involved in the regulation of lateral root initiation? Does the ASCO lncRNA have other functions within the plant, and which ones? It was shown by Bardou et al. (2014) that ASCO's overexpression leads to altered sensitivity to auxin. What about the impact of its suppression? Furthermore, are NSRs the only ASCO protein partners? Does ASCO interact with other components of the spliceosome machinery? Finally, what is the molecular mechanism through which ASCO regulates splicing of pre-mRNA targets?

My thesis project therefore aimed to elucidate certain of these biological questions. In the 1st chapter, I describe our efforts to characterize the transcriptome-wide impact of *NSRa* and *NSRb* suppression in the plant, as well as to identify at genome-wide scale the RNA targets of NSRs in order to investigate in which pathways they intervene. The 2nd chapter describes the major part of my thesis work, where we explored the impact of ASCO suppression in *Arabidopsis* plants, and looked for ASCO protein partners in the nucleus. Finally, the 3rd chapter of my manuscript discusses an unsuspected new link between ASCO and temperature sensing in the plant, opening interesting perspectives of ASCO role during cold stress responses in *Arabidopsis*. Overall, my thesis work aimed to uncover new biological roles for lncRNA-splicing factor complexes, trying to understand in particular how a long non-coding RNA can regulate alternative splicing processes in the context of plant development.

Results

2.1 NSRs modulate the transcriptome to regulate cross-talks between hormones and immune responses

2.1.1 Introduction

RBPs are a large class of proteins that were shown to be involved in various steps of post-transcriptional gene regulation (Lee and Kang, 2016). One of the main interests of the team is to understand the mechanisms underlying lncRNA modulation of RBPs action and how these interactions can lead to cellular outputs allowing the plant to adapt to its environment. NSRs are RBPs involved in auxin-regulated processes such as lateral root development. They localize in nuclear speckle particles and act as AS regulators, binding specific alternatively spliced mRNAs. They were also found to bind the lncRNA *ASCO*, which can compete with the binding of NSRs to specific mRNA targets (Bardou et al., 2014) as demonstrated using qRT-PCR of AS mRNAs. In order to better comprehend the NSRs' way of action in the plant, we initiated a study led by Jérémie Bazin to analyze genome-wide the impact of the *nsra/b* mutation on the transcriptome, especially during the plant response to an auxin stimulus, and identify the complete RNome able to bind to these RBPs.

In this chapter I will therefore present the publication that emerged from this study, unravelling the NSRs impact on the transcriptome and their involvement in the transcriptional response linked to auxin and immune responses. In this article, I contributed by performing qPCR analyses on the *nsr* mutants and by helping in the writing process and figure preparation. This publication will be followed by some complementary results I generated that were not included in the article. These results deepen the link between NSRs and the immune responses of the plant, and characterize the impact of *nsr* mutations on the establishment of plant defense.

2.1.2 Publication: Nuclear Speckle RNA Binding Proteins Remodel Alternative Splicing and the Non-coding Arabidopsis Transcriptome to Regulate a Cross-Talk between Auxin and Immune Responses



Nuclear Speckle RNA Binding Proteins Remodel Alternative Splicing and the Non-coding Arabidopsis Transcriptome to Regulate a Cross-Talk Between Auxin and Immune Responses

Jérémie Bazin^{1*}, Natali Romero¹, Richard Rigo¹, Celine Charon¹, Thomas Blein¹, Federico Ariel^{1,2} and Martin Crespi^{1*}

¹ CNRS, INRA, Institute of Plant Sciences Paris-Saclay IPS2, Univ Paris Sud, Univ Evry, Univ Paris-Diderot, Sorbonne Paris-Cite, Université Paris-Saclay, Orsay, France, ² Instituto de Agrobiotecnología del Litoral, CONICET, Universidad Nacional del Litoral, Santa Fe, Argentina

OPEN ACCESS

Edited by:

Dorothee Staiger,
Bielefeld University, Germany

Reviewed by:

Rossana Henriques,
University College Cork, Ireland
Heike Lange,
UPR2357 Institut de Biologie
Moléculaire des Plantes (IBMP),
CNRS, France

*Correspondence:

Jérémie Bazin
jeremie.bazin@free.fr
Martin Crespi
martin.crespi@u-psud.fr

Specialty section:

This article was submitted to
Plant Cell Biology,
a section of the journal
Frontiers in Plant Science

Received: 16 May 2018

Accepted: 27 July 2018

Published: 21 August 2018

Citation:

Bazin J, Romero N, Rigo R,
Charon C, Blein T, Ariel F and
Crespi M (2018) Nuclear Speckle
RNA Binding Proteins Remodel
Alternative Splicing
and the Non-coding Arabidopsis
Transcriptome to Regulate
a Cross-Talk Between Auxin
and Immune Responses.
Front. Plant Sci. 9:1209.
doi: 10.3389/fpls.2018.01209

Nuclear speckle RNA binding proteins (NSRs) act as regulators of alternative splicing (AS) and auxin-regulated developmental processes such as lateral root formation in *Arabidopsis thaliana*. These proteins were shown to interact with specific alternatively spliced mRNA targets and at least with one structured lncRNA, named *Alternative Splicing Competitor* RNA. Here, we used genome-wide analysis of RNAseq to monitor the NSR global role on multiple tiers of gene expression, including RNA processing and AS. NSRs affect AS of 100s of genes as well as the abundance of lncRNAs particularly in response to auxin. Among them, the *FPA* floral regulator displayed alternative polyadenylation and differential expression of antisense *COOLAIR* lncRNAs in *nsra/b* mutants. This may explain the early flowering phenotype observed in *nsra* and *nsra/b* mutants. GO enrichment analysis of affected lines revealed a novel link of NSRs with the immune response pathway. A RIP-seq approach on an NSR fusion protein in mutant background identified that lncRNAs are privileged direct targets of NSRs in addition to specific AS mRNAs. The interplay of lncRNAs and AS mRNAs in NSR-containing complexes may control the crosstalk between auxin and the immune response pathway.

Keywords: RNA binding proteins, RNP complexes, alternative splicing, immune response, auxin

INTRODUCTION

RNA binding proteins (RBPs) have been shown to affect all steps of post-transcriptional gene expression control, including alternative splicing (AS), silencing, RNA decay, and translational control (Bailey-Serres et al., 2009). The *Arabidopsis thaliana* genome encodes for more than 200 proteins predicted to bind RNAs. The picture becomes even more complex since over 500 proteins were found to bind polyA+ RNA in a recent study attempting to define the RNA interactome using affinity capture and proteomics (Marondedze et al., 2016). However, only a small subset of RBPs has been functionally assigned in plants. The versatility of RBPs on gene expression regulation has been recently highlighted by the identification of several among them acting at multiple steps of post-transcriptional gene regulation (Lee and Kang, 2016; Oliveira et al., 2017). During mRNA

maturation, the transcript acquires a complex of proteins at each exon–exon junction during pre-mRNA splicing that influences the subsequent steps of mRNA translation and decay (Maquat, 2004). Although all RBPs bind RNA, they exhibit different RNA-sequence specificities and affinities. As a result, cells are able to generate diverse ribonucleoprotein complexes (RNPs) whose composition is unique to each mRNA and these complexes are further remodeled during the life of the mRNA in order to determine its fate. One approach to determine RBP function consisted in the identification of all interacting molecules (the so-called RNPome) of a specific RNP and the conditions of their association. The ribonucleoprotein immunopurification assay facilitates the identification and quantitative comparison of RNA association to specific proteins under different experimental conditions. This approach has been successfully used to elucidate the genome-wide role of a number of plant RBPs involved in pre-mRNA splicing, stress granule formation or translational control (Sorenson and Bailey-Serres, 2014; Gagliardi and Matarazzo, 2016; Foley et al., 2017; Köster and Meyer, 2018).

The nuclear speckle RNA binding proteins (NSRs) are a family of RBPs that act as regulators of AS and auxin regulated developmental processes such as lateral root formation in *Arabidopsis thaliana*. These proteins were shown to interact with some of their alternatively spliced mRNA targets and at least with one structured lncRNA, named *Alternative Splicing Competitor RNA (ASCO)* (Bardou et al., 2014). Overexpression of ASCO was shown to affect AS of a subset of mRNA regulated by NSRs, similar to *nsra/b* double mutants, and ASCO was also shown to compete *in vitro* with the binding of one AS mRNA target. This study suggested that plant lncRNAs are able to modulate AS of mRNA by hijacking RBPs, such as NSRs, involved in splicing (Romero-Barrios et al., 2018). In addition, transcriptome analysis using microarrays and specific AS analysis on a subset of mRNAs suggested a role of NSR in transcriptome remodeling in response to auxin (Bardou et al., 2014).

Here we used genome wide analysis to monitor the NSR global role on multiple tiers of gene expression, including RNA processing and AS. This allowed us to find a new role of NSR in the control of flowering time regulators as well as to suggest that NSRs control the crosstalk between auxin and the immune response pathway.

RESULTS

Auxin Regulation of Gene Expression Is Altered in *nsra/b* Double Mutant

To characterize the role of NSRs in the control of auxin regulated gene expression, we performed paired-end strand specific RNA sequencing on the *nsra/nsrb* (*nsra/b*) double mutant and wild type (Col-0) seedlings treated for 24 h with the synthetic auxin NAA (100 nM) or a mock solution (Bardou et al., 2014; Tran et al., 2016) (Figure 1A).

In mock treated samples, 63 and 41 genes were found to be differentially up and down-regulated between mutant and wild type seedlings (Supplementary Table S1B). Remarkably, in response to auxin, we identified 709 and 465 genes

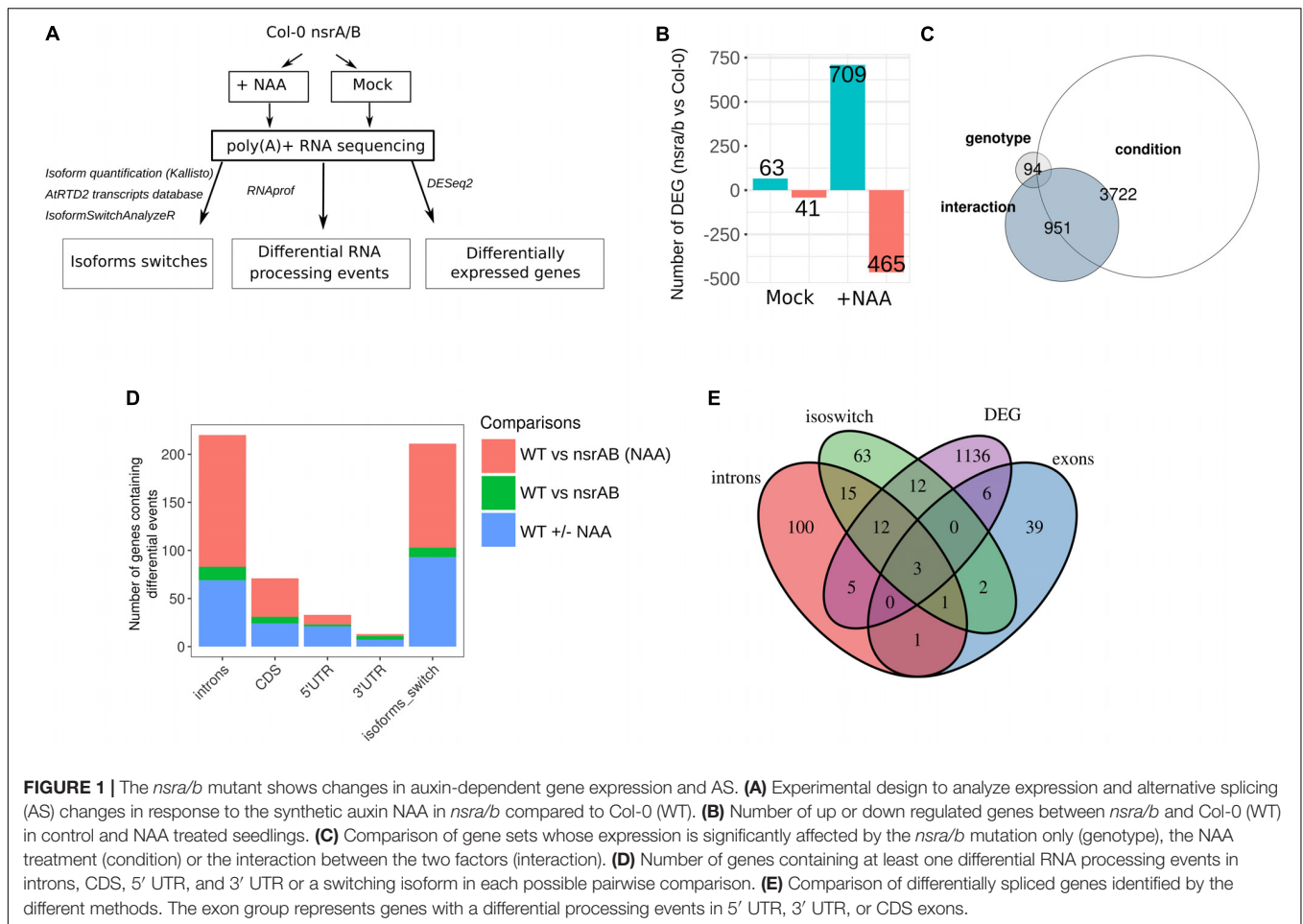
significantly up and down-regulated in *nsra/b*, compared to wild type (Figure 1B and Supplementary Table S1B). Principal component analysis (PCA) showed a dispersion of the data compatible with statistical comparisons between groups (Supplementary Figure S1). Multifactor analysis of differential gene expression further showed that *nsra/b* mutation has a major effect on auxin-regulated gene expression. Indeed, a set of 951 genes showed significant interaction between genotype and auxin regulation (Figure 1C and Supplementary Table S1B). This is in agreement with our previous findings indicating that NSRs mediate auxin regulation of gene expression (Bardou et al., 2014).

We have previously shown that NSRs modulate auxin-induced AS of a particular subset of genes using specific qRT-PCR assays (Bardou et al., 2014). We use now our RNA-seq dataset to characterize genome-wide effects of NSRs on AS and more generally on RNA processing (Figure 1A). To this end, we made use of the RNAprof software, which implements a gene-level normalization procedure and can compare RNA-seq read distributions on transcriptional units to detect significant profile differences. This approach allows *de novo* identification of RNA processing events independently of any gene feature or annotation independently of gene expression differences (Tran et al., 2016). RNAprof results were parsed to retain only highly significant differential RNA processing events ($p_{\text{adj}} < 10e-4$) and further crossed with gene annotation in order to classify them according to their gene features. The majority of events overlapped with intronic regions (Figure 1D and Supplementary Table S1C), which is in accordance with data showing that intron retention is the major event of AS in plants (Ner-Gaon et al., 2004). The effect of *nsra/b* on RNA processing and splicing is enhanced in response to NAA. In other words the vast majority of differential events between *nsra/b* and wild type plants were identified essentially in presence of auxin.

To further support the results from RNAprof and to gain knowledge on the functional consequences of NSR mediated AS events, we quantified mRNA transcript isoforms of the AtRTD2 database (Brown et al., 2017) using *kallisto* (Bray et al., 2016). Then, we searched for marked changes in isoform usage using IsoformSwitchAnalyzeR package (Vitting-Seerup and Sandelin, 2017), which allows statistical detection and visualization and prediction of functional consequences of isoform switching events. As a result, we identified 118 NSR-dependent isoform switching events including 108 only detected in NAA-treated samples (Figure 1E and Supplementary Table S1D). Comparison of gene sets affected in their steady state abundance, containing differential RNA processing or isoforms switching events in *nsra/b* highlighted the fact that most differentially spliced genes are not differentially expressed. In addition, over 35% of genes predicted with isoforms switching events were also found using RNAprof (Figure 1E).

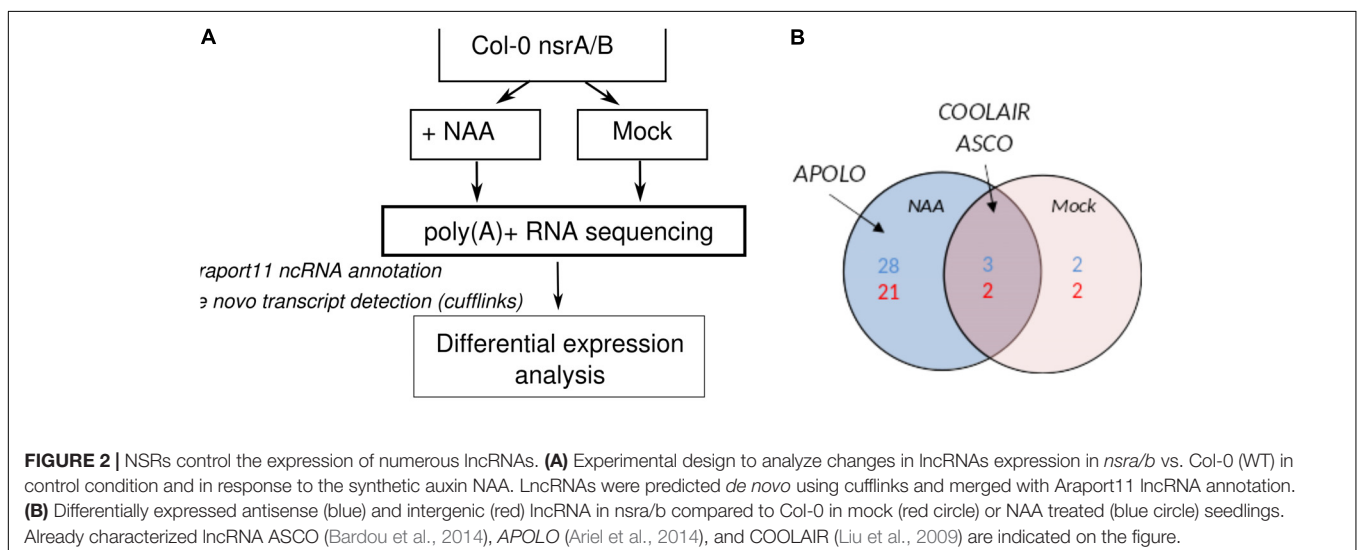
NSRs Affect the Abundance of Numerous LncRNAs

The activity of NSR proteins on AS is modulated by the lncRNA ASCO and the abundance of ASCO RNA is increased in *nsra/b* mutant (Bardou et al., 2014). Therefore, we conducted a global



analysis of lncRNAs detection and expression in our RNA-seq datasets. Annotated lncRNA (Araport11) were combined with *de novo* predicted transcripts and further classified based on their location in intergenic and antisense regions of coding genes

(Figure 2A). More than 2440 lncRNAs were detected in our RNAseq data with more than 1 TPM (Supplementary Table S1A) in at least three samples. In mock conditions, differential expression analysis served to identify five antisense and four



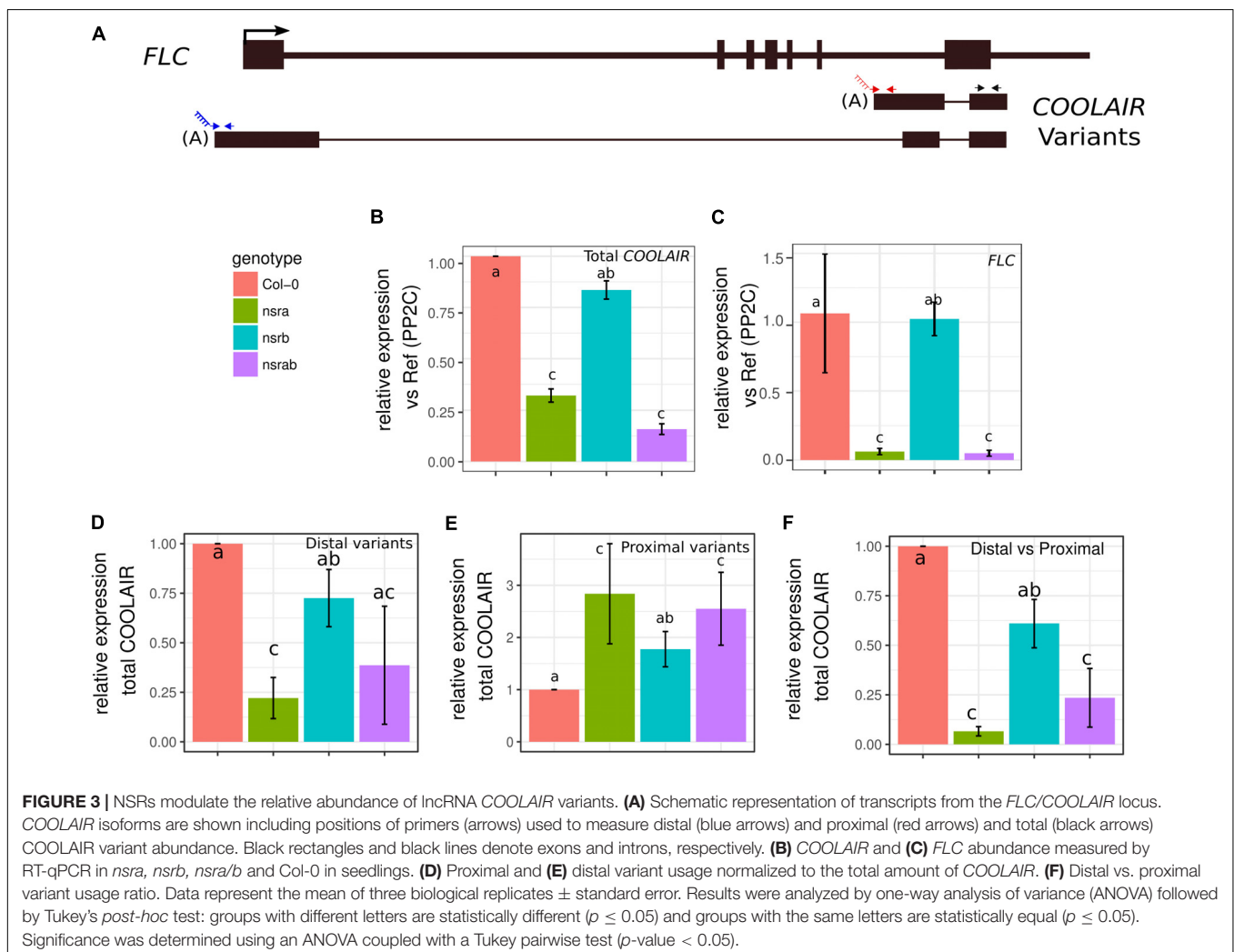
intergenic lncRNAs differentially expressed between mutant and wild type seedlings, whereas 31 intergenic and 23 antisense lncRNAs were found to be differentially regulated between mutant and wild type in the presence of auxin (Figure 2B). Differentially expressed lncRNAs included a number of well-characterized lncRNAs such as *APOLO*, which as been shown to influence root gravitropism in response to auxin via its action on PINOID protein kinase expression dynamics. In addition, the expression of lncRNA *ASCO*, shown to interact with NSR to modulate AS of its mRNA targets, was also affected in *nsra/b* suggesting a feedback regulation of NSR on *ASCO* lncRNA (Figure 2B).

NSR α Is Involved in the Control Flowering Time Through the Modulation of the *COOLAIR/FLC* Module

Interestingly, we also identified the lncRNA *COOLAIR* as down regulated in *nsra/b*, both in mock or NAA treated samples (Figure 2B). *COOLAIR* designate a set of transcripts expressed in antisense orientation of the locus encoding the floral repressor

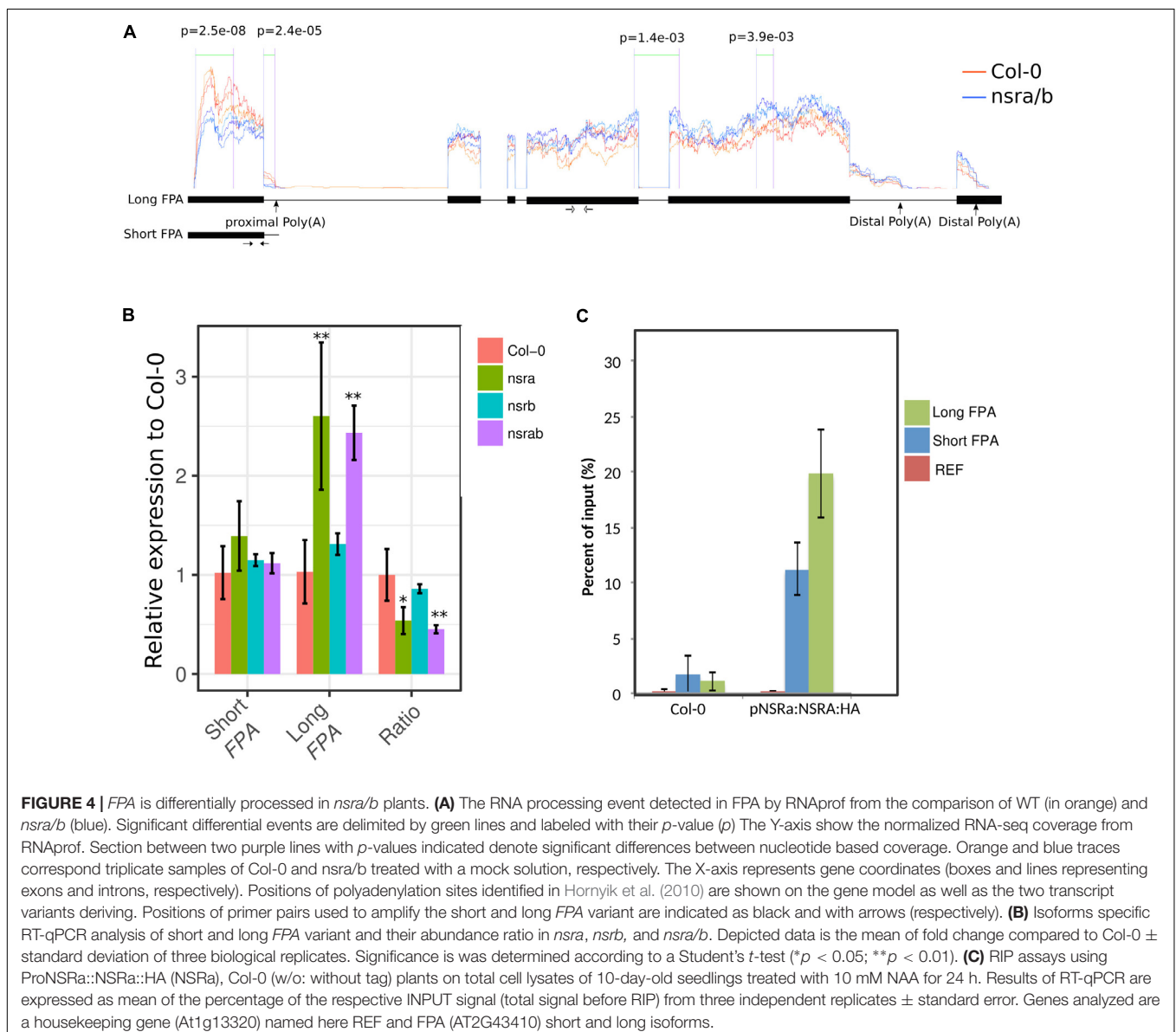
FLC (Whittaker and Dean, 2017). Two main classes of *COOLAIR* lncRNAs are produced by AS and polyadenylation of antisense transcripts generated from the *FLC* locus. One uses a proximal splice site and a polyadenylation site located in intron 6 of *FLC*, whereas the distal one results from the use of a distal splice and polyadenylation sites located in the *FLC* promoter (reviewed in Whittaker and Dean, 2017) (Figure 3A).

Strikingly, *FLC* is one of most deregulated genes in *nsra/b* mutants in control and NAA-treated samples. Notably, it was shown that a number of splicing and RNA processing factors control *FLC* expression by modulating the ratio of *COOLAIR* proximal and distal variants (Liu et al., 2009; Marquardt et al., 2014; Whittaker and Dean, 2017). Therefore, we determined the abundance and the ratio of *COOLAIR* variants in wild type, single *nsra*, *nsrb* and the double *nsra/b* mutants in control and NAA treated conditions using a dedicated strand-specific RT-qPCR assay (Marquardt et al., 2014). First, we confirmed that total *COOLAIR* and *FLC* abundance was decreased in *nsra* and *nsra/b* but not *nsrb* (Figures 3B,C). More importantly, we found that relative usage of the short (proximal) variant of *COOLAIR* increased by twofold in *nsra* and *nsra/b* but not in



nsrb leading to an increase of the ratio of distal vs. proximal COOLAIR isoforms in the same genotypes (Figures 3D–F). When analyzing the relative abundance of both variants against a housekeeping gene, we determined the decrease of total COOLAIR transcripts associated with a specific decrease of the distal variants. In contrast, proximal variant abundance remains stable (Supplementary Figure S2), leading to a change in relative variant usage (Figures 3D,E). Interestingly, the proximal COOLAIR variant was associated with a down-regulation of *FLC* and an early flowering phenotype (Marquardt et al., 2014). Together, these results suggest that the modulation of COOLAIR polyadenylation and/or splicing in *nsra* mutants contributes to the control of *FLC* expression. In addition, RNAprof also identified that the mRNA coding for the FPA protein (Horniyk et al., 2010) was differentially processed in *nsra/b* seedling treated with NAA (Figure 4A). The differential RNA processing event

occurred at the end of intron 1, which has been shown to contain an alternative polyadenylation site necessary for FPA negative autoregulation (Horniyk et al., 2010). RNAprof analysis hinted a significant reduction of the short FPA variant in *nsra/b* mutant compared to Col-0 (Figure 4A). RT-qPCR analysis using isoform specific primers (Figure 4A) showed that the long isoform accumulated in *nsra* and *nsra/b* but not in *nsrb* whereas the short isoform remained unaffected (Figure 4B). Hence, our data suggested that the use of the proximal polyA site is reduced in *nsra* and *nsra/b* mutant, which is predicted to lead to an increase of the full-length functional FPA. Interestingly, FPA was shown to favor proximal COOLAIR variants forms (Horniyk et al., 2010), suggesting that the effect of NSR mutation on COOLAIR variant ratio may be mediated by changes in FPA polyadenylation site usage. To address this potential mechanism, we checked whether COOLAIR or FPA are direct targets of



NSRa by RNA immunoprecipitation (RIP) using transgenic lines expressing a tagged version of the NSRa protein. Although we did not find *COOLAIR* binding to NSRa, both the long and the short *FPA* variant were enriched in the RIP assay supporting the idea that NSRa directly influences the processing of *FPA* mRNA (Figure 4C). Given the critical role of *FPA*, *COOLAIR*, and *FLC* in flowering, we hypothesized that NSRa may be involved in the control of flowering time. Indeed, we observed that *nsra/b* mutant displays an early flowering phenotype (Figure 5A). We then quantified this phenotype by counting the number of rosette leaves when the flower stem emerged from the plants. Data showed that *nsra* and *nsra/b* but not *nsrb* display an early flowering phenotype (Figure 5B), which is consistent with a lower expression of *FLC* in *nsra* and *nsra/b* mutants only (Figure 4C). Altogether, our results indicate that NSRa-dependent modulation of *FPA* polyadenylation may impact the activity of the *COOLAIR/FLC* module, affecting flowering time in Arabidopsis.

NSRs Affect Auxin-Dependent Expression of Biotic Stress Response Genes

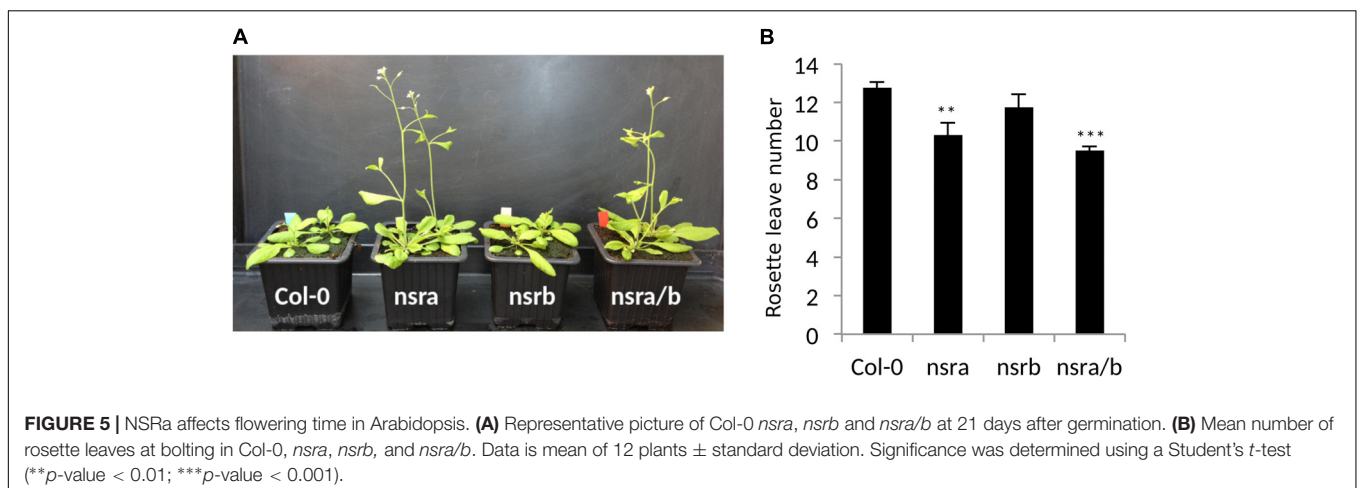
To extend our understanding on the genome-wide roles of NSRs in the control of auxin-dependent gene expression, we searched the putative function of differentially expressed and/or spliced gene groups using clustering and Gene Ontology (GO) enrichment analyses. Hierarchical clustering of differentially expressed genes determine two clusters of genes showing opposite expression patterns in response to NAA in *nsra/b* as compared to wild type plants (Figure 6A). GO analyses revealed that cluster 2 (Figure 6B), e.g., genes up-regulated by NAA in wild type plants but down-regulated by NAA in *nsra/b* is significantly enriched for genes belonging to GO categories such as “response to hormone” (FDR < 1e-6); “response to water deprivation” (FDR < 5e-9). On the other hand cluster 3 genes (Figure 6C), e.g., down-regulated or not affected by NAA in wild type but up-regulated in the mutant are highly significantly enriched for GO categories related to pathogen responses such as “response to biotic stimulus”

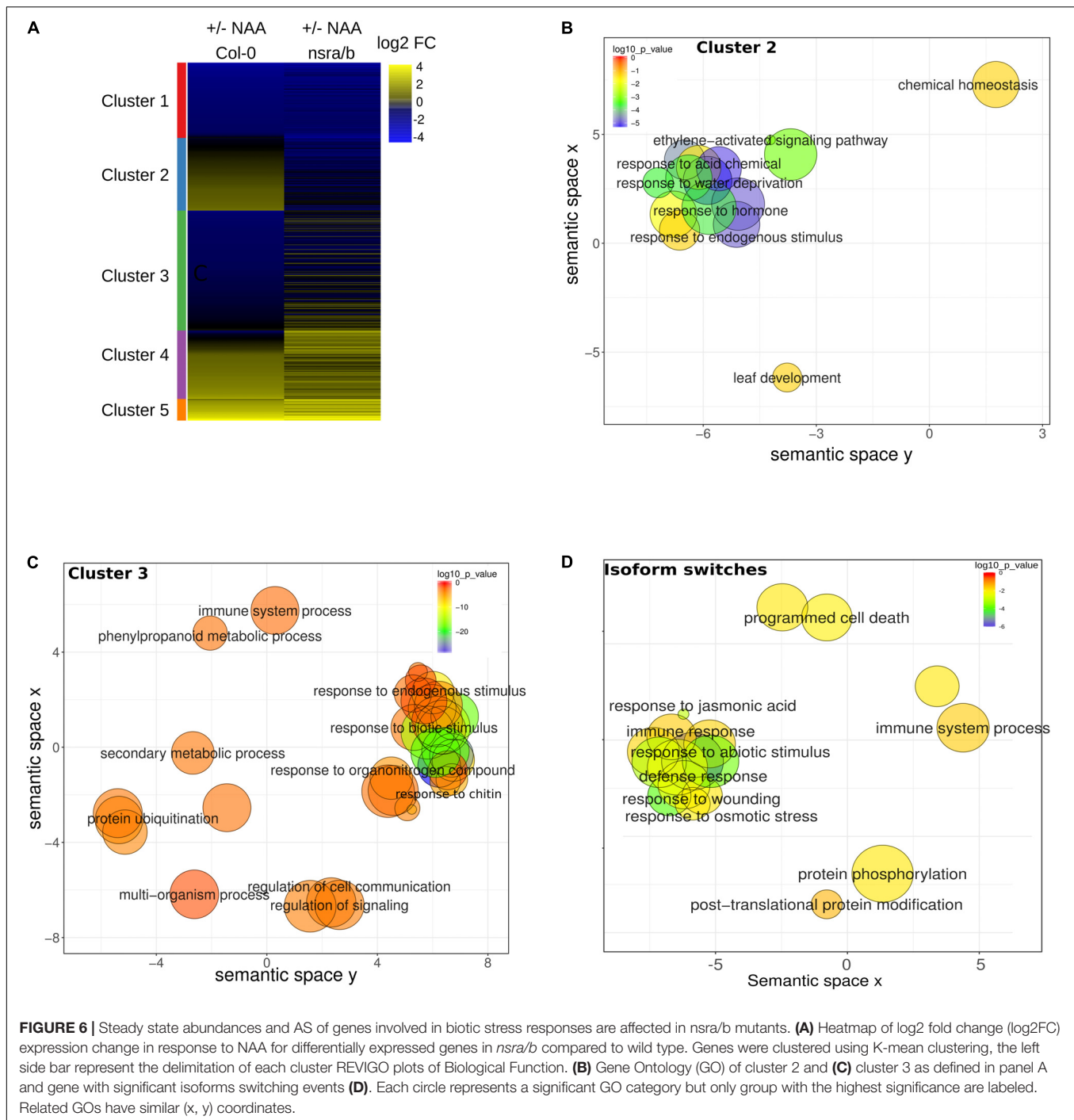
(FDR < 5e-16); “response to chitin” (FDR < 1e-26). We then confirmed the results of RNA-seq datasets (Figure 7) by RT-qPCR analysis of a small subset of genes belonging to clusters 2 and 3.

Given the important effect of NSRs on AS regulation, we also examined the putative function of differentially spliced genes having a switch in isoform usage. Strikingly, we identified a number of AS proteins located upstream of the immune response pathway. They include the MKP2 phosphatase (Lumbreras et al., 2010), the Toll/interleukin receptor (TIR) domain-containing protein TN1 and three members of the jasmonate co-receptor family (JAZ7, JAZ6, and JAZ2). In agreement, GO enrichment analysis of genes predicted to have significant isoforms switching events between *nsra/b* and Col-0 revealed a strong enrichment toward biological functions related to biotic stress responses (Figure 6D).

NSRa Directly Recognizes Transcripts Involved in Biotic Stress Responses

To address the question whether these targets are directly related to NSR function and/or indirectly affected by other proteins, we aimed to identify direct targets of NSRs using a genome-wide RIP-seq approach. We focused our analysis on NSRa as it is globally more highly expressed than NSRb (Bardou et al., 2014). Transgenic lines expressing an epitope tagged version of NSRa under its native promoter in the *nsra* mutant genetic background were used to avoid interference with the endogenous version of NSRa. Ten days-old seedlings treated for 24 h with NAA were used to match the transcriptome analysis. Immunoprecipitation was performed on UV cross-linked tissue using HA antibodies and mouse IgG as negative control (Figure 8A). NSRa-HA was detected from the input sample as well as from the eluate of the immunoprecipitation when it was performed with an HA antibody but not when mouse IgG were used (Figure 8B) qRT-PCR analysis of previously identified targets and a randomly selected abundant housekeeping gene confirmed the specific enrichment of target genes in the RIP sample compared to the input (Figure 8C). In addition, RNA extracted from mock IP eluate did not give

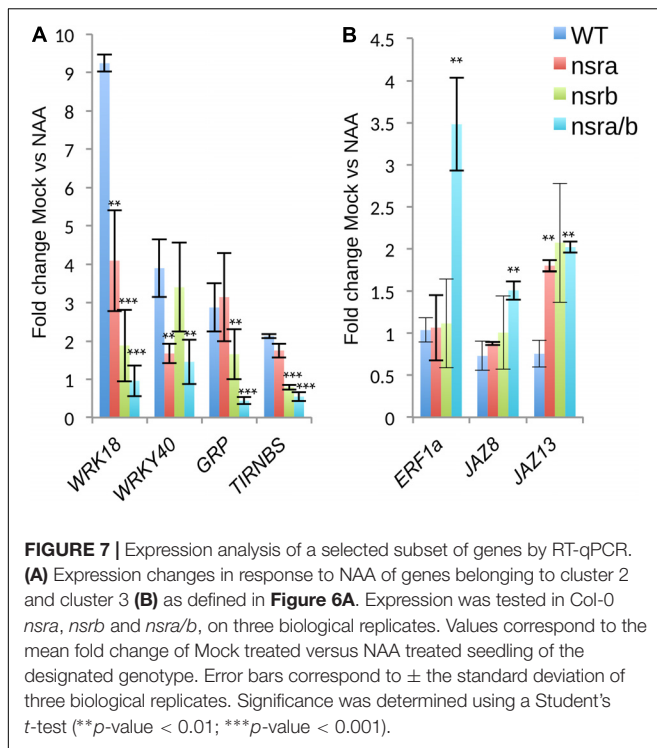




detectable amount of RNA supporting the specificity of this assay. Total RNA-seq libraries were prepared in duplicate from input, RIP and Mock samples. PCA and correlation analysis showed a dispersion of the data compatible with statistical comparisons between groups (**Supplementary Figure S3**). To detect putative NSRa targets, we used a multi-factor differential expression analysis using DESeq2 in order to identify transcripts significantly enriched in RIP as compared to the input (FDR < 0.01; log₂FC > 2) that were depleted from Mock samples. After

filtering out all transcripts with less than two TPM in RIP libraries, we finally identified 342 putative targets of NSRa (**Figure 9A**).

Comparing this list of genes with those differentially expressed in *nsra/b* in mock or NAA treated seedling, we found that 33% of putative target genes were also deregulated in *nsra/b* (**Figure 9B**). Further examination of putative targets genes revealed that the large majority of these genes are up-regulated in *nsra/b* suggesting that NSRs are negatively controlling their transcript abundance



in vivo (Figure 9D). GO enrichment analysis revealed that putative NSRa targets (Figure 9E) are enriched for genes involved in biological processes associated with defense responses such as “response to chitin” (FDR < 1.76e-9), “response to wounding” (FDR < 2.6e-3) or “immune system processes” (FDR < 1.7e-3). Interestingly, NSR target genes were also enriched for the GO category “regulation of transcription, DNA-templated” (FDR < 1.6e-8). Further examination of targets genes belonging to this GO category revealed that 56 transcription factors (TFs) are likely to be direct targets of NSRa (Supplementary Table S1E). Among them, we found the mRNA encoding the MYC2 TF, a key regulator of immune responses (Kazan and Manners, 2013) as well as nine *WRKY* and seven *ERF* TF transcripts, which both classes have been associated with the regulation of the plant immune response (Pandey and Somssich, 2009; Huang et al., 2016). Ten putative target genes were selected for RT-qPCR validation of the RIP assay. Among them, seven showed a significant enrichment over the input samples (Figure 9C) further supporting the genome-wide approach of NSRa target identification. Together, these results suggest that direct recognition of a subset of defense response genes by NSRa may affect their steady state abundance during auxin response.

LncRNAs Are Overrepresented Among NSRa Targets

It was previously demonstrated that a direct interaction between NSR and the lncRNA *ASCO* is able to modulate NSR function (Bardou et al., 2014). Thus, we thoroughly analyzed global lncRNA abundance in RIP-seq datasets. Interestingly, lncRNAs appeared among the most highly enriched transcripts within the

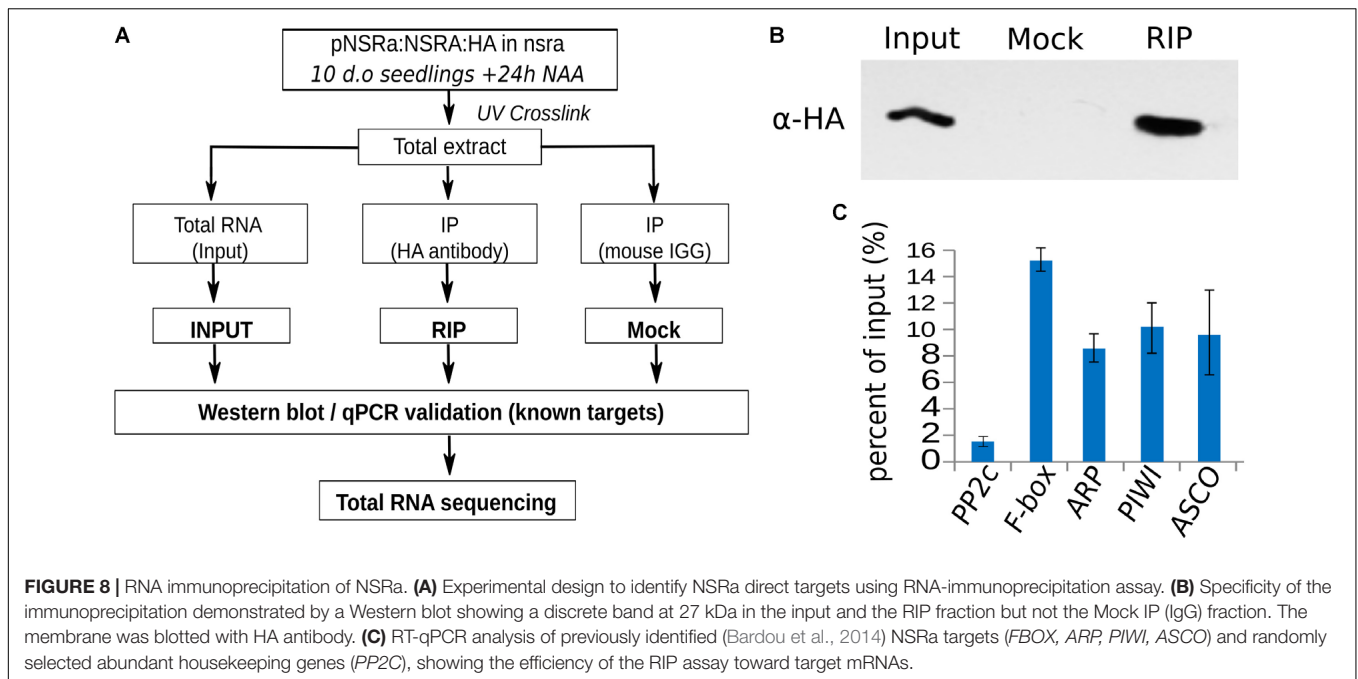
putative targets of NSRa. We found that, out of the 342 putative NSRa targets, 53 were lncRNA including 20 and 33 intergenic and antisense lncRNA, respectively (Figure 10A). In fact, relatively to the total number of lncRNAs detected in the input, lncRNAs were significantly enriched over mRNA in the set of putative targets transcripts (hypergeometric test: 1.9 fold, *p*-value < 4.06e-4) (Figure 10B).

We further validated the NSR-lncRNA interaction by RIP-qPCR. We found four out of five lncRNAs enriched over the input RNA in NSRa RIP samples (Figure 10C). Analyses of target lncRNA expression in *nsra/b* revealed that, similarly to the behavior of *ASCO*, seven target lncRNAs are significantly upregulated in the *nsra/b* mutant (Figures 10D,E). Together, these results suggest that lncRNAs are overrepresented among targets of NSRa and that NSRs might control the accumulation of lncRNA *in vivo*. Future works on the interplay between lncRNA and mRNAs in NSR-containing complexes should shed light on their global impact over the transcriptome.

DISCUSSION

In agreement with our previous study based on microarrays, a novel thorough analysis of *nsra/b* transcriptome using RNA-seq has revealed an important role of these RBPs in the control of auxin-responsive genes. A previous study monitoring AS changes of a subset of 288 genes using high-resolution real-time PCR, first uncovered the important roles of NSR in auxin-driven AS changes and targeted RIP-qPCR showed that both NSR proteins were able to bind AS mRNA targets *in planta* (Bardou et al., 2014). Our global AS analysis further confirmed this function of NSRs on AS modulation and demonstrated the impact of these proteins at genome-wide level. However, our RIP-seq global analysis of NSR targets did not show a strong enrichment toward AS modulated transcripts. Instead, a large fraction of NSR targets were transcriptionally upregulated in *nsra/b*, suggesting that NSR may play a direct role in controlling their stability or transcription. Several splicing factors have been shown to affect transcription by interacting with the transcriptional machinery and to modulate Pol II elongation rates (Kornblihtt et al., 2004). In addition, specific RBPs deposited during pre-mRNA splicing at exon-exon splicing junctions, can influence their mRNA decay (Lumbreras et al., 2010; Nishtala et al., 2016). Further dissection of the NSR recognition sites on mRNAs may support a role of NSRs on mRNA decay.

The combination of our RNA-seq and RIP-seq approaches revealed that lncRNAs are privileged targets of NSRa and that a significant fraction of the auxin-responsive non-coding transcriptome is deregulated in the *nsra/b* genetic background. This is in accordance with our previous results showing that the specific interaction of NSR with the *ASCO* lncRNA is able to modify AS pattern of a subset of NSR-target genes. Our study suggests that NSRs may play a broader role in lncRNA biology. In particular, we found that a large majority of lncRNAs targeted by NSRa are upregulated in *nsra/b*, suggesting a new role of these proteins in the control of lncRNA transcription and/or stability. So far, very little is known about lncRNA biogenesis,



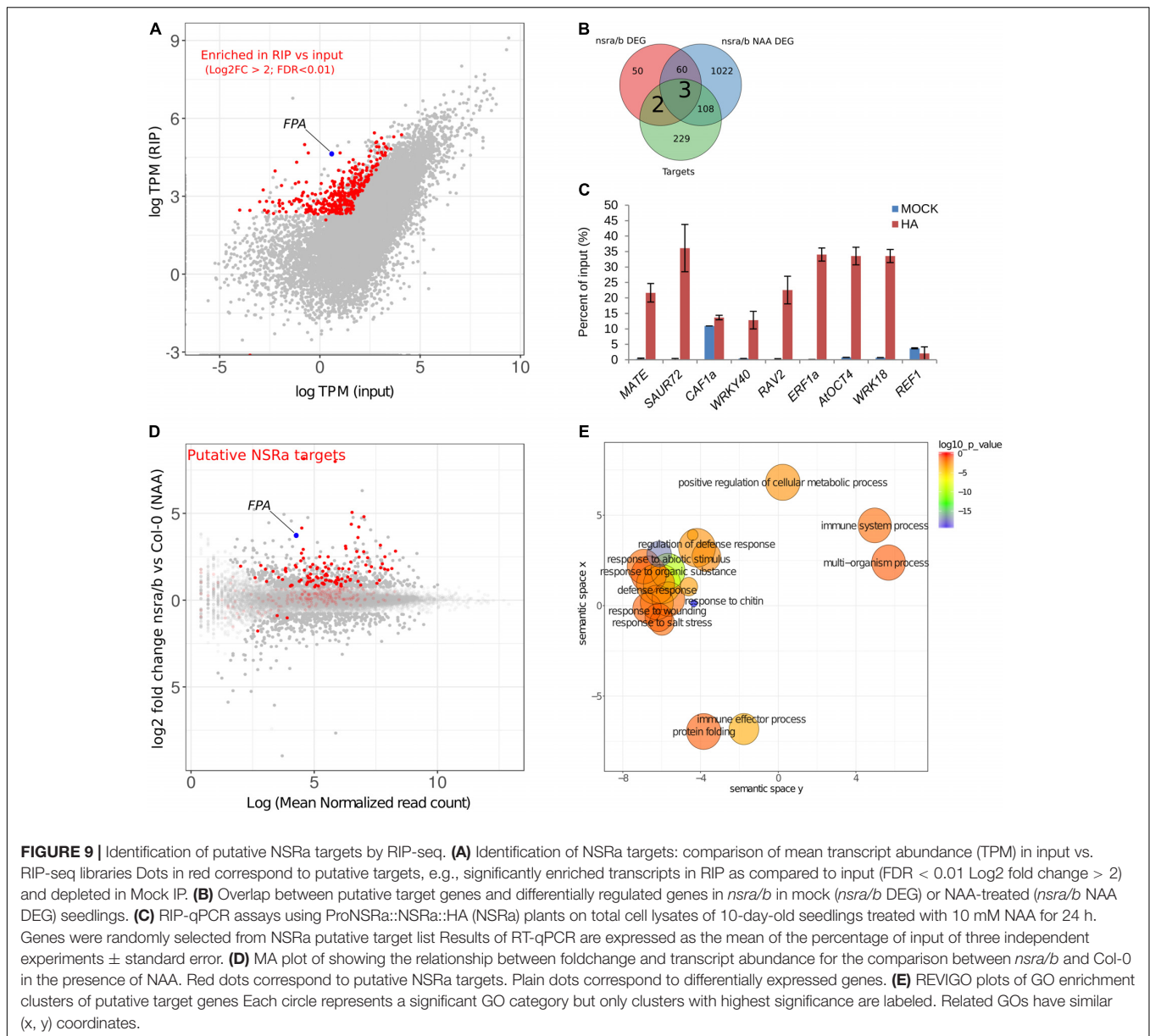
especially in plants. Other RBPs have been shown to affect lncRNA abundance. For instance several members of the cap binding complex such as CBP20, CBP80, and SERRATE have been shown to co-regulate the abundance of a large subset of lncRNAs in Arabidopsis seedlings (Liu et al., 2012). Interestingly, these three proteins, like NSRs, have also been associated with major roles in the control of AS patterns (Raczynska et al., 2010, 2014). This suggests that the splicing machinery might be used to control lncRNAs abundance in the nucleus and that the interplay between lncRNA and mRNAs may be an emerging mechanism in splicing regulation. Further genetic dissection is required to determine whether NSRs are involved in the same pathway that CBP20, CPB80, and SERRATE.

The strong deregulation of the *FLC/COOLAIR* module in *nsra/b* led us to identify a new role of NSR α in the control of flowering time. A number of forward genetic screenings aiming to identify new genes controlling flowering time through FLC expression modulation have consistently identified RNA processing and splicing factors that promote formation of the short *COOLAIR* isoforms, such as *FCA*, *FPA*, *HLP1*, *GRP7* and the core spliceosome component *PRP8a* (Deng and Cao, 2017). Loss of function mutants of these factors lead to a reduced usage of *COOLAIR* proximal polyadenylation site and an increase of *FLC* transcription which is associated with late flowering phenotypes (Deng and Cao, 2017). Interestingly, our analysis of the *FLC/COOLAIR* module in *nsr* mutants revealed an opposite role of NSR α in *COOLAIR* polyadenylation site usage, leading to the increased use of *COOLAIR* proximal polyadenylation site, and reduced *FLC* levels associated with an early flowering phenotype.

We also identified a new role of NSRs in the regulation of auxin-mediated expression and AS of transcripts related to biotic stress response. Interestingly, it has been shown for

several years that natural (i.e., IAA) and synthetic (i.e., NAA) auxins can promote pathogen virulence of *P. syringae* (Mutka et al., 2013). More recently, a conserved pathway of auxin biosynthesis was demonstrated in *Pseudomonads* as contributing to pathogen virulence in *Arabidopsis thaliana* (McClerkin et al., 2018). However, little is known on the specific plant factors that modulate immune responses upon endogenous or pathogen produced auxins. Our work shows that NSRs do not affect the global auxin responses but rather have an impact on the abundance of mRNAs coding for proteins involved in plant immune response, suggesting that these RBPs may participate in the regulation of plant defense by endogenous or pathogen-produced auxins.

In higher plants, AS plays a key role in gene expression as shown by the fact that 60–70% of intron-containing genes undergoes alternative processing. Several genome-wide studies of AS has shown that this mechanism may represent a way to enhance the ability for plant cells to cope with stress via the modulation of transcriptome plasticity. Here we show that among the genes with significant isoforms switching events in *nsra/b* mutant treated with auxin, we identified several genes involved in the modulation of the MAPK kinase modules, a core regulator of defense responses. They included MKP2 phosphatase which functionally interacts with MPK3 and MPK6 to mediate disease response in Arabidopsis (Lumbreras et al., 2010) and PTI-4 kinase which was found in MPK6 containing complexes *in vivo* and was shown to function in the MPK6 signaling cascade (Forzani et al., 2011). As activation of MAPK signaling cascades regulate the expression of 1000s of downstream targets genes, we can speculate that a large fraction of the transcriptome change observed in *nsra/b* mutant could be a consequence of AS defect of genes involved in such early phase of the defense response pathway.



MATERIALS AND METHODS

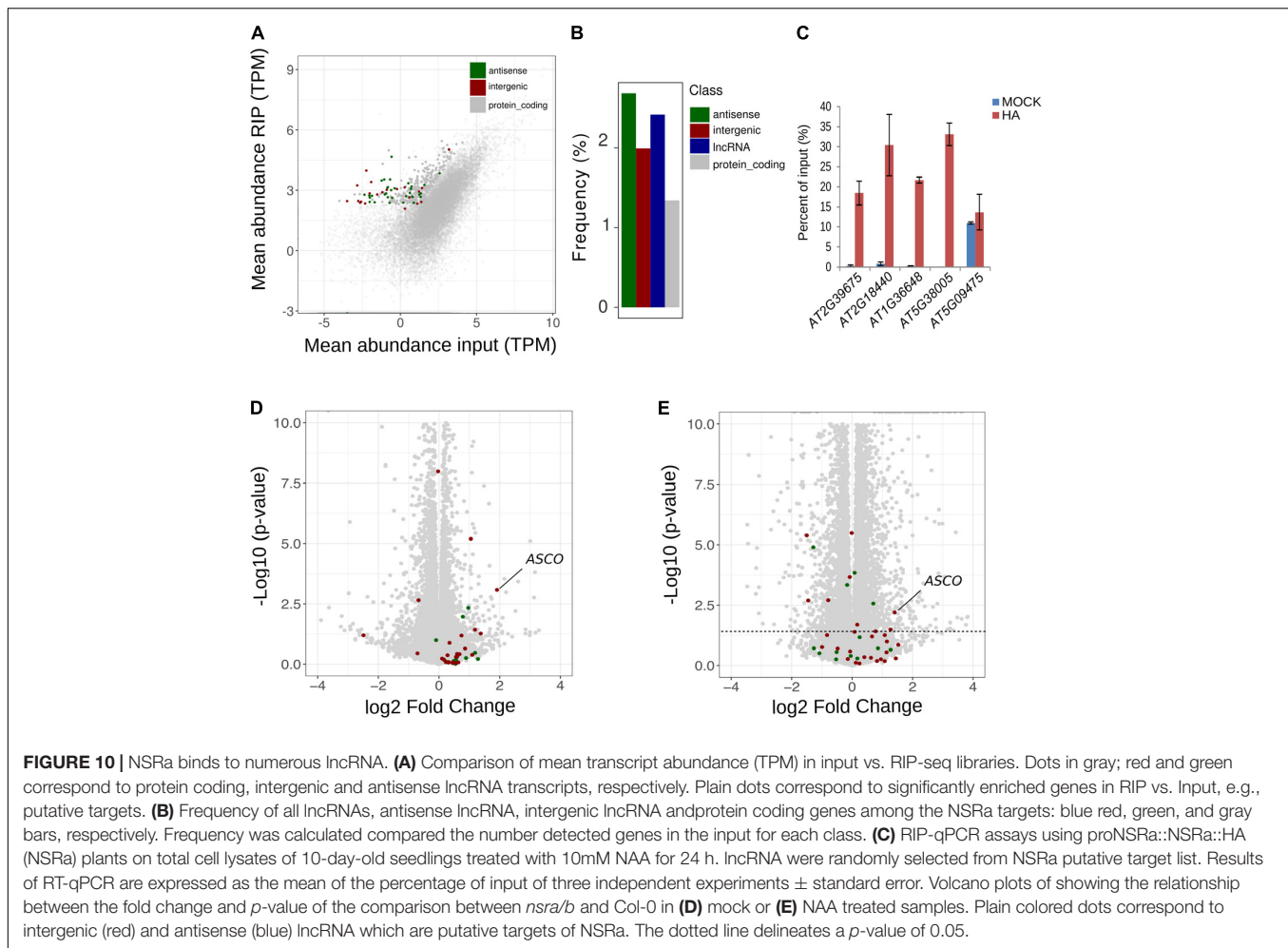
Plant Material and Treatments

All mutants were in the Columbia-0 (Col-0) background. *Atnsra* (SALK_003214) and *Atnsrb* (Sail_717) were from the SALK and SAIL T-DNA collections, respectively. For RIP, a lines expressing pNSRa::NRSa-HA in *Atnsra* or pNSRa::NRSb-HA in *Atnsrb* were used (Bardou et al., 2014). Plants were grown on soil in long day (16 h light/8 h dark) conditions at 23°C. For RNA-sequencing and RIP-seq WT and *nsra/nsrb* were grown on nylon membrane (Nitex 100 μm) in plate filled with 1/2MS medium for 10 days and then transferred for 24 h to 1/2MS medium containing 100 nM NAA or a mock solution before the whole seedlings were harvested. For flowering time analysis, plants were grown under long day conditions and the number of rosette

leave were counted from 12 plants when the flower stem was 1 cm tall.

RNA Sequencing Analysis

Stranded mRNA sequencing libraries were performed on three biological replicate of Col-0, *nsra/b* treated with a 100 nM NAA or a mock solution. One μg of total RNA from Col-0 and *nsra/b* seedlings was used for library preparation using the Illumina TruSeq Stranded mRNA library prep kit according to the manufacturer instruction. Libraries were sequenced on an HiSeq2000 sequencer using 150 nt pair-end read mode. A minimum 28 Million of were obtained for each sample, quality filtered using fastqc (Andrews, 2010) with default parameters and aligned using tophat (Trapnell et al., 2012) with the following arguments: -g 1 -i 5 -p



6 -I 2000 -segment-mismatches 2 -segment-length 20 -library-type fr-firststrand. Read were counted using SummarizeOverlap function from the GenomicRange R package (Lawrence et al., 2013) using strand specific and Union mode. Differential gene expression analysis was done one pairwise comparison using DESeq2 (Love et al., 2014) with FDR correction of the p -value. K-mean clustering analysis was performed in R on scaled log₂ fold change data and the optimal number of cluster was determined using the elbow method. Heatmap was plotted using heatmap.2 function of the gplots package (Warnes et al., 2009). Sequence files have been submitted to the NCBI GEO database under accession GSE65717 and GSE116923.

Gene Ontology Analysis

Gene ontology enrichment analysis was done using the AgriGO server¹ using default parameters. Lists of GO terms were visualized using REVIGO² and plotted in R. Only GO terms with a dispensability factor over 0.5 were printed in REVIGO plots.

¹<http://bioinfo.cau.edu.cn/agriGO/>

²<http://revigo.irb.hr/>

AS Analysis

RNAprof (v1.2.6) was used on BAM alignment files with the following parameters: LIBTYPE = fr-unstranded, SEQTYPE = “-Pair”, MIS = 1000. All possible pairwise comparisons were computed. Overlap of differential events ($pval < 1e-04$) with gene annotation was done using *findOverlaps* of the GenomicRanges Package in R and custom in house scripts. Only events that were completely included in gene feature (e.g., intron, exons, 3' UTR, and 5' UTR) were kept for further analysis.

For isoforms switching identification, transcript isoforms abundance was quantified with pseudo alignment read count with *kallisto* (Bray et al., 2016), on all isoforms of the AtRTD2 database (Zhang et al., 2017). Then the IsoformSwitchAnalyzeR package was used to detect significant changes in isoform usage. Only significant switches ($p_{adj} < 0.1$) were kept for further analyses (Vitting-Seerup and Sandelin, 2017).

RNA Immunoprecipitation and Sequencing (RIP-Seq)

NSRa protein tagged with HA was immunoprecipitated from the *nrsa* mutant background expressing the pNSRa::NSRa-HA

construct (Bardou et al., 2014). Briefly, 10 day old seedlings treated with 100 nM NAA for 24 h were irradiated three times with UV using a UV crosslinker CL-508 (Uvitec) at 0.400 J/cm². Plants were ground in liquid nitrogen and RNA-IP was performed as in Sorenson and Bailey-Serres (2014) with the following modification: immunoprecipitation (IP) was performed using anti mouse HA-7 monoclonal antibody (Sigma) and the negative IP (Mock) was done using anti mouse IgG (Millipore). RNA was eluted from the beads with 50 U proteinase K (RNase grade, Invitrogen) in 2 µl of RNase inhibitor at 55°C for 1 h in wash buffer and extracted using Trizol according to manufacturer instructions. A 10th of the input fraction was saved for RNA and protein extraction. For western blot analysis, proteins were extracted from the beads and input fraction with 2X SDS-loading Buffer for 10 min at 75°C, directly loaded on SDS PAGE, transferred onto Nitrocellulose membranes and blotted with HA-7 antibody. For RT-qPCR analysis, RNA was reverse transcribed with Maxima Reverse Transcriptase (Thermo) using random Hexamer priming. cDNA from input, IP and Mock were amplified with primers listed in **Supplementary Table S2**. Results were analyzed using the percentage of input method. First, Ct values of input sample (10% of volume) were adjusted to 100% as follows: Adjusted Ct input = Raw Ct input - log₂(10). Percentage of input was calculated as follow: 100 * 2^(Adjusted Ct input - Ct IP). Results are mean of three independent experiments. Student's *t*-test was performed to determine significance. For RNA-seq: input mock and IP RNA were depleted of rRNA using the plant leaf ribozero kit (Illumina) and libraries were prepared using the Illumina TruSeq Stranded mRNA library prep kit according to the manufacturer instruction but omitting the polyA RNA purification step and sequenced on a NextSeq500 sequencer (Illumina) using single-end 75 bp reads mode. Sequence files have been submitted to the NCBI GEO database under accession GSE116914.

Analysis of RIP-Seq Data

Reads were mapped using STAR (Dobin et al., 2013) and TPM was calculated using RSEM (Li and Dewey, 2011). Read were counted using SummarizeOverlap function from the GenomicRange R package (Lawrence et al., 2013) using strand specific and *Union* mode. To identify putative NSRa targets we used pairwise comparison with DESeq2 package. Only genes significantly enriched in IP with anti HA as compared with the anti-mouse IgG (mock) IP were kept for further analysis (log₂FC ≥ 1; FDR < 0.01). Putative targets genes were defined as gene highly enriched in the IP with anti HA compared to their global level in input used for the IP (log₂FC > 2; FDR < 0.01). To reduce noise associated with low read counts, we excluded from this list any gene with less than two TPM in at least one of the RIP-seq libraries.

REFERENCES

Andrews, S. (2010). *FastQC: A Quality Control Tool for High Throughput Sequence Data*. Available at: <http://www.bioinformatics.babraham.ac.uk/projects/fastqc>

Measuring Distal and Proximal COOLAIR Variants

This was performed essentially as in Marquardt et al. (2014). 5 µg of total RNA was reverse transcribed with and oligo(dT) primer. qPCR was performed with set of primers specific to distal and proximal COOLAIR described in Marquardt et al. (2014). qPCR reactions were performed in triplicates for each sample. Average values of the triplicates were normalized to the expression of total COOLAIR quantified in the same sample.

AUTHOR CONTRIBUTIONS

JB designed study, performed the experiments, analyzed the data, and wrote the article. NR, FA, RR, and CC performed the experiments and participated in writing. TB analyzed the data. MC designed the study and wrote the paper.

FUNDING

This work was supported by grants of The King Abdulla University of Science and Technology (KAUST) International Program OCRF-2014-CRG4 and The LIA (Associated International Laboratory) of CNRS NOCOSYM and 'Laboratoire d'Excellence (LABEX)' Saclay Plant Sciences (SPS; ANR-10-LABX-40) and the ANR grant SPLISIL, France.

SUPPLEMENTARY MATERIAL

The Supplementary Material for this article can be found online at: <https://www.frontiersin.org/articles/10.3389/fpls.2018.01209/full#supplementary-material>

FIGURE S1 | (A) Pearson correlation matrix heatmap with dendograms showing the relative distance between each poly(A)+ RNA-seq samples. **(B)** PCA analysis showing the effect of auxin and genotype on the variance between samples.

FIGURE S2 | (A) Proximal and **(B)** distal variant relative abundance normalized to an housekeeping transcript (PP2C). Error bars correspond to ± the standard deviation of three biological replicates. Significance was determined using a Student's *t*-test (***) *p*-value < 0.001).

FIGURE S3 | (A) Pearson correlation matrix heatmap with dendograms showing the relative distance between each sample of the RIP-seq experiments. **(B)** PCA analysis showing the effect the variance between samples.

TABLE S1 | Summary of RNA-seq and RIP-seq data analysis. **(A)** Description of spreadsheet tab. **(B)** Differential gene expression analysis. **(C)** RNA prof analysis. **(D)** Expression and usage of all isoforms from genes containing at least one isoforms switching event. **(E)** NSRa targets identified by RIP. **(F)** Transcription Factor identified in NSRa targets.

TABLE S2 | Sequence of primers used in this study.

Ariel, F., Jegu, T., Latrasse, D., Romero-Barrios, N., Christ, A., Benhamed, M., et al. (2014). Noncoding transcription by alternative RNA polymerases dynamically regulates an auxin-driven chromatin loop. *Mol. Cell* 55, 383–396. doi: 10.1016/j.molcel.2014.06.011

- Bailey-Serres, J., Sorenson, R., and Juntawong, P. (2009). Getting the message across: cytoplasmic ribonucleoprotein complexes. *Trends Plant Sci.* 14, 443–453. doi: 10.1016/j.tplants.2009.05.004
- Bardou, F., Ariel, F., Simpson, C. G., Romero-Barrios, N., Laporte, P., Balzergue, S., et al. (2014). Long noncoding RNA modulates alternative splicing regulators in *Arabidopsis*. *Dev. Cell* 30, 166–176. doi: 10.1016/j.devcel.2014.06.017
- Bray, N. L., Pimentel, H., Melsted, P., and Pachter, L. (2016). Near-optimal probabilistic RNA-seq quantification. *Nat. Biotechnol.* 34, 525–527. doi: 10.1038/nbt.3519
- Brown, J. W., Calixto, C. P., and Zhang, R. (2017). High-quality reference transcript datasets hold the key to transcript-specific RNA-sequencing analysis in plants. *New Phytol.* 213, 525–530. doi: 10.1111/nph.14208
- Deng, X., and Cao, X. (2017). Roles of pre-mRNA splicing and polyadenylation in plant development. *Curr. Opin. Plant Biol.* 35, 45–53. doi: 10.1016/j.pbi.2016.11.003
- Dobin, A., Davis, C. A., Schlesinger, F., Drenkow, J., Zaleski, C., Jha, S., et al. (2013). STAR: ultrafast universal RNA-seq aligner. *Bioinformatics* 29, 15–21. doi: 10.1093/bioinformatics/bts635
- Foley, S. W., Kramer, M. C., and Gregory, B. D. (2017). RNA structure, binding, and coordination in *Arabidopsis*. *Wiley Interdiscip. Rev. RNA* 8:e1426. doi: 10.1002/wrna.1426
- Forzani, C., Carreri, A., de la Fuente van Bentem, S., Lecourieux, D., Lecourieux, F., and Hirt, H. (2011). The *Arabidopsis* protein kinase Pto-interacting 1-4 is a common target of the oxidative signal-inducible 1 and mitogen-activated protein kinases. *FEBS J.* 278, 1126–1136. doi: 10.1111/j.1742-4658.2011.08033.x
- Gagliardi, M., and Matarazzo, M. R. (2016). RIP: RNA immunoprecipitation. *Methods Mol. Biol.* 1480, 73–86.
- Horniyk, C., Terzi, L. C., and Simpson, G. G. (2010). The spen family protein FPA controls alternative cleavage and polyadenylation of RNA. *Dev. Cell* 18, 203–213. doi: 10.1016/j.devcel.2009.12.009
- Huang, P.-Y., Catinot, J., and Zimmerli, L. (2016). Ethylene response factors in *Arabidopsis* immunity. *J. Exp. Bot.* 67, 1231–1241. doi: 10.1093/jxb/erv518
- Kazan, K., and Manners, J. M. (2013). MYC2: the master in action. *Mol. Plant* 6, 686–703. doi: 10.1093/mp/sss128
- Kornblihtt, A. R., de la Mata, M., Fededa, J. P., Munoz, M. J., and Noguez, G. (2004). Multiple links between transcription and splicing. *RNA* 10, 1489–1498.
- Köster, T., and Meyer, K. (2018). Plant ribonomics: proteins in search of RNA partners. *Trends Plant Sci.* 23, 352–365. doi: 10.1016/j.tplants.2018.01.004
- Lawrence, M., Huber, W., Pagès, H., Aboyoun, P., Carlson, M., Gentleman, R., et al. (2013). Software for computing and annotating genomic ranges. *PLOS Comput. Biol.* 9:e1003118. doi: 10.1371/journal.pcbi.1003118
- Lee, K., and Kang, H. (2016). Emerging roles of RNA-binding proteins in plant growth, development, and stress responses. *Mol. Cells* 39, 179–185. doi: 10.14348/molcells.2016.2359
- Li, B., and Dewey, C. N. (2011). RSEM: accurate transcript quantification from RNA-seq data with or without a reference genome. *BMC Bioinformatics* 12:323. doi: 10.1186/1471-2105-12-323
- Liu, F., Marquardt, S., Lister, C., Swiezewski, S., and Dean, C. (2009). Targeted 3' processing of antisense transcripts triggers *Arabidopsis* FLC chromatin silencing. *Science* 327, 94–97.
- Liu, J., Jung, C., Xu, J., Wang, H., Deng, S., Bernad, L., et al. (2012). Genome-wide analysis uncovers regulation of long intergenic noncoding RNAs in *Arabidopsis*. *Plant Cell* 24, 4333–4345. doi: 10.1105/tpc.112.102855
- Love, M. I., Huber, W., and Anders, S. (2014). Moderated estimation of fold change and dispersion for RNA-seq data with DESeq2. *Genome Biol.* 15:550. doi: 10.1101/002832
- Lumbreras, V., Vilela, B., Irar, S., Solé, M., Capellades, M., Valls, M., et al. (2010). MAPK phosphatase MKP2 mediates disease responses in *Arabidopsis* and functionally interacts with MPK3 and MPK6. *Plant J.* 63, 1017–1030. doi: 10.1111/j.1365-313X.2010.04297.x
- Maquat, L. E. (2004). Nonsense-mediated mRNA decay: splicing, translation and mRNP dynamics. *Nat. Rev. Mol. Cell Biol.* 5, 89–99.
- Marondedze, C., Thomas, L., Serrano, N. L., Lilley, K. S., and Gehring, C. (2016). The RNA-binding protein repertoire of *Arabidopsis thaliana*. *Sci. Rep.* 6:29766. doi: 10.1038/srep29766
- Marquardt, S., Raitskin, O., Wu, Z., Liu, F., Sun, Q., and Dean, C. (2014). Functional consequences of splicing of the antisense transcript COOLAIR on FLC transcription. *Mol. Cell* 54, 156–165. doi: 10.1016/j.molcel.2014.03.026
- McClerkin, S. A., Lee, S. G., Harper, C. P., Nwumeh, R., Jez, J. M., and Kunkel, B. N. (2018). Indole-3-acetaldehyde dehydrogenase-dependent auxin synthesis contributes to virulence of *Pseudomonas syringae* strain DC3000. *PLOS Pathog.* 14:e1006811. doi: 10.1371/journal.ppat.1006811
- Mutka, A. M., Fawley, S., Tsao, T., and Kunkel, B. N. (2013). Auxin promotes susceptibility to *Pseudomonas syringae* via a mechanism independent of suppression of salicylic acid-mediated defenses. *Plant J.* 74, 746–754. doi: 10.1111/tpj.12157
- Ner-Gaon, H., Halachmi, R., Savaldi-Goldstein, S., Rubin, E., Ophir, R., and Fluhr, R. (2004). Intron retention is a major phenomenon in alternative splicing in *Arabidopsis*. *Plant J.* 39, 877–885.
- Nishtala, S., Neelamraju, Y., and Janga, S. C. (2016). Dissecting the expression relationships between RNA-binding proteins and their cognate targets in eukaryotic post-transcriptional regulatory networks. *Sci. Rep.* 6:25711. doi: 10.1038/srep25711
- Oliveira, C., Faoro, H., Alves, L. R., and Goldenberg, S. (2017). RNA-binding proteins and their role in the regulation of gene expression in *Trypanosoma cruzi* and *Saccharomyces cerevisiae*. *Genet. Mol. Biol.* 40, 22–30. doi: 10.1590/1678-4685-GMB-2016-0258
- Pandey, S. P., and Somssich, I. E. (2009). The role of WRKY transcription factors in plant immunity. *Plant Physiol.* 150, 1648–1655.
- Raczynska, K. D., Simpson, C. G., Ciesiolka, A., Szewc, L., Lewandowska, D., McNicol, J., et al. (2010). Involvement of the nuclear cap-binding protein complex in alternative splicing in *Arabidopsis thaliana*. *Nucleic Acids Res.* 38, 265–278. doi: 10.1093/nar/gkp869
- Raczynska, K. D., Stepien, A., Kierzkowski, D., Kalak, M., Bajczyk, M., McNicol, J., et al. (2014). The SERRATE protein is involved in alternative splicing in *Arabidopsis thaliana*. *Nucleic Acids Res.* 42, 1224–1244. doi: 10.1093/nar/gkt894
- Romero-Barrios, N., Legascue, M. F., Benhamed, M., Ariel, F., and Crespi, M. (2018). Splicing regulation by long noncoding RNAs. *Nucleic Acids Res.* 46, 2169–2184. doi: 10.1093/nar/gky095
- Sorenson, R., and Bailey-Serres, J. (2014). Selective mRNA sequestration by oligouridylate-binding protein 1 contributes to translational control during hypoxia in *Arabidopsis*. *Proc. Natl. Acad. Sci. U.S.A.* 111, 2373–2378. doi: 10.1073/pnas.1314851111
- Tran, V. D. T., Souiai, O., Romero-Barrios, N., Crespi, M., and Gautheret, D. (2016). Detection of generic differential RNA processing events from RNA-seq data. *RNA Biol.* 13, 59–67. doi: 10.1080/15476286.2015.1118604
- Trapnell, C., Roberts, A., Goff, L., Pertea, G., Kim, D., Kelley, D. R., et al. (2012). Differential gene and transcript expression analysis of RNA-seq experiments with TopHat and Cufflinks. *Nat. Protoc.* 7, 562–578. doi: 10.1038/nprot.2012.016
- Vitting-Seerup, K., and Sandelin, A. (2017). The landscape of isoform switches in human cancers. *Mol. Cancer Res.* 15, 1206–1220. doi: 10.1158/1541-7786.MCR-16-0459
- Warnes, G. R., Bolker, B., Bonebakker, L., Gentleman, R., Huber, W., Liaw, A., et al. (2009). *gplots: Various R programming Tools for Plotting Data. R Package Version 2.*
- Whittaker, C., and Dean, C. (2017). The FLC locus: a platform for discoveries in epigenetics and adaptation. *Annu. Rev. Cell Dev. Biol.* 33, 555–575. doi: 10.1146/annurev-cellbio-100616-060546
- Zhang, R., Calixto, C. P. G., Marquez, Y., Venhuizen, P., Tzioutziou, N. A., Guo, W., et al. (2017). A high quality *Arabidopsis* transcriptome for accurate transcript-level analysis of alternative splicing. *Nucleic Acids Res.* 45, 5061–5073. doi: 10.1093/nar/gkx267

Conflict of Interest Statement: The authors declare that the research was conducted in the absence of any commercial or financial relationships that could be construed as a potential conflict of interest.

Copyright © 2018 Bazin, Romero, Rigo, Charon, Blein, Ariel and Crespi. This is an open-access article distributed under the terms of the Creative Commons Attribution License (CC BY). The use, distribution or reproduction in other forums is permitted, provided the original author(s) and the copyright owner(s) are credited and that the original publication in this journal is cited, in accordance with accepted academic practice. No use, distribution or reproduction is permitted which does not comply with these terms.

2.1.4 Complementary results

This article shows that NSRs impact the transcriptome in response to auxin, especially via the regulation of defense response genes expression. Furthermore, NSRa was found to bind hundreds of RNAs, a third of them having also their expression regulated by NSRs. Surprisingly, a significant portion of these mRNA targets are known to be involved in plant immune responses, suggesting a putative role of NSRs in the establishment of plant defenses to biotic stresses.

In order to assess the role of these RBPs in plant immunity, I performed some additional experiments. The sensing of biotic stresses by the plant is highly complex and involves various signaling networks, one of them being the sensing of PAMPs such as flagellin peptide 22 (flg22) (Boller and Felix, 2009). A simple way to mimic a bacterial attack consists in the addition of flg22 into the plant growth media, therefore triggering defense responses in whole seedlings, leaves and roots. (Zipfel et al., 2004; Millet et al., 2010). *NSRb* expression was already characterized as being responsive to an auxin stimulus (Bardou et al., 2014). Since NSRs regulate the expression of auxin and immune response related transcripts, the regulation of their expression after a biotic stimulus was explored. Interestingly, *NSRb* expression was also significantly induced by flg22 perception, reaching a plateau after 3h of treatment (Figure 10B). As occurred for an auxin stimulus, *NSRa* expression stayed unchanged after flg22 addition (Figure 10A).

Moreover, flg22 strongly affects root growth and architecture mainly due to the defined trade-off between immune and hormonal signaling (Gomez-Gomez et al., 1999; Navarro et al., 2008; Lozano-Duran et al., 2013). Hence, the root architecture of *nsr* single and double mutants was analyzed when grown in media supplemented with various concentrations of flg22 (Figure 10C, 10D, 10E). The *nsr* single mutants do not exhibit any significant growth defects when grown in control conditions, whereas *nsra/b* double mutants develop fewer lateral roots than the WT, leading to a reduced lateral root density. This phenotype was already described in Bardou et al, 2014 and was accentuated by an auxin treatment. When grown in media supplemented with 0,1µM of flg22, *nsra* and *nsra/b* grow a shorter primary root compared to the WT (Figure 10C), whereas *nsrb* forms less LRs (Figure 10D). These defects result in a reduced LR density for all genotypes (Figure 10E). With a higher flg22 concentration in the media, *nsrb* and *nsra/b* develop less LRs than the WT. The *nsra/b* double mutant shows a significant reduction in LR density, stronger than the one observed in *nsr* single mutants (Figure 10C, 10D, 10E). This additive phenotype suggests that even if *NSRb* is the only one to have its expression regulated by flg22, both *NSRa* and *NSRb* participate in the establishment of the plant response to flg22.

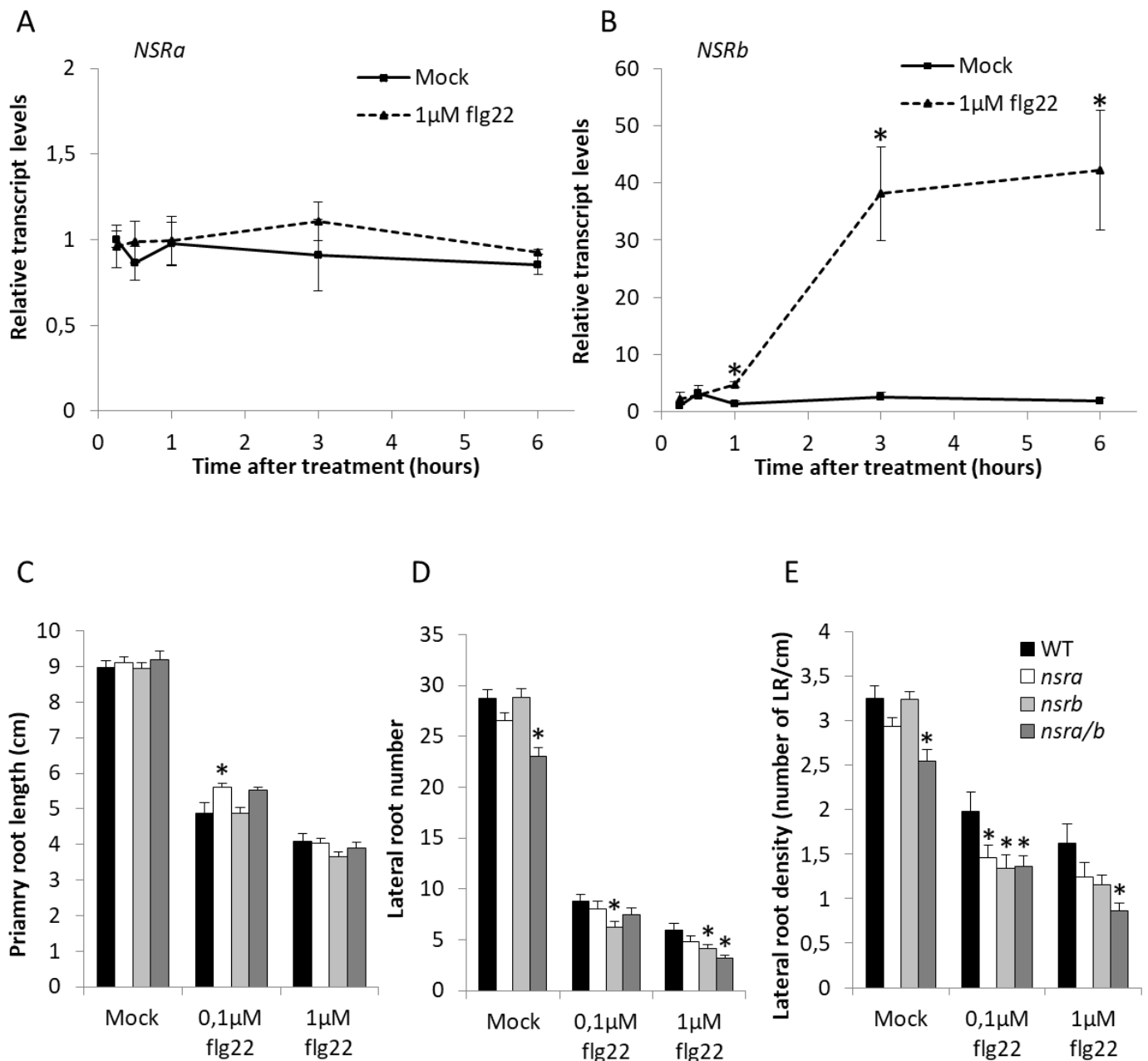


Figure 10. *nsr* mutants exhibit an altered response to flg22.

A, B. Time-course analysis of *NSRa* (A) and *NSRb* (B) transcript levels in WT after a flg22 treatment. RNAs were extracted from 11-day-old WT roots. The asterisk (*) indicates a significant difference as determined by Student's t test ($P < 0,05$, $n = 3$). Error bars show mean \pm standard deviation.

C, D, E. Mean of primary root length (C), lateral root number (D) and lateral root density (E) of WT, *nsra*, *nsrb* and *nsra/b* mutant lines 9 days after transfer in 1/2MS supplemented with various flg22 concentrations. The asterisk (*) indicates a significant difference as determined by Student's t test ($P < 0,05$, $n \geq 22$).

Error bars show mean \pm standard error.

The sensing of PAMPs by the plant represents one of many mechanisms occurring during defense responses. To go further in the understanding of NSRs role in plant immunity, an analysis of *NSR*s expression upon pathogen infection was conducted (Figure 11A, 11B, 11C, 11D). By searching among publicly available data on the Genevestigator database, we could find that *NSRb* but not *NSRa* expression was highly induced by the infection of various pathogens, including different *Pseudomonas syringae* strains (Figure 11A, 11B). *Pseudomonas syringae* is a major plant pathogen, infecting a wide range of species. This bacterial hemibiotroph initiates the infection with an epiphytic phase upon arrival on the surface of the plant, followed by an endophytic phase in the apoplast. The bacteria enter the plant through natural openings such as stomata or accidental wounds (Beattie and Lindow, 1995; Hirano and Upper, 2000; Melotto et al., 2006). *NSRb* expression is induced about 4 times after 1h of infection with *Pseudomonas syringae* pv. *Tomato* (*Pst*) DC3000 (Figure 11A). 1h of flg22 treatment induced a similar induction of *NSRb* expression, suggesting that PAMP sensing may be one of the stimuli triggering *NSRb* induction. Moreover, the *Pseudomonas syringae* strain pv. *maculicola* (*Psm*) ES4326 was found to increase *NSRb* expression by 25 times, here in non-inoculated upper rosette leaves 48h after infection (Figure 11B). This suggests that *NSRb* expression is also induced at a systemic scale, and could be dependent on the immunity state of the plant. *Psm* ES4326 was shown to induce more severe infection reactions compared to *Pst* DC3000, including higher SA accumulation in the plant and a larger number of genes with deregulated expression after infection (Wang et al., 2008). The higher induction of *NSRb* caused by the infection with *Psm* ES4326 may be linked to the plant's higher sensitivity to this strain.

The fungal pathogen *Botrytis cinerea* was also shown to induce *NSRb* expression 14h after infection (Figure 11C). This pathogen is considered the second most important fungal plant pathogen and serves as a model for necrotrophic fungi (Dean et al., 2012; van Kan 2006). It uses a wide range of toxins (Williamson et al., 2007) as well as the plant's own defense system to attack plant cells (Govrin et al., 2006). Finally, the infection by the oomycete *Phytophthora parasitica*, a biotrophic pathogen with a wide spectrum of host's expression, was also found to increase *NSRb* expression (Figure 11D). All of these transcriptomic data tend to show that *NSRb* expression is regulated by defense signals that are common to a wide range of biotic stimuli, rather than being regulated by a specific pathogen. *NSRb* responds to infection by bacteria, fungi and oomycetes, and this independently of their infection strategy suggesting a wide role in plant defense.

Since *NSRb* expression was upregulated by various types of pathogen infections, the *nsr* mutants were used to assess NSRs involvement in defense responses. First, the *Pst* DC3000 strain was used to test *nsr* mutant response to a hemibiotrophic pathogen (this

strain was kindly provided by Sophie Piquerez from Moussa Benhamed's lab). 5 week-old rosettes were either sprayed or inoculated with a bacterial solution containing *Pst* DC3000 strain. 48h after infection the *nsra/b* double mutant displayed some lesion areas that could not be observed in the WT (Figure 11E). Moreover, *Pst* DC3000 strain displayed a higher growth in *nsra/b* leaves compared to WT, suggesting that this mutant is more sensitive to this pathogen (Figure 11F). A similar result was obtained after direct inoculation with the bacterial solution, where the *nsra/b* double mutant exhibited once again a significantly lower resistance to the pathogen (Figure 11G). The *nsra/b* mutant exhibits a higher sensitivity to *Pst* DC3000 either after spraying or direct inoculation with the bacteria, suggesting that its sensitivity does not rely on the entry of the bacteria into the plant. These results also indicate that the absence of both *NSRa* and *NSRb* impairs the proper immune response of the plant and leads to a higher proliferation of *Pst* DC3000 inside plant cells.

After assessing their sensitivity to a bacterial hemibiotroph, the *nsr* mutants were subjected to an infection with the necrotrophic fungi *Botrytis cinerea* (kindly provided by Gwilherm Brisou from Abdel Bendahmane's lab). This time the *nsra*, *nsrb* and *nsra/b* mutants were subjected to infection with a *B. cinerea* spore suspension. All mutant lines displayed larger lesion areas compared to the WT, the double mutant exhibiting an additive phenotype with more severe lesions and a broader yellow infection zone (Figure 11H, 11I). Here, the mutation of one of the *NSRs* is sufficient to induce higher sensitivity to the fungi, meanwhile the double mutant's additive phenotype pinpoints the synergy of both *NSRs* in defense response establishment. Even though *NSRb* is the only one to have its expression regulated by biotic stimulus, both *NSRa* and *NSRb* seem to participate in the immune response and allow the plant to better cope with a pathogen attack. In the presence of PAMPs, *NSRs* participate in the maintenance of root growth and could therefore represent a new splicing regulator governing the plant growth / defense balance.

2.1.5 Discussion

NSRs were firstly described as SFs playing a role in the auxin response, binding to auxin-related transcripts and allowing their proper splicing (Bardou et al 2014). Bazin and colleagues (2018) have shown that *NSRs* participate in the reshaping of the plant transcriptome in response to auxin, and bind to a significant portion of the transcripts they regulate. Curiously, several of these targets are mainly associated with the immune response of the plant (Figure 12).

Plant immunity is intrinsically linked to phytohormone signaling in the plant (Pieterse et al., 2012). Pathogens have developed numerous ways to take advantage of their hosts,

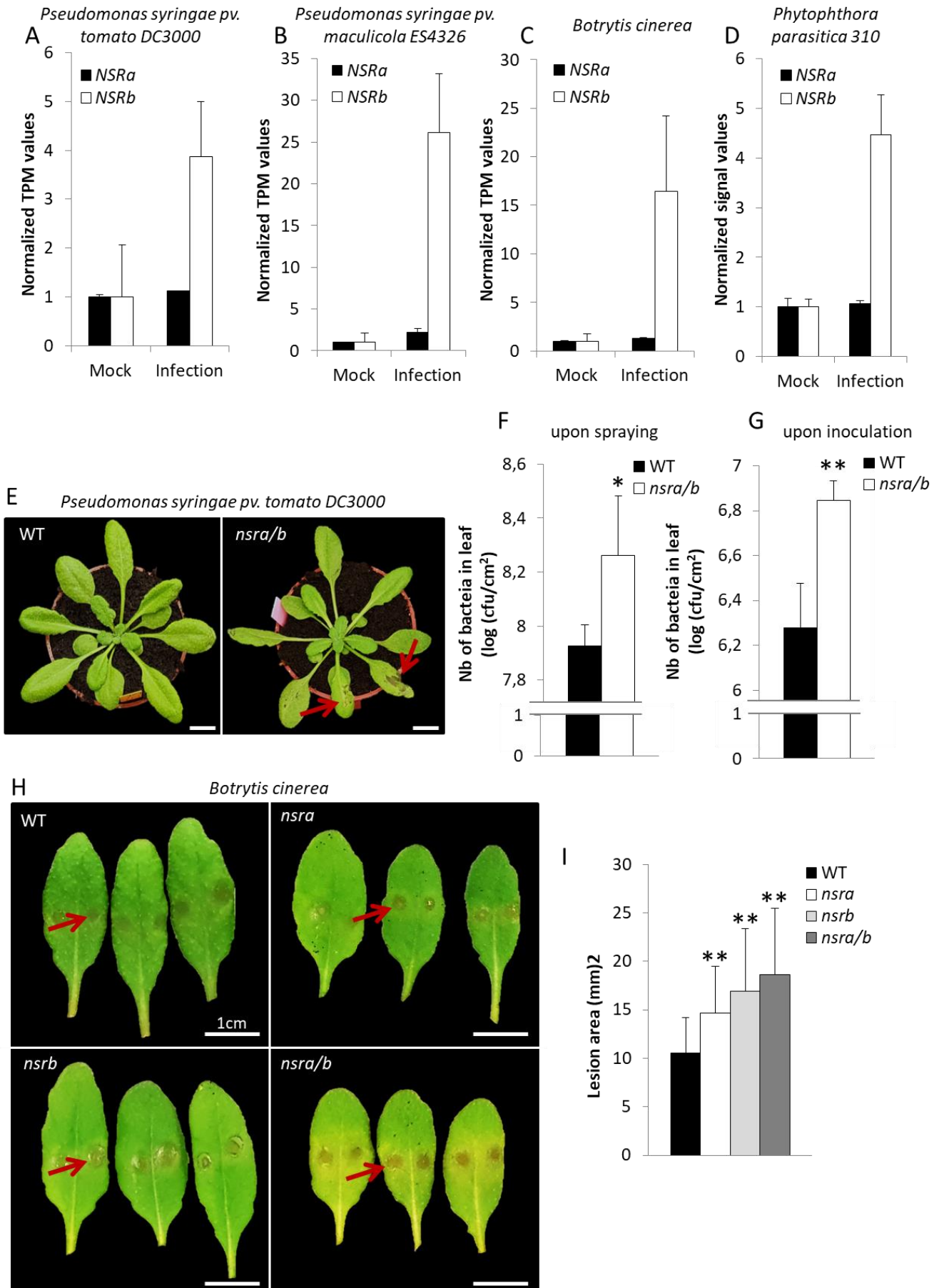


Figure 11. NSRs participate in the plant response to pathogens.

A, B, C, D. Normalized TPM (A, B, C) or signal (D) values for *NSRa* and *NSRb* upon infection with various pathogens retrieved from the Genevestigator database (<https://genevestigator.com/>). Expression values for both mock inoculation and pathogen infection are displayed. Error bars show mean \pm standard deviation.

E. Representative picture of 5-week-old WT and *nsra/b* rosettes sprayed with a *Pseudomonas syringae* pv. *tomato strain DC3000* suspension (OD = 0,1). Pictures were taken 48h after the spraying. Scale bars correspond to 1cm. Red arrows pinpoint disease lesions.

F. Growth of *Pseudomonas syringae* pv. *tomato strain DC3000* in rosette leaves. 5-week-old WT and *nsra/b* rosettes were sprayed with either a bacterial suspension (OD = 0,1) or with a mock solution. Leaf disks were harvested 2 days after the spraying.

G. Growth of *Pseudomonas syringae* pv. *tomato strain DC3000* in rosette leaves. 5-week-old WT and *nsra/b* rosettes were inoculated with either a bacterial suspension (OD = 0,001) or with a mock solution. Leaf disks were harvested 2 dpi.

In F and G, the quantification corresponds to the number of bacteria per square cm of leaf surface. Error bars show mean \pm standard deviation. The asterisks (*, **) indicate a significant difference as determined by Student's t-test (respectively: * $P < 0,05$; ** $P < 5 \times 10^{-4}$; $n = 6$).

H. Representative picture of 5-week-old WT, *nsra*, *nsrb* and *nsra/b* rosettes treated with a *Botrytis cinerea* spore suspension (5×10^{-5} spores per mL). Pictures were taken 2dpi. Scale bars correspond to 1cm. Red arrows pinpoint disease lesions.

I. Lesion area measurements on rosette leaves infected by *B. cinerea*. 5-week-old WT, *nsra*, *nsrb* and *nsra/b* rosettes were treated with either a *B. cinerea* spore suspension (5×10^{-5} spores per mL) or with a mock solution. Lesion areas were measured 2dpi using ImageJ package (<https://imagej.nih.gov/ij/>).

In F and D, error bars show mean \pm standard deviation. The asterisks (**) indicate a significant difference as determined by Student's t-test (** $P < 5 \times 10^{-4}$; $n \geq 42$).

notably by using effectors to rewire these signaling circuitries, and to suppress or evade plant's immune response. Jasmonic acid (JA) and salicylic acid (SA) are considered as the major immunity hormones, and usually exhibit antagonistic effects (Figure 12). JA is mainly produced upon infection by necrotrophs or herbivore attacks, whereas SA allows the plant to survive biotrophic infection (Browse 2009, Vlot et al., 2009). However, auxins were shown to modulate the plant immune signaling network as well (Kazan & Manners 2009). They act as essential virulence factors for gall-forming pathogens and root-associated bacteria (Spaepen and Vanderleyden, 2011). Nevertheless, their importance was also described during infection by leaf spotting pathogens such as the strains regulating *NSRb* expression: *Pst* DC3000 and *Psm* ES4326 (Chen et al., 2007; Mutka et al., 2013; Navarro et al., 2006; Wang et al., 2007). Host auxin signaling is required for normal susceptibility to *Pst* DC3000 and participates in the suppression of SA-mediated defenses. Indeed, impaired auxin perception leads to increased bacterial growth levels, mainly due to increased auxin levels and decreased SA-mediated responses (Djami-Tchatchou et al., 2020). Similarly, SA was demonstrated to repress auxin signaling, notably by stabilizing Aux/IAA auxin-response repressors (Figure 12) (Wang et al., 2007). Another study demonstrated that blocking auxin signaling either through mutations in the auxin pathway or by pharmacological interference with the auxin response impairs resistance to the necrotroph *B. cinerea* (Llorente et al., 2008).

JA is the main hormone participating in the response to necrotrophs, and shares a similar signaling pathway with auxin. Many studies have therefore shown that auxin promotes JA signaling, and reversely (Figure 12) (Yang et al., 2019). The *nsra/b* mutant exhibits a reduced sensitivity to auxin which leads to an altered root architecture (Bardou et al., 2014). This impaired auxin sensitivity could explain the *nsr* mutants higher sensitivity to infection by various pathogens. Since the *nsra/b* mutant was more sensitive to both hemibiotrophic and necrotrophic pathogens, it would be interesting to investigate its resistance to purely biotrophic pathogens such as *Phytophthora parasitica*, which was already found to regulate *NSRb* expression. Knowing the connection between auxins, JA and SA, the analysis of *NSR* expression changes in signaling mutants of these phytohormone pathways would help understanding in which steps of the immune response *nsr* mutants are affected. Furthermore, it would be helpful to test the application of exogenous SA or JA and see if it could restore a WT pathogen resistance in *nsr* mutants.

There is a growing number of studies showing the importance of splicing factors in the regulation of plant immune responses (Rigo et al., 2019). NSRs are not core components of the spliceosome machinery and are therefore not essential for the splicing process itself. However, they were shown to regulate both expression and splicing of a large set of defense

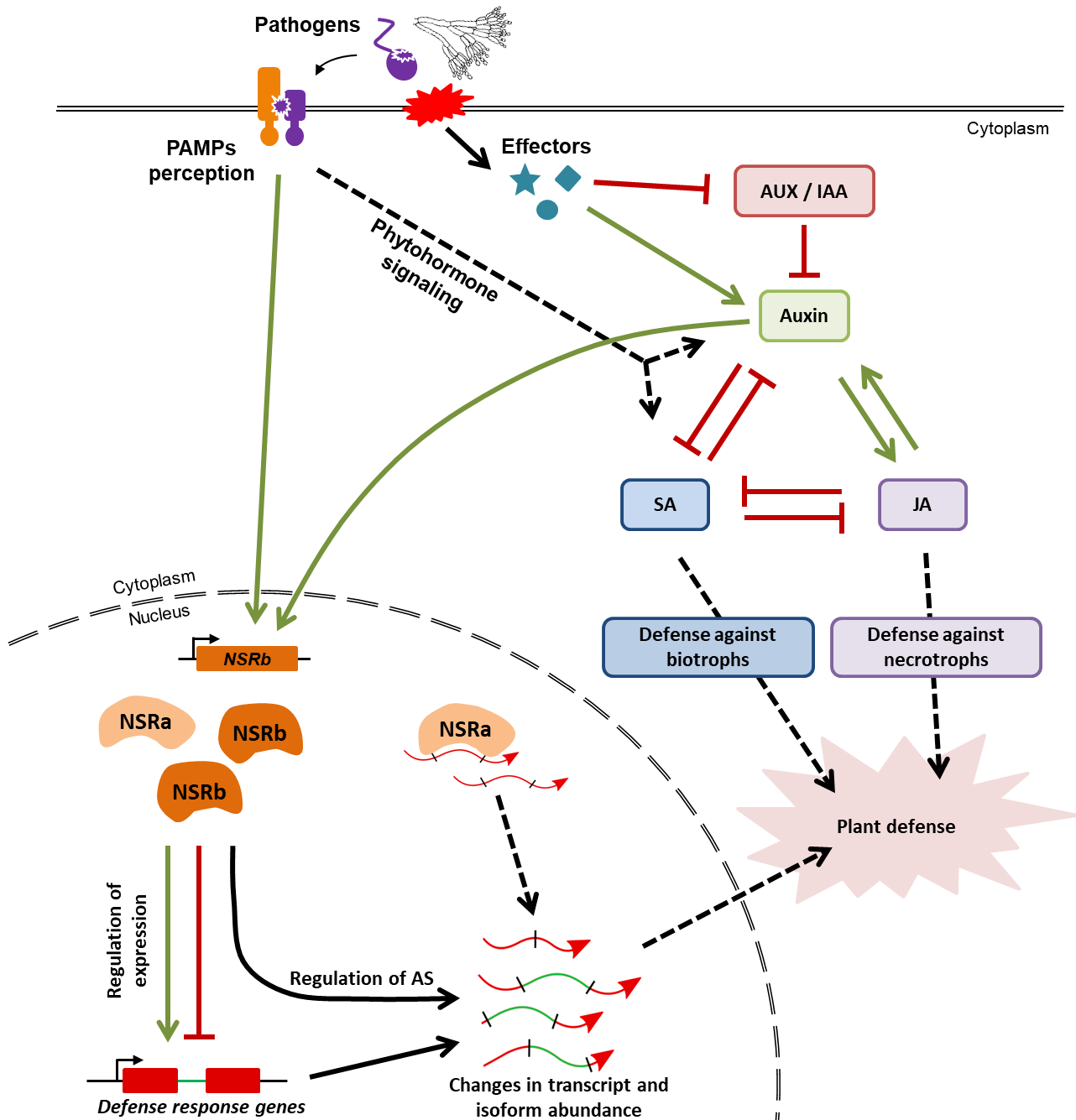


Figure 12. NSRs and their involvement in plant defense responses.

Pathogens harbor PAMPs that are perceived by plant cells, leading to changes in phytohormone balance. The perception of flg22, a bacterial PAMP, leads to *NSRb* induction. Pathogens can also inject effectors into plants cells in order to alter plant defense responses. These effectors can repress Aux/IAA inhibitors, causing an increase in auxin accumulation and associated auxin signaling. Auxin stimuli also induces *NSRb* expression. Auxin and salicylic acid (SA) are mutually antagonistic, as SA and jasmonic acid (JA) which respectively induce defenses against biotrophs and necrotrophs. On the contrary, JA and auxin signals mutually induce each other. NSRa and NSRb both contribute to proper expression and splicing of defense and auxin responsive genes. NSRa directly recognizes a subset of defense response genes, potentially affecting their steady state abundance. NSRs therefore shape a dynamic pool of transcripts related to auxin and defense responses, which contributes to the proper establishment of plant defenses against pathogens.

related genes in the presence of auxin. Hence, these SR proteins may represent one of the actors gathering auxin signaling and defense responses.

Interestingly, NSR function was found to be regulated by their interaction with the lncRNA *ASCO*, notably during the plant response to auxin (Bardou et al., 2014). *ASCO* is able to hijack NSRs and alter their binding to their mRNA targets. In the article presented in this chapter, NSRa was also found to bind to a subset of other lncRNAs. Indeed, 53 (15% of total targets) of NSRa transcript targets were characterized as lncRNAs. The NSRs could therefore represent one of the integrators of plant stress signals via their binding to various non-coding transcripts, whose expression is known to be highly stress- and cell-specific. By their abundance and/or their interactions with lncRNAs, NSRs could fine-tune the expression and splicing changes of many stress-related genes. This would allow the plant to reshape its transcriptome for the better, and to adapt to its changing environment.

2.1.6 Materials and Methods

2.1.6.1 Plant material and growth conditions

All mutants were in the Columbia-0 (Col-0) background. For all plant pathogen experiments, plants were grown on soil in short day conditions (8h light/16 h dark) at 20°C.

2.1.6.2 Infection tests

For bacterial infection tests, the *Pseudomonas syringae* pv. *tomato* DC3000 (*Pst* DC300) strain was used. *Pst* DC3000 cultures were grown at 30 °C on selective media (NYGA medium supplemented with 100 µg/ml rifampicin). On the day of the infection, overnight cultures were centrifuged, washed and resuspended in 10 mM MgCl₂. The bacterial suspension was adjusted to either OD₆₀₀ = 0,1 for spraying assay or OD₆₀₀ = 0,001 for inoculation. The ODs were adjusted in a 10 mM MgCl₂ + 0.04% Silwet-L-77 solution. 5-week-old plants were either sprayed with the *Pst* DC3000 suspension until completely covered or infiltrated with the solution using a 1-mL syringe. 2 leaves were infiltrated per plant. Plants were left for incubation for 2 days in a saturating humidity environment. For the determination of bacterial population, 2 leaf disks (1cm²) were collected from 6 plants for each genotype and for each treatment. Leaf disks were ground and 800µL of 10 mM MgCl₂ solution was added to the samples. The resulting bacterial suspension was serially diluted 1:10 and plated on selective NYGA media. Bacterial populations were determined as log of colony forming units (cfu) per leaf area (cm²) 2-days post inoculation. For infection tests by fungi, *Botrytis cinerea* was used for the infection. *Botrytis cinerea* was grown in Petri dishes containing

Potato Dextrose Agar (PDA) for 2 weeks at 21°C in the dark. Spore inoculums were prepared by harvesting spores at the surface of the Petri dish by adding Potato Dextrose Broth (PDB). The spore suspension was filtered through Miracloth (Merck) to remove hyphae and was adjusted to a concentration of 5×10^5 spores/mL. Plants were inoculated by depositing 5 µL droplets of the spore suspension on top of leaves. 2 droplets of spore suspension were deposited per leaf, 3 leaves were inoculated per plant and 8 plants were inoculated per genotype. Inoculated plants were maintained at high humidity with a transparent cover in the growth chamber, and symptom development was observed at 2 dpi. Lesion areas were measured for each infected spot using the ImageJ package (<https://imagej.nih.gov/ij/>).

2.1.6.3 Root growth analysis

For analysis of flagellin impact on root architecture, plants were previously grown 5 days on solid 1/2MS medium + 1% sucrose and then transferred for additional 9 days in liquid 1/2MS media + 1% sucrose supplemented or not with 0,1 µM or 1 µM of synthetic flg22 peptide (GeneCust). For each plantlet, lateral roots were counted, and the primary root length was measured using the RootNav software (Pound et al., 2013). Experiments were done at least two times, with a minimum of 22 plants per genotype and condition. Statistical tests were performed using the Student's T-test ($P < 0,05$) using wild-type values as reference.

2.1.6.4 RNA extraction and RT-qPCR analyses

Total RNA was extracted using Quick-RNA Kit (ZYMO RESEARCH), and DNase treatment was performed according to the manufacturer's protocol. One µg of DNase-free RNA was reverse transcribed using Maxima H Minus Reverse Transcriptase (Thermo Scientific). cDNA was then amplified in RT-qPCRs using LightCycler 480 SYBR Green I Master (Roche) and transcript-specific primers on a Roche LightCycler 480 thermocycler following standard protocol (45 cycles, 60°C annealing). Experiments were done in biological triplicates with at least three technical replicates. Expression was normalized to 2 constitutive genes (AT1G13320 and AT4G26410) (Czechowski et al., 2005). For analysis of gene expression after a flg22 kinetic, plants were previously grown 9 days on solid 1/2MS medium + 1% sucrose and then transferred for additional 24 h in liquid 1/2MS medium + 1% sucrose before adding or not 1 µM of flg22. Roots from 8 plants were pooled for each replicate. Error bars on qRT-PCR experiments represent standard deviations, and significant differences were determined using Student's t-test ($P \leq 0,05$, $n \geq 3$ biological replicates). All the used primers are listed in the Table 1.

Table 1
List of primers used for RT-qPCR in Chapter 1

	AGI	Gene	Oligo Sequence	Reference / Information
RT-qPCR	AT1G13320	<i>Housekeeping ref 1 PP2A F</i>	TAACGTGGCCAAAATGATGC	Czechowski et al., 2005
	AT1G13320	<i>Housekeeping ref 1 PP2A R</i>	GTTCTCCACAACCGCTTGGT	Czechowski et al., 2005
	AT4G26410	<i>Housekeeping ref 2 F</i>	GAGCTGAAGTGGCTTCCATGAC	Czechowski et al., 2005
	AT4G26410	<i>Housekeeping ref 2 R</i>	GGTCCGACATACCCATGATCC	Czechowski et al., 2005
	AT1G76940	<i>NSRa F</i>	CTCAGGGACATTGTGGTACG	
	AT1G76940	<i>NSRa R</i>	CTACACTCTCCGCGCATCTT	
	AT1G21320	<i>NSRb F</i>	GAGGATCGAGGTATCCCCCA	
	AT1G21320	<i>NSRb R</i>	CATTAATGGACCAGCTTCTTCAGA	

2.1.6.5 Expression data

All the data were retrieved from the Genevestigator database (<https://genevestigator.com/>). ArrayExpress identifiers are indicated for each experiment. For data from infection with *Pst* DC3000, rosette leaves from Col-0 6 week-old plants were inoculated with either *Pst* DC3000 carrying empty vector pVSP61 or with a Mock solution. The infiltrated leaves were harvested 1h after the inoculation (AT-00742). For data from infection with *Pseudomonas syringae* pv. *maculicola* ES4326, 5- to 6-week-old Col-0 plants were inoculated with *Psm* ES4326 by infiltrating bacterial suspension (OD600 = 0,005; 1.6×10^6 cfu/mL) into three lower rosette leaves of each plant. The plants were incubated for 48h and then non-inoculated upper rosette leaves were harvested (AT-00744). For data from infection with *Botrytis cinerea*, rosette leaves from Col-0 28 day-old plants were sprayed with either a *Botrytis cinerea* spore suspension ($2,5 \times 10^5$ spores/mL) or with a Mock solution. Infected leaves were harvested 14h after the spraying (AT-00736). For data from infection with *Phytophthora parasitica*, Col-0 plants were grown for 15 days on agar medium (1xMS, 1% sucrose, 2% agar) then for 1 month in new Petri dishes containing a strip of 1xMS agar medium underneath 10 mL of liquid 0,1xMS medium, under short day (8h light / 16h dark) at 25°C. Col-0 roots were inoculated with *Phytophthora parasitica* 310 strain (10^6 zoospores per Petri dish with 10 plants) and collected 30h after infection (AT-00425).

2.1.7 References

- Bardou F, Ariel F, Simpson CG, Romero-Barrios N, Laporte P, Balzergue S, Brown JWS, Crespi M** (2014) Long noncoding RNA modulates alternative splicing regulators in Arabidopsis. *Dev Cell* **30**: 166–176
- Bazin J, Romero N, Rigo R, Charon C, Blein T, Ariel F, Crespi M** (2018) Nuclear Speckle RNA Binding Proteins Remodel Alternative Splicing and the Non-coding Arabidopsis Transcriptome to Regulate a Cross-Talk Between Auxin and Immune Responses. *Front Plant Sci* **9**: 1209
- Beattie GA, Lindow SE** (1995) The secret life of foliar bacterial pathogens on leaves. *Annu Rev Phytopathol* **33**: 145–172
- Boller T, Felix G** (2009) A renaissance of elicitors: perception of microbe-associated molecular patterns and danger signals by pattern-recognition receptors. *Annu Rev Plant Biol* **60**: 379–406
- Browse J** (2009) Jasmonate passes muster: a receptor and targets for the defense hormone. *Annu Rev Plant Biol* **60**: 183–205
- Chen Z, Agnew JL, Cohen JD, He P, Shan L, Sheen J, Kunkel BN** (2007) *Pseudomonas syringae* type III effector AvrRpt2 alters Arabidopsis thaliana auxin physiology. *Proc Natl Acad Sci U S A* **104**: 20131–20136
- Czechowski T, Stitt M, Altmann T, Udvardi MK, Scheible W-R** (2005) Genome-Wide Identification and Testing of Superior Reference Genes for Transcript Normalization in Arabidopsis. *Plant Physiol* **139**: 5–17
- Dean R, Van Kan JAL, Pretorius ZA, Hammond-Kosack KE, Di Pietro A, Spanu PD, Rudd JJ, Dickman M, Kahmann R, Ellis J, et al** (2012) The Top 10 fungal pathogens in molecular plant pathology. *Mol Plant Pathol* **13**: 414–430
- Djami-Tchatchou AT, Harrison GA, Harper CP, Wang R, Prigge MJ, Estelle M, Kunkel BN** (2020) Dual Role of Auxin in Regulating Plant Defense and Bacterial Virulence Gene Expression During *Pseudomonas syringae* PtoDC3000 Pathogenesis. *Mol Plant-Microbe Interact* **33**: 1059–1071
- Gómez-Gómez L, Felix G, Boller T** (1999) A single locus determines sensitivity to bacterial flagellin in Arabidopsis thaliana. *Plant J* **18**: 277–284
- Govrin EM, Rachmilevitch S, Tiwari BS, Solomon M, Levine A** (2006) An Elicitor from *Botrytis cinerea* Induces the Hypersensitive Response in Arabidopsis thaliana and Other Plants and Promotes the Gray Mold Disease. *Phytopathology* **96**: 299–307
- Hirano SS, Upper CD** (2000) Bacteria in the leaf ecosystem with emphasis on *Pseudomonas syringae*-a pathogen, ice nucleus, and epiphyte. *Microbiol Mol Biol Rev* **64**: 624–653
- Kazan K, Manners JM** (2009) Linking development to defense: auxin in plant-pathogen interactions. *Trends Plant Sci* **14**: 373–382
- Lee K, Kang H** (2016) Emerging Roles of RNA-Binding Proteins in Plant Growth, Development, and Stress Responses. *Mol Cells* **39**: 179–185
- Llorente F, Muskett P, Sánchez-Vallet A, López G, Ramos B, Sánchez-Rodríguez C, Jordá L, Parker J, Molina A** (2008) Repression of the auxin response pathway increases Arabidopsis susceptibility to necrotrophic fungi. *Mol Plant* **1**: 496–509

- Lozano-Durán R, Macho AP, Boutrot F, Segonzac C, Somssich IE, Zipfel C** (2013) The transcriptional regulator BZR1 mediates trade-off between plant innate immunity and growth. *Elife* **2**: e00983
- Melotto M, Underwood W, Koczan J, Nomura K, He SY** (2006) Plant stomata function in innate immunity against bacterial invasion. *Cell* **126**: 969–980
- Millet YA, Danna CH, Clay NK, Songnuan W, Simon MD, Werck-Reichhart D, Ausubel FM** (2010) Innate Immune Responses Activated in *Arabidopsis* Roots by Microbe-Associated Molecular Patterns. *Plant Cell* **22**: 973 LP-990
- Mutka AM, Fawley S, Tsao T, Kunkel BN** (2013) Auxin promotes susceptibility to *Pseudomonas syringae* via a mechanism independent of suppression of salicylic acid-mediated defenses. *Plant J* **74**: 746–754
- Navarro L, Dunoyer P, Jay F, Arnold B, Dharmasiri N, Estelle M, Voinnet O, Jones JDG** (2006) A plant miRNA contributes to antibacterial resistance by repressing auxin signaling. *Science* **312**: 436–439
- Navarro L, Bari R, Achard P, Lisón P, Nemri A, Harberd NP, Jones JDG** (2008) DELLAs control plant immune responses by modulating the balance of jasmonic acid and salicylic acid signaling. *Curr Biol* **18**: 650–655
- Pieterse CMJ, Van der Does D, Zamioudis C, Leon-Reyes A, Van Wees SCM** (2012) Hormonal modulation of plant immunity. *Annu Rev Cell Dev Biol* **28**: 489–521
- Pound MP, French AP, Atkinson JA, Wells DM, Bennett MJ, Pridmore T** (2013) RootNav: navigating images of complex root architectures. *Plant Physiol* **162**: 1802–1814
- Rigo R, Bazin J, Crespi M, Charon C** (2019) Alternative Splicing in the Regulation of Plant–Microbe Interactions. *Plant Cell Physiol*. doi: 10.1093/pcp/pcz086
- Spaepen S, Vanderleyden J** (2011) Auxin and plant-microbe interactions. *Cold Spring Harb Perspect Biol*. doi: 10.1101/cshperspect.a001438
- van Kan JAL** (2006) Licensed to kill: the lifestyle of a necrotrophic plant pathogen. *Trends Plant Sci* **11**: 247–253
- Vlot AC, Dempsey DA, Klessig DF** (2009) Salicylic Acid, a multifaceted hormone to combat disease. *Annu Rev Phytopathol* **47**: 177–206
- Wang D, Pajerowska-Mukhtar K, Culler AH, Dong X** (2007) Salicylic Acid Inhibits Pathogen Growth in Plants through Repression of the Auxin Signaling Pathway. *Curr Biol* **17**: 1784–1790
- Wang L, Mitra RM, Hasselmann KD, Sato M, Lenarz-Wyatt L, Cohen JD, Katagiri F, Glazebrook J** (2008) The genetic network controlling the *Arabidopsis* transcriptional response to *Pseudomonas syringae* pv. *maculicola*: roles of major regulators and the phytotoxin coronatine. *Mol Plant Microbe Interact* **21**: 1408–1420
- Williamson B, Tudzynski B, Tudzynski P, Van Kan Janal** (2007) *Botrytis cinerea*: the cause of grey mould disease. *Mol Plant Pathol* **8**: 561–580
- Yang J, Duan G, Li C, Liu L, Han G, Zhang Y, Wang C** (2019) The Crosstalks Between Jasmonic Acid and Other Plant Hormone Signaling Highlight the Involvement of Jasmonic Acid as a Core Component in Plant Response to Biotic and Abiotic Stresses. *Front Plant Sci* **10**: 1349

Zipfel C, Robatzek S, Navarro L, Oakeley EJ, Jones JDG, Felix G, Boller T (2004) Bacterial disease resistance in Arabidopsis through flagellin perception. Nature 428: 764–767

2.2 The lncRNA *ASCO* interacts with highly conserved splicing factors and is involved in the plant response to stresses

2.2.1 Introduction

The previous chapter unveiled new roles of NSR splicing factors in the regulation of transcript and isoform abundance, especially during the sensing of stresses by the plant. Moreover, NSRs were shown to be novel actors of the plant response to biotic stress, allowing the resistance to various pathogens.

Another main objective of the team is to understand lncRNAs impact on plant development. The lncRNA *ASCO* was found to interact *in vivo* with NSRs and to compete *in vitro* for the binding of these proteins with their mRNA targets. *ASCO*'s overaccumulation leads to splicing defects in NSR mRNA targets, as observed in the *nsra/b* double mutant. Similarly, *nsra/b* mutants as well as *ASCO* overexpressing lines exhibit an altered response to auxin, notably in the process of lateral root (LR) formation (Bardou et al., 2014). In the article presented in the chapter 1, lncRNAs were shown to be overrepresented among NSRa targets. Hence, *ASCO* is not the only lncRNA being able to bind these splicing factors, suggesting that NSRs way of function is more complex than expected.

Based on these observations, we wondered about *ASCO*'s role in the plant. Is *ASCO*'s function only restricted to auxin response? Is this function only NSR-dependent? Are there other *ASCO* partners in the cell?

In this second chapter I will present new findings uncovering the roles of *ASCO* in the plant. It will be presented under the form of an article that includes most of my thesis results and where I participated as a first author. I conducted all the experiments concerning plant phenotyping at the macroscopic and molecular levels, the characterization of *ASCO* deregulated lines and the validation of AS events in plants showing altered *ASCO* levels. This publication will be followed by some complementary results I generated and that were not included in the article.

2.2.2 Publication: The Arabidopsis lncRNA *ASCO* modulates the transcriptome through interaction with splicing factors

The *Arabidopsis* lncRNA *ASCO* modulates the transcriptome through interaction with splicing factors

Richard Rigo^{1,†}, Jérémie Bazin^{1,†}, Natali Romero-Barrios¹, Michaël Moison^{1,2}, Leandro Lucero², Aurélie Christ¹, Moussa Benhamed¹, Thomas Blein¹, Stéphanie Huguet¹, Céline Charon¹, Martin Crespi^{1,*}  & Federico Ariel^{2,**} 

Abstract

Alternative splicing (AS) is a major source of transcriptome diversity. Long noncoding RNAs (lncRNAs) have emerged as regulators of AS through different molecular mechanisms. In *Arabidopsis thaliana*, the AS regulators NSRs interact with the *ALTERNATIVE SPLICING COMPETITOR* (*ASCO*) lncRNA. Here, we analyze the effect of the knock-down and overexpression of *ASCO* at the genome-wide level and find a large number of deregulated and differentially spliced genes related to flagellin responses and biotic stress. In agreement, *ASCO*-silenced plants are more sensitive to flagellin. However, only a minor subset of deregulated genes overlaps with the AS defects of the *nsra/b* double mutant, suggesting an alternative way of action for *ASCO*. Using biotin-labeled oligonucleotides for RNA-mediated ribonucleoprotein purification, we show that *ASCO* binds to the highly conserved spliceosome component PRP8a. *ASCO* overaccumulation impairs the recognition of specific flagellin-related transcripts by PRP8a. We further show that *ASCO* also binds to another spliceosome component, Smd1b, indicating that it interacts with multiple splicing factors. Hence, lncRNAs may integrate a dynamic network including spliceosome core proteins, to modulate transcriptome reprogramming in eukaryotes.

Keywords core splicing factors; flagellin; long noncoding RNA; PRP8a; Smd1b

Subject Category RNA Biology

DOI 10.15252/embr.201948977 | Received 31 July 2019 | Revised 9 March 2020 | Accepted 10 March 2020 | Published online 14 April 2020

EMBO Reports (2020) 21: e48977

Introduction

Alternative splicing (AS) of pre-mRNAs represents a major mechanism boosting eukaryotic transcriptome and proteome complexity [1]. In recent years, the advent of novel sequencing technologies

allowed us to analyze entire genomes and complete pools of transcripts, leading to the identification of a wide variety of mRNA isoforms in higher organisms. More than 90% of intron-containing genes in humans and over 60% in plants are alternatively spliced [2–4]. The significant diversity in the number of transcripts compared to the number of genes suggests that a complex regulation occurs at transcriptional and post-transcriptional levels [5]. Many mRNA isoforms derived from the same DNA locus are tissue-specific or are accumulated under particular conditions [6]. In humans, numerous studies suggest that the misregulation of RNA splicing is associated with several diseases [7–10]. In plants, AS plays an important role in the control of gene expression for an adequate response to stress conditions [11–19]. Alternative splicing modulates gene expression mainly by (i) increasing gene-coding capacity, thus proteome complexity, through the generation of a subset of mRNA isoforms derived from a single locus and/or (ii) triggering mRNA degradation through the introduction of a premature termination codon in specific isoforms that would lead to nonsense-mediated decay (NMD). Besides the finding of an increasing number of AS events on mRNAs, next-generation sequencing technologies led to the identification of thousands of RNAs with no or low coding potential (the so-called noncoding RNAs, ncRNAs), which are classified by their size and location with respect to coding genes [20]. The long ncRNAs (lncRNAs, over 200 nt) act directly in a long form or may lead to the production of small ncRNAs (smRNAs) acting through base pairing recognition of their mRNA targets. There is growing evidence that large amounts of lncRNAs accumulate in particular developmental conditions or during diseases, suggesting that they participate in a wide range of biological processes. In recent years, several lncRNAs from higher organisms have been characterized as modulators of virtually every step of gene expression through interaction with proteins involved in chromatin remodeling, transcriptional control, co- and post-transcriptional regulation, miRNA processing, and protein stability during various developmental processes [20–22]. In particular, a growing number of lncRNAs have been linked to the

1 Institute of Plant Sciences Paris-Saclay (IPS2), CNRS, INRA, Universities Paris-Sud, Evry and Paris-Diderot, Sorbonne Paris-Cite, University of Paris-Saclay, Orsay, France

2 Instituto de Agrobiotecnología del Litoral, CONICET, FBCB, Universidad Nacional del Litoral, Santa Fe, Argentina

*Corresponding author. Tel: +33 1 69153304; E-mail: martin.crespi@ips2.universite-paris-saclay.fr

**Corresponding author. Tel: +54 342 4511370; E-mail: fariel@santafe-conicet.gov.ar

†These authors contributed equally to this work

modulation of AS in both plants and animals [23]. The main mechanisms involving lncRNAs in AS modulation have been classified as follows: (i) lncRNAs interacting with splicing factors [24–28]; (ii) lncRNAs forming RNA–RNA duplexes with pre-mRNA molecules [29,30]; and (iii) lncRNAs affecting chromatin remodeling of alternatively spliced target genes [31,32].

In *Arabidopsis thaliana*, the lncRNA *ASCO* (*ALTERNATIVE SPLICING COMPETITOR*; AT1G67105) is recognized *in vivo* by the plant-specific NUCLEAR SPECKLE RNA-BINDING PROTEINS (NSRs), involved in splicing [24]. Interestingly, there is no evidence that *ASCO* undergoes splicing, although it is recognized by splicing factors. The analysis of a transcriptomic dataset of the *nsra/b* mutant compared to wild-type (WT) plants revealed an important number of intron retention events and differential 5' start or 3' end in a subset of genes, notably in response to auxin [33]. Indeed, the *nsra/b* mutant exhibits diminished auxin sensitivity, e.g., lower lateral root (LR) number than WT plants in response to auxin treatment. This phenotype was related to the one observed for *ASCO* overexpressing lines. Interestingly, the splicing of a high number of auxin-related genes was perturbed in *nsra/b* mutants and several of them behaved accordingly in the *ASCO* overexpressing lines. The *ASCO*-NSR interaction was then proposed to regulate AS during auxin responses in roots [24]. More recently, an RNA immunoprecipitation assay followed by RNA-seq (RIP-seq) served to identify genome-wide RNAs bound *in vivo* by NSRa [34]. Long ncRNAs transpired to be privileged direct targets of NSRs in addition to specific NSR-dependent alternatively spliced mRNAs, suggesting that other lncRNAs than *ASCO* may interact with NSRs to modulate AS [34].

In this work, we thoroughly characterize *ASCO* knocked-down plants and present its general role in AS regulation, not only in response to auxin treatment. A transcriptomic analysis of *ASCO* knocked-down seedlings revealed a misregulation of immune response genes and, accordingly, *ASCO* RNAi-silenced plants exhibited enhanced root growth sensitivity to flagellin 22 (flg22). The transcriptomic analysis of the *ASCO* overexpressing versus *ASCO* knocked-down seedlings revealed distinct and overlapping effects on the entire mRNA population. Assessing the genome-wide impact of *ASCO* function on AS, we found many flg22-response regulatory genes to be differentially alternatively spliced in *ASCO*-deregulated lines. Surprisingly, the effect of *ASCO* knock-down on AS was clearly distinct from the defects of the *nsra/b* double mutant, suggesting that *ASCO* impacts AS through a different interaction with the splicing machinery. Searching for *ASCO*-interacting proteins, we found SmD1b and PRP8a, two core components of the spliceosome that recognize subsets of AS-regulated flg22-regulatory genes, also differentially spliced in *prp8-7* [35] and *smd1b* mutants. Furthermore, *ASCO* overexpression competes for PRP8a binding to particular mRNA targets. Hence, lncRNAs may interact with key conserved components of the spliceosome to integrate a dynamic splicing network that modulates transcriptome diversity in eukaryotes.

Results

The *ASCO* lncRNA participates in lateral root formation

It was previously shown that *ASCO* overexpression results in a lower number of LRs in response to auxin treatment, a phenotype

related to that of the *nsra/b* mutant, suggesting that increasing *ASCO* expression may lead to a titration of NSR activity in splicing [34]. To understand the role of *ASCO* in plant development, we generated independent RNAi lines to downregulate the levels of *ASCO* expression (RNAi-*ASCO1* and RNAi-*ASCO2*, Fig EV1A and B). Under control growth conditions, RNAi-*ASCO* plants do not exhibit significant changes in primary root growth when compared to Col-0 WT (Fig EV1C), whereas both independent lines showed an enhanced LR density in response to auxin treatment (Fig EV1D), the opposite phenotype to the one displayed by the *ASCO* overexpressing lines [24]. Furthermore, we transformed *A. thaliana* with a construct bearing 2,631 bp of the *ASCO* promoter region controlling the expression of the fusion reporter genes *GFP-GUS* (*proASCO::GFP-GUS*). The *proASCO* construct includes the full intergenic region upstream of *ASCO* in addition to the first fifteen nucleotides from the transcription start site of the *ASCO* locus (position of the first ATG found in the locus) fused to the reporter genes (Fig EV1E). In roots, *proASCO::GFP-GUS* was active very early in LR development, in pericycle cells undergoing the first division (Fig EV1F), whereas activity was then restricted to the vasculature adjacent to the LR primordium between stages II and VIII of LR development [36]. Thus, *ASCO* expression pattern is in agreement with the LR-related phenotype of RNAi-*ASCO* plants.

Deregulation of *ASCO* expression triggers a transcriptional response to biotic stress

In order to decipher the role of *ASCO* in the regulation of gene expression at a genome-wide level, we performed RNA-seq with *A. thaliana* 14-day-old seedlings RNAi-*ASCO1* versus WT Columbia (Col-0) accession in standard growth conditions. Overall, more genes were upregulated (321) than downregulated (178) in *ASCO*-silenced plants (Fig 1A). Over 90% of deregulated transcripts correspond to protein-coding genes, according to Araport11 gene annotation (Fig 1B; Table EV1). To extend our understanding on the genome-wide role of *ASCO* in the control of gene expression, we searched the putative function of differentially expressed genes using Gene Ontology (GO). This analysis revealed a clear enrichment of deregulated genes involved in immune and defense responses (FDR < 8e-4), as well as related pathways such as “response to chitin” and “glucosinolate metabolic pathways” (Fig 1C). Interestingly, related pathways were also partially observed in *nsra/b* mutants in response to auxin [34]. The upregulation of biotic stress-related genes was validated by RT-qPCR in both RNAi-*ASCO* lines compared to WT for a subset of 6 chosen transcription factors (TFs) which have been linked to the response to pathogens (Fig EV2A): *STZ/ZAT10* (AT1G27730) encodes for a Zn-finger TF involved in the response to oxidative stress [37] and acts as a negative regulator of methyl jasmonate (MeJA) biosynthesis [38], MYB29 (AT5G07690) positively regulates the biosynthesis of aliphatic glucosinolate (AGSL), an essential defense secondary metabolite in *A. thaliana* [39], WRKY33 (AT2G38470) controls the ABA biosynthetic pathway in response to the necrotrophic fungi *Botrytis cinerea* [40], ERF6 (AT4G17490) is a positive regulator of the MeJA and ethylene-mediated defense against *B. cinerea* [41], ERF104 (AT5G61600) participates in the ethylene-dependent response to flg22 [42], and ERF105 (AT5G51190) was shown to be strongly regulated in response to chitin [43] and to bind to the GCC-

box pathogenesis-related promoter element [44]. Remarkably, all of these pathogen-related TFs are transcriptionally overaccumulated in control conditions in the RNAi-*ASCO* plants (Fig EV2A), indicating that the deregulation of *ASCO* expression triggers molecular defense responses likely through the induction of pathogen-related TFs.

It is known that peptides corresponding to the most conserved domains of eubacterial flagellins (flg) act as potent elicitors in *A. thaliana*. Notably, flg22 causes callose deposition, induction of genes encoding for pathogenesis-related proteins, and a strong inhibition of growth including root development [45–47]. Thus, we first assessed the transcriptional accumulation over time of *ASCO* in response to flg22. As shown in Fig EV2B, *ASCO* accumulation in roots was not significantly affected by flg22, compared to *CYP81F2* used as a positive control (Fig EV2C) [48]. Then, we characterized the physiological response of both *ASCO* RNAi-silenced lines to the

exogenous treatment with flg22. Five-day-old plantlets were treated or not for 9 additional days with 0.1 or 1 μM flg22. Strikingly, the roots of RNAi-*ASCO1* and 2 plants exhibited a normal development in control conditions (Fig EV3A and B), whereas they were more sensitive to flg22 treatment, exhibiting a significantly shorter primary root (Figs 1D and EV3C) but a minor reduction in the number of total LRs, resulting in a higher density of LRs (Fig 1E). Cell wall staining and microscopic observation allowed us to quantify meristem size and determine that RNAi-*ASCO* plants show a reduction of the meristematic zone in response to flg22, e.g., shorter distance between the quiescent center and the beginning of the transition zone (Fig 1F and G). This reduction in size is the result of a significantly lower number of cells forming the root meristematic zone (Fig EV3D). Together with the physiological phenotype, we characterized the molecular response to this elicitor. A small subset

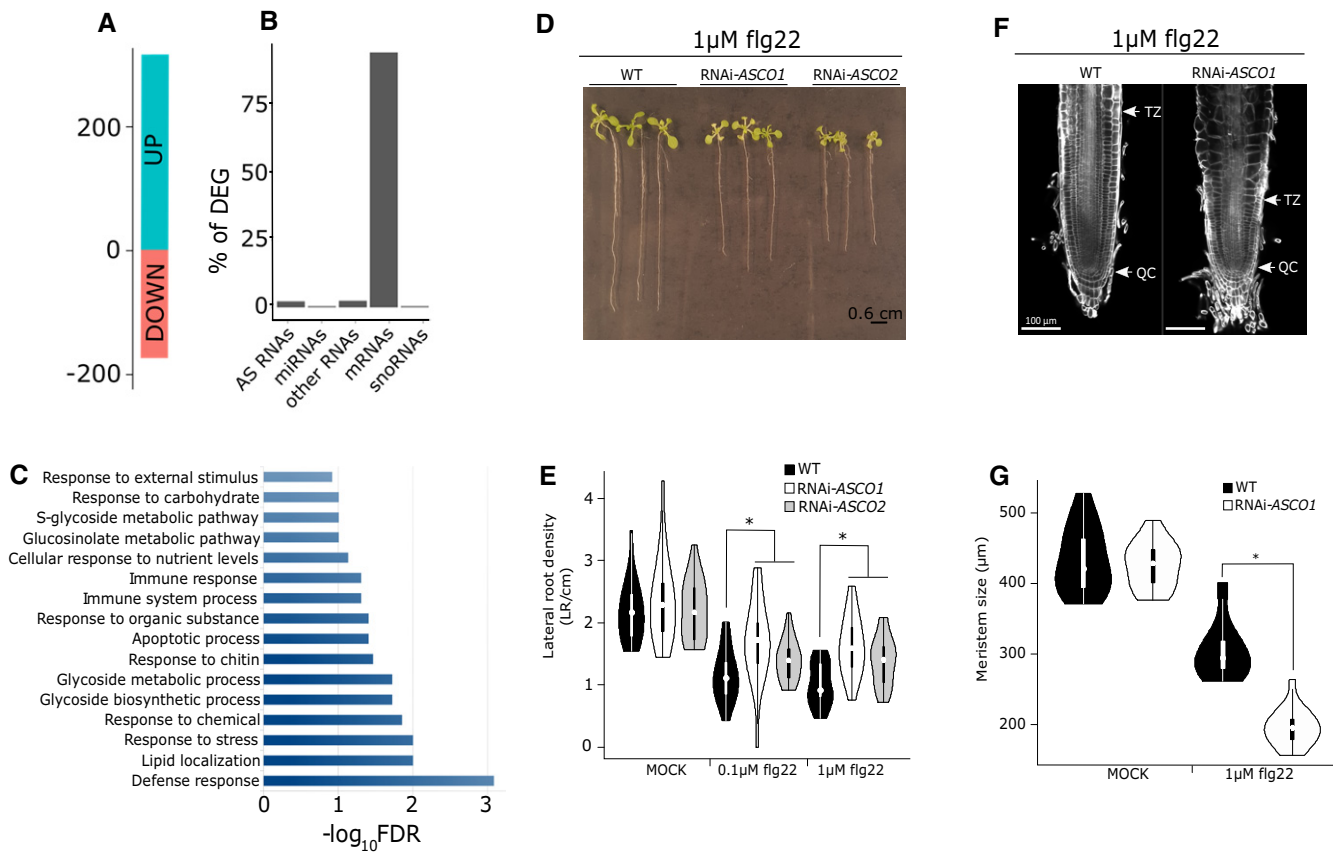


Figure 1. *ASCO* modulates steady-state levels of transcripts involved in plant immune responses affecting the sensitivity to flg22 peptide.

- A Number of differentially up- and downregulated genes (DEG) in RNAi-*ASCO1* seedlings as compared to wild type (WT) according to the RNA-seq data (FDR < 0.01, $|\log_2\text{FC}| \geq 0.75$).
- B Fraction of DEG found in each transcript class as defined in the Araport11 gene annotation. AS stands for antisense.
- C Enriched Gene Ontology (GO) of DEG in RNAi-*ASCO1* seedlings as compared to WT, x-axis represents the $-\log_{10}$ FDR for the enrichment of each GO category over genome frequency.
- D Representative picture of 14-day-old plants grown 9 days in liquid 1/2MS supplemented with 1 μM flg22. The scale bar representing 0.6 cm is included in the picture.
- E Lateral root density of WT and two independent RNAi-*ASCO* lines 9 days after transfer in 1/2MS supplemented with 0.1 or 1 μM flg22.
- F Representative picture of root apical meristems after cell wall staining, in response to flg22. TZ: transition zone; QC: quiescent center.
- G Root apical meristem size of WT and RNAi-*ASCO1* (e.g. distance from QC to TZ in μm).

Data information: Error bars indicate the standard error. The asterisk (*) indicates a significant difference as determined by Mann–Whitney's *U*-test ($P < 0.05$, $n = 18$ biological replicates).

of flg22-responsive genes was chosen [49–51] to assess putative expression changes due to *ASCO* knock-down. In mock conditions, RNAi-*ASCO* lines exhibited an increased expression for certain flg22-responsive genes tested (Fig EV3E). Interestingly, this subset of genes suffered an overall lower induction after 3 h of flg22 in RNAi-*ASCO* plants (Fig EV3F), in agreement with the previously observed altered sensitivity to flg22 of RNAi-*ASCO* roots.

To further demonstrate the link between *ASCO* and the response to flg22, we searched for additional independent *Arabidopsis* lines exhibiting a deregulation in *ASCO* accumulation. We characterized two insertional mutants located at the 5' region (*asco-1*) and the 3' region of the locus (*asco-2*; Fig EV4A). The first line, *asco-1*, resulted in an overexpressor of a truncated *ASCO* version (lacking a minor portion of the 5' region), whereas the *asco-2* T-DNA line shows minor changes in *ASCO* expression (Fig EV4B and C). Interestingly, the nearly 50-fold overaccumulation of *ASCO* RNA in *asco-1* plants do not yield any significant root growth phenotype, possibly a slight reduction in LR density (Fig EV4D and E). Accordingly, when we assessed two independent 35S:*ASCO* overexpressing lines, reaching an overaccumulation of 1,000–2,500-fold RNA levels (Fig EV4B), plants exhibit a longer main root and a lower density of LRs in response to flg22 (Fig EV4F and G). Therefore, *ASCO* participates in the regulation of biotic stress-related genes, shaping root architecture in response to flg22.

***ASCO* modulates the alternative splicing of a subset of pathogen-related mRNAs with unaltered accumulation**

Considering that overexpression of *ASCO* affected the AS of NSR mRNA targets [24], we searched for mis-spliced genes potentially explaining the global physiological impact of *ASCO* deregulation. To this end, we used two complementary approaches to detect both differential AS based on annotated isoforms (Reference Transcript Dataset for *A. thaliana*, AtRTD2) [52] and potentially nonannotated differential RNA processing events using RNAprof [33,52]. Based on RNAprof, a total of 303 differential RNA processing events in 281 distinct genes were identified comparing RNAi-*ASCO* with WT plants in control growth conditions (Dataset EV2), whereas the SUPPA2 method [53] identified 205 genes with evidence of differential AS in the AtRTD2 database. Comparison of the two analyses with differentially expressed genes (DEG) in RNAi-*ASCO* lines revealed that most differentially alternatively spliced (DAS) genes are not differentially accumulated (Fig 2A). In addition, our analyses showed the complementarity between the two approaches since only 24 common DAS genes were identified by both methods. Classification of the location and the relative isoform accumulation (up or down) of these events revealed that the majority of them were located in introns and had higher read coverage in RNAi-*ASCO* plants, suggesting that *ASCO* inhibited proper intron splicing on these genes (Fig 2B). Nevertheless, we also identified differential events located within 5'UTR, CDS, or 3'UTR suggesting that other RNA processing events, in addition to intron retention, such as alternative transcription start sites or polyadenylation sites, are affected by *ASCO* expression levels. Analysis of differential AS events with SUPPA revealed 317 significant DAS events ($|\text{dPSI}| > 0.1$, $P < 0.01$) on 205 unique genes from the AtRTD2 transcript annotation database (Dataset EV3). Similarly to the analysis with RNAprof, most of these events corresponded to intron retention (62%) but we also

identified a significant number of alternative 3' splice site and alternative 5' splice site selection modulated in *ASCO* knock-down lines (Fig 2C). To determine the most significant impact of the AS events, we sought to identify isoform switching events (i.e., co-ordinated variations in abundance of two isoforms) using the IsoformSwitchAnalyzeR package (Dataset EV4) [54]. Strikingly, isoform switching events were detected for 52 genes, out of which 12 and 34 were common cases detected by RNAprof and AtRTD2-SUPPA, respectively (Fig 2D). *In silico* analysis of the protein sequences derived from switching isoforms indicated that the AS events may lead to (i) change of ORF length, (ii) gain or loss of conserved PFAM protein domain and signal peptides, and (iii) change of the coding potential and the sensitivity to NMD (Fig 2E). Since AS can often trigger NMD, an important mechanism of plant gene expression regulation [55], we compared DAS genes to those transcripts overaccumulated in the double mutant of the NMD factor homologs *UP FRAMESHIFT1* (*UPF1*) and *UPF3*, *upf1-upf3* [56]. As shown in Fig 2F, 66 and 29 genes regulated by NMD were reported by RNAprof and AtRTD2-SUPPA as alternatively spliced in RNAi-*ASCO* plants, respectively. Hence, the majority of AS events controlled by *ASCO* seem to be independent of the UPF1-UPF3-mediated RNA quality control machinery, at least in the conditions previously assessed.

Furthermore, we performed RNA-seq with 14-day-old seedlings 35S:*ASCO1* versus Col-0 WT plants in standard growth conditions. Interestingly, there is a minimal overlap between DEG and DAS genes in WT versus RNAi-*ASCO1* and 35S:*ASCO1*. Strikingly, the up- and down-deregulation of *ASCO* resulted in alternative subsets of DAS genes, including only 120 common DAS between RNAi-*ASCO1* and 35S:*ASCO1*, compared to 227 and 137 excluding events, respectively (Fig 3A). Further comparison of DEG fold change revealed a global correlation of gene expression changes in 35S:*ASCO1* and RNAi-*ASCO1* as compared to WT. However, we show that particular subsets of genes responded to the down- or upregulation of *ASCO* (Fig 3B). Similarly, in these lines we compared the dPSI (difference of Percent Spliced In), which represents the change of each AS event. The analysis revealed that the group of 120 common AS events are positively correlated between the two lines as compared to wild type (Fig 3C). In addition, this also revealed that dPSI of AS events significantly regulated in response to either overexpression or silencing of *ASCO*, respectively, was not correlated between the two lines (Fig 3C). Overall, the effect of *ASCO* silencing was more extensive on DAS, compared to its overexpression.

In order to better understand the impact of *ASCO* deregulation on the plant response to flg22, we focused on the transcriptional accumulation of specific genes. Strikingly, several pathogen-related genes appeared differentially spliced in the RNAi-*ASCO1* line although they were not affected in their global expression levels (Fig 3A). These AS events include two members from the NB-LRR disease resistance genes: *RPP4* [57] and *RLM3* [58], as well as the splicing regulatory serine-rich protein-coding gene *SR34* (AT1G02840), needed for accurate response to pathogens [59]. The splicing of the *SR34* own pre-mRNA is auto-regulated and depends on the activity of immune response factors [60]. Other relevant AS targets are *SNC4* (AT1G66980) which encodes a receptor-like kinase that participates in the activation of the defense response, and its AS is impaired in defense-related mutants, affecting the response to pathogens [60]; *SEN1* (AT4G35770), a senescence marker gene

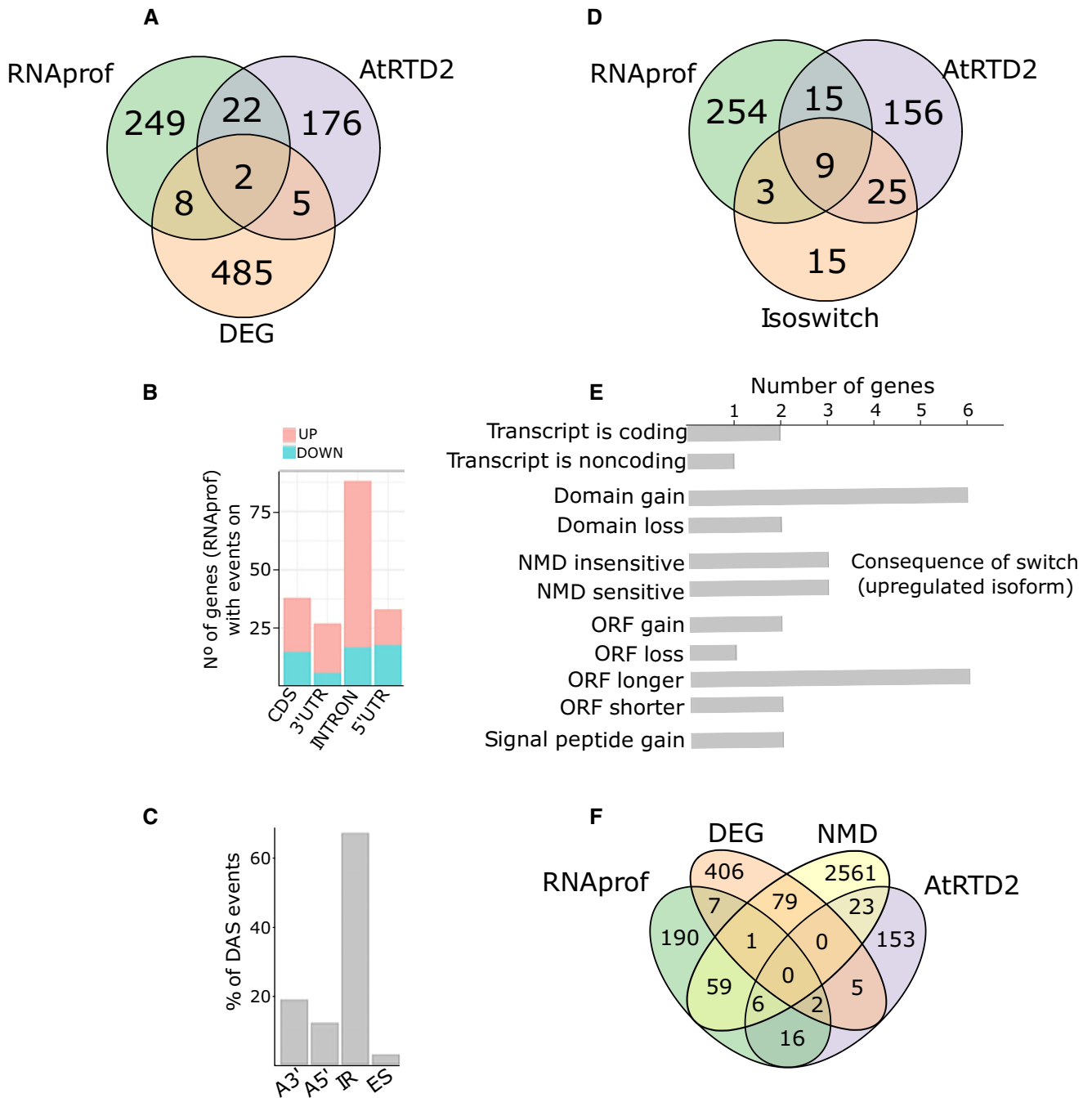


Figure 2. ASCO modulates alternative splicing.

- A Comparison of differentially processed transcripts (RNAprof) and differentially AS genes (AtRTD2-SUPPA) with differentially expressed genes (DEG).
- B Number of genes containing at least one differential RNA processing event (as defined by RNAprof $P_{adj} < 0.001$) in CDS, introns, 5'UTR and 3'UTR between RNAi-*ASCO1*, and WT. Up and down fractions correspond to increase or decrease, respectively, of RNA-seq coverage in RNAi-*ASCO1* for each specified gene feature.
- C Proportion of DAS events identified by AtRTD2-SUPPA in RNAi-*ASCO1* compared to WT; alternative 3' site (A3'), alternative 5' site (A5'), intron retention (IR), exon skipping (ES).
- D Comparison of differentially processed transcripts (RNAprof) and differentially AS genes (AtRTD2-SUPPA) with genes showing significant isoform switch events (Isoswitch).
- E Summary of the predicted consequence of the isoform switch events as shown by the feature acquired by the upregulated isoform. ncRNA stands for noncoding RNA, and NMD stands for nonsense-mediated decay.
- F Comparison of differentially processed transcripts (RNAprof), differentially AS genes (AtRTD2-SUPPA), and differentially expressed genes (DEG) with genes significantly upregulated in the *upf1-upf3* mutant [56], indicating genes potentially regulated by NMD.

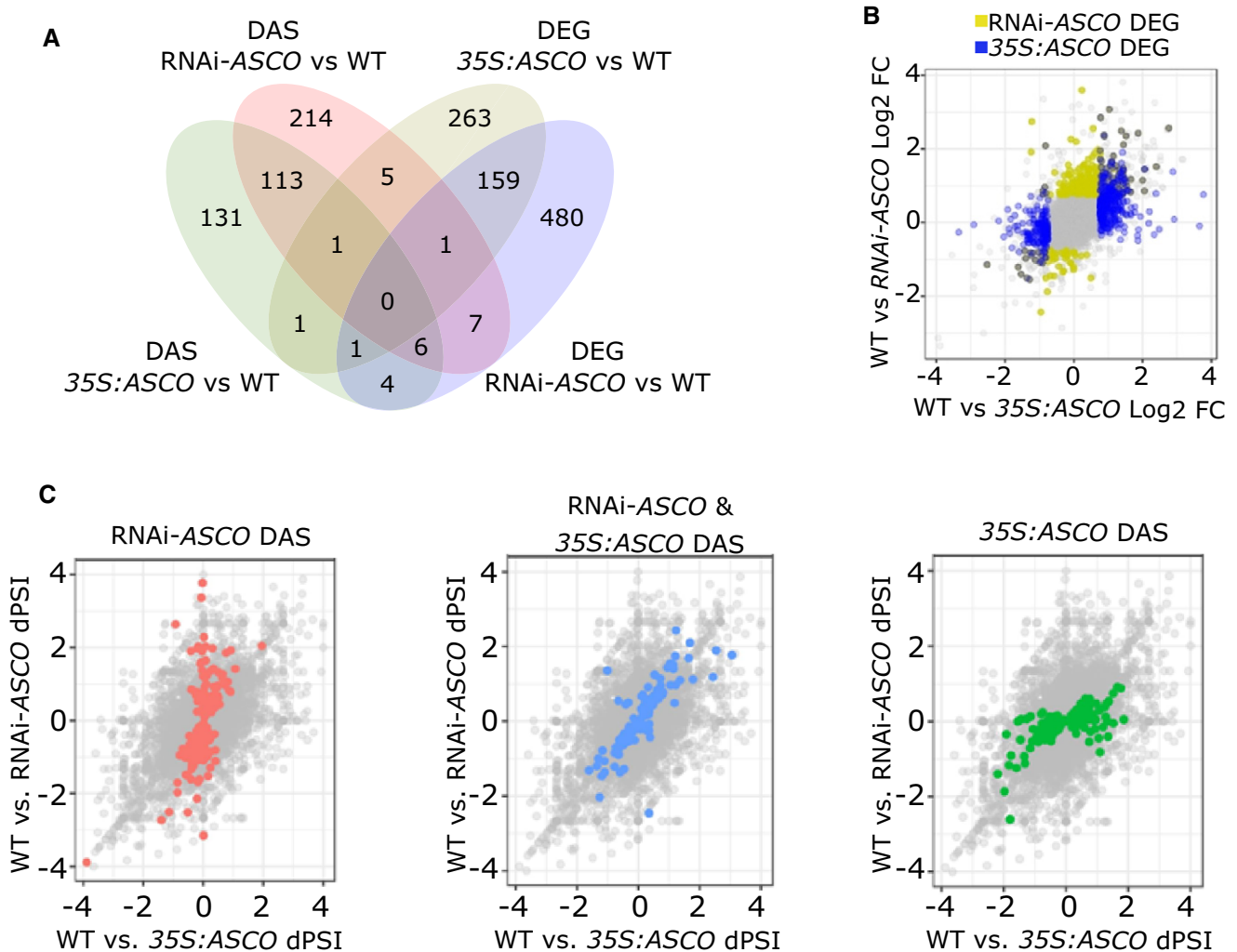


Figure 3. RNAi-ASCO and 35S:ASCO lines share common and distinct subsets of DEG and DAS targets.

- A Overlap between differentially expressed (DEG) and spliced (DAS) genes in RNAi-ASCO and 35S:ASCO as compared to WT.
- B Scatter plot showing the respective gene expression fold change in RNAi-ASCO and 35S:ASCO lines as compared to WT. Genes showing significant changes in RNAi-ASCO and 35S:ASCO are highlighted as yellow and blue dots, respectively.
- C Scatter plots showing the respective percent spliced in difference (dPSI) in RNAi-ASCO and 35S:ASCO lines as compared to WT. Genes showing significant changes in RNAi-ASCO, 35S:ASCO, or in both lines are highlighted as red, green, or blue dot, respectively. Gray dots represent all AS events.

primarily regulated by salicylic acid (SA)- and MeJA-dependent signaling pathways [61] and *NUDIX HYDROLASE7* (*NUDT7*, AT4G12720) which regulates defense and cell death against biotrophic pathogens [62]. Another interesting target is *EPITHIOSPECIFIER PROTEIN* (*ESP*, AT1G54040) a gene involved in plant defense to insects which is differentially spliced in response to MeJA [63] although this gene was also differentially expressed in RNAi-ASCO plants. We also included in the following analysis a NAD(P)-binding Rossmann-fold protein family gene (*NRG*, AT2G29290), exhibiting drastically altered AS upon *ASCO* knock-down. DAS events in the chosen genes mentioned above, first identified *in silico* (Fig 4A and D, Appendix Fig S1), were validated by RT-PCR and polyacrylamide gel electrophoresis by calculating the ratio between alternatively spliced and fully spliced isoforms (isoform ratio, Figs 4B and C, and 4E and F, Appendix Fig S2). All events tested excepting *RLM3*

displayed significant changes in isoform ratio. Most events led to changes in conserved protein domains (Fig 4 and Appendix Fig S2). For instance, retention of the last intron in *RPP4* gave place to a protein predicted with a lower number of LRR repeat as previously observed in other R-genes such as *RPS4* [64]. Splicing events in *SR34* and *ESP* were further validated by quantitative RT-qPCR where each differential event was normalized with respect to an internal gene probe (called INPUT) which corresponds to a common exon. This allowed for the calculation of the splicing index (defined in the methods section, Appendix Fig S3). Splicing index was not calculated for the other chosen genes due to technical difficulties in primer designing. Altogether, our results indicate that the knock-down of *ASCO* expression affects the AS of a subset of genes whose isoforms distribution may modulate the pathogen-related transcriptome and affect the response to flg22.

ASCO interacts with the spliceosome core components PRP8a and Smd1b

The fact that ASCO interacts with NSRs strongly suggested that its deregulation would affect a large subset of NSR-targeted AS events. Surprisingly, DAS genes in the RNAi-ASCO and 35S:ASCO plants only partially coincide with those in *nsra/b* double mutants (in response to auxin or not). In all, out of the 589 DAS events identified in *nsra/b* compared to WT, only 140 (32%) are common with RNAi-ASCO1 and 109 (33%) with 35S:ASCO, representing 24 and

19% of all DAS events in the *nsra/b* mutant, respectively (Fig EV5A). Furthermore, *nsra/b* plants do not respond to flg22 in the same way as RNAi-ASCO plants (Fig EV5B and C), indicating that ASCO further modulates AS in an NSR-independent manner by an unknown mechanism, notably affecting the response to biotic stress. Therefore, in order to decipher the AS-related complexes implicating ASCO, we performed an antisense oligonucleotide-based pull-down method, related to the chromatin isolation by RNA Purification (ChIRP) [65,66] using nuclear extracts to purify ASCO-containing RNPs. Eighteen biotinylated probes matching ASCO were

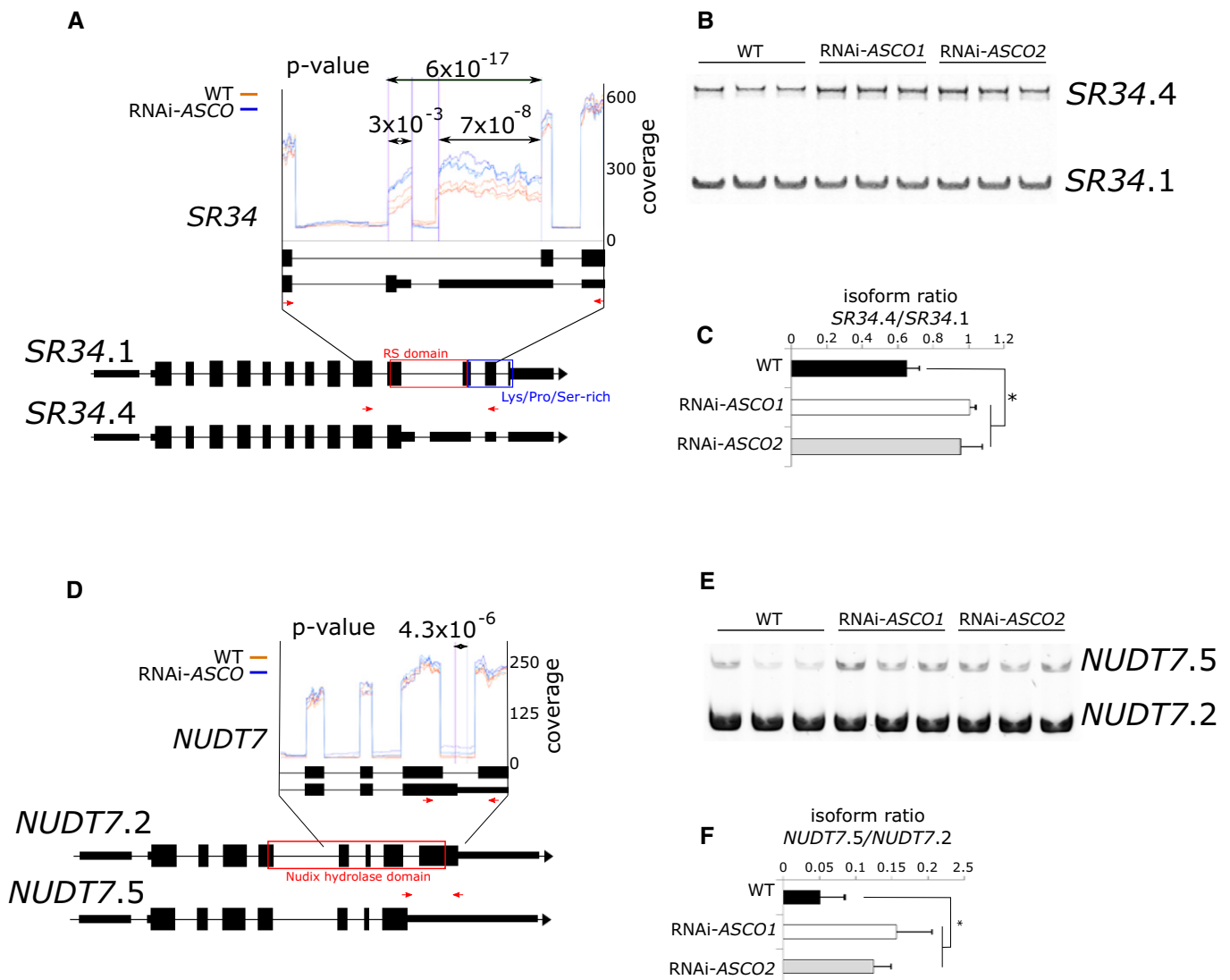


Figure 4. Validation of AS events in RNAi-ASCO lines.

A–F (A, D) Differential RNA processing events of *SR34* (AT1G02840) and *NUDT7* (AT4G12720) transcripts detected by RNAprof from the comparison of RNA-seq libraries of 14-day-old WT (red) and RNAi-ASCO1 (blue) plants. Three biological replicates were used. Vertical purple lines and *P*-values indicate significant differential processing events. Structure of *SR34* (A) and *NUDT7* (D) RNA isoforms. Large black boxes indicate exons, narrow black boxes indicate UTRs, and black lines indicate introns. Colored boxes indicate protein domains affected by an AS event. RS domain: Arg/Ser-rich domain. Red arrows indicate probes used for gel electrophoresis. Protein domains were retrieved from Uniprot database (<https://www.uniprot.org>). (B, E) Analyses of RT-PCR products of *SR34* (B) and *NUDT7* (E) transcripts on 8% acrylamide gel. (C, F) Quantification of the ratio of *SR34* (C) and *NUDT7* (D) isoforms detected in the gel in (B) and (E), respectively. RNAs were extracted from WT and RNAi-ASCO1 14-day-old plants. The asterisk (*) indicates a significant difference as determined by Student's *t*-test ($P < 0.05$, $n = 3$ biological replicates). Error bars show mean \pm standard deviation.

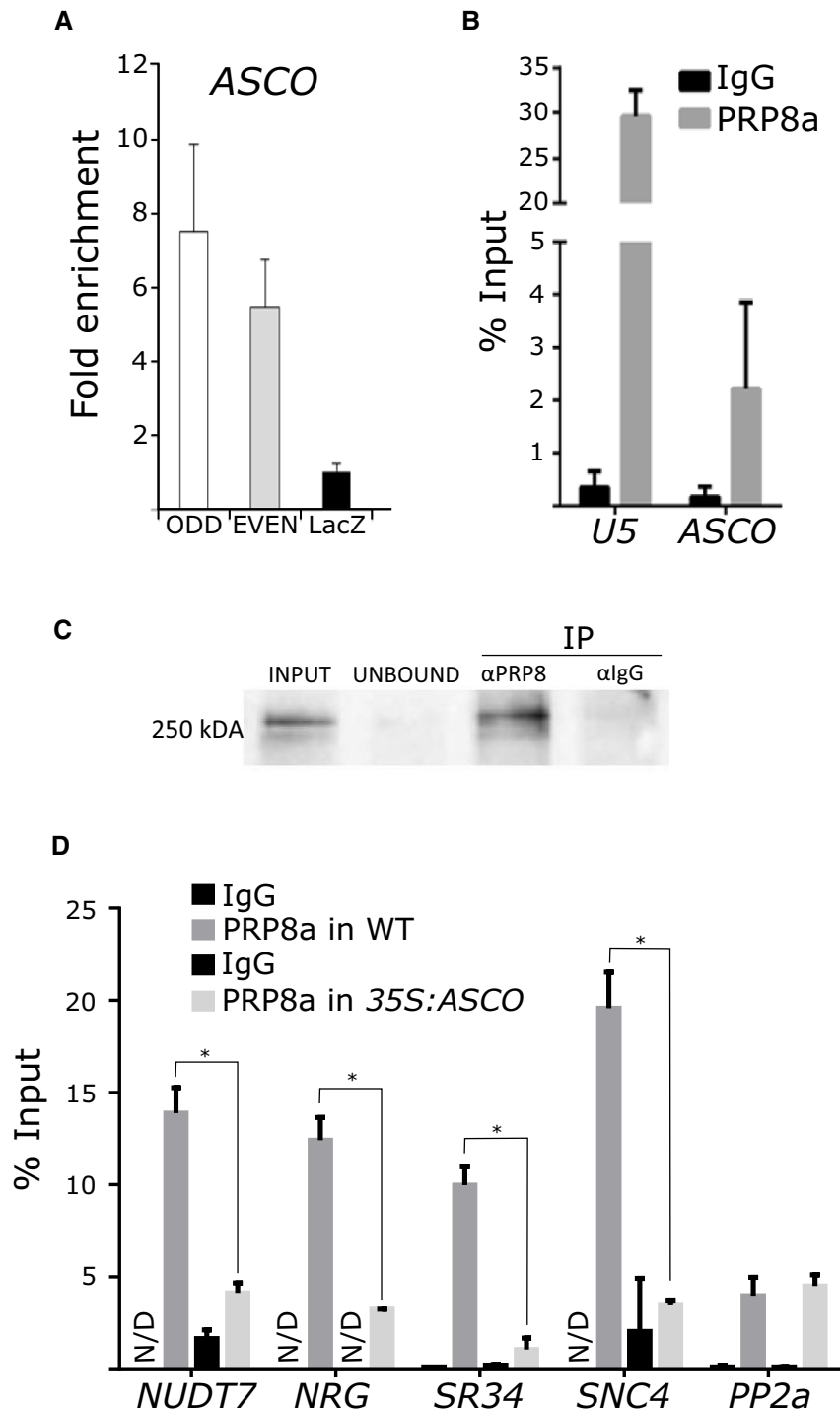


Figure 5. *ASCO* modulates the activity of the spliceosome component PRP8a.

A Analysis of *ASCO* enrichment by ChIRP using two sets of independent biotinylated probes ODD and EVEN compared to negative control with probes designed against the *LacZ* RNA. The fold enrichment was calculated between ODD or EVEN samples against LacZ. These samples were used for protein precipitation and mass spectrometry analyses (ChIRP-MS), from which PRP8a was identified as a potential *ASCO* partner.

B Validation of PRP8a-*ASCO* interaction by PRP8a-RIP. *U5* RNA was used as a positive control.

C Immunoblot analysis was performed during PRP8a immunoprecipitation (IP). The same volume of input, unbound fraction was loaded as well as 20% of the eluted IP fraction. α -PRP8a and α -IgG: IP performed with anti-PRP8a or control rabbit IgG antibody, respectively.

D PRP8a recognition of a subset of DAS RNAs is impaired in the *35S:ASCO* plants. A housekeeping gene (*PP2a*, AT1G13320) RNA was used as a negative control.

Data information: In (B and D), the results are expressed as a percentage of the input for PRP8a RIP followed by RT-qPCR, and IgG RIP was used as a negative control. Error bars represent the standard error of 3 biological replicates. N/D stands for nondetectable. The asterisk (*) indicates a significant difference as determined by Student's *t*-test ($P < 0.05$, $n = 3$).

used in independent sets called EVEN and ODD, respectively (Dataset EV5). ASCO-ChiRP was performed in 4 biological replicates for each set of probes: ODD, EVEN, and an additional set matching the *LacZ* RNA, used as a negative control. ASCO enrichment was corroborated by ChiRP followed by RNA purification and RT-qPCR (Fig 5A). We then performed a mass spectrometry on the proteins from the purified ASCO-containing RNP to identify potential ASCO protein partners. Strikingly, among the RNA-related proteins identified in the EVEN and ODD samples, but not in the *LacZ*, we found the pre-mRNA-processing-splicing factor 8A, PRP8a. PRP8 is a core component of the spliceosome and is highly conserved in higher organisms; null mutations generally result in embryonic lethality [67]. In *Arabidopsis*, a PRP8a leaky mutation was found to also affect the AS of the *COOLAIR* lncRNA [68] and results in a high number of intron retention events [35]. Therefore, we developed specific antibodies against PRP8a and we tested them in immunolocalization experiments that revealed a nuclear localization pattern (Appendix Fig S4) similar to what was previously observed in *Drosophila* [69]. In order to validate the interaction with ASCO *in vivo*, we performed a RNA immunoprecipitation assay followed by qPCR (RIP-qPCR) from nuclear extracts. We show that PRP8a can recognize the spliceosomal *U5* RNA [70] taken as a positive control, as well as the ASCO lncRNA (Fig 5B). The efficiency of the PRP8a immunoprecipitation (IP) was assessed by Western blot comparing nuclei input samples, against the unbound fraction after IP, as well as the anti-PRP8a IP and the anti-IgG IP (Fig 5C). We then assessed the binding of PRP8a to the pathogen-related mRNAs differentially spliced in the RNAi-ASCO lines. PRP8a was indeed able to interact with 4 of these ASCO-related DAS genes. Furthermore, their binding was impaired upon the overexpression of ASCO (Fig 5D), hinting at an ASCO-mediated competition of these mRNAs inside the PRP8a-containing spliceosome complex. Interestingly, ASCO is overaccumulated in the *prp8-7* mutant allele [35] (Fig 6A), as it occurs in the *nsra/b* mutant plants [24]. Remarkably, similar AS defects were shown between the *prp8-7* mutant and RNAi-ASCO lines for pathogen-related genes (Fig 6B and C, Appendix Fig S5), indicating that the flg22 differential phenotype of RNAi-ASCO plants may be related to the interaction with the spliceosome components. Recently, we identified another core component of the spliceosome, Smd1b, linked both to AS and the recognition of aberrant ncRNAs to trigger gene silencing [71]. Interestingly, ASCO expression levels are also increased in the *smd1b* mutant (Fig 6D), exhibiting the same transcript accumulation as in *prp8-7* and *nsra/b* mutants. Hence, we wondered whether this other core component of the spliceosome also interacts with ASCO lncRNA. Using *pUBI:Smd1b-GFP* plants (*smd1b* mutant background) [71], we performed a RIP assay and found that Smd1b also recognizes ASCO *in vivo* (Fig 6E) as well as the *U6* RNA taken as a positive control. Furthermore, Smd1b recognizes the four pathogen-related transcripts assessed (Fig 6F) although only two out of three pathogen-related transcripts assessed were DAS in *smd1b* mutants: *ESP*, *SR34*, but not *NUDT7* (Fig 6G and H, Appendix Fig S5). *SNC4* total transcript levels were dramatically reduced in the *smd1b* mutant, hindering the analysis of relative isoforms accumulation (Appendix Fig S5J). Altogether, our results indicate that ASCO, an apparently intron-less lncRNA, interacts with PRP8a and Smd1b, two core components of the spliceosome, contributing to determine the dynamic ratio between hundreds of alternatively spliced mRNAs, notably pathogen-related

genes. Hence, lncRNAs appear as possible dynamic interactors of multiple core components of the splicing machinery, likely modulating the splicing patterns of particular subsets of mRNAs.

Discussion

Long noncoding RNAs modulate splicing regulatory networks

We show here that reducing ASCO expression has a major effect on AS at the genome-wide level in plants. In animals, different splicing factors can recognize lncRNAs *in vivo* [23], e.g., Y-BOX BINDING PROTEIN 1 (YBX1) [72], POLY(RC) BINDING PROTEINS 1 and 2 (PCBP1/2), FOX proteins [73], and the serine-rich splicing factors, such as SRSF6 [74], among others. The lncRNA *GOMAFU*, for example, is recognized through a tandem array of UACUAAC motifs by the splicing factor SF1, which participates in the early stages of spliceosome assembly [75]. Furthermore, *GOMAFU* was found to directly interact with the splicing factors QUAKING homolog QKI and SRSF1 [25]. In adult mice, *GOMAFU* is expressed in a specific group of neurons and has been implicated in retinal cell development [76,77], brain development [78], and post-mitotic neuronal function [79]. *GOMAFU*'s downregulation leads to aberrant AS patterns of typically schizophrenia-associated genes [25]. Other lncRNAs recognized by splicing factors are *NUCLEAR PARSPECKLE ASSEMBLY TRANSCRIPT 1 (NEAT1)* and *NEAT2* (also known as *METASTASIS ASSOCIATED LUNG ADENOCARCINOMA TRANSCRIPT 1; MALAT1*) [80]. RNA FISH analyses revealed an intimate association of *NEAT1* and *MALAT1* with the SC35 splicing factor containing nuclear speckles in both human and mouse cells, suggesting their participation in pre-mRNA splicing. Indeed, the ASCO lncRNA also interacts with NSRs and Smd1b both localized in nuclear speckles [24,71], whereas we show here that PRP8a seems to have nuclear localization in *Arabidopsis*. It was shown that *NEAT1* localizes to the speckles periphery, whereas *MALAT1* is part of the polyadenylated component of nuclear speckles [80]. *MALAT1* acts as an oncogene transcript, and its aberrant expression is involved in the development and progression of many types of cancers [81–83]. *MALAT1* can promote metastasis by interacting with the proline- and glutamine-rich splicing factor SFPQ, blocking its tumor suppression activity [26]. In plants, little is known about the interaction between splicing factors and lncRNAs [20,23]. NSRs are a family of RNA-binding proteins that act as regulators of AS and auxin-regulated developmental processes such as lateral root formation in *A. thaliana*. These proteins were first shown to interact with some of their alternatively spliced pre-mRNA targets and ASCO lncRNA [24]. More recently, a RIP-seq approach on an NSRa fusion protein in *A. thaliana* mutant background allowed the identification of genome-wide NSR targets, e.g., specific alternatively spliced mRNAs as well as a plethora of lncRNAs, including ASCO [34]. Strikingly, ASCO was detected albeit not among the most abundant NSRa-interacting lncRNA, suggesting the existence of an intricate network of multiple lncRNAs and splicing factors interactions. In fact, we showed here that the impact of ASCO deregulation on AS at a genome-wide level barely overlaps with the defects observed in the *nsra/b* mutant background (with or without auxin), indicating that ASCO and NSRs participate in common as well as in independent molecular mechanisms related to AS.

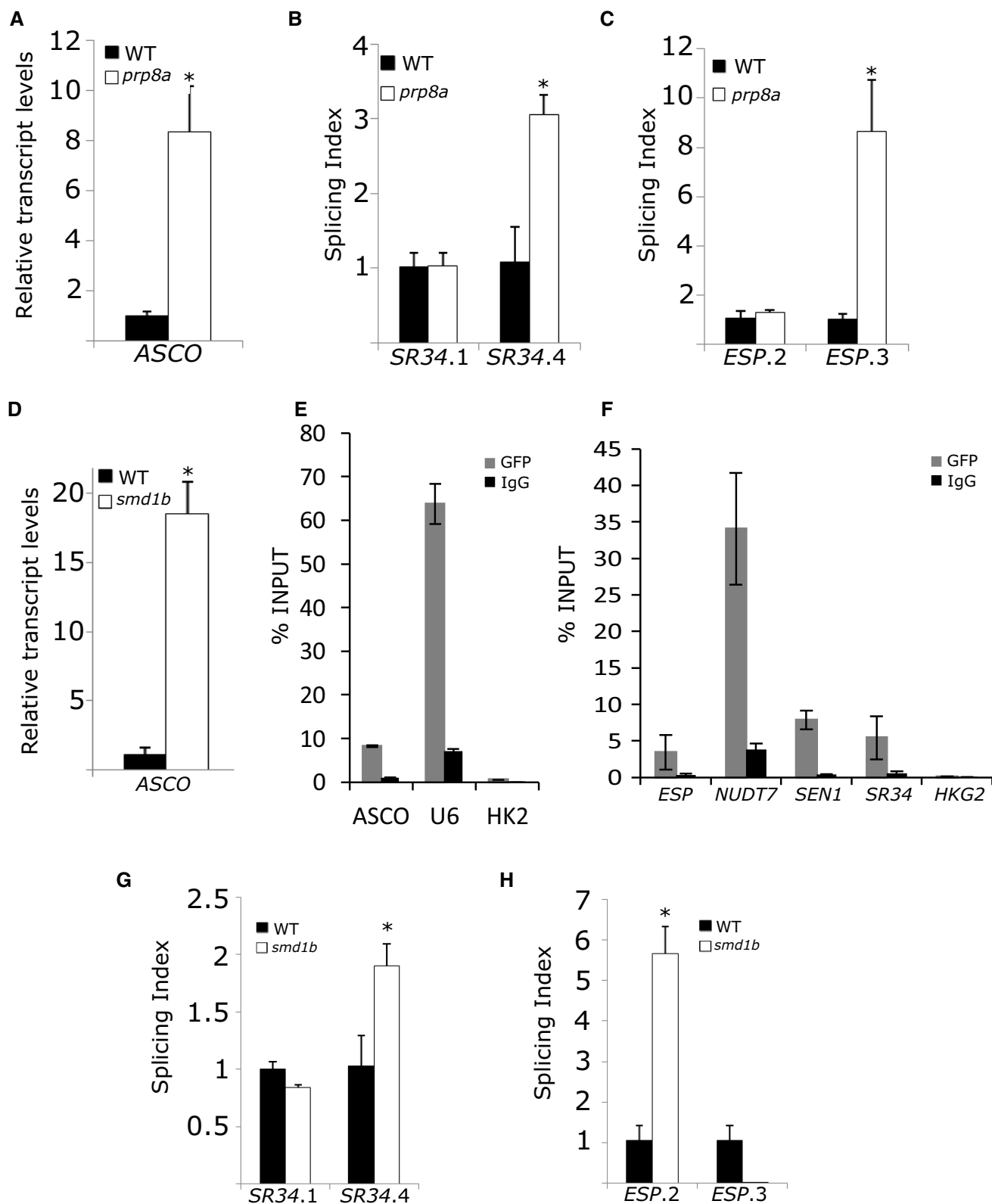


Figure 6.

Figure 6. PRP8a and Smd1b regulate AS of ASCO mRNA targets.

- A ASCO transcript levels in WT and *prp8-7* mutants.
 B, C *prp8-7* leaky mutant displays similar AS events as observed in RNAi-ASCO. Quantification of *SR34* (B) and *ESP* (C) isoforms splicing index by RT-qPCR.
 D ASCO transcript levels in *smd1b* mutant. In A and D, RNAs were extracted from WT, *prp8-7*, and *smd1b* 14-day-old plants.
 E Smd1b can bind ASCO *in vivo*. *U6* RNA was used as a positive control and a housekeeping gene (*HKG2*, AT4G26410) RNA as a negative control. The results were expressed as % INPUT in Smd1b-GFP RIP and IgG RIP used as a negative control.
 F Smd1b recognizes *in vivo* the RNAs of 4 genes regulated by ASCO. The results were expressed as % INPUT in Smd1b-GFP RIP and IgG RIP used as a negative control.
 G, H *smd1b* mutant displays similar AS events as observed in RNAi-ASCO. Quantification of *SR34* (G) and *ESP* (H) isoforms splicing index by RT-qPCR.
 Data information: The asterisk (*) indicates a significant difference as determined by Student's *t*-test ($P < 0.05$, $n = 3$ biological replicates). Error bars show mean \pm standard error.

The ASCO lncRNA knocked-down plants show altered sensitivity to flagellin

The comparison of the transcriptome of RNAi-ASCO and 35S:ASCO plants revealed common and specific subsets of DAS genes. This dual effect caused by the up- or downregulation of ASCO accumulation hints to the potential relevance of a stoichiometric factor impacting the action of ASCO within the spliceosome. ASCO-silenced plants exhibit an enhanced sensitivity to flg22, in contrast to 35S:ASCO and *nsra/b* plants. In agreement, overexpressing ASCO plants and *nsra/b* mutants behave similarly in response to auxin [24]. Interestingly, auxin signaling is known to control the balance between growth and immunity [84]. The auxin response was recently identified as a major component of the root transcriptional response to beneficial and pathogenic bacteria elicitors and is thought to mediate the observed reshaping of the root system in response to bacterial defense elicitors [85]. Our results suggest that ASCO has a wider function than the simple titration of NSR activity. Remarkably, we now determined that ASCO is recognized by additional splicing factors: the spliceosome core components PRP8a and Smd1b. Accordingly, RNAi-ASCO lines and a *prp8-7* leaky mutant exhibit similar AS defects of flg22-regulated genes. However, *smd1b* mutants resulted in a deregulated ratio of isoforms of only *ESP* and *SR34*, but not *NUDT7*. The milder effect of ASCO-related Smd1b over the subset of pathogen-related genes may be due to a compensatory role of Smd1a in the *smd1b* background. Core splicing factors null mutants usually give very severe phenotypes or embryo lethality, and *smd1b* mutation was proposed to be partially compensated by Smd1a [71]. Thus, the *prp8-7* leaky allele and the *smd1b* compensated mutant both exhibit partial effects on global constitutive splicing. Altogether, our results indicate that a complex network of lncRNAs and splicing factors involving ASCO, PRP8a, Smd1b, and NSRs dynamically shapes transcriptome diversity, integrating developmental, and environmental cues, thus conditioning the response to biotic stress (Fig 7).

In *Arabidopsis*, the lncRNA *ELF18-INDUCED LONG NONCODING RNA 1 (ELENA1)* is regulated by the perception of the translation elongation factor Tu (*elf18*) and it was identified as a factor enhancing resistance against *Pseudomonas syringae*. It was shown that *ELENA1* directly interacts with Mediator subunit 19a (*MED19a*), modulating the enrichment of *MED19a* on the *PATHOGENESIS-RELATED GENE1 (PR1)* promoter [86]. Several other examples of lncRNAs mediating the environmental control of gene expression illustrate the relevance of the noncoding transcriptome as a key integration factor between developmental and external cues [68,87–89]. The sensitivity to pathogens has been shown to be affected in

spliceosome-related mutants. For instance, it was recently reported that the *prp40c* mutants display an enhanced tolerance to *Pseudomonas syringae* [90]. On the other hand, several other splicing-related genes have been identified as positive regulators of plant immunity against *Pseudomonas* [91–93]. Therefore, the modulation of the expression and activity of splicing-related components appear to be important for the proper response to pathogens.

lncRNAs as highly variable components of the conserved spliceosomal machinery

Here, we show that the highly structured lncRNA *ASCO*, which does not seem to contain introns, is capable to interact with PRP8a and modulate PRP8a binding to ASCO-related AS targets. The spliceosome is a large complex composed of five different small nuclear ribonucleoprotein complexes subunits (snRNPs). Each subunit includes noncoding and nonpolyadenylated small nuclear uridine (U)-rich RNAs (U snRNAs) and core spliceosomal proteins, along with more than 200 non-snRNPs splicing factors [94]. PRP8a is one of the largest and most highly conserved proteins in the nucleus of eukaryotic organisms. It occupies a central position in the catalytic core of the spliceosome and has been implicated in several crucial molecular rearrangements [67]. In *Arabidopsis*, analysis of *PRP8a* leaky mutation suggests that PRP8a recognizes the lncRNA *COOLAIR in vivo* to modulate its AS [68] hinting at an interaction with lncRNAs. *COOLAIR* designates a set of transcripts expressed in antisense orientation of the locus encoding the floral repressor *FLC* [95]. Two main classes of *COOLAIR* lncRNAs are produced by AS and polyadenylation of antisense transcripts generated from the *FLC* locus. One uses a proximal splice site and a polyadenylation site located in intron 6 of *FLC*, whereas the distal one results from the use of a distal splice and polyadenylation sites located in the *FLC* promoter [95]. Notably, *prp8-7* partial loss of function leads to a reduced usage of *COOLAIR* proximal polyadenylation site and an increase of *FLC* transcription which is associated with late-flowering phenotypes [68,95]. Interestingly, the *FLC/COOLAIR* module is strongly deregulated in the *nsra/b* double mutant and NSRa was linked to flowering time further supporting multiple interactions of lncRNAs and the splicing machinery [34]. Although NSRa-COOLAIR interaction seems not to occur, it was proposed that the control of NSRa over *COOLAIR* involves the direct interaction and processing of the polyadenylation regulatory gene *FPA* [34]. In the model legume *Medicago truncatula*, the NSRs closest homolog, RNA-BINDING PROTEIN 1 (RBP1), is localized in nuclear speckles where many components of the splicing machinery are hosted in plant cells. Remarkably, RBP1 interacts with a highly

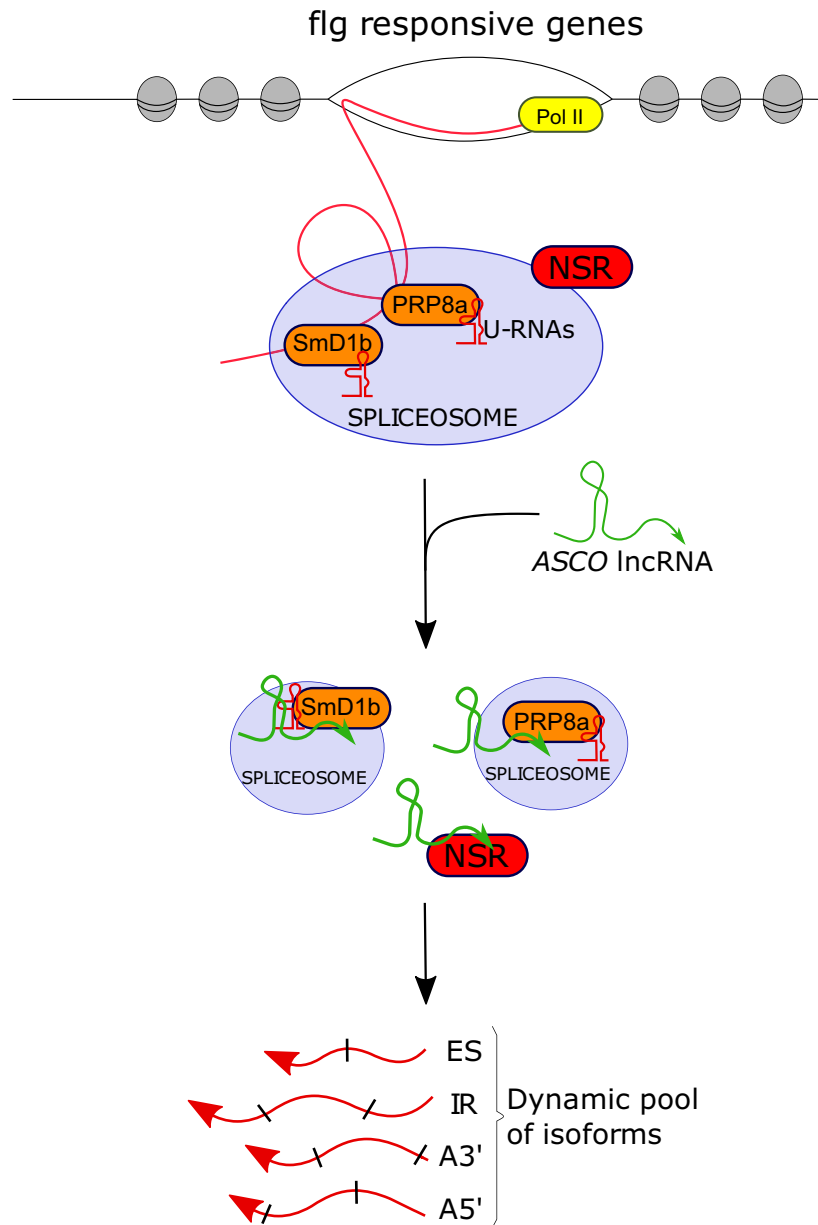


Figure 7. The interaction of ASCO lncRNA and the spliceosome components PRP8a and SmD1b shapes the transcriptional response to flg22 modulating alternative splicing.

Proposed mechanism of ASCO lncRNA action. ASCO hijacks NSR proteins to modulate the population of alternatively spliced transcripts. Additionally, ASCO is recognized by PRP8a and SmD1b, two core components of the spliceosome, conditioning the SmD1b/PRP8a-dependent transcriptome diversity in response to flagellin.

structured lncRNA, *EARLY NODULIN 40 (ENOD40)*, which participates in root symbiotic nodule organogenesis [96–98]. *ENOD40* is highly conserved among legumes and was also found in other species such as rice (*Oryza sativa*) [99], but shows no homology to ASCO lncRNA [24]. In contrast to the nuclear localization of *Arabidopsis* ASCO, *ENOD40* was found both in the nucleus and in the cytoplasm, and it is able to relocalize RBP1 from nuclear speckles into cytoplasmic granules during nodulation [98]. These observations suggested a role of the lncRNA *ENOD40* in nucleocytoplasmic trafficking, potentially modulating RBP1-dependent splicing and further supporting the multiple interactions of

lncRNAs with splicing regulators. A major result shown here is that ASCO is recognized by PRP8a and SmD1b, two central regulators of splicing and not only by the NSR proteins which are plant-specific “peripheral” regulators of splicing. Indeed, the *nsra/b* null double mutants did not display major phenotypes in contrast to null PRP or SmD components. The identification of how the ASCO lncRNA interacts with PRP8a will certainly contribute to understanding the intricate network of lncRNA-mediated regulation of core splicing factors, thus opening wide perspectives for the use of lncRNAs in the modulation of the dynamic population of alternatively spliced mRNAs in higher organisms. Interestingly, a search for ASCO

homologs across the Brassicaceae family reveals that 9 additional copies of *ASCO* exist in *A. thaliana* and related sequences are also present in other Brassicaceae species, including *A. halleri* and *A. lyrata*, and the more distant species *Capsella rubella* and *Capsella grandiflora* (Appendix Fig S6A). However, none of the four detectable *A. thaliana* *ASCO*-like homologs suffered any significant alteration in RNAi-*ASCO* and 35S:*ASCO* lines (Appendix Fig S6B), suggesting that none of them seem to compensate for the absence or overaccumulation of the *ASCO* lncRNA. The existence of *ASCO*-like sequences in other species suggests that conserved lncRNA-mediated mechanisms of AS regulation may occur through the interaction with highly conserved splicing factors. As PRP8a and Smd1b as well as the snRNAs are highly conserved spliceosomal components in contrast to the outstanding variability of lncRNA sequences along evolution, our results hint at a yet undiscovered evolutionary layer in the fine-tuning of AS in specific cell types and different environmental conditions without affecting essential splicing activity. Structure and short sequences inside lncRNAs may contribute to the evolution of splicing regulatory networks in eukaryotes.

Materials and Methods

Plant material and growth conditions

All the lines used in this study were in the *A. thaliana* Columbia-0 (Col-0) background. We used the *nsra/b* double mutant and the *ASCO* overexpressing lines from [Ref. 24]. The insertion lines WiscDsLoxHs110_08A (*asco-1*) and SAIL_812_C08 (*asco-2*) were obtained from the T-DNA mutant collection at the Salk Institute Genomics Analysis Laboratory (SIGnAL, <http://signal.salk.edu/cgi-bin/tdnaexpress>) via NASC (<http://arabidopsis.info/>). Seeds from *ppr8-7* in the T line Col-0 background [35] and *smd1b* [71] mutants were provided by H. Vaucheret. The *pUBQ10:Smd1b-GFP* line was used for RNA immunoprecipitation assays. Plants were grown at 20°C with a 16-h light/8-h dark photoperiod (long days) on solid half-strength Murashige and Skoog (1/2MS) medium.

Generation of transgenic lines

Pro*ASCO*::GUS transgenic lines

The promoter region of *ASCO* (2631-bp upstream of the transcription start) was amplified from *A. thaliana* genomic DNA using gene-specific primers listed in Dataset EV5. The amplicon was subcloned into the pENTR/D-TOPO vector and recombined in a pKGWFS7 binary destination vector, upstream of the *GFP*, and *GUS* sequences. Pro*ASCO*::*GUS* constructs were transferred into *A. thaliana* by standard Agrobacterium-mediated protocol [100]. Three lines were selected based on 3:1 segregation for the transgene (single insertion) and brought to T3 generation where the transgene was in a homozygous state. All lines behave similarly as for *GUS* expression.

RNAi-*ASCO* knocked-down lines

The first 233-bp of the *ASCO* transcript was amplified from *A. thaliana* genomic DNA using gene-specific primers listed in Dataset EV5. Amplicons were subcloned into the pENTR/D-TOPO

vector and recombined in a pFRN binary destination vector [101] to target the *ASCO* RNA by long dsRNA hairpin formation.

Root growth analysis

For analysis of auxin impact on root architecture, plants were grown as described in [Ref. 24]. Briefly, seeds were sterilized and directly sown on plates containing 1/2MS medium supplemented or not with 100 nM NAA. Plantlet root architecture was analyzed using the RootNav software after 7 days of growth [102]. For analysis of flagellin impact on root architecture, plants were previously grown 5 days on solid 1/2MS medium + 1% sucrose and then transferred for additional 9 days in liquid 1/2MS media + 1% sucrose supplemented or not with 0.1 μM or 1 μM of synthetic flg22 peptide (GeneCust). For each plantlet, lateral roots were counted, and the primary root length was measured using the RootNav software. Experiments were done at least two times, with a minimum of 16 plants per genotype and condition. Statistical tests were performed using the Mann–Whitney's *U*-test ($P < 0.05$) using wild-type values as reference.

Root meristem measurements

Plants were grown as for root growth analysis in response to flg22. The treated plants were stained with SCR1 Renaissance 2200 (Renaissance Chemicals) as described in [Ref. 103]. Images were obtained with LSM880 (Zeiss) confocal microscope. The SR2200 fluorescence was excited with a 405 nm laser line and emission recorded between 410 and 686 nm (405/410–686). Cell counting and primary root meristem measurements were performed using ImageJ package (<https://imagej.nih.gov/ij/>). Experiments were done two times, with a minimum of 18 plants per genotype and condition. Statistical tests were performed using the Student's *t*-test ($P < 0.05$).

Histochemical GUS staining

Histochemical GUS staining was performed according to [Ref. 104]. Briefly, 10-day-old plantlets grown in standard conditions were fixed in cold 90% acetone and incubated overnight at 37°C in the GUS staining buffer. Roots were subsequently fixed in 4% paraformaldehyde for 1 h and washed several times in 70% ethanol before a final wash in 10% glycerol prior observation. Images were acquired using an AxiolmagerZ2 microscope (Zeiss).

RNA extraction and RT-PCR analyses

Total RNA was extracted using Quick-RNA Kit (ZYMO RESEARCH), and DNase treatment was performed according to the manufacturer's protocol. One μg of DNase-free RNA was reverse transcribed using Maxima H Minus Reverse Transcriptase (Thermo Scientific). cDNA was then amplified in RT-qPCRs using LightCycler 480 SYBR Green I Master (Roche) and transcript-specific primers on a Roche LightCycler 480 thermocycler following standard protocol (45 cycles, 60°C annealing). Experiments were done in biological triplicates with at least three technical replicates. Expression was normalized to 2 constitutive genes (AT1G13320 and AT4G26410) [105]. For analysis of flg22 impact on gene expression, plants were

previously grown 9 days on solid 1/2MS medium + 1% sucrose and then transferred for additional 24 h in liquid 1/2MS medium + 1% sucrose before adding or not 1 μ M of flg22. Five plantlets were pooled for each replicate. The fold induction of expression after flg22 treatment was normalized to the WT response considered as 100%. For analysis of gene expression after a flg22 kinetic, roots from 8 plants were pooled for each replicate. For AS analysis, isoform-specific primers were designed for each differential event and the signal was normalized with respect to an internal gene probe (called INPUT) corresponding to a common exon for each group of transcripts. This allows differentiating the change of each isoforms independently of the expression level of the studied gene (splicing index) in each sample [33]. The splicing index was calculated following this equation: $\text{splicing index} = 2^{[\Delta Ct(\text{specific isoform}) - \Delta Ct(\text{INPUT})]}$. Error bars on qRT-PCR experiments represent standard deviations, and significant differences were determined using Student's *t*-test ($P \leq 0.05$, $n \geq 3$ biological replicates). All the used primers are listed in Dataset EV5.

For RT-PCR analysis, the amplification was performed using Phusion High-Fidelity DNA Polymerase and transcript-specific primers as manufacturer's protocol. PCR products were separated on an 8% polyacrylamide gel stained with SYBR Gold (Thermo Fischer Scientific) and revealed using a ChemiDoc MP Imaging System (Bio-Rad). Band intensity was quantified using ImageJ package (<https://imagej.nih.gov/ij/>). Isoform ratio was calculated as the ratio of intensity of the two bands corresponding either to the alternatively spliced or to spliced transcript isoforms, respectively.

Transcriptome studies

Total RNA was extracted using RNeasy Plant Mini Kit (Qiagen) from whole 14-day-old Col-0, 35S:ASCO1, and RNAi-ASCO1 plants grown on 1/2MS medium. Three independent biological replicates were produced per genotype. For each biological repetition and each point, RNA samples were obtained by pooling RNA from more than 200 plants. After RNA extraction, polyA RNAs were purified using Dynabeads mRNA DIRECT Micro Kit (Ambion). Libraries were constructed using the Truseq Stranded mRNA Sample Prep Kit (Illumina®). Sequencing was carried out at the POPS Transcriptomic Platform, Institute of Plant Sciences Paris-Saclay in Orsay, France. The Illumina HiSeq2000 technology was used to perform paired-end 100-bp sequencing. A minimum of 30 million of paired-end reads by sample were generated. RNA-seq preprocessing included trimming library adapters and quality controls with Trimmomatic [106]. Paired-end reads with Phred Quality Score Qscore > 20 and read length > 30 bases were kept, and ribosomal RNA sequences were removed with SortMeRNA [107]. Processed reads were aligned using Tophat2 with the following arguments: `-max-multihits 1 -i 20 -min-segment-intron 20 -min-coverage-intron 20 -library-type fr-firststrand -microexon-search -I 1,000 -max-segment-intron 1,000 -max-coverage-intron 1,000 -b2-very-sensitive`. Reads overlapping exons per genes were counted using the FeatureCounts function of the Rsubreads package using the GTF annotation files from the Araport11 repository (https://www.araport.org/downloads/Araport11_Release_201606/annotation/Araport11_GFF3_genes_transposons.201606.gff.gz). Significance of differential gene expression was estimated using DEseq2 [108], and the FDR correction of the

P-value was used during pairwise comparison between genotypes. A gene was declared differentially expressed if its adjusted *P*-value (FDR) was ≤ 0.01 and its absolute fold change was ≥ 1.5 .

Gene Ontology analysis

Gene Ontology enrichment analysis was done using AgriGO (<http://bioinfo.cau.edu.cn/agriGO>) and default parameters.

AS analysis

The RNA profile analysis was performed using the RNAprof software (v1.2.6) according to [Ref. 33]. Briefly, RNAprof software allows detection of differential RNA processing events from the comparison of nucleotide level RNA-seq coverage normalized for change in gene expression between conditions. Here, the RNAprof analysis compared RNA-seq data from biological triplicates of WT, RNAi-ASCO1, and 35S:ASCO1 lines. Differentially processed regions genes were filtered as follows: fold change > 2 and $P < 0.001$. Overlap between gene features and differentially processed regions was done using in-house R scripts (https://github.com/JBazinIPS2/Bioinfo/blob/master/RNAProf_events_selection.Rrst). Only regions fully included in a gene features were kept for further analysis. The RNAprof software archive, including documentation and test sets, is available at the following address: <http://rna.igmors.u-psud.fr/Software/rnaprof.php>. Transcript level quantification was performed using pseudo-alignment counts with kallisto [109] on AtRTD2 transcripts sequences (https://ics.hutton.ac.uk/atRTD/RTD2/AtRTDv2_QUASI_19April2016.fa) with a K-mer size of 31-nt. Differential AS events in the AtRTD2 database were detected using SUPPA2 with default parameters [53]. Only events with an adjusted $P < 0.01$ were kept for further analysis. Isoforms switch identification was performed with the IsoformSwitchAnalyzeR package [54] according to [34].

Whole-mount immunolocalization

Specific rabbit polyclonal antibodies were developed against PRP8a using the peptide TNKEKRERKVDDED (Li International). Five-day-old seedlings were fixed with 4% paraformaldehyde in microtubule stabilization buffer (MTSB) [110] for 1 h and rinsed once in glycine 0.1 M and twice with MTSB. Cell walls were partially digested for 45 min at 37°C in cellulase R10 1% w/v (Onozuka), pectolyase 1% w/v, and cytohelicase 0.5% w/v (Sigma) solution. After two PBS washes, root tissues were squashed on polylysine-treated glass slides (VWR International) and dipped in liquid nitrogen. The coverslip was then removed, and the slides were left to dry. After 2 rinses with PBS and 2 with PBS-0.1% Triton, they were treated with BSA 3% in PBS-Triton buffer for 1 h and incubated with the anti-PRP8a antibody (dilution 1:400) for 16 h at 4°C in a humid chamber. After incubation, slides were rinsed 8–10 times with PBS-Triton and incubated for 1 h at 37°C with the secondary antibody (anti-Rabbit IgG coupled to Alexa Fluor® 594, dilution 1:500; Thermo Scientific) and rinsed 10 times with PBS-Triton and once with PBS. Slides were mounted in Vectashield® containing DAPI (VECTOR Laboratories). Images were obtained with LSM880 (Zeiss) confocal microscope equipped with Plan-Apochromat 63 \times /NA1.40 Oil M27 lens. Dapi and Alexa 594 fluorescences were, respectively, excited with 405 nm and 561 nm diodes and recorded between 410–500 nm and 570–695 nm.

LncRNA-bound nuclear protein isolation by RNA purification

A method adapted from the ChIRP protocol [65,66,111] was developed to allow identification of nuclear proteins bound to specific lncRNAs. Briefly, plants were *in vivo* crosslinked, and nuclei of cells purified and extracted through sonication. The resulting supernatant was hybridized against biotinylated complementary oligonucleotides that tile the lncRNA of interest, and putative lncRNA-containing protein complexes were isolated using magnetic streptavidin beads. Co-purified ribonucleoprotein complexes were eluted and used to purify RNA or proteins, which were later subject to downstream assays for identification and quantification.

Probe design

Antisense 20-nt oligonucleotide probes were designed against the ASCO full-length sequence (AT1G67105) using an online designer at <http://singlemoleculfish.com/>. All probes were compared with the *A. thaliana* genome using the BLAST tool at the NCBI, and probes returning noticeable homology to non-ASCO targets were discarded. Eighteen probes were finally generated and split into two sets based on their relative positions along the ASCO sequence, such as EVEN-numbered and ODD-numbered probes were separately pooled. A symmetrical set of probes against *LacZ* RNA [66] was also used as the mock control. All probes were ordered biotinylated at the 3' end (Invitrogen).

Crosslinking and ribonucleoprotein complexes purification

For protein extraction, approximately 250 g of 7-day-old Col-0 plants grown on solid half-strength MS medium was irradiated three times with UV using a CROSSLINKER[®] CL-508 (Uvitec) at 0.400 J/cm². For RNA extraction, 10 g of 7-day-old Col-0 plants grown on solid half-strength MS medium was crosslinked under vacuum for 15 min with 37 ml of 1% (v/v) formaldehyde. The reaction was stopped by adding 2.5 ml of 2 M glycine, and seedlings were rinsed with Milli-Q purified water. For both crosslinking methods, 6 g of the fixed material was ground in liquid nitrogen and added to 50-ml tubes with 25 ml of extraction buffer 1–15 ml of plant material ground to fine dust (the nuclei were prepared starting with 30 fifty-milliliter tube; buffer 1: 10 mM Tris-HCl pH 8, 0.4 M sucrose, 10 mM MgCl₂, 5 mM β-mercaptoethanol, 1 ml/30 g of sample powder Protease Inhibitor Sigma Plant P9599). The solution was then filtered through Miracloth membrane (Sefar) into a new tube, and 5 ml of extraction buffer 2 (10 mM Tris-HCl pH 8, 0.25 M sucrose, 10 mM MgCl₂, 5 mM β-mercaptoethanol, 1% Triton X-100, 50 μl protease inhibitor) was added. The solution was then centrifuged, the supernatant discarded and the pellet was resuspended in 500 μl of extraction buffer 3 (10 mM Tris-HCl pH 8, 1.7 M sucrose, 2 mM MgCl₂, 5 mM β-mercaptoethanol, 0.15% Triton X-100, 50 μl protease inhibitor) and layered on top of fresh extraction buffer 3 in a new tube. After centrifugation at 13,000 rpm for 2 min at 4°C to pellet nuclei, the supernatant was discarded and the pellet resuspended in 300 μl of nuclei lysis buffer (50 mM Tris-HCl pH 7, 1% SDS, 10 mM EDT, 1 mM DTT, 50 μl protease inhibitor, 10 μl RNase inhibitor per tube) to degrade nuclear membranes. Samples were sonicated three times in refrigerated BIORUPTOR Plus (Diagenode), 10 cycles 30 s ON–30 sec OFF in a Diagenode TPX microtube M-50001. After centrifugation, the supernatant was transferred to a new tube and diluted two times volume in hybridization buffer

(50 mM Tris-HCl pH 7, 750 mM NaCl, 1% SDS, 15% formamide, 1 mM DTT, 50 μl protease inhibitor, 10 μl RNase inhibitor). One hundred pmol of probes were added to samples and incubated 4 h at 50°C in a thermocycler. Samples were transferred to tubes containing Dynabeads-Streptavidin C1 (Thermo Fisher Scientific) and incubated 1 h at 50°C. Then, samples were placed on a magnetic field and washed three times with 1 ml of wash buffer (2× SSC, 0.5% SDS, 1 mM DTT, 100 μl protease inhibitor).

Protein purification

Samples for protein extraction were DNase-treated according to the manufacturer (Thermo Scientific). After addition of 1.8 ml of TCA-acetone (5 ml 6.1 N TCA + 45 ml acetone + 35 μl β-mercaptoethanol), samples were incubated overnight at –80°C. After centrifugation at 44,000 g for 20 min and 4°C, the supernatant was discarded and 1.8 ml of acetone wash buffer (120 ml acetone, 84 μl β-mercaptoethanol) was added to the samples. Then, samples were incubated 1 h at –20°C and centrifuged again at 40,000 g for 20 min and 4°C. The supernatant was discarded, and the dry pellet was used for mass spectrometry analysis.

RNA purification

Samples for RNA extraction were boiled for 15 min after washing with 1 ml of wash buffer (2× SSC, 0.5% SDS, 1 mM DTT, 100 μl protease inhibitor). Beads were removed in a magnetic field, and TRIzol/chloroform RNA extraction was performed according to the manufacturer (Sigma). RNAs were precipitated using 2 volumes EtOH 100, 10% 3 M sodium acetate, and 1 μl glycogen and washed with EtOH 70%. RNAs were kept at –20°C before use for reverse transcription and RT-qPCR analysis.

Liquid Chromatography–Mass Spectrometry (LC-MS) analysis

Proteins purified from ribonucleoprotein complexes were analyzed using the King Abdullah University of Science and Technology proteomic facilities. Dry pellets of samples purified with either ODD, EVEN, or *LacZ* probe sets were solubilized in trypsin buffer (Promega) for digestion into small peptides. The solubilized peptides were then injected into a Q Exactive[™] HF hybrid quadrupole-Orbitrap mass spectrometer (Thermo Scientific) with a Liquid Chromatography (LC) Acclaim PepMap C18 column (25 cm length × 75 μm I.D. × 3 μm particle size, 100 Å porosity, Dionex). Data were analyzed for each sample using Mascot software (Matrix Science), with a minimal sensitivity of 2 detected peptides per identified protein.

RNA immunoprecipitation

Eleven-day-old plants grown in Petri dishes were irradiated three times with UV using a CL-508 cross-linker (Uvitec) at 0.400 J/cm². Briefly, fixed material was ground in liquid nitrogen and homogenized and nuclei isolated and lysed according to [Ref. 112]. RNA immunoprecipitation was basically performed as described by [Ref. 113]. The nuclei extract (input) was used for immunoprecipitation with 50 μl of Dynabeads-Protein A (Thermo Fisher Scientific) and 1 μg of anti-GFP antibodies (Abcam ab290) or anti-PRP8a (Li International), respectively. Beads were washed twice for 5 min at 4°C with wash buffer 1 (150 mM NaCl, 1% Triton X-100, 0.5% Nonidet

P-40, 1 mM EDTA, and 20 mM Tris–HCl, pH 7.5) and twice with wash buffer 2 (20 mM Tris–HCl, pH 8) and finally resuspended in 100 μ l Proteinase K buffer (100 mM Tris–HCl, pH 7.4, 50 mM NaCl, and 10 mM EDTA). Twenty microliters were saved for further immunoblot analysis. After Proteinase K (Ambion AM2546) treatment, beads were removed with a magnet, and the supernatants were transferred to a 2-ml tube. RNA was extracted using TRI Reagent (Sigma-Aldrich) as indicated by the manufacturer. Eighty microliters of nuclei extracts was used for input RNA extraction. The immunoprecipitation and input samples were treated with DNase, and random hexamers were used for subsequent RT. Quantitative real-time PCR reactions were performed using specific primers (Dataset EV5). Results were expressed as a percentage of cDNA detected after immunoprecipitation, taking the input sample as 100%. For Western blot analysis, immunoprecipitated proteins were eluted by incubating 20 μ l of beads in 20 μ l of 2 \times SDS-loading buffer without β -mercaptoethanol (100 mM Tris–HCl pH 6.8, 20% glycerol, 12.5 mM EDTA, 0.02% bromophenol blue) at 50°C for 15 min. Input, unbound and eluted fractions were boiled in 2 \times SDS-loading buffer with 1% β -mercaptoethanol for 10 min, loaded onto a 4–20% Mini-PROTEAN[®] TGX[™] Precast Protein Gels (Bio-Rad), and transferred onto a PVDF membrane using the Mini Trans-Blot[®] Cell system (Bio-Rad) for 3 h at 70 V. Membranes were blocked in 5% dry nonfat milk in PBST and probed using PRP8a antibody (1:500) and an HRP coupled anti-Rabbit secondary antibody (Bio-Rad, 1:10,000). All antibodies were diluted in 1% dry nonfat milk in PBST. Blots were revealed with the Clarity ECL substrate according the manufacturer instruction (Bio-Rad) and imaged using the ChemiDoc system (Bio-Rad).

Data availability

Data were deposited in CATdb database [114] (<http://tools.ips2.u-psud.fr/CATdb/>) with ProjectID NGS2016-07-ASCOncRNA. This project was submitted from CATdb into the international repository GEO (<http://www.ncbi.nlm.nih.gov/geo>) with accession number GSE135376.

Expanded View for this article is available online.

Acknowledgements

Synthetic flg22 peptide was kindly provided by J. Colcombet (IPS2). Seeds from the *prp8-7* [35,113] and the *smd1b* [71] mutants were kindly provided by H. Vaucheret. We thank Wil Prall for critical reading of the manuscript. This work was supported by grants from ANPCyT (PICT 2016-0289 and -0007, Argentina), CNRS (Laboratoire International Associé NOCOSYM), the “Laboratoire d’Excellence (LABEX)” Saclay Plant Sciences (SPS; ANR-10-LABX-40), the Ministère Français de l’Enseignement Supérieur et de la Recherche (RR), and the ANR grants (ANR-15-CE20-0002-01 EPISYM and ANR 16-CE20-0003-04 SPLISIL) as well as the EPIMMUNITY International project between IPS2, France and KAUST University, Saudi Arabia. The POPS platform benefits from the support of the LabEx Saclay Plant Sciences-SPS (ANR-10-LABX-0040-SPS).

Author contributions

RR, JB, NR-B, MM, LL, AC, CC, and FA performed the experiments; SH was in charge of the RNA-seq libraries preparation and sequencing; TB, RR, JB, CC, MB, MC, and FA analyzed the data; JB performed bioinformatic analyses; JB,

MC, and FA designed the experiments; MC and FA conceived the study and wrote the manuscript.

Conflict of interest

The authors declare that they have no conflict of interest.

References

1. Chaudhary S, Khokhar W, Jabre I, Reddy ASN, Byrne LJ, Wilson CM, Syed NH (2019) Alternative splicing and protein diversity: plants versus animals. *Front Plant Sci* 10: 708
2. Wang B-B, O’Toole M, Brendel V, Young ND (2008) Cross-species EST alignments reveal novel and conserved alternative splicing events in legumes. *BMC Plant Biol* 8: 17
3. Marquez Y, Brown JWS, Simpson C, Barta A, Kalyna M (2012) Transcriptome survey reveals increased complexity of the alternative splicing landscape in *Arabidopsis*. *Genome Res* 22: 1184–1195
4. Gerstein MB, Rozowsky J, Yan K-K, Wang D, Cheng C, Brown JB, Davis CA, Hillier L, Sisu C, Li JJ *et al* (2014) Comparative analysis of the transcriptome across distant species. *Nature* 512: 445–448
5. Syed NH, Kalyna M, Marquez Y, Barta A, Brown JWS (2012) Alternative splicing in plants – coming of age. *Trends Plant Sci* 17: 616–623
6. Djebali S, Davis CA, Merkel A, Dobin A, Lassmann T, Mortazavi A, Tanzer A, Lagarde J, Lin W, Schlesinger F *et al* (2012) Landscape of transcription in human cells. *Nature* 489: 101–108
7. Boon K-L, Grainger RJ, Ehsani P, Barrass JD, Auchynnikava T, Inglehearn CF, Beggs JD (2007) *prp8* mutations that cause human retinitis pigmentosa lead to a U5 snRNP maturation defect in yeast. *Nat Struct Mol Biol* 14: 1077–1083
8. Tanackovic G, Ransijn A, Ayuso C, Harper S, Berson EL, Rivolta C (2011) A missense mutation in PRPF6 causes impairment of pre-mRNA splicing and autosomal-dominant retinitis pigmentosa. *Am J Hum Genet* 88: 643–649
9. Yoshida K, Sanada M, Shiraishi Y, Nowak D, Nagata Y, Yamamoto R, Sato Y, Sato-Otsubo A, Kon A, Nagasaki M *et al* (2011) Frequent pathway mutations of splicing machinery in myelodysplasia. *Nature* 478: 64–69
10. Faial T (2015) RNA splicing in common disease. *Nat Genet* 47: 105–105
11. Palusa SG, Ali GS, Reddy ASN (2007) Alternative splicing of pre-mRNAs of *Arabidopsis* serine/arginine-rich proteins: regulation by hormones and stresses. *Plant J* 49: 1091–1107
12. Tanabe N, Kimura A, Yoshimura K, Shigeoka S (2009) Plant-specific SR-related protein atSR45a interacts with spliceosomal proteins in plant nucleus. *Plant Mol Biol* 70: 241–252
13. Filichkin SA, Priest HD, Givan SA, Shen R, Bryant DW, Fox SE, Wong W-K, Mockler TC (2010) Genome-wide mapping of alternative splicing in *Arabidopsis thaliana*. *Genome Res* 20: 45–58
14. Reddy ASN, Marquez Y, Kalyna M, Barta A (2013) Complexity of the alternative splicing landscape in plants. *Plant Cell* 25: 3657–3683
15. Ding F, Cui P, Wang Z, Zhang S, Ali S, Xiong L (2014) Genome-wide analysis of alternative splicing of pre-mRNA under salt stress in *Arabidopsis*. *BMC Genom* 15: 431
16. Zhan X, Qian B, Cao F, Wu W, Yang L, Guan Q, Gu X, Wang P, Okusolubo TA, Dunn SL *et al* (2015) An *Arabidopsis* PWI and RRM motif-containing protein is critical for pre-mRNA splicing and ABA responses. *Nat Commun* 6: 8139
17. Laloum T, Martín G, Duque P (2018) Alternative splicing control of abiotic stress responses. *Trends Plant Sci* 23: 140–150

18. Jabre I, Reddy ASN, Kalyna M, Chaudhary S, Khokhar W, Byrne LJ, Wilson CM, Syed NH (2019) Does co-transcriptional regulation of alternative splicing mediate plant stress responses? *Nucleic Acids Res* 47: 2716–2726
19. Rigo R, Bazin JRM, Crespi M, Charon CL (2019) Alternative splicing in the regulation of plant-microbe interactions. *Plant Cell Physiol* 60: 1906–1916
20. Ariel F, Romero-Barrios N, Jégu T, Benhamed M, Crespi M (2015) Battles and hijacks: noncoding transcription in plants. *Trends Plant Sci* 20: 362–371
21. Zhang Y, Zhang X-O, Chen T, Xiang J-F, Yin Q-F, Xing Y-H, Zhu S, Yang L, Chen L-L (2013) Circular intronic long noncoding RNAs. *Mol Cell* 51: 792–806
22. Song X, Liu G, Huang Z, Duan W, Tan H, Li Y, Hou X (2016) Temperature expression patterns of genes and their coexpression with lncRNAs revealed by RNA-Seq in non-heading Chinese cabbage. *BMC Genom* 17: 297
23. Romero-Barrios N, Legascue MF, Benhamed M, Ariel F, Crespi M (2018) Splicing regulation by long noncoding RNAs. *Nucleic Acids Res* 46: 2169–2184
24. Bardou F, Ariel F, Simpson CG, Romero-Barrios N, Laporte P, Balzergue S, Brown JWS, Crespi M (2014) Long noncoding RNA modulates alternative splicing regulators in *Arabidopsis*. *Dev Cell* 30: 166–176
25. Barry G, Briggs JA, Vanichkina DP, Poth EM, Beveridge NJ, Ratnu VS, Nayler SP, Nones K, Hu J, Bredy TW et al (2014) The long non-coding RNA Gomafu is acutely regulated in response to neuronal activation and involved in schizophrenia-associated alternative splicing. *Mol Psychiatry* 19: 486–494
26. Ji Q, Zhang L, Liu X, Zhou L, Wang W, Han Z, Sui H, Tang Y, Wang Y, Liu N et al (2014) Long non-coding RNA MALAT1 promotes tumour growth and metastasis in colorectal cancer through binding to SFPQ and releasing oncogene PTBP2 from SFPQ/PTBP2 complex. *Br J Cancer* 111: 736–748
27. West JA, Davis CP, Sunwoo H, Simon MD, Sadreyev RI, Wang PI, Tolstorukov MY, Kingston RE (2014) The long noncoding RNAs NEAT1 and MALAT1 bind active chromatin sites. *Mol Cell* 55: 791–802
28. Kong Y, Hsieh C-H, Alonso LC (2018) A lncRNA at the CDKN2A/B locus with roles in cancer and metabolic disease. *Front Endocrinol* 9: 405
29. Beltran M, Puig I, Pena C, Garcia JM, Alvarez AB, Pena R, Bonilla F, de Herreros AG (2008) A natural antisense transcript regulates Zeb2/Sip1 gene expression during Snail1-induced epithelial-mesenchymal transition. *Genes Dev* 22: 756–769
30. Villamizar O, Chambers CB, Riberdy JM, Persons DA, Wilber A (2016) Long noncoding RNA Saf and splicing factor 45 increase soluble Fas and resistance to apoptosis. *Oncotarget* 7: 13810–13826
31. Gonzalez I, Munita R, Agirre E, Dittmer TA, Gysling K, Misteli T, Luco RF (2015) A lncRNA regulates alternative splicing via establishment of a splicing-specific chromatin signature. *Nat Struct Mol Biol* 22: 370–376
32. Conn VM, Hugouvieux V, Nayak A, Conos SA, Capovilla G, Cildir G, Jourdain A, Tergaonkar V, Schmid M, Zubieta C et al (2017) A circRNA from SEPALLATA3 regulates splicing of its cognate mRNA through R-loop formation. *Nat Plants* 3: 17053
33. Tran VDT, Souiai O, Romero-Barrios N, Crespi M, Gautheret D (2016) Detection of generic differential RNA processing events from RNA-seq data. *RNA Biol* 13: 59–67
34. Bazin J, Romero N, Rigo R, Charon C, Blein T, Ariel F, Crespi M (2018) Nuclear speckle RNA binding proteins remodel alternative splicing and the non-coding *Arabidopsis* transcriptome to regulate a cross-talk between auxin and immune responses. *Front Plant Sci* 9: 1209
35. Sasaki T, Kanno T, Liang S-C, Chen P-Y, Liao W-W, Lin W-D, Matzke AJM, Matzke M (2015) An Rtf2 domain-containing protein influences Pre-mRNA splicing and is essential for embryonic development in *Arabidopsis thaliana*. *Genetics* 200: 523–535
36. Malamy JE, Benfey PN (1997) Organization and cell differentiation in lateral roots of *Arabidopsis thaliana*. *Development* 124: 33–44
37. Munekage YN, Inoue S, Yoneda Y, Yokota A (2015) Distinct palisade tissue development processes promoted by leaf autonomous signalling and long-distance signalling in *Arabidopsis thaliana*. *Plant Cell Environ* 38: 1116–1126
38. Pauwels L, Morreel K, De Witte E, Lammertyn F, Van Montagu M, Boerjan W, Inzé D, Goossens A (2008) Mapping methyl jasmonate-mediated transcriptional reprogramming of metabolism and cell cycle progression in cultured *Arabidopsis* cells. *Proc Natl Acad Sci USA* 105: 1380–1385
39. Li Y, Sawada Y, Hirai A, Sato M, Kuwahara A, Yan X, Hirai MY (2013) Novel insights into the function of *Arabidopsis* R2R3-MYB transcription factors regulating aliphatic glucosinolate biosynthesis. *Plant Cell Physiol* 54: 1335–1344
40. Liu S, Kracher B, Ziegler J, Birkenbihl RP, Somssich IE (2015) Negative regulation of ABA signaling by WRKY33 is critical for *Arabidopsis* immunity towards *Botrytis cinerea* 2100. *Elife* 4: e07295
41. Moffat CS, Ingle RA, Wathugala DL, Saunders NJ, Knight H, Knight MR (2012) ERF5 and ERF6 play redundant roles as positive regulators of JA/Et-mediated defense against *Botrytis cinerea* in *Arabidopsis*. *PLoS ONE* 7: e35995
42. Bethke G, Unthan T, Uhrig JF, Pöschl Y, Gust AA, Scheel D, Lee J (2009) Flg22 regulates the release of an ethylene response factor substrate from MAP kinase 6 in *Arabidopsis thaliana* via ethylene signaling. *Proc Natl Acad Sci USA* 106: 8067–8072
43. Libault M, Wan J, Czechowski T, Udvardi M, Stacey G (2007) Identification of 118 *Arabidopsis* transcription factor and 30 ubiquitin-ligase genes responding to chitin, a plant-defense elicitor. *Mol Plant Microbe Interact* 20: 900–911
44. O'Malley RC, Huang S-SC, Song L, Lewsey MG, Bartlett A, Nery JR, Galli M, Gallavotti A, Ecker JR (2016) Cistrome and episcistrome features shape the regulatory DNA landscape. *Cell* 166: 1598
45. Gómez-Gómez L, Felix G, Boller T (1999) A single locus determines sensitivity to bacterial flagellin in *Arabidopsis thaliana*. *Plant J* 18: 277–284
46. Beck M, Wyrtsch I, Strutt J, Wimalasekera R, Webb A, Boller T, Robatzek S (2014) Expression patterns of flagellin sensing 2 map to bacterial entry sites in plant shoots and roots. *J Exp Bot* 65: 6487–6498
47. Poncini L, Wyrtsch I, Déneraud Tendon V, Vorley T, Boller T, Geldner N, Métraux J-P, Lehmann S (2017) In roots of *Arabidopsis thaliana*, the damage-associated molecular pattern AtPep1 is a stronger elicitor of immune signalling than flg22 or the chitin heptamer. *PLoS ONE* 12: e0185808
48. Denoux C, Galletti R, Mammarella N, Gopalan S, Werck D, De Lorenz G, Ferrari S, Ausubel FM, Dewdney J (2008) Activation of defense response pathways by OGs and Flg22 elicitors in *Arabidopsis* seedlings. *Mol Plant* 1: 423–445
49. Asai T, Tena G, Plotnikova J, Willmann MR, Chiu W-L, Gomez-Gomez L, Boller T, Ausubel FM, Sheen J (2002) MAP kinase signalling cascade in *Arabidopsis* innate immunity. *Nature* 415: 977–983
50. Zipfel C (2009) Early molecular events in PAMP-triggered immunity. *Curr Opin Plant Biol* 12: 414–420

51. Boudsocq M, Willmann MR, McCormack M, Lee H, Shan L, He P, Bush J, Cheng S-H, Sheen J (2010) Differential innate immune signalling via Ca(2+) sensor protein kinases. *Nature* 464: 418–422
52. Zhang R, Calixto CPG, Marquez Y, Venhuizen P, Tzioutziou NA, Guo W, Spensley M, Entizne JC, Lewandowska D, Ten Have S et al (2017) A high quality *Arabidopsis* transcriptome for accurate transcript-level analysis of alternative splicing. *Nucleic Acids Res* 45: 5061–5073
53. Trincado JL, Entizne JC, Hysenaj G, Singh B, Skalic M, Elliott DJ, Eyraas E (2018) SUPPA2: fast, accurate, and uncertainty-aware differential splicing analysis across multiple conditions. *Genome Biol* 19: 40
54. Vitting-Seerup K, Sandelin A (2019) IsoformSwitchAnalyzer: analysis of changes in genome-wide patterns of alternative splicing and its functional consequences. *Bioinformatics* 35: 4469–4471
55. Kalyna M, Simpson CG, Syed NH, Lewandowska D, Marquez Y, Kusenda B, Marshall J, Fuller J, Cardle L, McNicol J et al (2012) Alternative splicing and nonsense-mediated decay modulate expression of important regulatory genes in *Arabidopsis*. *Nucleic Acids Res* 40: 2454–2469
56. Drechsel G, Kahles A, Kesarwani AK, Stauffer E, Behr J, Drewe P, Rättsch G, Wachter A (2013) Nonsense-mediated decay of alternative precursor mRNA splicing variants is a major determinant of the *Arabidopsis* steady state transcriptome. *Plant Cell* 25: 3726–3742
57. Mohr TJ, Mammarella ND, Hoff T, Woffenden BJ, Jelesko JG, McDowell JM (2010) The *Arabidopsis* downy mildew resistance gene RPP8 is induced by pathogens and salicylic acid and is regulated by W box cis elements. *Mol Plant Microbe Interact* 23: 1303–1315
58. Staal J, Kaliff M, Dewaele E, Persson M, Dixelius C (2008) RLM3, a TIR domain encoding gene involved in broad-range immunity of *Arabidopsis* to necrotrophic fungal pathogens. *Plant J* 55: 188–200
59. Xu S, Zhang Z, Jing B, Gannon P, Ding J, Xu F, Li X, Zhang Y (2011) Transportin-SR is required for proper splicing of resistance genes and plant immunity. *PLoS Genet* 7: e1002159
60. Zhang Z, Liu Y, Ding P, Li Y, Kong Q, Zhang Y (2014) Splicing of receptor-like kinase-encoding SNC4 and CERK1 is regulated by two conserved splicing factors that are required for plant immunity. *Mol Plant* 7: 1766–1775
61. Schenk PM, Kazan K, Rusu AG, Manners JM, Maclean DJ (2005) The SEN1 gene of *Arabidopsis* is regulated by signals that link plant defence responses and senescence. *Plant Physiol Biochem* 43: 997–1005
62. Straus MR, Rietz S, Loren V, van Themaat E, Bartsch M, Parker JE (2010) Salicylic acid antagonism of EDS1-driven cell death is important for immune and oxidative stress responses in *Arabidopsis*. *Plant J* 62: 628–640
63. Kissen R, Hyldebakk E, Wang C-WW, Sørmo CG, Rossiter JT, Bones AM (2012) Ecotype dependent expression and alternative splicing of epithiospecifier protein (ESP) in *Arabidopsis thaliana*. *Plant Mol Biol* 78: 361–375
64. Zhang X-C, Gassmann W (2007) Alternative splicing and mRNA levels of the disease resistance gene RPS4 are induced during defense responses. *Plant Physiol* 145: 1577–1587
65. Chu C, Qu K, Zhong FL, Artandi SE, Chang HY (2011) Genomic maps of long noncoding RNA occupancy reveal principles of RNA-chromatin interactions. *Mol Cell* 44: 667–678
66. Ariel F, Jegu T, Latrasse D, Romero-Barrios N, Christ A, Benhamed M, Crespi M (2014) Noncoding transcription by alternative RNA polymerases dynamically regulates an auxin-driven chromatin loop. *Mol Cell* 55: 383–396
67. Grainger RJ, Beggs JD (2005) Prp8 protein: at the heart of the spliceosome. *RNA* 11: 533–557
68. Marquardt S, Raitskin O, Wu Z, Liu F, Sun Q, Dean C (2014) Functional consequences of splicing of the antisense transcript COOLAIR on FLC transcription. *Mol Cell* 54: 156–165
69. Claudius A-K, Romani P, Lamkemeyer T, Jindra M, Uhlirva M (2014) Unexpected role of the steroid-deficiency protein ecdysoneless in pre-mRNA splicing. *PLoS Genet* 10: e1004287
70. Koncz C, Dejong F, Villacorta N, Szakonyi D, Koncz Z (2012) The spliceosome-activating complex: molecular mechanisms underlying the function of a pleiotropic regulator. *Front Plant Sci* 3: 9
71. Elvira-Matelot E, Bardou F, Ariel F, Jauvion V, Bouteiller N, Le Masson I, Cao J, Crespi MD, Vaucheret H (2016) The nuclear ribonucleoprotein SmD1 interplays with splicing, RNA quality control, and posttranscriptional gene silencing in *Arabidopsis*. *Plant Cell* 28: 426–438
72. Suresh PS, Tsutsumi R, Venkatesh T (2018) YBX1 at the crossroads of non-coding transcriptome, exosomal, and cytoplasmic granular signaling. *Eur J Cell Biol* 97: 163–167
73. Yin Q-F, Yang L, Zhang Y, Xiang J-F, Wu Y-W, Carmichael GG, Chen L-L (2012) Long noncoding RNAs with snoRNA ends. *Mol Cell* 48: 219–230
74. Kong J, Sun W, Li C, Wan L, Wang S, Wu Y, Xu E, Zhang H, Lai M (2016) Long non-coding RNA LINC01133 inhibits epithelial-mesenchymal transition and metastasis in colorectal cancer by interacting with SRSF6. *Cancer Lett* 380: 476–484
75. Tsuiji H, Yoshimoto R, Hasegawa Y, Furuno M, Yoshida M, Nakagawa S (2011) Competition between a noncoding exon and introns: gomafu contains tandem UACUAAC repeats and associates with splicing factor-1. *Genes Cells* 16: 479–490
76. Rapicavoli NA, Blackshaw S (2009) New meaning in the message: noncoding RNAs and their role in retinal development. *Dev Dyn* 238: 2103–2114
77. Rapicavoli NA, Poth EM, Blackshaw S (2010) The long noncoding RNA RNCR2 directs mouse retinal cell specification. *BMC Dev Biol* 10: 49
78. Mercer TR, Qureshi IA, Gokhan S, Dinger ME, Li G, Mattick JS, Mehler MF (2010) Long noncoding RNAs in neuronal-glia fate specification and oligodendrocyte lineage maturation. *BMC Neurosci* 11: 14
79. Sone M, Hayashi T, Tarui H, Agata K, Takeichi M, Nakagawa S (2007) The mRNA-like noncoding RNA Gomafu constitutes a novel nuclear domain in a subset of neurons. *J Cell Sci* 120: 2498–2506
80. Hutchinson JN, Ensminger AW, Clemson CM, Lynch CR, Lawrence JB, Chess A (2007) A screen for nuclear transcripts identifies two linked noncoding RNAs associated with SC35 splicing domains. *BMC Genom* 8: 39
81. Wang J, Pan Y, Wu J, Zhang C, Huang Y, Zhao R, Cheng G, Liu J, Qin C, Shao P et al (2016) The association between abnormal long noncoding RNA MALAT-1 expression and cancer lymph node metastasis: a meta-analysis. *Biomed Res Int* 2016: 1823482
82. Zhang R, Xia Y, Wang Z, Zheng J, Chen Y, Li X, Wang Y, Ming H (2017) Serum long non coding RNA MALAT-1 protected by exosomes is up-regulated and promotes cell proliferation and migration in non-small cell lung cancer. *Biochem Biophys Res Commun* 490: 406–414
83. Malakar P, Shilo A, Mogilevsky A, Stein I, Pikarsky E, Nevo Y, Benyamini H, Elgavish S, Zong X, Prasanth KV et al (2017) Long noncoding RNA MALAT1 promotes hepatocellular carcinoma development by SRSF1 upregulation and mTOR activation. *Can Res* 77: 1155–1167
84. Huot B, Yao J, Montgomery BL, He SY (2014) Growth-defense trade-offs in plants: a balancing act to optimize fitness. *Mol Plant* 7: 1267–1287
85. Stringlis IA, Proietti S, Hickman R, Van Verk MC, Zamioudis C, Pieterse CMJ (2018) Root transcriptional dynamics induced by beneficial

- rhizobacteria and microbial immune elicitors reveal signatures of adaptation to mutualists. *Plant J* 93: 166–180
86. Liang N, Cheng D, Cui J, Dai C, Luo C, Liu T, Li J (2017) Vernalisation mediated lncRNA-like gene expression in *Beta vulgaris*. *Funct Plant Biol* 44: 720
 87. Heo JB, Sung S (2011) Vernalization-mediated epigenetic silencing by a long intronic noncoding RNA. *Science* 331: 76–79
 88. Kim D-H, Sung S (2012) Environmentally coordinated epigenetic silencing of FLC by protein and long noncoding RNA components. *Curr Opin Plant Biol* 15: 51–56
 89. Kindgren P, Ard R, Ivanov M, Marquardt S (2018) Transcriptional read-through of the long non-coding RNA SValka governs plant cold acclimation. *Nat Commun* 9: 4561
 90. Hernando CE, Hourquet MG, de Leone MJ, Careno D, Iserle J, Garcia SM, Yanovsky MJ (2019) A role for Pre-mRNA-PROCESSING PROTEIN 40C in the control of growth, development, and stress tolerance in *Arabidopsis thaliana*. *Front Plant Sci* 10: 1019
 91. Monaghan J, Xu F, Gao M, Zhao Q, Palma K, Long C, Chen S, Zhang Y, Li X (2009) Two Prp19-like U-box proteins in the MOS4-associated complex play redundant roles in plant innate immunity. *PLoS Pathog* 5: e1000526
 92. Palma K, Zhao Q, Cheng YT, Bi D, Monaghan J, Cheng W, Zhang Y, Li X (2007) Regulation of plant innate immunity by three proteins in a complex conserved across the plant and animal kingdoms. *Genes Dev* 21: 1484–1493
 93. Xu F, Xu S, Wiermer M, Zhang Y, Li X (2012) The cyclin L homolog MOS12 and the MOS4-associated complex are required for the proper splicing of plant resistance genes. *Plant J* 70: 916–928
 94. Herold N, Will CL, Wolf E, Kastner B, Urlaub H, Lührmann R (2009) Conservation of the protein composition and electron microscopy structure of *Drosophila melanogaster* and human spliceosomal complexes. *Mol Cell Biol* 29: 281–301
 95. Whittaker C, Dean C (2017) The FLC locus: a platform for discoveries in epigenetics and adaptation. *Annu Rev Cell Dev Biol* 33: 555–575
 96. Crespi MD, Jurkevitch E, Poirer M, d'Aubenton-Carafa Y, Petrovics G, Kondorosi E, Kondorosi A (1994) enod40, a gene expressed during nodule organogenesis, codes for a non-translatable RNA involved in plant growth. *EMBO J* 13: 5099–5112
 97. Charon C, Sousa C, Crespi M, Kondorosi A (1999) Alteration of enod40 expression modifies *Medicago truncatula* root nodule development induced by *Sinorhizobium meliloti*. *Plant Cell* 11: 1953–1966
 98. Campalans A, Kondorosi A, Crespi M (2004) Enod40, a short open reading frame-containing mRNA, induces cytoplasmic localization of a nuclear RNA binding protein in *Medicago truncatula*. *Plant Cell* 16: 1047–1059
 99. Gulyaev AP, Roussis A (2007) Identification of conserved secondary structures and expansion segments in enod40 RNAs reveals new enod40 homologues in plants. *Nucleic Acids Res* 35: 3144–3152
 100. Clough SJ, Bent AF (1998) Floral dip: a simplified method for *Agrobacterium*-mediated transformation of *Arabidopsis thaliana*. *Plant J* 16: 735–743
 101. Ariel F, Brault-Hernandez M, Laffont C, Huault E, Brault M, Plet J, Moison M, Blanchet S, Ichanté JL, Chabaud M et al (2012) Two direct targets of cytokinin signaling regulate symbiotic nodulation in *Medicago truncatula*. *Plant Cell* 24: 3838–3852
 102. Pound MP, French AP, Atkinson JA, Wells DM, Bennett MJ, Pridmore T (2013) RootNav: navigating images of complex root architectures. *Plant Physiol* 162: 1802–1814
 103. Musielak TJ, Schenkel L, Kolb M, Henschen A, Bayer M (2015) A simple and versatile cell wall staining protocol to study plant reproduction. *Plant Reprod* 28: 161–169
 104. Latrasse D, Jégu T, Meng P-H, Mazubert C, Hudik E, Delarue M, Charon C, Crespi M, Hirt H, Raynaud C et al (2013) Dual function of MIPS1 as a metabolic enzyme and transcriptional regulator. *Nucleic Acids Res* 41: 2907–2917
 105. Czechowski T, Stitt M, Altmann T, Udvardi MK, Scheible W-R (2005) Genome-wide identification and testing of superior reference genes for transcript normalization in *Arabidopsis*. *Plant Physiol* 139: 5–17
 106. Bolger AM, Lohse M, Usadel B (2014) Trimmomatic: a flexible trimmer for Illumina sequence data. *Bioinformatics* 30: 2114–2120
 107. Kopylova E, Noé L, Touzet H (2012) SortMeRNA: fast and accurate filtering of ribosomal RNAs in metatranscriptomic data. *Bioinformatics* 28: 3211–3217
 108. Love MI, Huber W, Anders S (2014) Moderated estimation of fold change and dispersion for RNA-seq data with DESeq2. *Genome Biol* 15: 550
 109. Bray NL, Pimentel H, Melsted P, Pachter L (2016) Near-optimal probabilistic RNA-seq quantification. *Nat Biotechnol* 34: 525–527
 110. Pasternak T, Tietz O, Rapp K, Begheldo M, Nitschke R, Ruperti B, Palme K (2015) Protocol: an improved and universal procedure for whole-mount immunolocalization in plants. *Plant Methods* 11: 50
 111. Chu C, Chang HY (2016) Understanding RNA-chromatin interactions using chromatin isolation by RNA purification (ChIRP). *Methods Mol Biol* 1480: 115–123
 112. Gendrel A-V, Lippman Z, Martienssen R, Colot V (2005) Profiling histone modification patterns in plants using genomic tiling microarrays. *Nat Methods* 2: 213–218
 113. Carlotto N, Wirth S, Furman N, Ferreyra Solari N, Ariel F, Crespi M, Kobayashi K (2016) The chloroplastic DEVH-box RNA helicase INCREASED SIZE EXCLUSION LIMIT 2 involved in plasmodesmata regulation is required for group II intron splicing. *Plant Cell Environ* 39: 165–173
 114. Gagnot S, Tamby J-P, Martin-Magniette M-L, Bitton F, Taconnat L, Balzergue S, Aubourg S, Renou J-P, Lecharny A, Brunaud V (2008) CATdb: a public access to *Arabidopsis* transcriptome data from the URGV-CATMA platform. *Nucleic Acids Res* 36: D986–D990
 115. Thorvaldsdóttir H, Robinson JT, Mesirov JP (2013) Integrative genomics viewer (IGV): high-performance genomics data visualization and exploration. *Brief Bioinform* 14: 178–192

Expanded View Figures

Figure EV1. The response to auxin is altered in RNAi-*ASCO* lines.

- A *ASCO* transcript levels in two independent 14-day-old RNAi-*ASCO* lines compared to WT. Error bars represent standard deviation. The asterisk (*) indicates a significant difference as determined by Student's *t*-test ($P < 0.05$, $n = 3$ biological replicates).
- B RNA-seq read coverage on *ASCO* lncRNA in RNAi-*ASCO* and WT seedlings RNA-seq data. The region cloned to generate dsRNA is indicated on the gene structure. Coverage plots were made with IGV software [115] using normalized (read per million) bigwig files. The same scale (0–200) was used for each track.
- C, D Primary root length (C) and lateral root density (D) of WT and two independent RNAi-*ASCO* lines grown on media with or without 100 nM NAA and measured 7 days after germination. The asterisk (*) indicates a significant difference as determined by Mann–Whitney's *U*-test ($P < 0.05$, $n = 16$ biological replicates). Errors bars show mean value \pm standard deviation.
- E Scheme of the transcriptional fusion to *GFP::GUS* used to analyze the *ASCO* promoter activity.
- F Activity of *proASCO* during LR development. Scale bar corresponds to 20 μm .

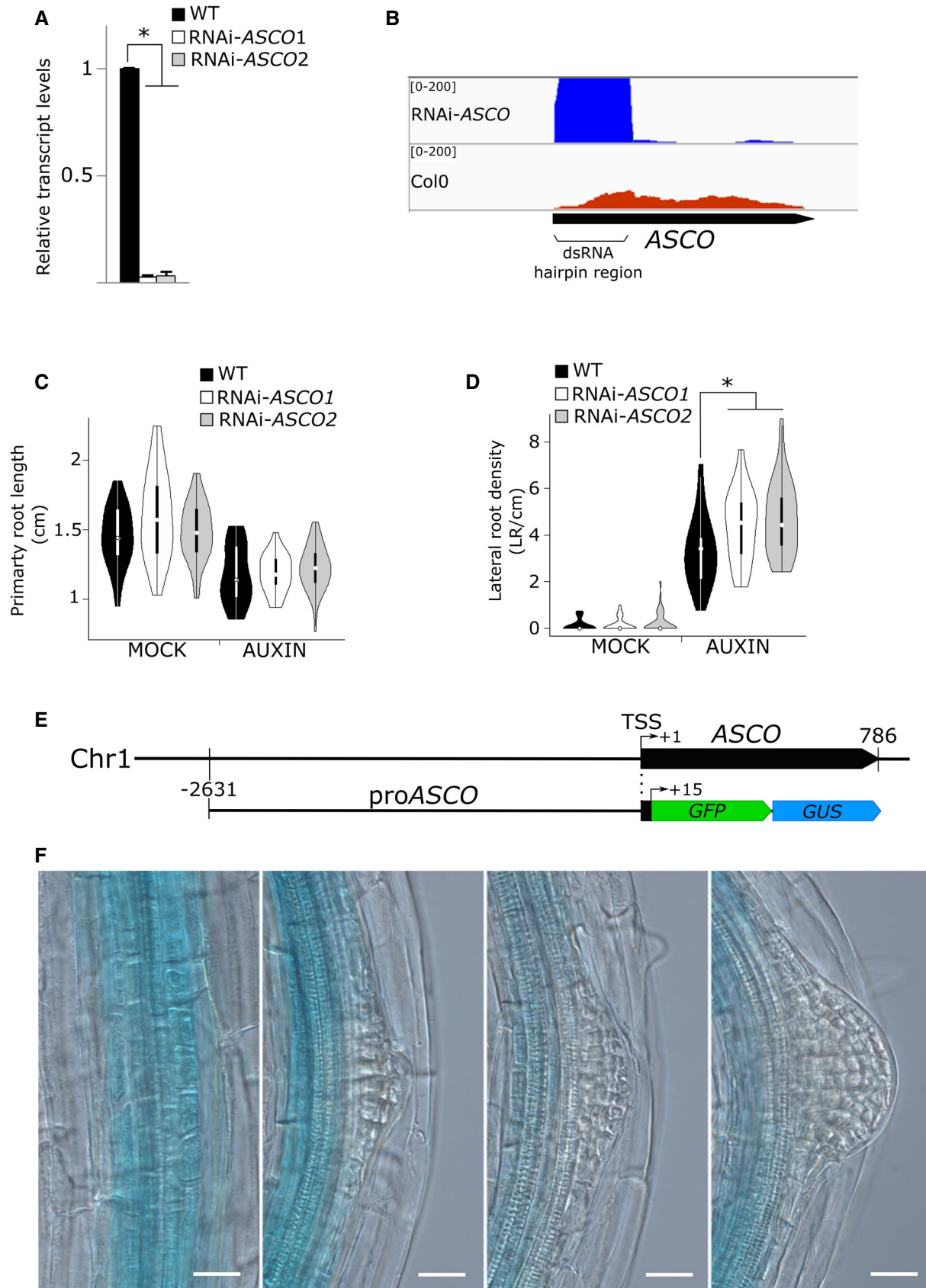


Figure EV1.

Figure EV2. Expression of immunity-related TF in RNAi-ASCO lines and ASCO expression in roots during flg22 treatment.

- A Transcript levels of stress-related DEG identified in the RNA-seq data in the WT and the two independent RNAi-ASCO lines, measured by RT-qPCR. RNAs were extracted from 14-day-old plants. Data are mean of 3 independent biological replicates. Error bars represent standard deviation. The asterisk (*) indicates a significant difference as determined by Student's *t*-test ($P < 0.05$, $n = 3$ biological replicates).
- B, C Time-course analysis of *ASCO* (B) and *CYP81F2* (C, AT5G57220) expression levels after treatment with media supplemented or not with 1 μ M flg22. RNAs were extracted from 10-day-old plants. Data are mean of 3 independent biological replicates. Error bars represent standard deviation.

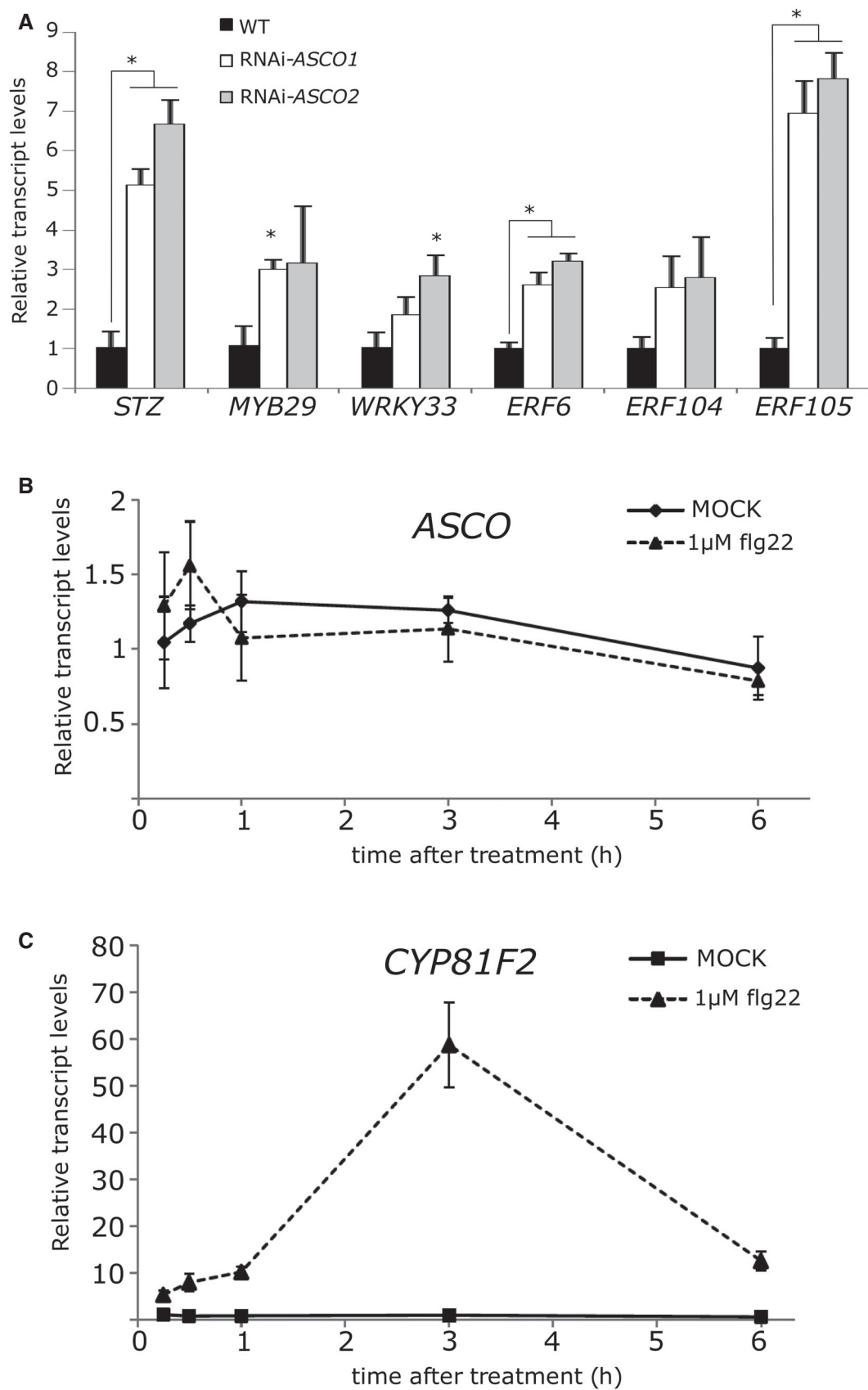


Figure EV2.

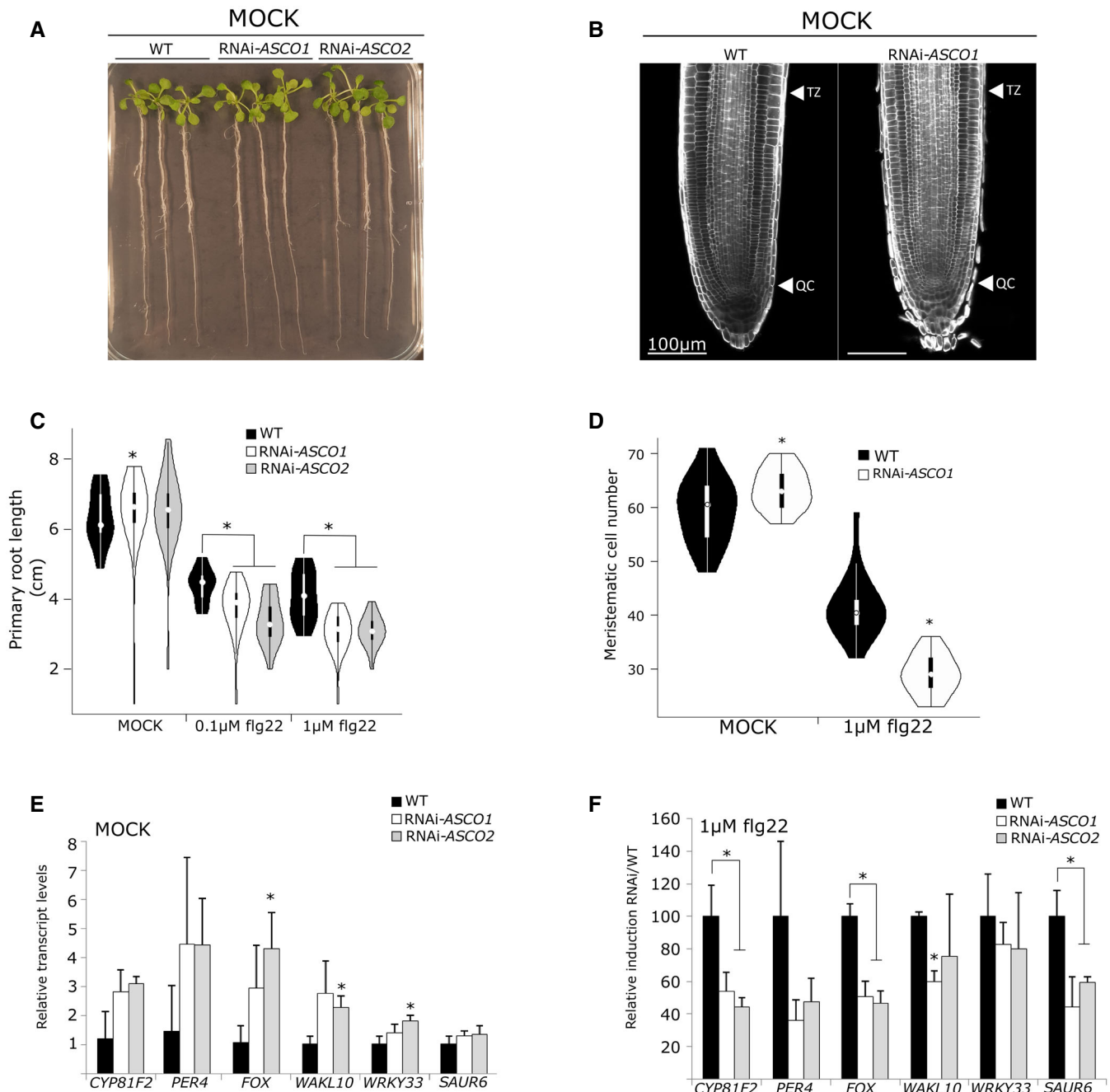


Figure EV3. The response to flg22 is altered in RNAi-ASCO lines.

- A** Representative picture of 14-day-old plants grown 9 days in liquid 1/2MS corresponding to Mock condition. The scale bar representing 0.6 cm is included in the picture.
- B** Representative picture of root apical meristems after cell wall staining, in mock condition. TZ: transition zone; QC: quiescent center.
- C** Primary root length of WT and two independent RNAi-ASCO lines 9 days after transfer in 1/2 MS supplemented with 0.1 or 1 µM flg22. The asterisk (*) indicates a significant difference as determined by Mann–Whitney’s *U*-test ($P < 0.05$, $n = 18$).
- D** Meristematic cell number in WT and RNAi-ASCO1 primary root apex, treated or not with 1 µM flg22. The asterisk (*) indicates a significant difference as determined by Mann–Whitney’s *U*-test ($P < 0.05$, $n = 18$ biological replicates).
- E** Relative transcript levels of a subset of flg22 responsive genes in control conditions (AGIs are indicated in Dataset EV5). RNAs were extracted from 10-day-old plants. Data are mean of three independent biological replicates. Error bars represent standard deviation. The asterisk (*) indicates a significant difference as determined by Student’s *t*-test ($P < 0.05$, $n = 3$ biological replicates).
- F** Relative modulation of the same genes as in (E), in response to flg22. Results are normalized against the response in WT plants, taken as 100%. Error bars represent standard deviation. The asterisk (*) indicates a significant difference as determined by Student’s *t*-test ($P < 0.05$, $n = 3$ biological replicates).

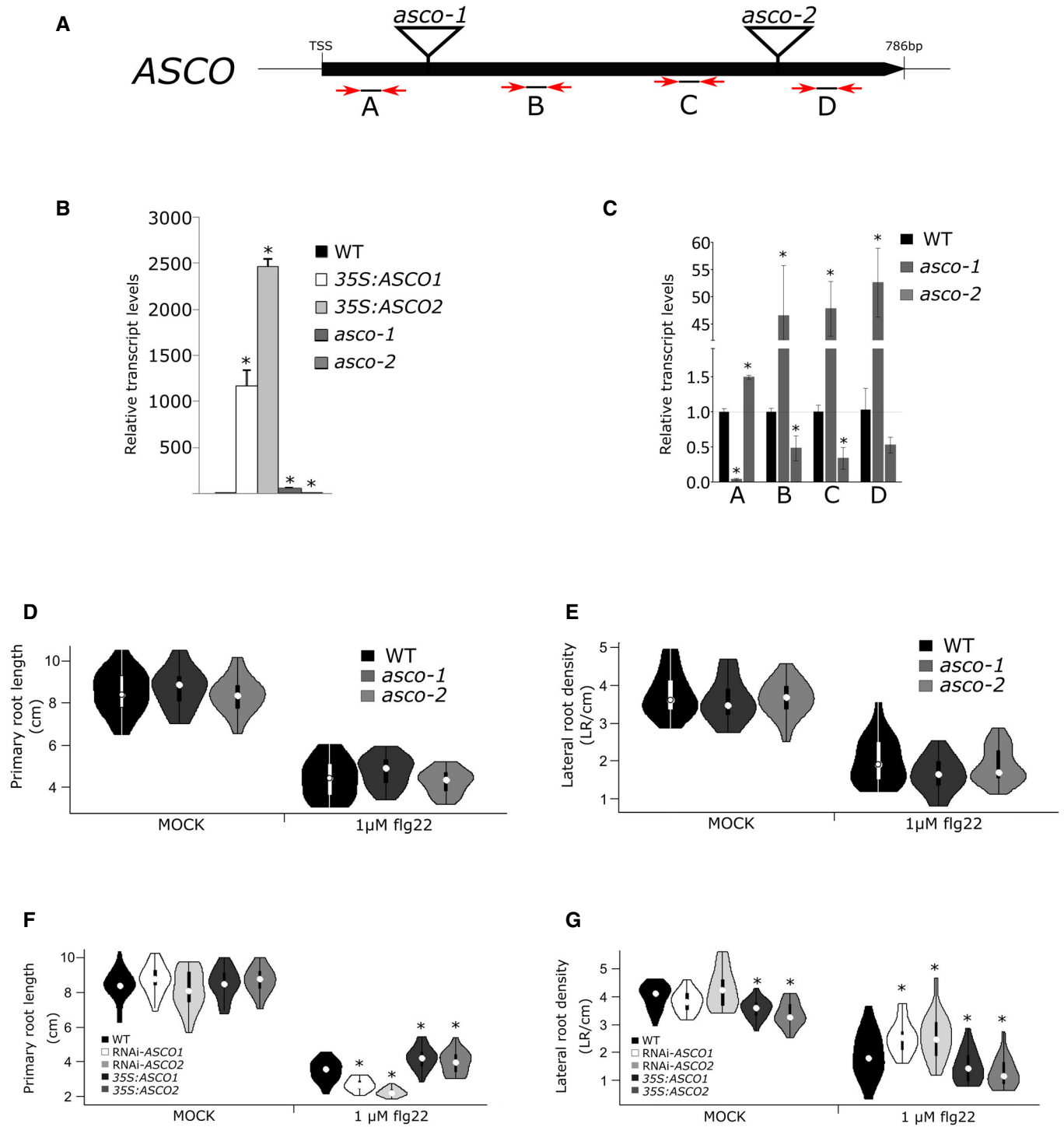
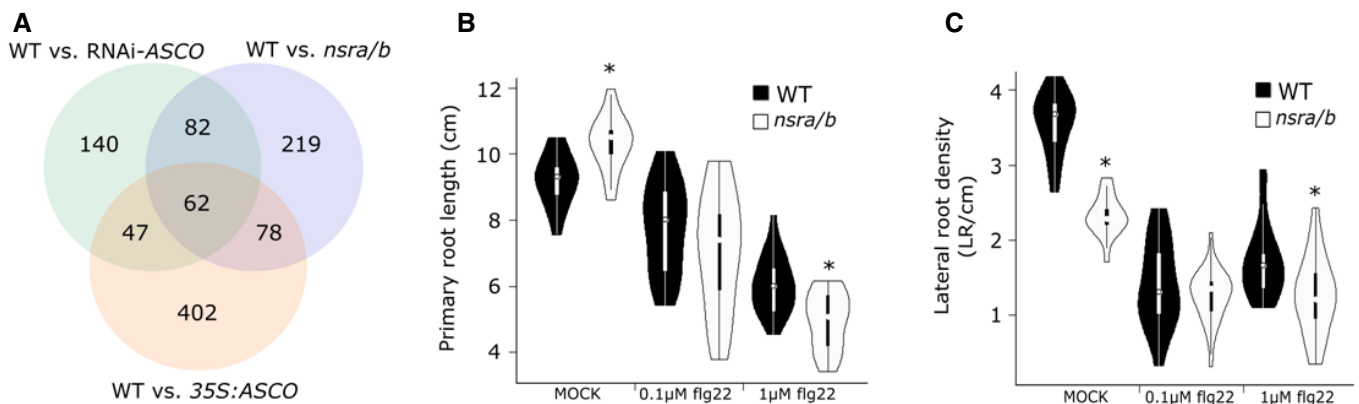


Figure EV4.

Figure EV4. ASCO insertion mutants do not exhibit drastic changes in RNA accumulation.

- A Scheme of T-DNA insertions along *ASCO* locus in *asco-1* and *asco-2* mutants. Red arrows indicate probes used for qPCR expression analysis.
- B Relative *ASCO* transcript levels in two independent 14-day-old 35-*ASCO* lines, *asco-1*, and *asco-2* compared to WT. Error bars represent standard deviation. The asterisk (*) indicates a significant difference as determined by Student's *t*-test ($P < 0.05$, $n = 3$ biological replicates).
- C Quantification of *ASCO* transcript levels targeting different regions of the locus by RT-qPCR in WT and *asco* mutants. A, B, C, and D probe positions are indicated in (A). The error bars represent standard deviation between 3 biological replicates, and (*) indicates a significant difference as determined by Student's *t*-test ($P < 0.05$, $n = 3$ biological replicates).
- D, E Primary root length (D) and lateral root density (E) of WT, *asco-1*, and *asco-2* plants 9 days after transfer in 1/2MS supplemented with 1 μ M flg22. The asterisk (*) indicates a significant difference as determined by Mann-Whitney's *U*-test ($P < 0.05$, $n = 24$ biological replicates). Error bars show mean value \pm standard deviation.
- F, G Primary root length (F) and lateral root density (G) of WT, two RNAi-*ASCO*, and two 35S:*ASCO* independent lines 9 days after transfer in 1/2MS supplemented with 1 μ M flg22. Error bars indicate the standard error. The asterisk (*) indicates a significant difference as compared to the WT, determined by Mann-Whitney's *U*-test ($P < 0.05$, $n = 24$ biological replicates). Error bars show mean value \pm standard deviation.

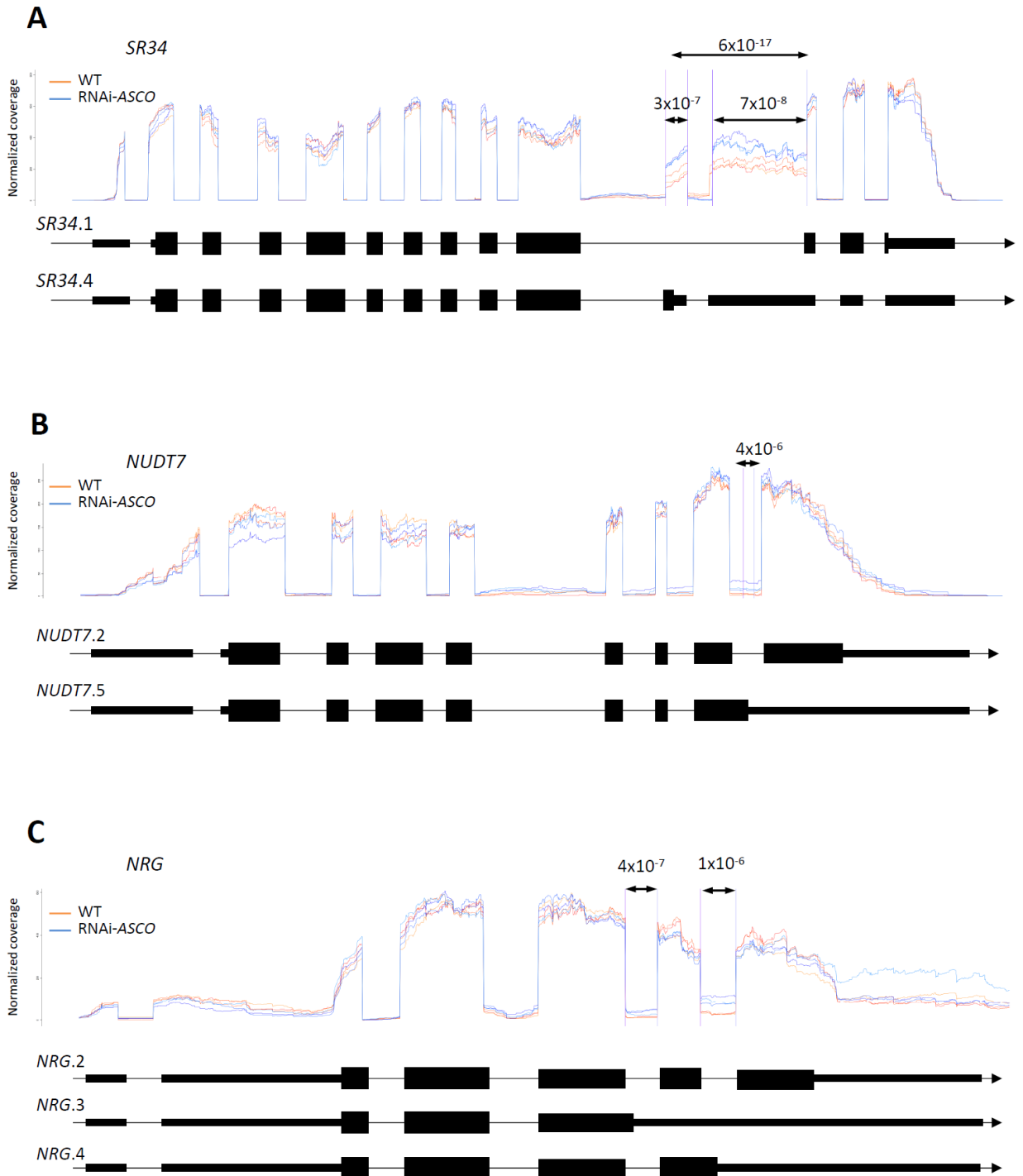
**Figure EV5. nsra/b affects root responses to flg22 and splicing of subsets of genes partially overlapping with RNAi-*ASCO* and 35S:*ASCO*.**

- A Overlap between differentially spliced events in RNAi-*ASCO*, 35S:*ASCO* and WT and *nsra/b* mutant, and WT treated with NAA [24].
- B, C Primary root length (B) and lateral root density (C) of WT and *nsra/b* double mutants 9 days after transfer in 1/2MS supplemented with 1 μ M flg22. Error bars show mean value \pm standard deviation. The asterisk (*) indicates a significant difference as determined by Mann-Whitney's *U*-test ($P < 0.05$, $n = 16$ biological replicates).

Appendix (Rigo et al., 2020)

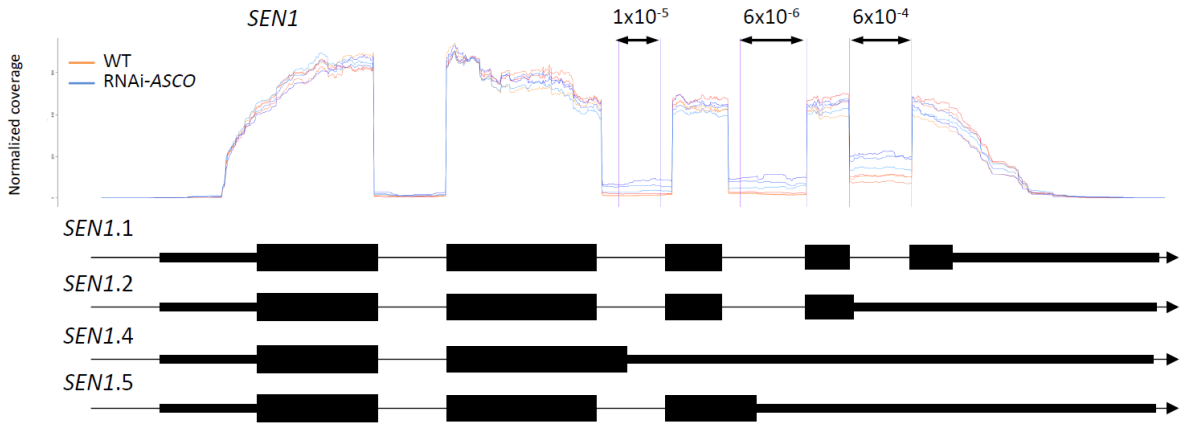
Table of contents:	Page
Appendix Figures S1	2
Appendix Figures S2	4
Appendix Figures S3	6
Appendix Figures S4	7
Appendix Figures S5	8
Appendix Figures S6	9

Appendix Figure S1

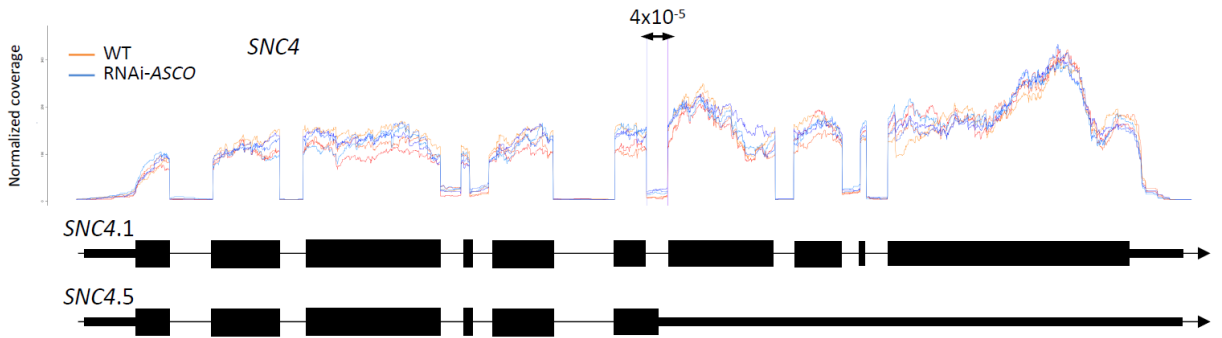


Appendix Figure S1

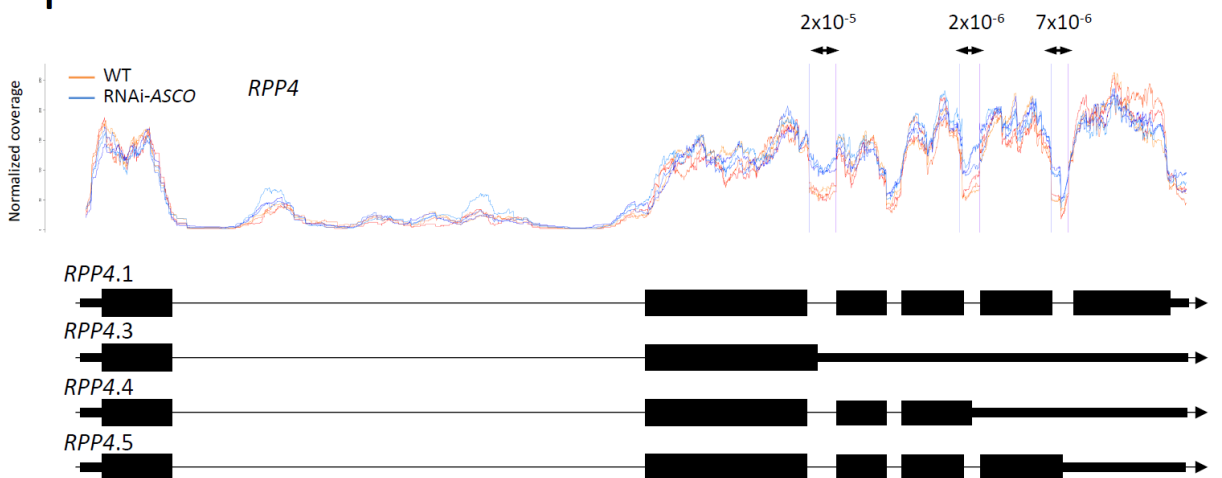
D



E



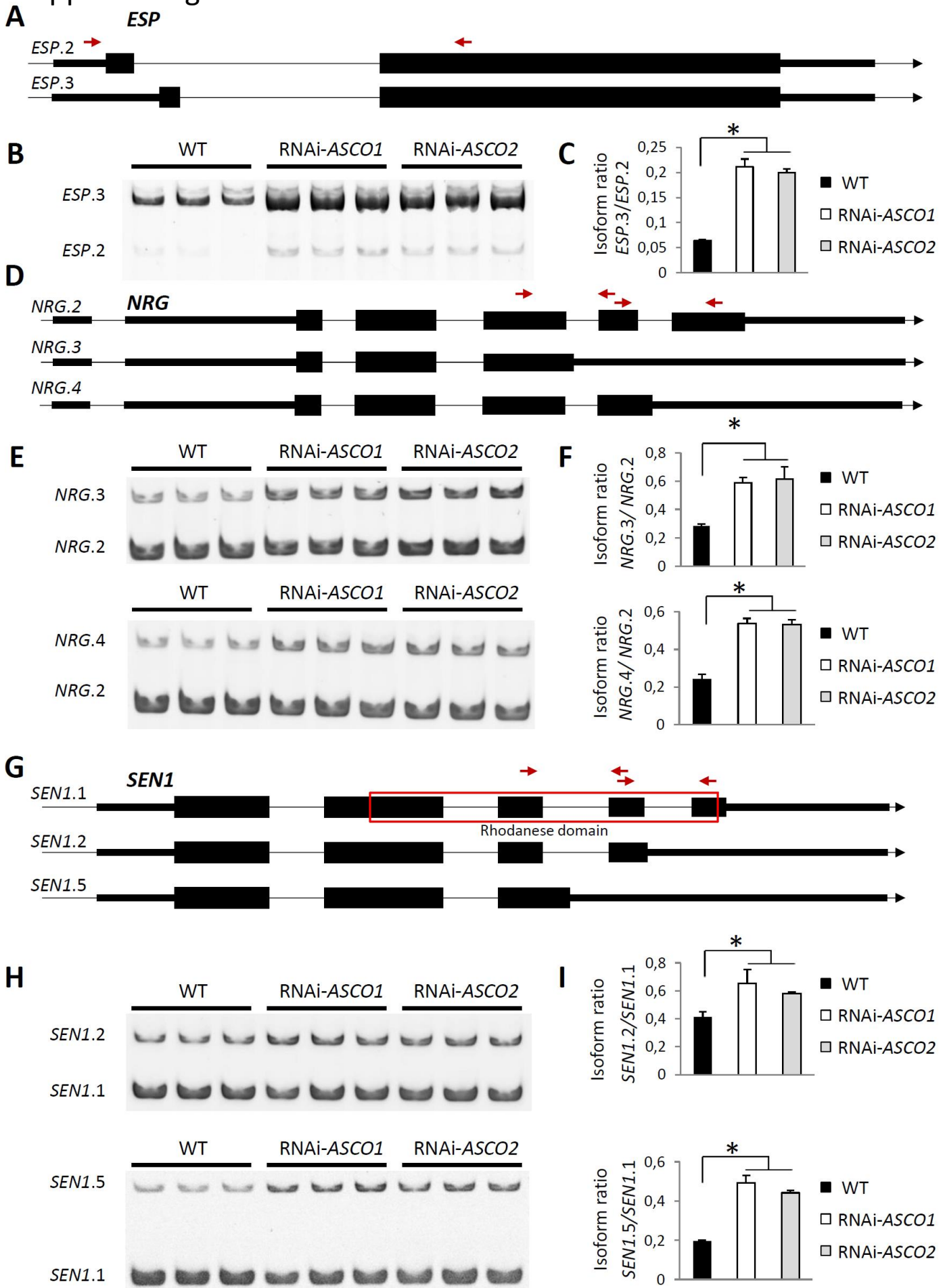
F



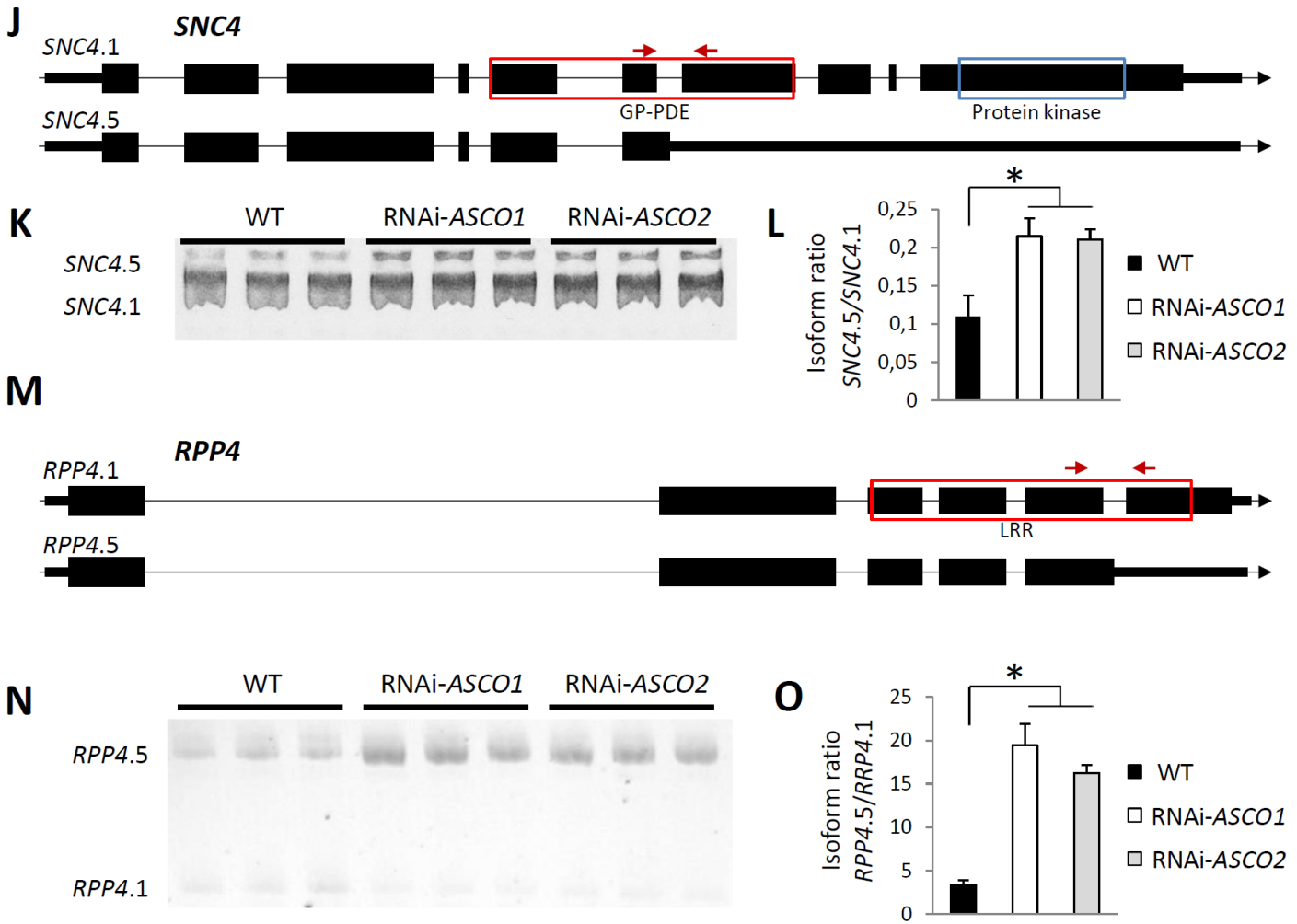
Appendix Figure S1. Differential RNA processing events identified in RNAi-ASCO

A, B, C, D, E, F Differential RNA processing events of *SR34* (AT1G02840, **A**), *NUDT7* (AT4G12720, **B**), *NRG* (AT2G29290, **C**), *SEN1* (AT4G35770, **D**), *SNC4* (AT1G66980, **E**) and *RPP4* (AT4G16860, **F**) transcripts detected by RNAprof. Blue and red lines represent RNA-seq read coverage normalized for gene expression differences in WT and RNAi-ASCO biological replicate, respectively. Three biological replicates were used for the analyses. Vertical purple lines and p-values indicate significant differential processing events. Each profile is associated with the structure of the corresponding RNA isoforms. Large black boxes indicate exons, narrow black boxes indicate UTRs and black lines indicate introns.

Appendix Figure S2



Appendix Figure S2

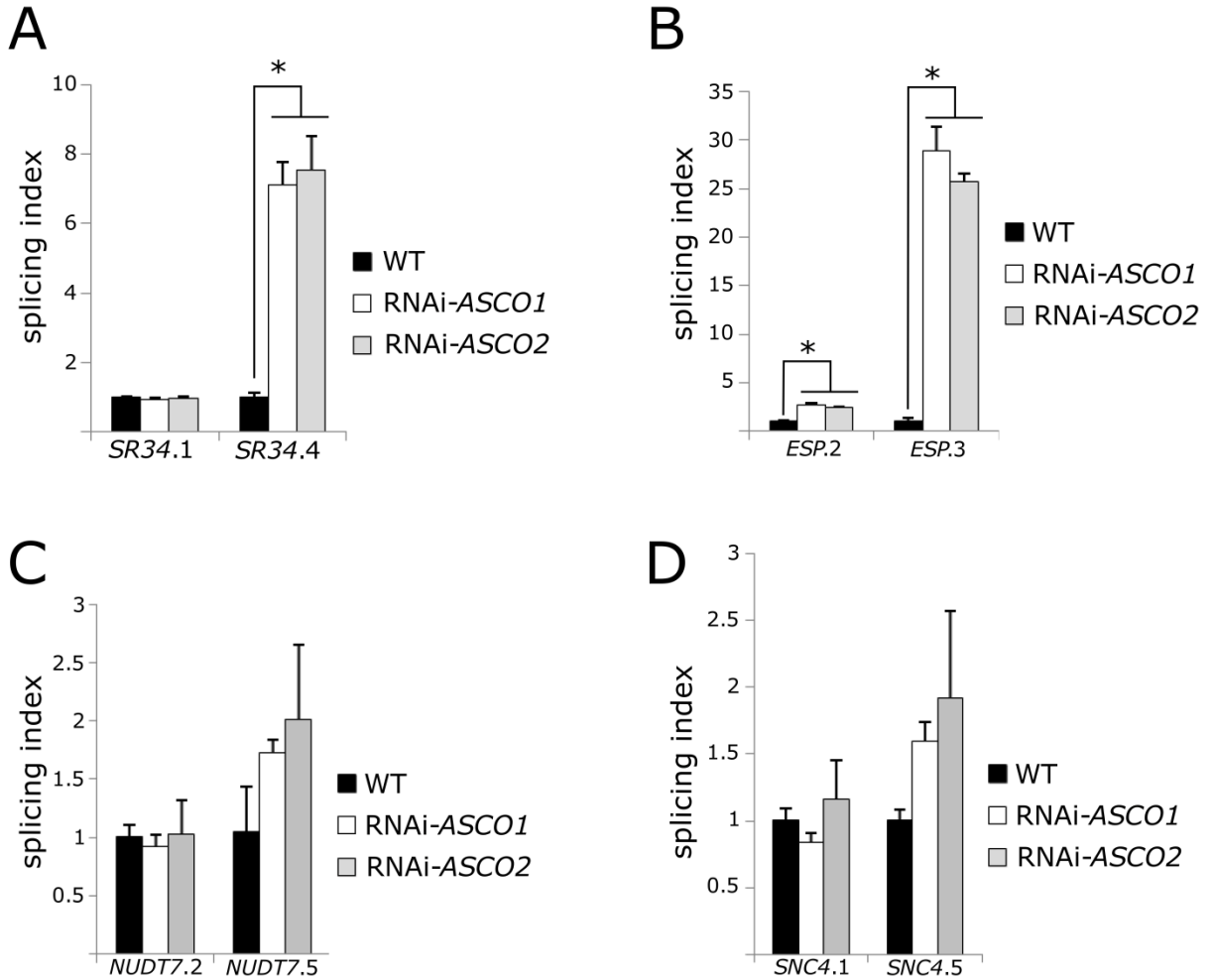


Appendix Figure S2. Validation of AS events in RNAi-ASCO lines

A-O (A, D, G, J, M) Structure of *ESP* (AT1G54040, A), *NRG* (D), *SEN1* (G), *SNC4* (J) and *RPP4* (M) RNA isoforms. The structure of each associated RNA isoform is represented as follows: large black boxes indicate exons, narrow black boxes indicate UTRs, black lines indicate introns. Red arrows indicate probes used for gel electrophoresis. Colored boxes indicate protein domains affected by an AS event. GP-PDE: glycerophosphodiester phosphodiesterase domain; LRR: Leucine-rich repeats. (B, E, H, K, N) Analyses of RT-PCR products of corresponding transcripts on 8% acrylamide gel. (C, F, I, L, O) Quantification of the ratio of the corresponding isoforms detected in gels in B, E, H, K and N, respectively.

Data information: RNAs were extracted from WT and RNAi-ASCO 14-day-old plants. The asterisk (*) indicates a significant difference as determined by Student's T test ($p < 0.05$, $n = 3$ biological replicates). Error bars show mean value \pm standard deviation

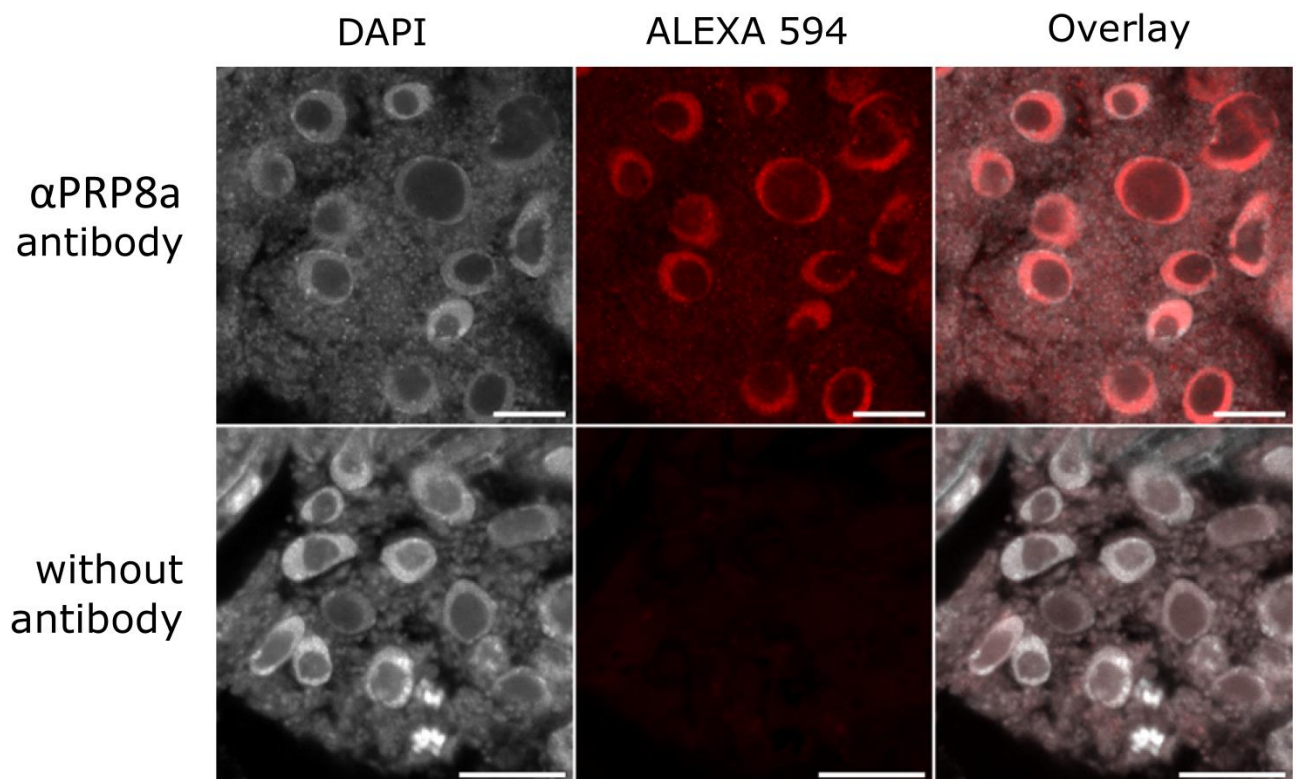
Appendix Figure S3



Appendix Figure S3. qPCR analysis of several AS events identified in RNAi-ASCO lines

A, B, C and D Quantification of *SR34* (**A**), *ESP* (**B**), *NUDT7* (**C**) and *SNC4* (**D**) isoforms splicing by splicing index RT-qPCR. The asterisk (*) indicates a significant difference as determined by Student's T test ($p < 0.05$, $n = 3$ biological replicates). Error bars show mean value +/- standard deviation.

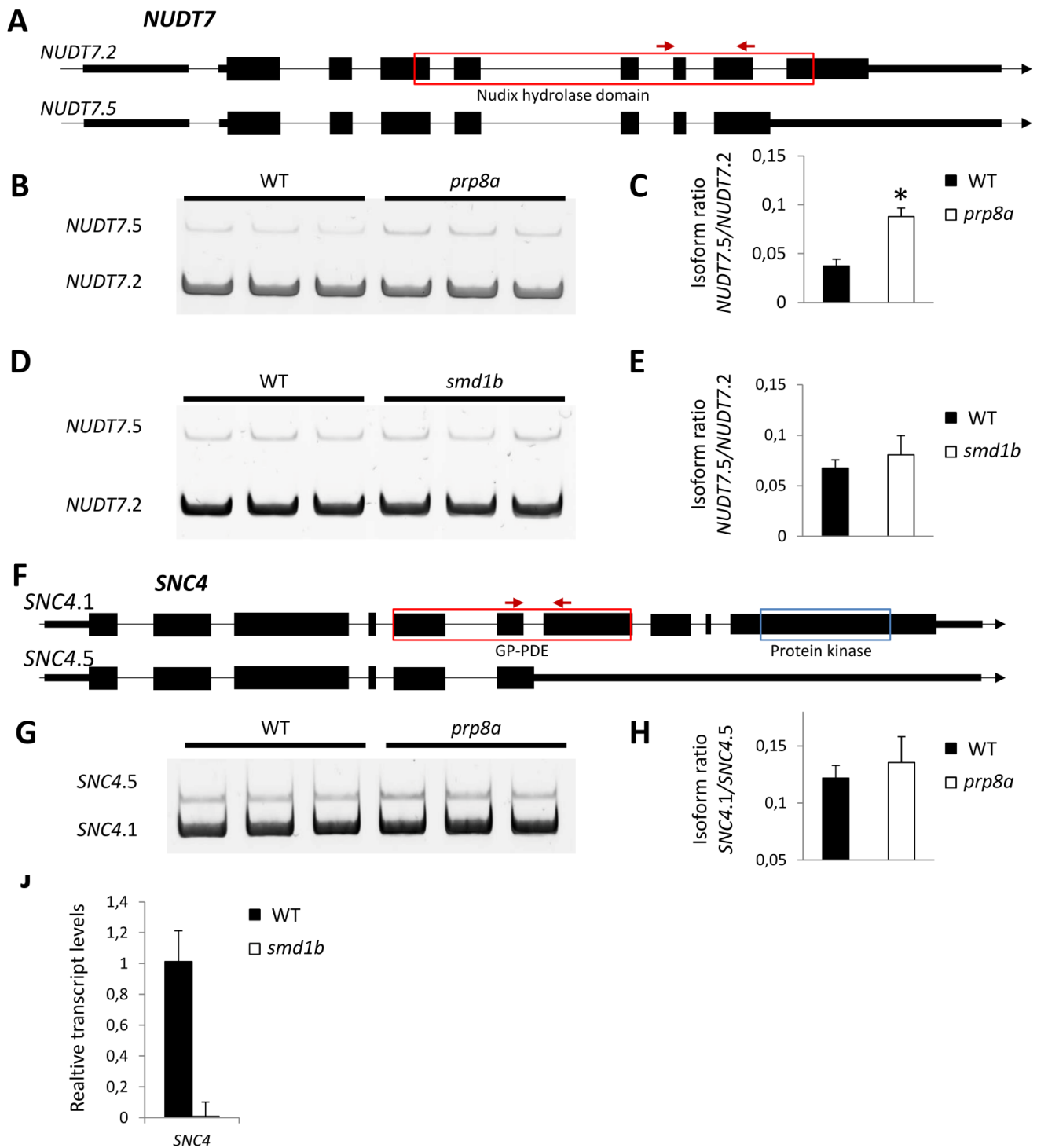
Appendix Figure S4



Appendix Figure S4. Novel specific antibody against AtPRP8a confirmed the protein localization in the cell nucleus

Whole-mount immunolocalization using the specific antibody against PRP8a. The signals of DAPI (grey channel) and AtPRP8a protein (red channel) colocalized in the nuclei of *A. thaliana* WT plants. The negative control corresponds to the immunolocalization assay without anti-AtPRP8a antibody. Scale bar represents 10 μm .

Appendix Figure S5



Appendix Figure S5. Analyses of *NUDT7* and *SNC4* in the *smd1b* background

A-H (A, F) Structure of *NUDT7* (A) and *SNC4* (F) RNA isoforms. Large black boxes indicate exons, narrow black boxes indicate UTRs, black lines indicate introns. Red arrows indicate probes used for gel electrophoresis. Colored boxes indicate the position of protein domains affected by an AS event. GP-PDE: glycerophosphodiester phosphodiesterase domain. Protein domains were retrieved from Uniprot database (<https://www.uniprot.org>). **(B, D, G)** Analyses of RT-PCR products of corresponding transcripts on 8% acrylamide gel in *prp8a* (B, G) and *smd1b* (D) mutants, respectively. **(C, E, H)** Quantification of the ratio of the corresponding isoforms detected in gels in B, D and G, respectively.

J *SNC4* transcript levels in *smd1b* mutant compared to WT. RNAs were extracted from WT, *prp8a* and *smd1b* 14-day-old plants.

Data information: The asterisk (*) indicates a significant difference as determined by Student's T test ($p < 0.05$, $n = 3$ biological replicates).

Appendix Figure S6

A

A. thaliana

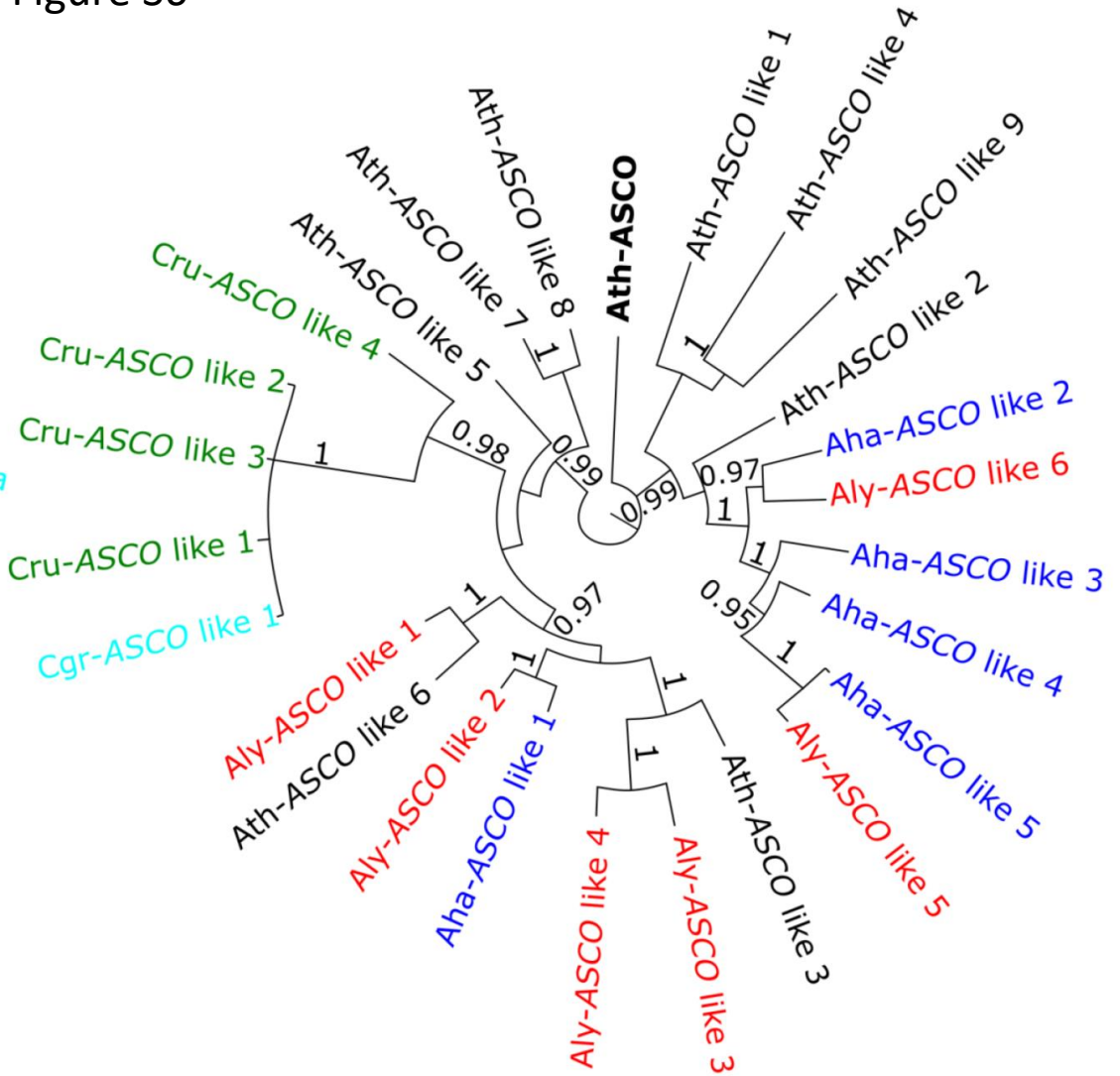
A. lyrata

A. halleri

C. rubella

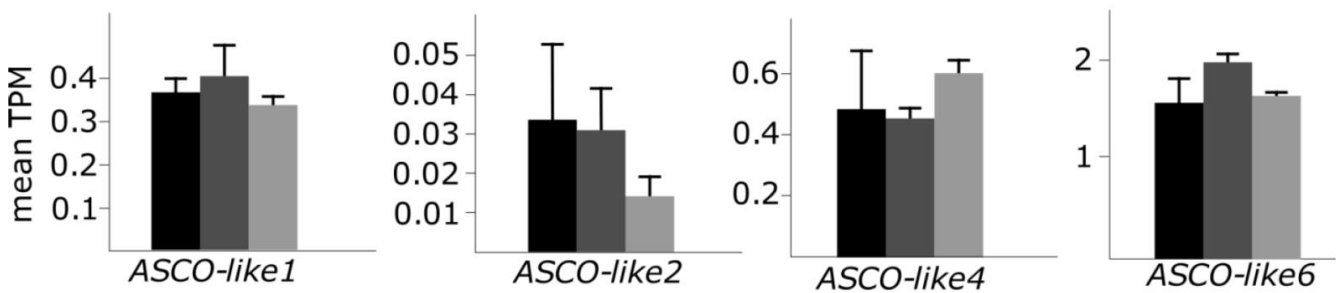
C. grandiflora

0.2



B

■ WT ■ 35S:ASCO ■ RNAi-ASCO



Appendix Figure S6. Identification of ASCO homologs in *A.thaliana* and other species from the Brassicaceae family

A Maximum likelihood tree depicting the evolutionary history of ASCO in the Brassicaceae family. Bootstrap support values are indicated above branches. Sequences identifiers are colored by species.

B Normalized expression level of detectable ASCO-like transcripts in WT, RNAi-ASCO and 35S:ASCO RNA-seq data.(Error bars show mean tpm value +/- standard deviation).

2.2.3 Complementary results

This article sheds light on *ASCO*'s role at the transcriptome level, and notably how it interacts with conserved components of the spliceosome machinery. Moreover, *ASCO* was found to regulate both expression and AS of a large subset of defense-related genes. This part will add some complementary results concerning *ASCO*'s expression patterns in the plant, and how they could be linked to its function.

To investigate *ASCO*'s expression in the plant, pro*ASCO*::GUS lines were used and examined after GUS staining (Figure 13). In 10-day-old seedlings, a GUS staining was observed in the hypocotyl and the shoot apical meristem (Figure 13A), in vascular tissues and guard cells of the cotyledons (Figures 13A and 13B), and in vascular tissues of the root (Figures 13A and 13C). No expression was detected in emerging LRs (Figure 13C), as well as in the primary root apex (Figure 13D). It was already shown that *ASCO* expression is specifically downregulated in roots but not in whole seedlings upon auxin treatment (Romero-Barrios thesis, 2016). Auxin mainly accumulates at the root tip (Grieneisen et al., 2007; Overvoorde et al., 2010) and in lateral root primordia (LRP) when the new LR starts to form (Du and Scheres, 2017). Indeed an auxin signaling cascade occurs in xylem-pole-pericycle (XPP) cells, where INDOLE-3-ACETIC ACID28 (IAA28) and ARF binding factors (ARF5, 6, 7, 8, and 19) allow the control of *GATA23* expression, leading to the specification of lateral root founder cells (LRFCs) (De Rybel et al., 2010). *ASCO*'s expression decrease is concomitant with the progressive formation of the new LR organ and could be due to the accumulation of auxin and activation of its associated signaling pathway. To take a closer look at *ASCO*'s expression in root cell-types, expression data from FACS-isolated root cells was analyzed (Rich-Griffin et al., 2020). Transgenic lines specifically expressing GFP in epidermis (atrachoblast, *pGL2:GFP*), cortex (*pCORTEX:GFP*), or pericycle (xylem pole, *E3754*) cells were used for protoplast generation, cell-sorting and subsequent sequencing. No *ASCO* expression could be detected in either epidermis or cortex cells (Figure 13E). Nevertheless, *ASCO* was found to be expressed in XPP cells (Figure 13E), which will give rise to LRFCs if exposed to appropriate stimuli. The detection of *ASCO* transcripts in this specific cell-type strengthens *ASCO*'s role in LR formation and suggests *ASCO* could represent one of the actors involved in LR organogenesis.

Root growth and LR organogenesis are known to integrate a plethora of environmental signals including nutrient availability in the soil such as nitrogen (N), one of the major mineral nutrients for plant growth (Hodge, 2004). Plants are able to assimilate various forms of nitrogen, including nitrate (NO_3^-) and ammonium (NH_4^+) (Vidal and Gutiérrez, 2008). Nitrate was shown to regulate root branching by its interaction with the auxin signaling

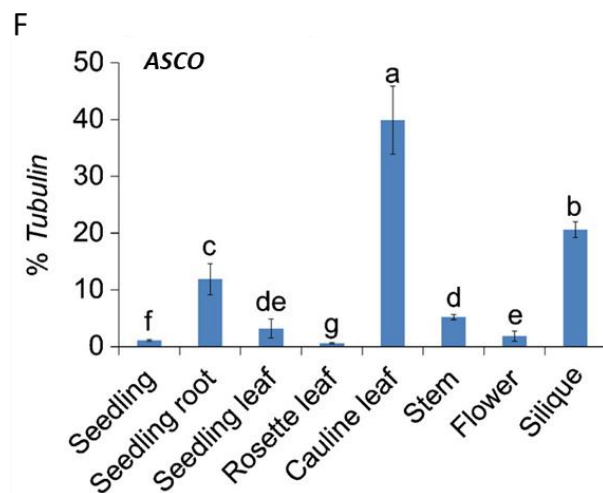
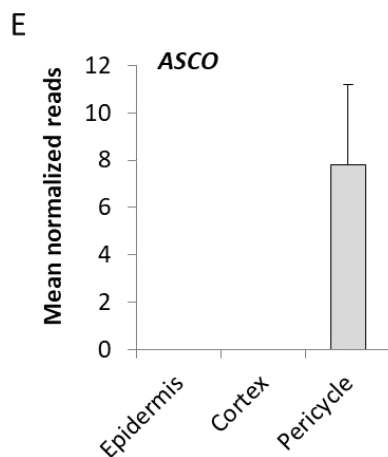
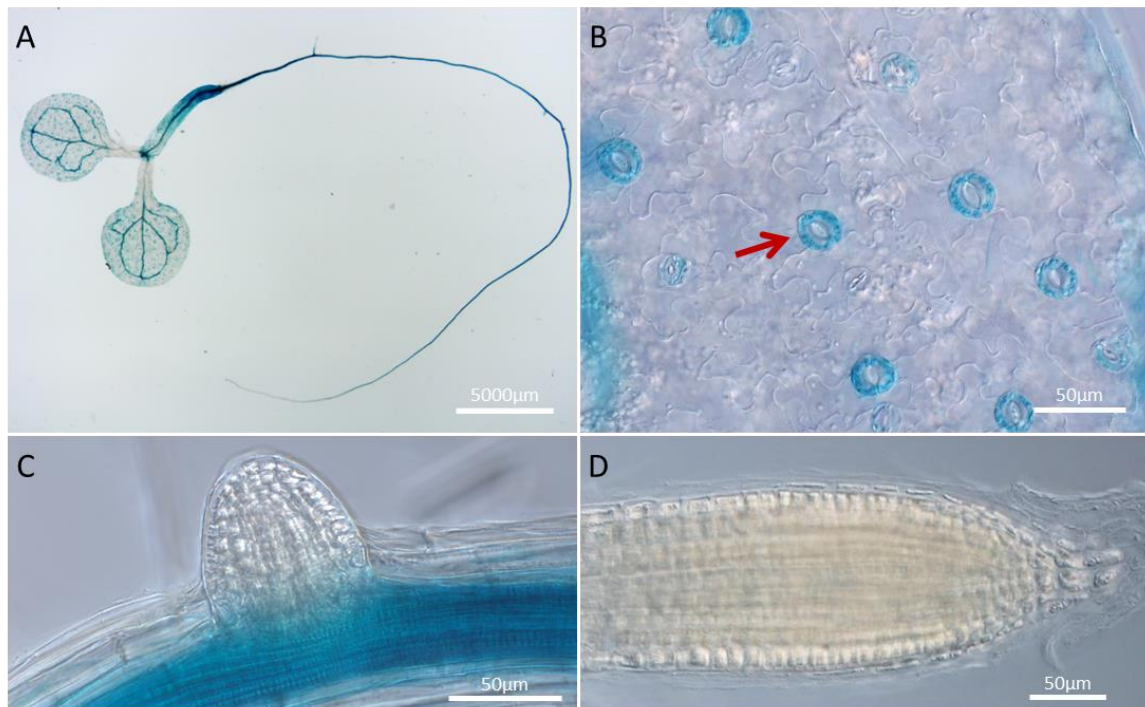


Figure 13. ASCO expression patterns in the plant.

A, B, C, D. Histochemical analyses of representative transgenic *A. thaliana* plants expressing a proASCO::GUS construct. Expression analyses in 10-day-old seedlings (A), in cotyledons (B), in emerging LR (C), and in the root apex (D). Red arrows highlight GUS staining in stomata of the cotyledon. Scale bars indicate corresponding distances in μm .

E. ASCO expression in FACS-isolated root cells. Lines specifically expressing GFP in epidermis (atrachoblast, *pGL2:GFP*), cortex (*pCORTEX:GFP*), or pericycle (xylem pole, *E3754*) cells were used for the analysis. Roots were treated with a mock solution prior to protoplast generation and cell-sorting. For each cell line, data represent mean normalized reads. Error bars show mean \pm standard deviation. Data were obtained from Rich-Griffin et al., 2020.

F. ASCO expression in different organs. Tissues were obtained at different developmental stages from 7-day-old seedlings and 40-day-old plants grown in soil. Expression levels were measured by qPCR and were normalized to tubulin expression levels. Error bars show mean \pm standard deviation. The different letters indicate significant differences as determined by Student's t test ($P < 0,05$, $n = 4$). Data were obtained from Liu et al., 2019.

pathway (Guo et al., 2002). Indeed, a high nitrate concentration inhibits LR growth, notably by acting on auxin transport inhibitors and leading to decreased auxin concentrations in the root (Guo et al., 2005; Tian et al., 2008; Asim et al., 2020). A recent study has shown that nitrate levels regulate the expression of a subset of 6 lncRNAs, including ASCO. For this analysis seedlings were plated in aseptic solution containing 2,5 mM ammonium succinate as the sole nitrogen source for 7 days, and then treated either with 10 mM KNO₃ or with 10 mM KCl as a control for 2 h. ASCO expression exhibited a 2,36 fold increase when treated with KNO₃ compared to control conditions (Liu et al., 2019). Therefore, ASCO expression either increases when plants are exposed to nitrate or decreases when plants are exposed to auxin, each of these two molecules respectively sending negative and positive signals for LR formation. Taken altogether, it suggests that ASCO's abundance may represent a negative marker of LR organogenesis.

To investigate ASCO's role along plant development, an analysis of its expression profile among different tissues was extracted from Liu et al., 2019. In concordance with the previous analyses, ASCO is highly expressed in seedling roots, but even higher expression was detected in siliques and cauline leaves (Figure 13F). This could suggest a putative role of ASCO in seed development or early embryogenesis.

To conclude this chapter, additional experiments concerning ASCO suppression effect on plant responses to flg22 were conducted. It was shown in the article presented in this chapter that both ASCO suppressed and overexpressing lines displayed an altered sensitivity to flg22. This was notably observed at the root growth level, where RNAi- and 35S-ASCO plants exhibited respectively higher and lower LR densities compared to WT when treated with flg22. Moreover, RNAi-ASCO lines also presented a shorter root apical meristem (RAM) when treated with this PAMP. The plant infection by pathogen influences cell cycle via different ways (Qi and Zhang, 2020), notably through the JA signaling pathway (Chen et al., 2011). Activation of PTI by infection with non-virulent *P. syringae* strains leads to enlarged mesophyll cells containing higher nuclear DNA content, suggesting a possible endoreplication in these host cells. A similar phenotype is observed when leaves are treated with flg22 (Hamdoun et al., 2013).

Hence, the impact of flg22 addition on cell division was investigated in both WT and RNAi-ASCO plants. For this end, seedlings were subjected to a 24h flg22 treatment and subsequently stained with 5-ethynyl-2'-deoxyuridine (EdU) to reveal cells exhibiting active DNA synthesis in the RAM (Figure 14A and 14B). Flg22 led to a 22% reduction of the division zone (DZ) size in WT plants, corresponding to the area where meristematic cells are actively dividing. Interestingly, RNAi-ASCO lines displayed a significantly higher DZ size in mock conditions compared to WT plants. Nevertheless, flg22 addition led to a 31% reduction

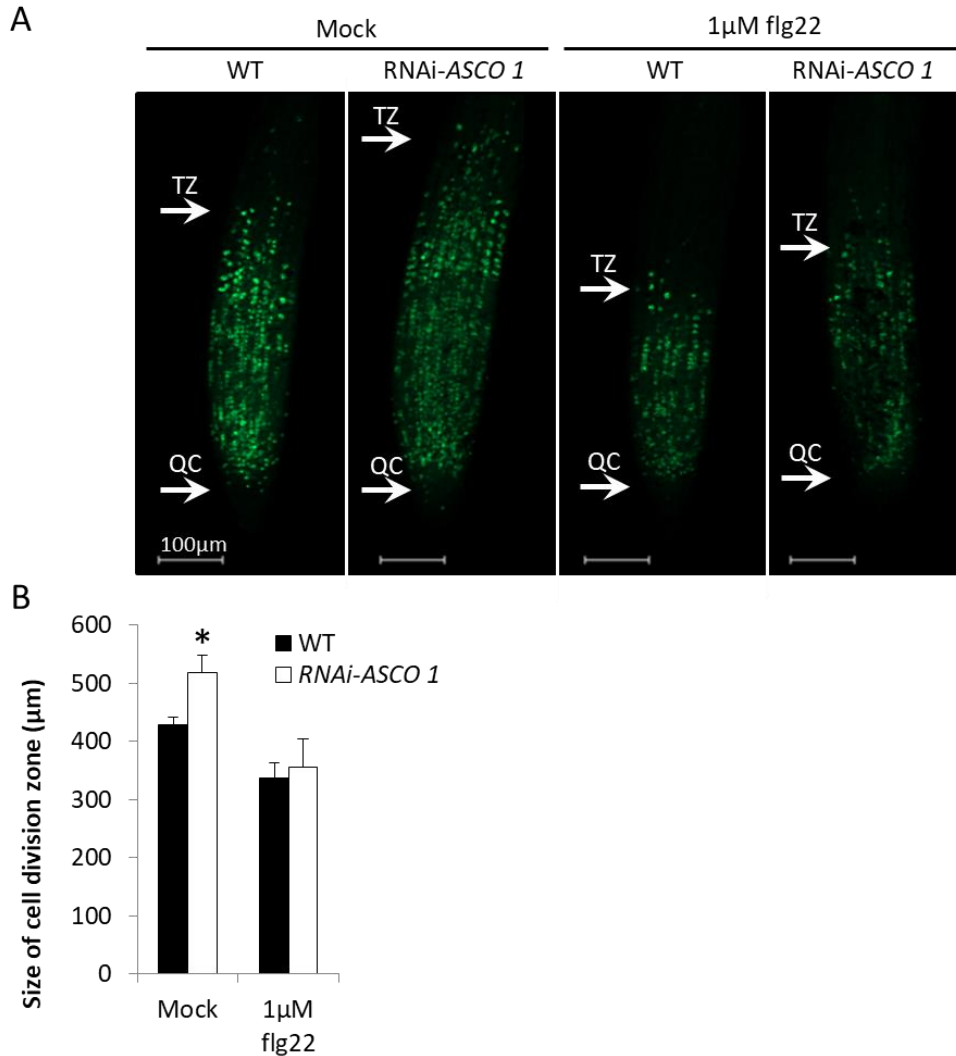


Figure 14. ASCO suppression leads to fewer cell divisions upon flg22 treatment.

A. Representative picture of root apical meristems after EdU staining, in response to a 24h flg22 treatment in WT and RNAi-ASCO 1 plants. TZ: transition zone; QC: quiescent center. Scale bars correspond to 100 μ m.

B. Size of cell division zone in WT and RNAi-ASCO 1 roots (e.g length of the zone comprising actively dividing cells at the root tip, in μ m) after a flg22 treatment. Error bars show mean \pm standard deviation. The asterisk (*) indicates a significant difference as determined by Student's t test ($P < 0,05$, $n \geq 8$).

of the DZ size in RNAi-*ASCO* lines (Figure 14A and 14B). In addition, root cells from RNAi-*ASCO* plants appeared more swollen along the root axis, suggesting an increased endoreplication in these cells (see Figure 1E of Rigo et al., 2020). All of this suggests that *ASCO*-suppressed plants may be more sensitive to the *flg22* impact on cell cycle. These results support the previously observed impact of *ASCO* suppression on root growth and plant response to *flg22*.

2.2.4 Discussion

All the presented experiments provide new evidence that the lncRNA *ASCO* is linked to the shaping of the root system architecture (RSA). The article included in this chapter reinforced the hypothesis that *ASCO* is involved in the root sensitivity to auxin, a major phytohormone controlling LR organogenesis. Indeed, *ASCO* overexpression lowers LR density, whereas its absence increases the formation of new LRs. Accordingly, *ASCO* expression is controlled by auxin abundance, where high auxin contents lead to a decrease of its expression in the roots (Bardou et al., 2014, Romero-Barrios 2016). On the contrary, high levels of nitrate, an inhibitor of LR growth, tend to increase *ASCO* transcript levels. Hence, *ASCO* abundance in XPP cells may represent one of the signals controlling LR development. When abundant, *ASCO* stands as a “no-go” signal for LR formation, mimicking lower auxin / high nitrate content and leading to a lower LR density along the root. Reversely, *ASCO* decrease or absence seems to copy high auxin content, promoting LR organogenesis.

Likewise, *ASCO* plays a role in root growth when the plant perceives biotic stresses such as the PAMP *flg22*. *Flg22* was demonstrated to trigger downregulation of auxin signaling notably through reduction in auxin receptors TIR1, AFB2, and AFB3 and upregulation of miR393 (Navarro et al., 2006). Consistently with this data, *flg22* application represses LR formation (Beck et al., 2014), mainly by impacting LR emergence (Kong et al., 2020). LRs represent a potential entry point for pathogens such as *Pst* DC3000 which gather around emerging LRs. Accordingly, mutants displaying reduced LR formation (*arf7*, *slr*, *arf7/19*, and *lbd16/lbd18/lbd33*) accumulate less *Pst* DC3000 after infection (Kong et al., 2020). Therefore, the regulation of LR formation during pathogen infection is a crucial aspect for limiting pathogen proliferation and entry in the plant. Defects in *ASCO* expression lead to higher LR density in response to *flg22*, resulting from an altered control of LR organogenesis and a reduced primary root growth caused by fewer cell divisions in the RAM. This enhanced LR density could engender a higher sensitivity to root pathogens, benefiting from the increase of “entrances” along the root. Infection tests with root pathogens would provide more insights in this aspect of *ASCO* function. The impact of *ASCO* suppression on primary

root growth still remains elusive knowing that it is not expressed in the RAM. *ASCO* may participate in the control of primary root elongation via an indirect auxin-dependent effect, this hormone being a major regulator of cell division and primary root growth (Dello Iorio et al., 2008; Zhao, 2010; Fendrych et al., 2018).

Beyond its role in plant development, *ASCO* could therefore link RSA shaping and defense responses, fine-tuning root architecture in response to pathogen infection. Moreover, its expression in leaves and especially stomata hints at other putative roles in the plant. Stomata regulate the flow of gases inside the plant, notably upon various abiotic stresses, but also serve as a defensive wall against pathogen entrance in leaves (Gudesblat et al., 2009). Knowing all the stress-related genes regulated by variations in *ASCO* expression, this lncRNA may act at different levels to help the plant cope with a fast-changing environment.

2.2.5 Material and Methods

2.2.5.1 Histochemical GUS staining

GUS staining was performed as previously described in the M&M of the article included in this chapter (Rigo et al., 2020).

2.2.5.2 *ASCO* expression data

For analysis of *ASCO* expression in various organs, the tissues were obtained at different developmental stages from seedlings grown on 1/2MS medium for 7 days (seedling, seedling root, and seedling leaf) and 40-day-old plants grown in soil (rosette leaf, cauline leaf, stem, flower, and silique). For more details concerning the data, see Liu et al., 2019. For analysis of *ASCO* expression within root cell types, 3 marker lines were used for the analysis: *pGL2:GFP* (epidermis atrichoblast; Lin et al. 2015), *pCORTEX:GFP* (cortex), and *E3754* (xylem-pole pericycle; Bargmann et al. 2013). Roots were treated with a mock solution prior to protoplast generation, cell-sorting and subsequent RNA sequencing. Read number at *ASCO*'s locus was extracted from RNAseq data. For more details concerning the data, see Rich-Griffin et al., 2020.

2.2.5.3 Cell division zone measurements

For analysis of flg22 impact on cell division zone, plants were previously grown 9 days on solid 1/2MS medium + 1% sucrose and then transferred for additional 24 h in liquid 1/2MS

medium + 1% sucrose before adding or not 1 μ M of flg22 for another 24h. 5-ethynyl-2'-deoxyuridine (EdU) was added (final concentration of 10 μ M) 30min before the end of the flg22 treatment to stain cells exhibiting active DNA synthesis. The cells were fixed with PBS 1X + 4% paraformaldehyde + 0,1% Triton X-100 and washed twice with PBS 1X + 3% BSA. Root tips were then transferred to a PBS 1X + 0,5% Triton X-100 solution and left to incubate for 20min at room temperature under shaking. Samples were then washed twice with PBS 1X + 3% BSA. For EdU fluorescent labeling, root tips were transferred to a Click-IT reaction mix (Invitrogen) and incubated for 30min under shaking in the dark. Samples were washed once with PBS 1X + 3% BSA and finally washed twice with PBS 1X. The samples were observed under a LSM880 (Zeiss) confocal microscope. Samples were excited with a 488 nm laser line and emission was recorded between 500 and 550 nm. Division zone was measured as the distance between the quiescent center and the transition zone where the fluorescent signal starts to fade. Measurements were performed using ImageJ software (<https://imagej.nih.gov/ij/>). The asterisk (*) indicates a significant difference as determined by Student's t-test ($P < 0.05$, $n = 8$ biological replicates). Error bars show mean \pm standard deviation.

2.2.6 References

- Asim M, Ullah Z, Oluwaseun A, Wang Q, Liu H** (2020) Signalling Overlaps between Nitrate and Auxin in Regulation of The Root System Architecture: Insights from the *Arabidopsis thaliana*. *Int J Mol Sci* **21**: 2880
- Bardou F, Ariel F, Simpson CG, Romero-Barrios N, Laporte P, Balzergue S, Brown JWS, Crespi M** (2014) Long noncoding RNA modulates alternative splicing regulators in *Arabidopsis*. *Dev Cell* **30**: 166–176
- Beck M, Wyrsh I, Strutt J, Wimalasekera R, Webb A, Boller T, Robatzek S** (2014) Expression patterns of flagellin sensing 2 map to bacterial entry sites in plant shoots and roots. *J Exp Bot* **65**: 6487–6498
- Chen Q, Sun J, Zhai Q, Zhou W, Qi L, Xu L, Wang B, Chen R, Jiang H, Qi J, et al** (2011) The Basic Helix-Loop-Helix Transcription Factor MYC2 Directly Represses *PLETHORA*; Expression during Jasmonate-Mediated Modulation of the Root Stem Cell Niche in *Arabidopsis*; *Plant Cell* **23**: 3335 LP-3352
- De Rybel B, Vassileva V, Parizot B, Demeulenaere M, Grunewald W, Audenaert D, Van Campenhout J, Overvoorde P, Jansen L, Vanneste S, et al** (2010) A Novel Aux/IAA28 Signaling Cascade Activates GATA23-Dependent Specification of Lateral Root Founder Cell Identity. *Curr Biol* **20**: 1697–1706
- Dello Ioio R, Nakamura K, Moubayidin L, Perilli S, Taniguchi M, Morita MT, Aoyama T, Costantino P, Sabatini S** (2008) A genetic framework for the control of cell division and differentiation in the root meristem. *Science* **322**: 1380–1384
- Du Y, Scheres B** (2018) Lateral root formation and the multiple roles of auxin. *J Exp Bot* **69**: 155–167

- Fendrych M, Akhmanova M, Merrin J, Glanc M, Hagihara S, Takahashi K, Uchida N, Torii KU, Friml J** (2018) Rapid and reversible root growth inhibition by TIR1 auxin signalling. *Nat plants* **4**: 453–459
- Grieneisen VA, Xu J, Marée AFM, Hogeweg P, Scheres B** (2007) Auxin transport is sufficient to generate a maximum and gradient guiding root growth. *Nature* **449**: 1008–1013
- Gudesblat GE, Torres PS, Vojnov AA** (2009) Stomata and pathogens: Warfare at the gates. *Plant Signal Behav* **4**: 1114–1116
- Guo F-Q, Wang R, Crawford NM** (2002) The Arabidopsis dual-affinity nitrate transporter gene AtNRT1.1 (CHL1) is regulated by auxin in both shoots and roots. *J Exp Bot* **53**: 835–844
- Guo Y, Chen F, Zhang F, Mi G** (2005) Auxin transport from shoot to root is involved in the response of lateral root growth to localized supply of nitrate in maize. *Plant Sci* **169**: 894–900
- Hamdoun S, Liu Z, Gill M, Yao N, Lu H** (2013) Dynamics of defense responses and cell fate change during Arabidopsis-Pseudomonas syringae interactions. *PLoS One* **8**: e83219–e83219
- Hodge A** (2004) The plastic plant: root responses to heterogeneous supplies of nutrients. *New Phytol* **162**: 9–24
- Kong X, Zhang C, Zheng H, Sun M, Zhang F, Zhang M, Cui F, Lv D, Liu L, Guo S, et al** (2020) Antagonistic Interaction between Auxin and SA Signaling Pathways Regulates Bacterial Infection through Lateral Root in Arabidopsis. *Cell Rep* **32**: 108060
- Liu F, Xu Y, Chang K, Li S, Liu Z, Qi S, Jia J, Zhang M, Crawford NM, Wang Y** (2019) The long noncoding RNA T5120 regulates nitrate response and assimilation in Arabidopsis. *New Phytol* **224**: 117–131
- Navarro L, Dunoyer P, Jay F, Arnold B, Dharmasiri N, Estelle M, Voinnet O, Jones JDG** (2006) A plant miRNA contributes to antibacterial resistance by repressing auxin signaling. *Science* **312**: 436–439
- Overvoorde P, Fukaki H, Beeckman T** (2010) Auxin control of root development. *Cold Spring Harb Perspect Biol* **2**: a001537
- Qi F, Zhang F** (2020) Cell Cycle Regulation in the Plant Response to Stress. *Front Plant Sci* **10**: 1765
- Rich-Griffin C, Eichmann R, Reitz MU, Hermann S, Woolley-Allen K, Brown PE, Wiwatdirekkul K, Esteban E, Pasha A, Kogel K-H, et al** (2020) Regulation of Cell Type-Specific Immunity Networks in Arabidopsis Roots. *Plant Cell* **32**: 2742 LP-2762
- Rigo R, Bazin J, Romero-Barrios N, Moison M, Lucero L, Christ A, Benhamed M, Blein T, Huguet S, Charon C, et al** (2020) The Arabidopsis lncRNA ASCO modulates the transcriptome through interaction with splicing factors. *EMBO Rep* **21**: e48977
- Romero-Barrios N** (2016) Non-codings RNAs, regulators of gene expression in Arabidopsis thaliana root developmental plasticity. <http://www.theses.fr>
- Tian Q, Chen F, Liu J, Zhang F, Mi G** (2008) Inhibition of maize root growth by high nitrate supply is correlated with reduced IAA levels in roots. *J Plant Physiol* **165**: 942–951
- Vidal EA, Gutiérrez RA** (2008) A systems view of nitrogen nutrient and metabolite responses in Arabidopsis. *Curr Opin Plant Biol* **11**: 521–529

Zhao Y (2010) Auxin biosynthesis and its role in plant development. *Annu Rev Plant Biol* **61**: 49–64

2.3 ASCO, a novel actor in temperature sensing?

2.3.1 Introduction

In nature, plants are challenged by changing environmental conditions, having them manage conflicting stresses simultaneously. They often have to cope with both biotic and abiotic stresses and coordinate defense responses in order to minimize fitness costs. Abiotic stresses such as drought, high salinity or temperature changes can lead to altered resistance to pathogens. These multi-layered responses require a complex network involving phytohormones, reactive oxygen species (ROS), and other signaling molecules, leading to the regulation of a whole set of stress-related genes (Bostock et al., 2014).

Variations in temperature greatly impact plant growth, development as well as plant's immunity (Wang et al., 2009). Indeed, high temperatures tend to enhance plant susceptibility to pests by suppressing SA responses and promoting pathogen virulence (Huot et al., 2017). On the contrary, low temperatures boost the SA pathway and limit pathogen propagation in the plant, therefore promoting immunity (Li et al., 2020). At the molecular scale, recent studies have shown that temperature is a major driver of changes in AS, mainly by impacting the splicing activity of major spliceosome components and splicing regulatory genes. Such regulations likely permit cascades of AS of downstream genes, modulating transcriptome shaping accordingly to the perceived stress (Calixto et al., 2018; Ling et al., 2018; Verhage et al., 2017).

Plants subjected to a severe heat stress exhibit a significant increase of intron retention (IR) events, which is due to the repression of the splicing machinery. Once the stress is relieved, the return to control-like splicing patterns yet requires a prior gradual heat treatment of the plants, known as priming. Indeed, if the plants are directly exposed to a lethal heat stress they will maintain a splicing repression mimicking stress conditions, even after stress removal. On the contrary, primed plants recover from the lethal heat stress and exhibit control-like AS patterns. Hence, heat-stress priming, among other regulations, was suggested to be established at a post-transcriptional level through splicing "memory" (Ling et al., 2018).

On the other hand, cold stress does not seem to block general splicing efficiency, but induces a rapid and massive wave of AS coincident with a transcriptional response. The AS of some TFs and SFs was demonstrated to be highly sensitive to even slight temperature drops, leading to AS cascades and subsequent fine-tuning of transcriptome content (Calixto et al., 2018). New players that are involved in cold acclimation and resistance to freezing

were discovered, such as U2B^{''}-LIKE (AT1G06960), a paralog of the U2B^{''} (AT2G30260) protein which binds to spliceosomal U2snRNA. Moreover, the *u2b^{''}-like* mutant exhibit higher sensitivity to freezing and harbors splicing defects in phytochrome-interacting factor PIF7 (AT5G61270), a regulator of the C-REPEAT BINDING FACTOR (CBF) pathway (Calixto et al., 2018). Therefore, the study of new splicing regulators represents a promising track for the understanding of splicing involvement in plant responses to temperature changes.

The expression level of the lncRNA *ASCO* is driven by phytohormone content, such as auxin or ABA (Romero-Barrios, 2016). The abundance of *ASCO* transcripts fine-tunes the response to biotic stimulus such as flg22. Moreover, this lncRNA was found to bind to specific components of the spliceosome machinery in order to modulate the AS of specific target genes (Rigo et al., 2020). Hence, it was suggested that *ASCO* may act as an integrator of various stress signals in the plant. A growing number of lncRNAs emerge as major regulators of stress responses, some of them being temperature responsive (Liu et al., 2010; Kindgren et al., 2018; Wang et al., 2019). Knowing the role of *ASCO* in biotic responses (chapter 2), we decided to investigate *ASCO*'s involvement in another type of stress: temperature changes.

In this chapter I will present new data linking *ASCO* and thermoregulation in the plant, and provide hints that broaden *ASCO*'s functions in *Arabidopsis thaliana*.

2.3.2 Results

2.3.2.1 ASCO suppression resembles to a cold treatment at the transcriptome level

In the former chapter, ASCO suppression was found to impact the response to biotic cues such as flg22. Indeed, the sequencing of RNAi-ASCO plants unveiled a large proportion of differentially expressed genes (DEGs) related to biotic stresses. Nevertheless, one of the most significant GO category among DEGs was “response to stress” (FDR < 5e-3), comprising a total of 51 genes linked to biotic stresses and 47 genes linked to abiotic stresses. It is known that a large set of genes intervenes during both biotic and abiotic responses, and some elicitors such as SA induce both resistance to biotrophic attack and resistance to abiotic stresses like drought or low temperatures (Baillio et al., 2019; Venegas-Molina et al., 2020; Saleem et al., 2020).

Therefore, we investigated if ASCO suppression impacted other pathways besides biotic responses in the plant. For this, the Genevestigator Signature tool was used, which allows to identify experiments or conditions giving similar expression results than the entered gene expression signature. Here, the top 300 DEGs identified from RNAi-ASCO lines (ranked based on their fold-changes (FCs)) were used as the expression signature input. The experiment that shared the most common deregulations with RNAi-ASCO lines was a cold treatment at 4°C on Col-0 plants (Figure 15A). Indeed, these genes regulated in both processes exhibit similar expression changes in both RNAi-ASCO and cold treated plants, some of them being key markers of cold sensing (Figure 15B). For example, *COR28* (AT4G33980) and *RD29A* (AT5G52310) are well-known cold-regulated (COR) genes (Thomashow, 1999; Fowler and Thomashow, 2002), meanwhile *ERF105* (AT5G51190) and *GIGANTEA* (AT1G22770) were shown to participate in cold acclimation of the plant (Bolt et al., 2017; Cao et al., 2005). Hence, ASCO suppression seems to “give a cold” to the plant and activates cold stress signaling. In addition to that, experiments involving SA treatments also resemble ASCO suppression (Figure 15B). SA impact on biotic stress has been well described so far (An and Mou, 2011). Nevertheless, various studies pointed out the involvement of SA in cold stress (Saleem et al., 2020), showing the perception of cold temperatures leads to SA accumulation in various species (Scott et al., 2004; Kosova et al., 2012). Furthermore, SA application leads to better resistance to cold and freezing conditions, notably via gene regulation and increase in antioxidant activity, compatible solute content and accumulation of various cold-responsive proteins (Saleem et al., 2020). The similarities

A

Experiment identifier	Experimental conditions	Relative similarity value
AT-00120 (1)	Cold (4°C) treatment / untreated green tissue samples (0,5h ; 1h and 3h of treatment, in Col-0 genotype)	1,234
AT-00016 (2)	<i>fas2-1</i> / Ler-0	1,225
AT-00216 (156)	Salicylic acid spraying / mock treated rosette leaf sample (28h of incubation after treatment, in CS57664 genotype)	1,222
AT-00216 (79)	Salicylic acid spraying / mock treated rosette leaf sample (28h of incubation after treatment, in CS57664 genotype)	1,218
AT-00644 (1)	Tunicamycin treatment / mock treated seedling samples (5h of treatment, in Col-0 genotype)	1,217
AT-00216 (157)	Salicylic acid spraying / mock treated rosette leaf sample (28h of incubation after treatment, in CS57664 genotype)	1,216
AT-00575 (4)	<i>pft1-2</i> / Col-0	1,208
AT-00664 (5)	H ₂ O ₂ treatment / mock treated seedling samples (3h of incubation after treatment, in <i>anac017-1</i> genotype)	1,206
AT-00661 (3)	<i>sid2-2</i> / Col-0 (9h after inoculation with <i>Alternaria brassicicola</i> strain ATCC96836)	1,201
AT-00058 (5)	Drought treatment / untreated aerial tissue samples (2h in dry laminar airflow, in Col-0 genotype)	1,200

B

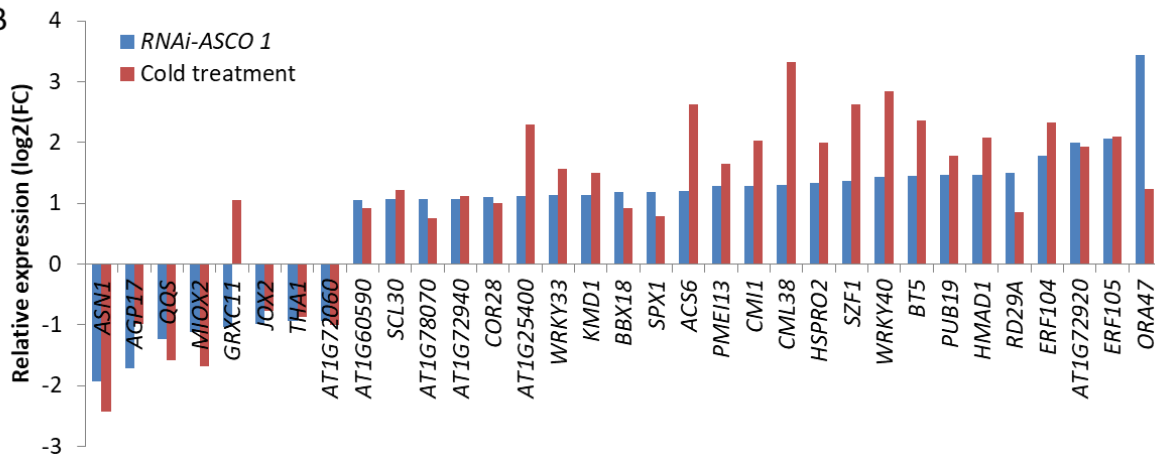


Figure 15. ASCO suppression induces a “cold-like” response in the plant.

A. Experiments that most resemble the expression deregulations observed in the RNAi-ASCO lines.

The 300 most deregulated (up- and downregulated) genes were selected from RNAi-ASCO / Col-0 RNAseq data and uploaded with their corresponding FC to the Signature tool of the Genevestigator software (<https://genevestigator.com/>). The transcriptome perturbations are ranked based on their relative similarity values.

B. Subset of common DEGs between RNAi-ASCO vs WT and the cold 4°C treatment vs WT. Genes were filtered based on their FC ($|\log_2FC| \geq 0,75$) and they false discovery values (FDR < 0,01).

between *ASCO* suppression and SA treatment hence reinforce *ASCO*'s link with cold stress responses in addition to biotic stresses.

2.3.2.2 *ASCO* regulates the expression of a large subset of cold-responsive genes

The Signature tool from Genevestigator gathered Affymetrix microarray data from *A. thaliana* to perform comparisons and similarity search of regulated genes. In order to have a more exhaustive landscape of the cold responsive transcriptome and explore in more detail the link between *ASCO* and cold responses, we used recently published transcriptomic data to carry out a comparison between our *ASCO* suppressed lines and cold treated plants (Calixto et al., 2018). In this study, deep RNA sequencing was performed on 5 week-old Col-0 plants subjected to a short and long-term kinetic at 4°C. Rosettes were sampled at 3 h intervals for the last day at 20°C, the first day at 4°C, and the fourth day at 4°C as described in Calixto et al., 2018. The analysis of RNAseq data determined both overall gene expression changes and individual transcript isoform levels. Taken altogether, 7302 genes had their expression significantly regulated throughout the low temperature kinetic. Strikingly, 58% of DEGs in RNAi-*ASCO* are cold-responsive, suggesting that the majority of genes affected by *ASCO* absence are also sensitive to low temperatures (Figure 16A). This provides strong evidence of *ASCO*'s involvement in the regulation of expression of cold-sensitive genes. As the transcriptomic analysis of RNAi-*ASCO* lines was performed under control conditions, this suggests that in the absence of *ASCO* the steady-state level of a subset of cold-related transcripts is altered.

Another question that arose was the regulation of *ASCO*'s expression upon cold treatment. For that purpose, *ASCO* expression levels were monitored through cold treatment kinetics at 4°C on Col-0 plants (Figure 16B). The expression of C-REPEAT BINDING FACTORS (*CBF1-3*), major actors of the cold signaling pathway (Liu et al., 2019), was also followed and used as a positive control of the low temperature response (Figure 16C). *ASCO* levels underwent a slight 1,5 fold increase upon 6h at 4°C, but the overall variations seemed negligible compared to the variations observed for *CBFs* genes. The expression levels of *ASCO*, the *NSRs*, *PRP8a* and *SmD1b* were also analyzed throughout the cold kinetic assay from Calixto et al., 2018. No significant expression changes could be found along the cold treatment kinetic for any of these splicing related actors. It was shown in chapter 2 that *ASCO* expression was not regulated by flg22 either, nevertheless changes in *ASCO* content were found to alter flg22 responses of the plant.

To go further in the characterization of ASCO's role in the response to low temperatures, WT and RNAi-ASCO plants were either placed at 21°C in control conditions or at 4°C for 3h, representing the time point where most of the transcriptional changes occur (Calixto et al., 2018). To evaluate putative defects in the cold signaling pathway, the expression of *CBF1*, 2 and 3, *INDUCER OF CBF EXPRESSION 1 and 2 (ICE1-2)* and well-known COR genes was investigated in control and low temperatures (AGIs are indicated in Table 2). *CBFs* are core transcriptional regulators of the cold signaling network and lead to the activation of a plethora of COR genes, resulting in cold acclimation and further freezing tolerance. These CBF factors are themselves activated by ICE1 and ICE2 MYC-like factors which undergo post-translational activation upon cold sensing (Kim et al., 2015; Liu et al., 2019; Tang et al., 2020). In control conditions, both independent RNAi-ASCO lines exhibited higher transcripts levels of *ICE1* and 2, *CBFs* and COR genes (Figure 16D). Some of these regulations were already observed in RNAseq data from RNAi-ASCO lines, except the changes for *CBFs* and *ICE* factors. These differences with RNAi-ASCO RNAseq data could be explained by the differences in the age of the used biological material and in the growth medium used for the cold treatment assay. These deregulations of expression further support ASCO's impact on the maintenance of steady state levels of major cold signaling genes. For the analysis of the molecular response to cold, gene expression inductions in RNAi-ASCO lines were compared to WT values set as a 100% response. Interestingly, ASCO suppressed lines exhibited lower inductions of expression for *CBF1*, *CBF2* and *COR15A* after 3h at 4°C (Figure 16E). *ICE1* and *ICE2* were not represented in this analysis as their expression does not change upon cold treatment but only their post-transcriptional regulation. These experiments therefore suggest that ASCO suppression alters the steady-state level of cold signaling genes, but also leads to changes in the induction level of cold-sensitive genes upon cold perception.

2.3.2.3 Deregulation of ASCO alters plant acclimation to cold temperatures

Various studies showed that the deregulation of cold response regulators such as ICE1 or *CBFs* modulates the response to low temperatures and plant tolerance to freezing (Gilmour et al., 2004; Xiang et al., 2008; Zhao et al., 2016). Indeed, perception of cold temperatures triggers dramatic changes in the plant transcriptome, proteome and metabolome. The sensing of cold notably leads to reduced plant growth and accumulation of cryoprotective molecules and specific pigments such as anthocyanins (Theocharis et al., 2012; Schulz et

A

DEG
RNAi-ASCO vs WT
 $|\log_2FC| \geq 0,75$;
 $p\text{-value} < 0,01$



DEG
4°C vs 20°C
 $|\log_2FC| \geq 1$;
 $p\text{-value} < 0,01$

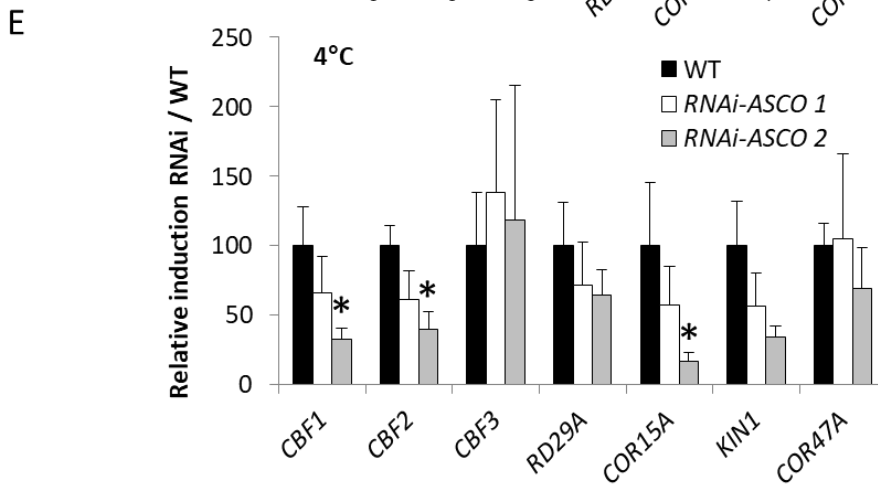
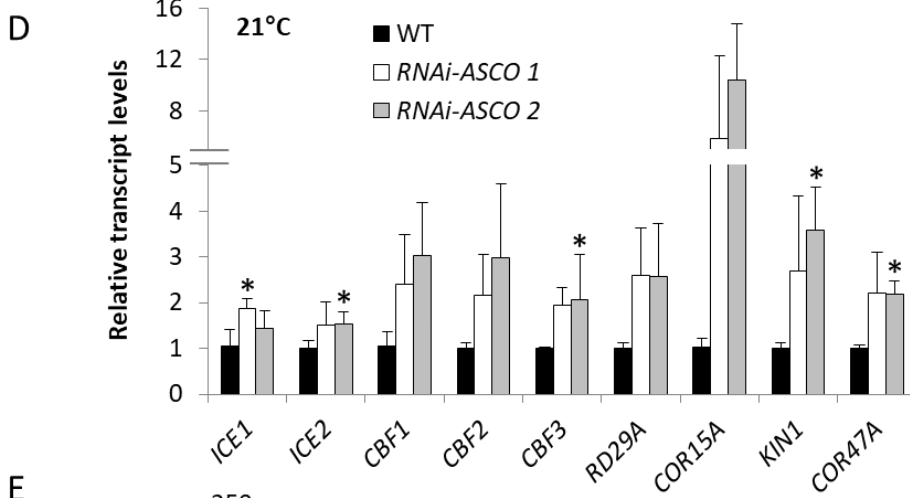
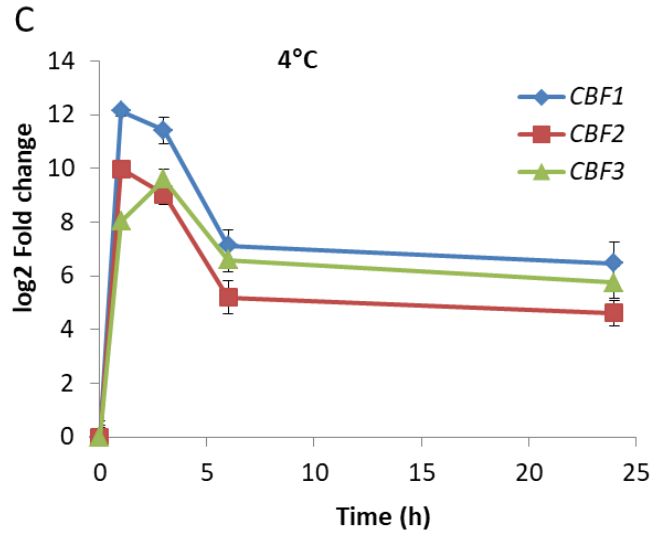
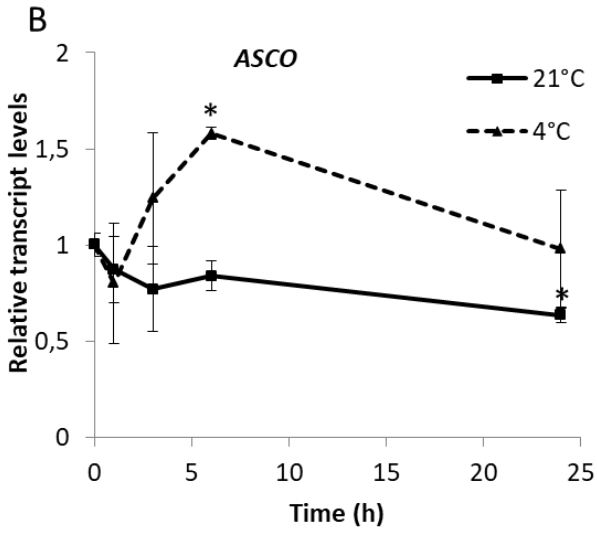


Figure 16. RNAi-ASCO lines show altered expression of cold-responsive genes.

A. Comparison of RNA-seq data from RNAi-ASCO vs WT and cold (4°C) treated plants (from Calixto et al., 2018). DEGs were filtered based on their FC and FDR values as stated on the Venn diagram.

B, C. Time-course analysis of ASCO (B) and CBFs (C; *CBF1*, AT4G25490 ; *CBF2*, AT4G25470; *CBF3*, AT4G25480) expression levels in WT plants after being transferred or not to cold (4°C) media. In (C), expression levels are represented as Log2-fold change values.

D. Relative transcript levels of a subset of cold responsive genes and cold response regulators in control conditions in WT and RNAi-ASCO plants (AGIs are indicated in Table 2).

E. Relative modulation of the same genes as in (D), in response to 3h in the cold (4°C). Results are normalized against the response in WT plants, taken as 100%. *ICE1* and *ICE2* were not displayed as they are not regulated by a cold treatment.

RNAs were extracted from 11-day-old WT plants transferred or not to cold (4°C). The asterisk (*) indicates a significant difference as determined by Student's t test ($P < 0,05$, $n = 3$). Error bars show mean \pm standard deviation.

al., 2016). Thus, together with the previously observed molecular response, the physiological phenotype of ASCO deregulated plants was characterized upon cold stress (Figure 17). Both RNAi- and 35S-ASCO lines were grown 10 days under classical growth conditions and then either kept 15 additional days under classical conditions, or placed at 4°C for 20 days to assess their cold acclimation. At the root growth level, RNAi-ASCO plants and especially RNAi-ASCO 2 lines developed shorter primary roots and have enhanced LR density in cold conditions (Figure 17A, 17B and 17C). However, this stunted growth was also observed in control temperature, suggesting a growth defect independent of a cold environmental effect. On the other hand, 35S-ASCO plants did not exhibit significant differences in root growth compared to the WT in cold conditions (Figure 17A, 17B and 17C). Noteworthy, the aerial parts of RNAi-ASCO lines appeared much darker than WT and 35S-ASCO plants (Figure 17A and 17D). Anthocyanins are one of the major pigments that provide red / purple color to leaves and protect plant tissues against many abiotic stresses including cold temperatures (Landi et al., 2015; Schulz et al., 2016). Anthocyanin content was therefore measured in aerial parts of ASCO deregulated lines grown in cold conditions (Figure 17E). Strikingly, RNAi-ASCO lines accumulated approximately 3 times more anthocyanins than WT plants subjected to long term low temperature. Conversely, 35S-ASCO plants presented WT-like anthocyanin content, with 35S-ASCO 1 lines presenting even lower levels than the WT. Rather than impacting the root growth in cold conditions, ASCO could participate in the regulation of pigment content in the aerial parts of the plant, potentially fine-tuning their acclimation to low temperatures.

2.3.2.4 ASCO-suppressed plant exhibit cold-induced AS events

In Rigo et al., 2020 the modulation of ASCO levels was found to alter the AS of transcripts involved in various pathways, including the response to pathogens. For this analysis, two complementary approaches were used to identify both differential AS based on annotated isoforms (AtRTD2) and potentially non-annotated differential RNA processing events using RNAprof (see Rigo et al., 2020 for method details). As the majority of DEGs in RNAi-ASCO plants were cold responsive, we also wondered if the differentially alternatively spliced (DAS) genes in these lines had their AS regulated by cold. Calixto et al., 2018 searched for genes presenting cold-induced AS events and identified a total of 2442 DAS genes throughout their cold kinetics. Respectively 25% and 40% of DAS genes from ASCO RNAprof and AtRTD2 analyses presented variations in AS in response to cold (Figure 18A). Interestingly, the DAS genes that were confirmed in RNAi-ASCO lines in Rigo et al., 2020 such as *SR34*, *SNC4*, *NUDT7* and *RPP4* were also detected as DAS in response to cold treatment. Remarkably, these genes are mainly described as actors of the defense responses to biotic stresses up to

now. So as for DEGs, *ASCO* suppression provokes cold-induced DAS events, and seems to mostly impact the AS of defense-related transcripts.

Nevertheless, we searched for other DAS events in *ASCO* silenced lines that could provide new hints on its way of action and impact on cold signaling. *ICE2* expression was previously shown to be upregulated in RNAi-*ASCO* plants. Surprisingly, the RNAprof analysis detected a significant retention of *ICE2*'s 1st intron in RNAi-*ASCO* lines, this AS event leading to a truncated protein lacking bHLH and ACT domains (Figure 18B). This event was not identified among cold-induced DAS events from Calixto et al., 2018. Given *ICE2* and *ICE1* are both at the beginning of the CBF-pathway and govern its activation, impacting the AS of these actors could greatly impact the CBF-pathway itself and therefore the plant acclimation to cold. The ratio between alternatively spliced (*ICE2.1*) and fully spliced isoform (*ICE2.3*) was investigated by qPCR in RNAi-*ASCO* plants under both control (Figure 18C) and low temperatures (Figure 18D). No significant differences in isoform ratios could be detected in *ASCO* suppressed lines in the tested conditions. The assay will need further investigation by testing *ICE2*'s splicing in the same conditions as the one used for the RNAseq experiment. Nonetheless, another major actor of the cold response was found in DAS analyses of RNAi-*ASCO* lines: *REGULATOR OF CBF GENE EXPRESSION 1* (*RCF1*, AT1G20920). This DEAD-box RNA helicase was shown to modulate the splicing of many cold-responsive transcripts and is required for cold tolerance (Guan et al., 2013). Moreover, Calixto et al., 2018 have shown that *RCF1* itself underwent AS upon low temperatures, suggesting the presence of an autoregulatory loop governing cold-responsive transcripts abundance. The regulation of *RCF1* splicing in *ASCO*-silenced lines grown under control conditions delivers additional clues that *ASCO* participates in the control of steady-state abundance of cold-related transcripts. Curiously, both cold-treated and *ASCO* suppressed plants display AS for the *HEAT SHOCK TRANSCRIPTION FACTOR A1D* (*HSFA1D*, AT1G32330), one of the major regulators of the heat shock response (Liu et al., 2011). *HSFA1D* exhibited rapid AS changes upon gradual temperature decrease, suggesting a putative role of this TF in both heat and cold sensing. The modulation of *HSFA1D*'s splicing by *ASCO* led us to investigate new hypotheses concerning *ASCO*'s role in temperature sensing in the plant.

2.3.2.5 Towards a new role of *ASCO* in heat sensing?

ASCO was already found to integrate many stresses notably by splicing modulation of various stress-related transcripts. A growing number of splicing regulators display new roles in the plant response to stresses. For instance, the spliceosome component U5-snRNP-interacting protein called STABILIZED1 (*STA1*, AT4G03430) was shown to modulate both

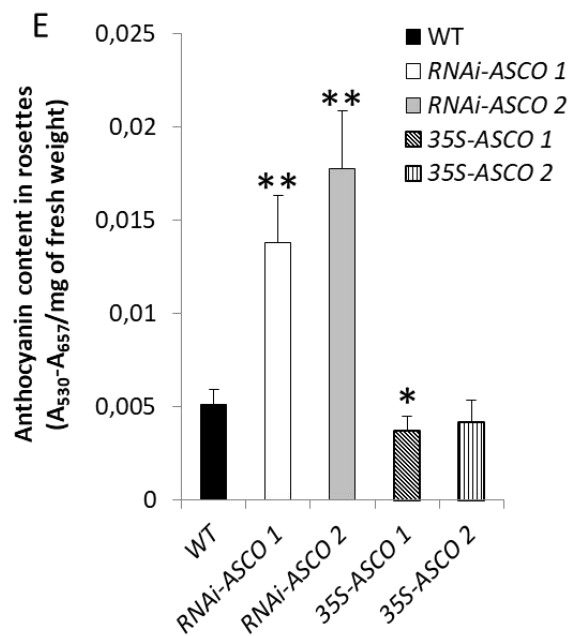
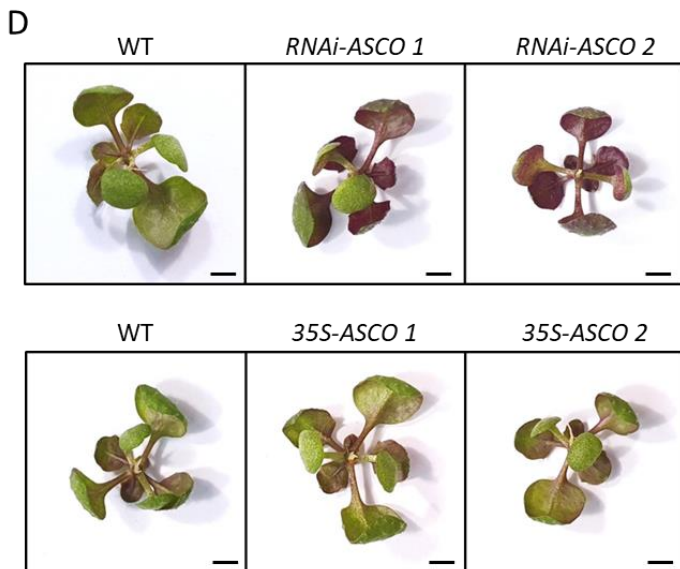
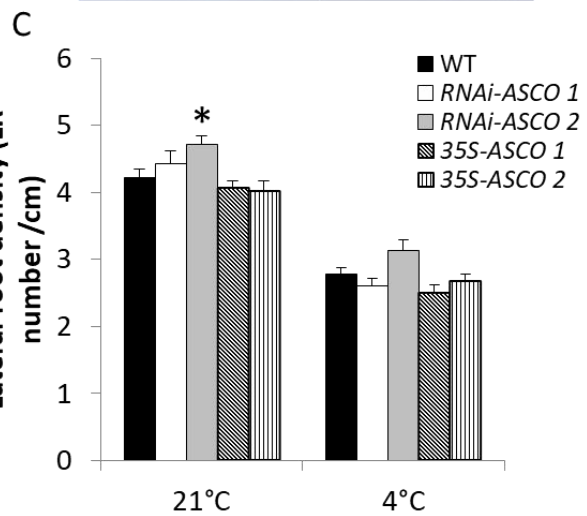
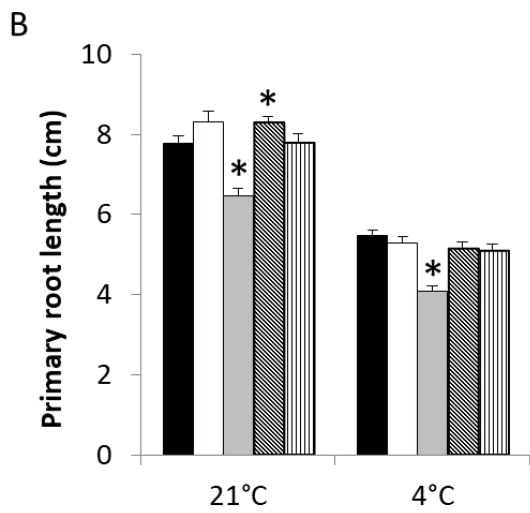
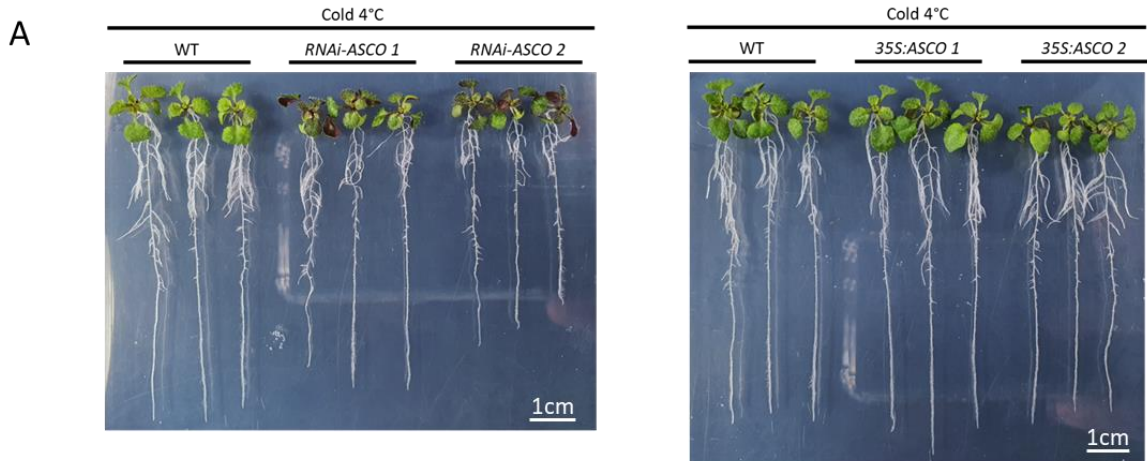


Figure 17. Deregulation of ASCO expression leads to an altered response to cold.

A. Representative picture of 30-day-old plants grown 20 days at 4°C on 1/2MS + 1% sucrose. Scale bar corresponds to 1 cm.

B, C. Primary root length (B) and lateral root density (C) of WT, RNAi-ASCO and 35S-ASCO lines 15 days at 21°C or 20 days after transfer at 4°C. The asterisk (*) indicates a significant difference as determined by Student's t-test (respectively: * $P < 0.05$, $n \geq 30$). Error bars show mean \pm standard error.

D. Representative picture of 30-day-old plant rosettes grown 20 days at 4°C. Note anthocyanin accumulation in leaves. Scale bars correspond to 2 mm.

E. Anthocyanin content of WT, RNAi-ASCO and 35S-ASCO rosettes 20 days after transfer at 4°C. The anthocyanin content is measured as the absorbance at 530nm normalized to rosettes' fresh weight. The asterisks (*, **) indicate a significant difference as determined by Student's t-test (respectively: * $P < 0.05$; ** $P < 5 \times 10^{-3}$, $n=5$). Error bars show mean \pm standard deviation.

splicing of cold-induced genes under low temperatures and heat shock proteins (HSPs) and heat shock factor (HSFs) under high temperatures (Lee et al., 2006; Kim et al., 2017; Kim et al., 2018). Indeed, this heat inducible gene is required for proper splicing of *HSFA3* and essential for subsequent thermotolerance (Kim et al., 2017). Given *ASCO*'s impact on some heat-shock factors' splicing, we analyzed *ASCO* expression levels upon heat stress among transcriptomic data. Ling and colleagues (2018) described the link between heat perception and heat priming, notably through the acquisition of a splicing memory allowing to cope with a lethal heat stress. This study compared transcriptomic variations in seedlings primed (Figure 19A) or non-primed (Figure 19B) with heat stress (see Ling et al., 2018 for further details). Interestingly, *ASCO* expression was found to be positively correlated with temperature changes, displaying a 4-fold induction peak at the very end of the heat acclimation period (Time-point (TP) 2 to TP4, Figure 19B). *ASCO* expression returned to control-like levels as soon as the heat stress was removed (TP5 and TP6). When primed plants were subjected again to severe heat stress, *ASCO* expression significantly increased but at a lower level than during the previous gradual heat acclimation (TP7). This priming allowed the plant to better survive to an upcoming lethal heat stress, and attenuated its associated transcriptomic changes. In absence of priming, the severe heat shock was lethal for the plants and induced persisting splicing blockage. In this case, *ASCO* expression level slightly augmented upon heat shock (TP10) but kept increasing even after stress removal (TP11) (Figure 19C). However, the variability in transcript values could not lend significant changes during this particular set-up. *ASCO* induction seems therefore to rely on the perception of heat stress by the plant, where slower and gradual priming provokes stronger expression increase. Splicing factors are known to respond to a large spectrum of stresses (Laloum et al., 2017). To go further in the analysis of *ASCO* way of action during heat stress, the expression of *ASCO* partners, the NSRs, was investigated during the heat priming assay. Strikingly, *NSRa* and *NSRb* exhibited completely opposite expression patterns upon heat sensing. *NSRa* displayed an expression pattern really similar to *ASCO*, with a sharper and earlier increase during the heat acclimation step (Figure 19E). Interestingly, *NSRa* levels slightly rose in both primed and non-primed plants after a short lethal heat stress, but remained a bit higher than control levels in primed plants after stress removal (Figure 19E and 19F). On the contrary, *NSRb* levels underwent a significant drop in expression as soon as the heat stress was applied, reaching non detectable transcript levels at TP3 (Figure 19G). The short lethal heat stress in both primed and non-primed plants caused a slight decrease in *NSRb* expression, but did not come out as significant in both cases (Figure 19G and 19H). The clear regulation of *ASCO* and *NSRs* expression upon heat sensing suggests a role of these actors during heat acclimation and response to high temperatures. On top of

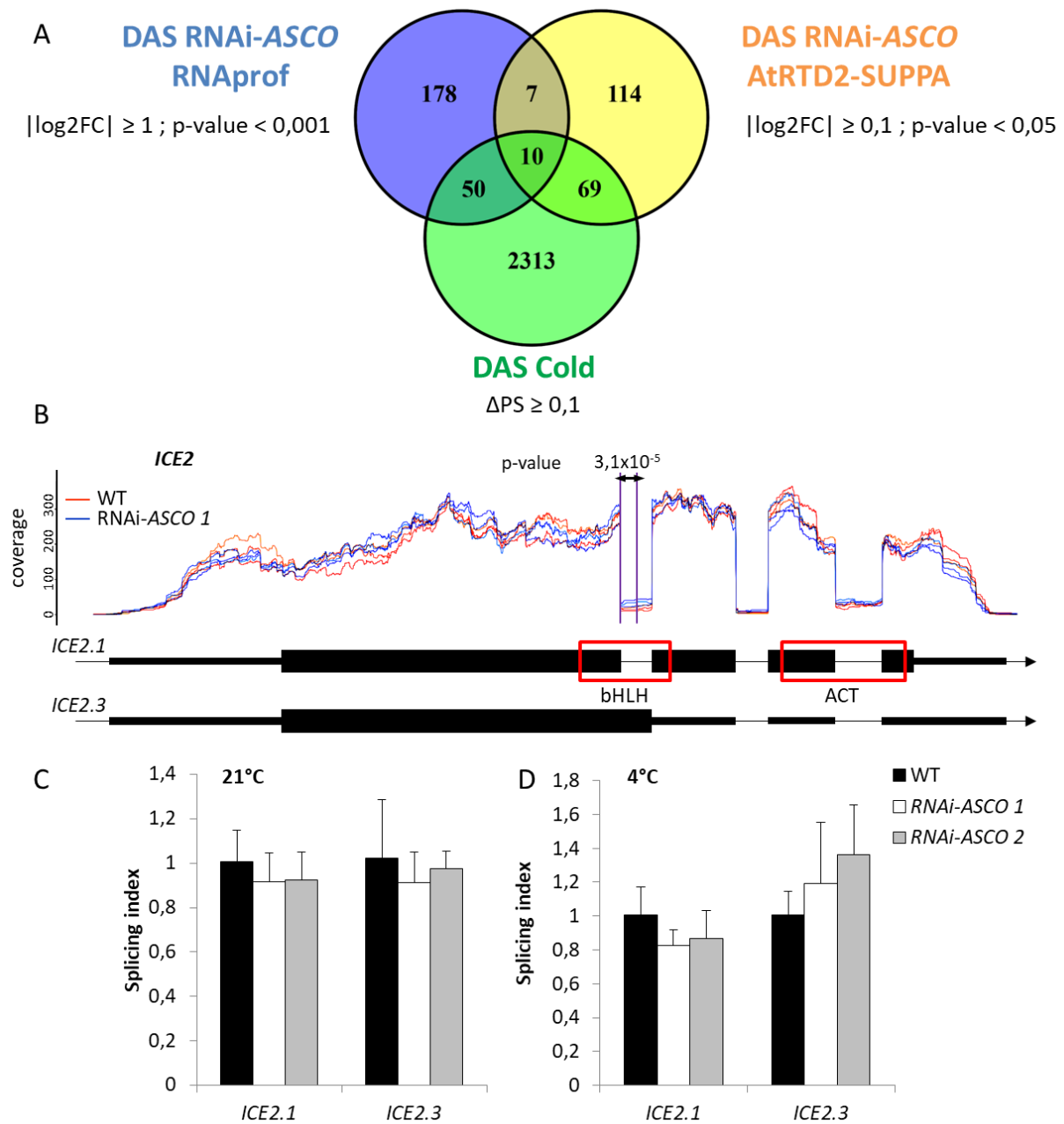


Figure 18. ASCO suppressed plants present cold-induced splicing events.

A. Comparison of differentially processed transcripts (DAS RNAprof) and differentially spliced genes (DAS AtRTD2-SUPPA) in RNAi-ASCO lines with differentially spliced genes in response to cold treatment (DAS Cold) (from Calixto et al., 2018). DAS genes were filtered based on their FC, FDR and ΔPS values as stated on the Venn diagram.

B. Differential RNA processing events of *ICE2* (AT1G12860) transcripts detected by RNAprof. Blue and red lines represent RNA-seq read coverage normalized for gene expression differences in WT and RNAi-ASCO 1 biological replicates, respectively. Three biological replicates were used for the analyses. Vertical purple lines and p-values indicate significant differential processing events. Each profile is associated with the structure of the corresponding RNA isoform. Large black boxes indicate exons, narrow black boxes indicate UTRs and black lines indicate introns. Colored boxes indicate protein domains affected by an AS event. bHLH: basic helix-loop-helix domain; ACT: Aspartate kinase, Chorismate mutase and TyrA domain.

C, D. Quantification of *ICE2* isoforms splicing at 21°C (C) and 4°C (D) by splicing index RT-qPCR. Error bars show mean \pm standard deviation.

that, certain ASCO AS targets such as *SR34* were also found to be regulated at both transcriptional and post-transcriptional levels by heat stress (Ling et al., 2018). *SR34* was found to be DAS in RNAi-ASCO lines but also upon biotic stresses and abiotic stresses such as cold or heat stress (Xu et al., 2011; Calixto et al., 2018; Ling et al., 2018). The high splicing plasticity of this SR protein could represent one of the main actors through which ASCO modulates AS and integrates various stresses in the plant.

2.3.3 Discussion

In this chapter we provided new hints that shed light on ASCO's role during the plant response to temperature changes. Indeed, nearly 60% of the genes that are deregulated by ASCO suppression also respond to the perception of cold temperatures. Some major regulators of the cold response such as *ICEs*, *CBFs* and *COR* genes had their expression deregulated in RNAi-ASCO lines under normal temperatures, and furthermore displayed altered expression induction upon cold sensing. Moreover, ASCO absence led to altered AS patterns of cold-sensitive genes such as *RCF1*, an RBP which regulates gene expression under cold stress and is required for proper splicing of cold-responsive genes (Guan et al., 2013). Interestingly, *RCF1* was shown to be coexpressed with another RNA helicase, the U5 small nuclear ribonucleoprotein helicase (*Brr2b*, AT2G42270) and together they impact *CBF* expression and participate in plant resistance to cold temperatures (Guan et al., 2013). In Rigo et al., 2020 the mass spectrometry analysis of ASCO-containing RNPs identified a subset of spliceosome components, including the Brr2b helicase. This putative interaction between ASCO and Brr2b together with its impact on *RCF1* splicing supports the need for further characterization of ASCO's role in cold sensing and acclimation. RIP assays targeting Brr2b or RCF1 will provide new insights in ASCO interaction network. Moreover, *brr2b* and *rcf1-1* mutants displayed reduced freezing tolerance, a phenotype that could not be tested for our ASCO suppressed lines due to a lack of appropriate similar equipment in our lab. Nevertheless, a stronger anthocyanin accumulation was observed upon cold acclimation at 4°C in RNAi-ASCO plants. These pigments belong to the major class of flavonoids, secondary plant metabolites which accumulate in response to various stresses including drought, cold and high light (Nakabayashi et al., 2014; Schulz et al., 2016; Winkel-Shirley 2002). The accumulation of anthocyanin derivatives was shown to reduce electrolyte leakage and enhance freezing tolerance (Schulz et al., 2016). The RNAi-ASCO lines could therefore display higher freezing tolerance as well, in concordance with their upregulation of *ICE*, *CBFs*, and *COR* genes which were also found to provide tolerance to low temperatures (Zhao et al., 2016). Anthocyanin production is also positively regulated by hormonal cues

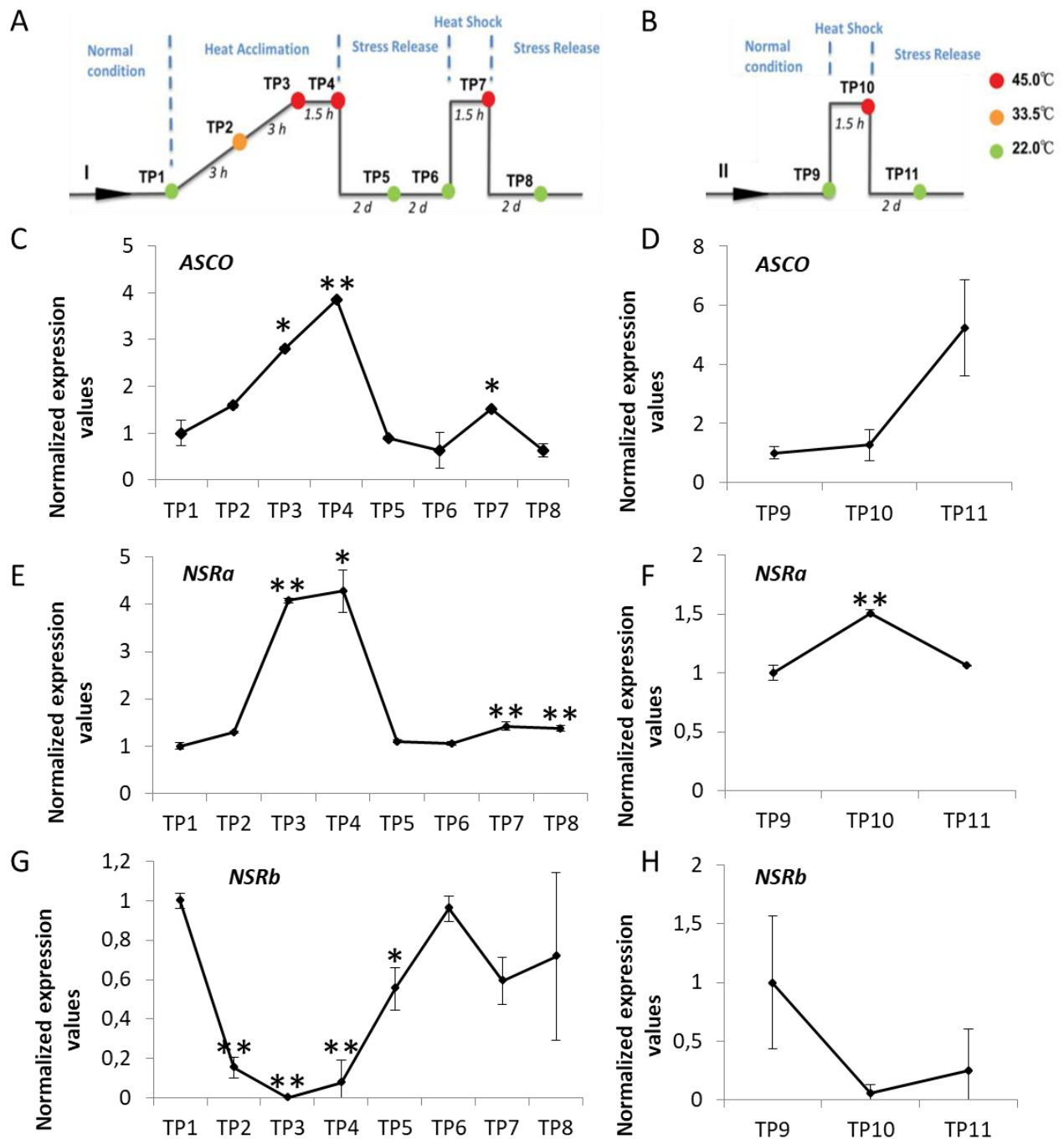


Figure 19. The NSR-ASCO complex is regulated by heat at the transcriptional level.

A, B. Experimental set-up of the heat-stress priming process. Seedlings grown under long days were either primed (A, acclimation before the heat shock) or not primed (B, direct heat shock) with heat stress. During priming, the temperature was increased uniformly from 22 to 45 °C over 6 h, sustained at 45 °C for 1.5 h, and then brought down sharply to 22 °C. For the heat-shock process, the temperature was rapidly increased from 22 to 45 °C and then dropped down to 22 °C sharply after 1.5 h. The temperature of each sample collection time-point (TP) and the interval between the TPs are indicated (extracted from Ling et al., 2018).

C, E, G. Normalized expression values of *ASCO* (C), *NSRa* (E) and *NSRb* (G) in primed seedlings.

D, F, H. Normalized expression values of *ASCO* (D), *NSRa* (F) and *NSRb* (H) in non-primed seedlings.

The asterisks (*, **) indicate a significant difference as determined by Student's t-test (respectively: * $P < 0,075$; ** $P < 0,05$; $n = 2$). Error bars show mean \pm standard deviation.

such as JA signaling (Shan et al., 2009). The ORA47 TF, a major regulator of JA and ABA biosynthesis (Chen et al., 2016) is cold-inducible and highly upregulated in RNAi-*ASCO* lines (Figure 15B). The deregulated expression of this TF could represent another path through which *ASCO* modulates the response to various stresses, including cold stress.

Neither *ASCO* nor its RBP partners were found to be regulated by a cold treatment at the transcriptional level. Intriguingly, *ASCO* and *NSRa* expression was clearly positively correlated with heat perception by the plant, whereas *NSRb* levels dropped to non-detectable levels upon high temperatures. Heat shock stress leads to major transcriptome changes including splicing blockage, altering both constitutive and alternative splicing in both animals and plants (Shukla et al., 1990; Fujikake et al., 2005; Chang et al., 2014; Lal et al., 2015). Changes in *ASCO* and NSRs abundance were shown to alter the expression and the AS of a large subset of genes (Bardou et al., 2014; Bazin et al., 2018, Rigo et al., 2020). As heat perception affects the expression of these splicing regulators, they may play a role in the fine-tuning of heat-associated transcriptome changes. In animals, the SRp38 protein acts as a general splicing repressor in response to heat shock. Heat perception induces dephosphorylation of this SR protein, leading to its activation and further splicing repression (Shin et al., 2004; Shi et al., 2007). In the absence of SRp38 and under heat stress, the splicing machinery keeps functioning but under suboptimal conditions, leading to affected cell survival. This data suggests that effective splicing modulation and/or repression is necessary for proper cell survival. Indeed, this splicing fine-tuning could diminish the production of inaccurately spliced transcripts and could also modulate protein translation by producing NMD-sensitive mRNAs, avoiding the cells to waste precious energy in translation during heat stress (Dutertre et al., 2011).

To date, such splicing repressors were not described in plants. However, some hypotheses emerge from the numerous pathways in which the *ASCO* lncRNA is involved. This lncRNA acts as splicing factor hijacker, competing with the binding of its RBP partners to their mRNA targets. Therefore, rather than completely blocking splicing *ASCO* could promote the accumulation of specific AS transcripts, allowing the plant to better cope with either biotic or abiotic stresses. Given its high accumulation in response to heat, the phenotypical analysis of *ASCO* suppressed lines under heat stress would provide insights in which specific signaling pathways this lncRNA acts. Moreover, it is the first time that *NSRa* and *NSRb* exhibit such opposite expression patterns in response to a stress, *NSRa* usually presenting stable expression among the tissues where it is expressed. On the contrary, *NSRb* was already found to be upregulated by auxin, flg22 and pathogen infection, suggesting this RBP is more involved in the response to biotic cues. Such differences open up new hypotheses on NSRs specificity, which may represent one key aspect of *ASCO*'s

versatile role during stress responses. Indeed, numerous studies pinpointed the role of SFs during plant response to stresses. GRP7 is a glycine-rich RBP involved in the response to drought, salt and cold (Kim et al., 2008; Yang et al., 2014). RBM25 is a putative component of the spliceosome which is essential for ABA responses and associated plant responses to osmotic stresses (Zhan et al., 2015; Cheng et al., 2017). SR45 is a SR protein that participates in reproductive processes but also acts as an immunity suppressor (Zhang et al., 2017). The diversity of stress-involved SFs let us catch a glimpse of this huge reservoir of transcriptome modulators. Hence, *ASCO*'s impact on the transcriptome and the associated AS output it provokes could directly rely on the ribonucleoprotein partner *ASCO* has at a specific time and in specific tissues. The investigation of *ASCO*'s partners especially during stresses will increase understanding of how this lncRNA works with other actors of the splicing process, and which molecular, cellular and phenotypical outputs it generates to regulate crucial processes such as plant acclimation to abiotic stresses and plant immunity.

2.3.4 Material and Methods

2.3.4.1 Plant material and growth conditions

All the lines used in these experiments are described in Rigo et al., 2020. Plants were grown at 21°C with a 16-h light/8-h dark photoperiod (long days) on solid half-strength Murashige and Skoog (1/2MS) medium supplemented with 1% sucrose.

2.3.4.2 Root growth analysis

For analysis of cold temperature impact on root architecture, plants were previously grown 10 days on solid 1/2MS medium + 1% sucrose and then were either kept 15 additional days in the same growth conditions, or transferred in a growth cabinet at 4°C with the same light conditions for 20 additional days. For each plantlet, the primary root length and lateral root count were measured using the RootNav software (Pound et al., 2013). Experiments were performed with a minimum of 30 plants per genotype and condition. Statistical tests were performed using Student's t-test ($P < 0,05$) using WT values as reference.

2.3.4.3 Anthocyanin extraction

For measurements of the anthocyanin content in cold-treated rosettes, plants were grown as stated in the "Root growth analysis" section. Method for anthocyanin extraction was adapted

from Feinbaum and Asubel (1988). Frozen plant tissue was ground (around 150mg, 6 rosettes per sample) and total pigments were extracted in a 99% ethanol / 1% HCl solution. Then, one volume of 3:1 H₂O/methanol solution was added to the extract. Chlorophyll was separated from the anthocyanins by the addition of one volume of chloroform. The samples were centrifuged 3 minutes at 6000g. The upper aqueous phase containing the anthocyanins was transferred to a new tube containing one volume of 3:1 H₂O/methanol solution. The quantity of anthocyanin pigments was determined by spectrophotometric measurements of the aqueous – methanol phase ($A_{530} - A_{657}$ was used as a measure of anthocyanin content) and normalized to the weight of tissue used in each sample. Experiments were performed with 5 replicates per genotype, each replicate containing 6 rosettes. Statistical tests were performed using Student's t-test ($P < 0,05$) using WT values as reference.

2.3.4.4 RNA extraction and RT–qPCR analyses

All the analyses were performed as described in Rigo et al., 2020. Experiments were done in biological triplicates with at least two technical replicates. For analysis of cold impact on gene expression, plants were previously grown 10 days on solid 1/2MS medium + 1% sucrose and then transferred for additional 24 h in liquid 1/2MS medium + 1% sucrose before adding or not cold (4°C) liquid media. Cold-treated plants were then kept at 4°C in growth chambers until the end of the treatment. Five plantlets were pooled for each replicate. The fold induction of expression after cold treatment was normalized to the WT response considered as 100%. Error bars on qRT–PCR experiments represent standard deviations, and significant differences were determined using Student's t-test ($P \leq 0.05$, $n \geq 3$ biological replicates). All the used primers and gene AGIs are listed in Table 2.

2.3.4.5 Genevestigator Signature tool

The Signature tool from Genevestigator was used to compare the list of DEGs in RNAi-ASCO 1 lines against the entire Genevestigator curated content (<https://genevestigator.com/>). The result shows conditions giving similar results (expression values) for the entered genes. The relative similarity indicates the degree of their resemblance: the higher the value, the higher the similarity relative to the average similarity. More precisely, if the similarity s_i is defined as $1/d_i$ with d_i the distance of category i to the signature, then the relative similarity R of a category c is calculated as:

Where s_i is the similarity of category i and I the set of all conditions. Due to software

$$R_{s_c} = \frac{s_c}{\frac{1}{N} \sum_{i \in I} s_i}$$

limitations, only the best 300 DEGs from RNAi-ASCO 1 lines presenting the highest FCs were used for the analysis. The top 10 experiments giving the most similar results were displayed along with their corresponding experimental conditions, relative similarity values and experiment identifiers. For the comparison of expression FCs between RNAi-ASCO 1 lines and cold treated plants, expression values were directly extracted from the Signature tool. Genes were filtered based on their FC ($|\log_2FC| \geq 0,75$) and their false discovery values ($FDR < 0,01$) for their representation on the graph.

2.3.4.6 Transcriptome and AS comparisons

All the methods for the analysis of transcriptomic data are described in Rigo et al., 2020. For the transcriptomic analysis of cold-treated plants, see Calixto et al., 2018. General linear models to determine differential expression at both gene and transcript levels were established using time and biological replicates as factors. 18 contrast groups were set up where corresponding time-points in the day 1 and day 4 at 4°C blocks were compared with those of the 20°C block. Genes were significantly differentially expressed at the gene level if they had at least two contrast groups at consecutive time points with adjusted $P < 0,01$ and ≥ 2 -fold change in expression in each contrast group. Genes/transcripts with significant DAS had at least two consecutive contrast groups with adjusted $P < 0,01$ and with these contrast groups having at least one transcript with $\geq 10\%$ change in expression ($\Delta PS \geq 0,1$). Both DEG and DAS genes identified in RNAi-ASCO 1 lines were compared to the whole list of DEG or DAS genes in response to cold (4°C) treatment. For the transcriptomic analysis of heat-treated plants, see Ling et al., 2018. Two replicate samples per time-point were used. Gene expression levels (here fragments per kilobase of transcript per million mapped reads, FPKM) were calculated using Cufflinks (Version 2.0.0). For each of the analyzed gene, expression values were normalized to TP1 levels corresponding to the plants under control conditions. Statistical tests were performed using Student's t-test ($P < 0,05$ or $P < 0,075$) using TP1 values as reference.

Table 2
List of primers used for RT-qPCR in Chapter 3

	AGI	Gene	Oligo Sequence	Reference / Information	
RT-qPCR	AT1G13320	<i>Housekeeping ref 1 PP2A F</i>	TACCGTGGCCAAAATGATGC	Czechowski et al., 2005	
	AT1G13320	<i>Housekeeping ref 1 PP2A R</i>	GTTCTCCACAACCGCTTGGT	Czechowski et al., 2005	
	AT4G26410	<i>Housekeeping ref 2 F</i>	GAGCTGAAGTGGCTTCCATGAC	Czechowski et al., 2005	
	AT4G26410	<i>Housekeeping ref 2 R</i>	GGTCCGACATACCCATGATCC	Czechowski et al., 2005	
	AT1G67105	<i>ASCO F</i>	CGCGTGGATAGGTAGGGTAC		
	AT1G67105	<i>ASCO R</i>	TGCGAGAAGAACGGTCCATA		
	AT3G26744	<i>ICE1 F</i>	AATTGGGGAACAGGGATTTG		
	AT3G26744	<i>ICE1 R</i>	CAACGGAGCTGTGAAACCAC		
	AT1G12860	<i>ICE2 F</i>	TCTTCAAGCTTGCATCCGTT		
	AT1G12860	<i>ICE2 R</i>	GTTGGCCTTTAGGACTTGGC		
	AT4G25490	<i>CBF1 F</i>	GGAGACAATGTTTGGGATGC		
	AT4G25490	<i>CBF1 R</i>	TTAGTAACTCCAAAGCGACACG		
	AT4G25470	<i>CBF2 F</i>	TGACGTGTCTTATGGAGCTA		
	AT4G25470	<i>CBF2 R</i>	CTGCACTCAAAAACATTTGCA		
	AT4G25480	<i>CBF3 F</i>	GATGACGACGTATCGTTATGGA		
	AT4G25480	<i>CBF3 R</i>	TACTACTCGTTTCTCAGTTTTACAAAC		
	AT5G52310	<i>RD29A F</i>	CTTGTCGACGAGAAGCAAAGAA		
	AT5G52310	<i>RD29A R</i>	TCTTGATGGAGAATTCGTGTCC		
	AT2G42540	<i>COR15A F</i>	GTCGTCGTTTCTCAACGCAAGA		
	AT2G42540	<i>COR15A R</i>	GCITTTCTCAGCTTCTTTACCCA		
	AT5G15960	<i>KIN1 F</i>	ATGCCITCCAAGCCGGTCAGAC		
	AT5G15960	<i>KIN1 R</i>	CCGGTCTTGTCTTACGAAGT		
	AT1G20440	<i>COR47A F</i>	TGTCATCGAAAAGCTTACCCGA		
	AT1G20440	<i>COR47A R</i>	ACCGGGATGGTAGTGAAACTG		
	Alternative splicing RT-qPCR	AT1G12860	<i>ICE2 INPUT</i>	TCTTCAAGCTTGCATCCGTT	
		AT1G12860	<i>ICE2 INPUT R</i>	GTTGGCCTTTAGGACTTGGC	
AT1G12860		<i>ICE2.1 F</i>	CCAAGATCAGCAAAATGGATAGAGC		
AT1G12860		<i>ICE2.1 & 3 R</i>	CAAGCTTGAAGAACTCGGTGG		
AT1G12860		<i>ICE2.3 F</i>	GGTTGCAAATGTAGATGGATAGAGC		
AT1G12860		<i>ICE2.1 & 3 R</i>	CAAGCTTGAAGAACTCGGTGG		

2.3.5 References

- An C, Mou Z** (2011) Salicylic acid and its function in plant immunity. *J Integr Plant Biol* **53**: 412–428
- Baillo EH, Kimotho RN, Zhang Z, Xu P** (2019) **Transcription Factors Associated with Abiotic and Biotic Stress Tolerance and Their Potential for Crops Improvement.** *Genes (Basel)*. doi: [10.3390/genes10100771](https://doi.org/10.3390/genes10100771)
- Bardou F, Ariel F, Simpson CG, Romero-Barrios N, Laporte P, Balzergue S, Brown JWS, Crespi M** (2014) Long noncoding RNA modulates alternative splicing regulators in Arabidopsis. *Dev Cell* **30**: 166–176
- Bolt S, Zuther E, Zintl S, Hinch DK, Schmülling T** (2017) ERF105 is a transcription factor gene of Arabidopsis thaliana required for freezing tolerance and cold acclimation. *Plant Cell Environ* **40**: 108–120
- Bostock RM, Pye MF, Roubtsova T V** (2014) Predisposition in Plant Disease: Exploiting the Nexus in Abiotic and Biotic Stress Perception and Response. *Annu Rev Phytopathol* **52**: 517–549
- Calixto CPG, Guo W, James AB, Tzioutziou NA, Entizne JC, Panter PE, Knight H, Nimmo HG, Zhang R, Brown JWS** (2018) Rapid and Dynamic Alternative Splicing Impacts the Arabidopsis Cold Response Transcriptome. *Plant Cell* **30**: 1424 LP-1444
- Cao S, Ye M, Jiang S** (2005) Involvement of GIGANTEA gene in the regulation of the cold stress response in Arabidopsis. *Plant Cell Rep* **24**: 683–690
- Chang C-Y, Lin W-D, Tu S-L** (2014) Genome-Wide Analysis of Heat-Sensitive Alternative Splicing in *Physcomitrella patens*; *Plant Physiol* **165**: 826 LP-840
- Chen H-Y, Hsieh E-J, Cheng M-C, Chen C-Y, Hwang S-Y, Lin T-P** (2016) ORA47 (octadecanoid-responsive AP2/ERF-domain transcription factor 47) regulates jasmonic acid and abscisic acid biosynthesis and signaling through binding to a novel cis-element. *New Phytol* **211**: 599–613
- Cheng C, Wang Z, Yuan B, Li X** (2017) RBM25 Mediates Abiotic Responses in Plants. *Front Plant Sci* **8**: 292
- Dutertre M, Sanchez G, Barbier J, Corcos L, Auboeuf D** (2011) The emerging role of pre-messenger RNA splicing in stress responses: sending alternative messages and silent messengers. *RNA Biol* **8**: 740–747
- Fowler S, Thomashow MF** (2002) Arabidopsis transcriptome profiling indicates that multiple regulatory pathways are activated during cold acclimation in addition to the CBF cold response pathway. *Plant Cell* **14**: 1675–1690
- Fujikake N, Nagai Y, Popiel HA, Kano H, Yamaguchi M, Toda T** (2005) Alternative splicing regulates the transcriptional activity of Drosophila heat shock transcription factor in response to heat/cold stress. *FEBS Lett* **579**: 3842–3848
- Gilmour SJ, Fowler SG, Thomashow MF** (2004) Arabidopsis transcriptional activators CBF1, CBF2, and CBF3 have matching functional activities. *Plant Mol Biol* **54**: 767–781
- Guan Q, Wu J, Zhang Y, Jiang C, Liu R, Chai C, Zhu J** (2013) A DEAD box RNA helicase is critical for pre-mRNA splicing, cold-responsive gene regulation, and cold tolerance in Arabidopsis. *Plant Cell* **25**: 342–356

- Huot B, Castroverde CDM, Velásquez AC, Hubbard E, Pulman JA, Yao J, Childs KL, Tsuda K, Montgomery BL, He SY** (2017) Dual impact of elevated temperature on plant defence and bacterial virulence in *Arabidopsis*. *Nat Commun* **8**: 1808
- Kim J, Jung H, Lee H, Kim K, Goh C-H, Woo Y, Oh S, Han Y, Kang H** (2008) Glycine-rich RNA-binding protein 7 affects abiotic stress responses by regulating stomata opening and closing in *Arabidopsis thaliana*. *Plant J* **55**: 455–466
- Kim G-D, Cho Y-H, Lee B-H, Yoo S-D** (2017) STABILIZED1 Modulates Pre-mRNA Splicing for Thermotolerance. *Plant Physiol* **173**: 2370 LP-2382
- Kim G-D, Yoo S-D, Cho Y-H** (2018) STABILIZED1 as a heat stress-specific splicing factor in *Arabidopsis thaliana*. *Plant Signal Behav* **13**: e1432955
- Kim YS, Lee M, Lee J-H, Lee H-J, Park C-M** (2015) The unified ICE–CBF pathway provides a transcriptional feedback control of freezing tolerance during cold acclimation in *Arabidopsis*. *Plant Mol Biol* **89**: 187–201
- Kindgren P, Ard R, Ivanov M, Marquardt S** (2018) Transcriptional read-through of the long non-coding RNA SVALKKA governs plant cold acclimation. *Nat Commun* **9**: 4561
- Kosová K, Prášil IT, Vítámvás P, Dobrev P, Motyka V, Floková K, Novák O, Turečková V, Rolčík J, Pešek B, et al** (2012) Complex phytohormone responses during the cold acclimation of two wheat cultivars differing in cold tolerance, winter Samanta and spring Sandra. *J Plant Physiol* **169**: 567–576
- Lal SV, Brahma B, Gohain M, Mohanta D, De BC, Chopra M, Dass G, Vats A, Upadhyay RC, Datta TK, et al** (2015) Splice variants and seasonal expression of buffalo HSF genes. *Cell Stress Chaperones* **20**: 545–554
- Landi M, Tattini M, Gould KS** (2015) Multiple functional roles of anthocyanins in plant-environment interactions. *Environ Exp Bot* **119**: 4–17
- Lee B, Kapoor A, Zhu J, Zhu J-K** (2006) STABILIZED1, a stress-upregulated nuclear protein, is required for pre-mRNA splicing, mRNA turnover, and stress tolerance in *Arabidopsis*. *Plant Cell* **18**: 1736–1749
- Li Z, Liu H, Ding Z, Yan J, Yu H, Pan R, Hu J, Guan Y, Hua J** (2020) Low Temperature Enhances Plant Immunity via Salicylic Acid Pathway Genes That Are Repressed by Ethylene. *Plant Physiol* **182**: 626–639
- Ling Y, Serrano N, Gao G, Atia M, Mokhtar M, Woo YH, Bazin J, Veluchamy A, Benhamed M, Crespi M, et al** (2018) Thermopriming triggers splicing memory in *Arabidopsis*. *J Exp Bot* **69**: 2659–2675
- Liu F, Marquardt S, Lister C, Swiezewski S, Dean C** (2010) Targeted 3' processing of antisense transcripts triggers *Arabidopsis* FLC chromatin silencing. *Science* **327**: 94–97
- Liu H-C, Liao H-T, Charng Y-Y** (2011) The role of class A1 heat shock factors (HSFA1s) in response to heat and other stresses in *Arabidopsis*. *Plant Cell Environ* **34**: 738–751
- Liu Y, Dang P, Liu L, He C** (2019) Cold acclimation by the CBF–COR pathway in a changing climate: Lessons from *Arabidopsis thaliana*. *Plant Cell Rep* **38**: 511–519

- Nakabayashi R, Yonekura-Sakakibara K, Urano K, Suzuki M, Yamada Y, Nishizawa T, Matsuda F, Kojima M, Sakakibara H, Shinozaki K, et al** (2014) Enhancement of oxidative and drought tolerance in *Arabidopsis* by overaccumulation of antioxidant flavonoids. *Plant J* **77**: 367–379
- Pound MP, French AP, Atkinson JA, Wells DM, Bennett MJ, Pridmore T** (2013) RootNav: navigating images of complex root architectures. *Plant Physiol* **162**: 1802–1814
- Rigo R, Bazin J, Romero-Barrios N, Moison M, Lucero L, Christ A, Benhamed M, Blein T, Huguet S, Charon C, et al** (2020) The *Arabidopsis* lncRNA ASCO modulates the transcriptome through interaction with splicing factors. *EMBO Rep* **21**: e48977
- Romero-Barrios N** (2016) Non-coding RNAs, regulators of gene expression in *Arabidopsis thaliana* root developmental plasticity.
- Saleem M, Fariduddin Q, Janda T** (2020) Multifaceted Role of Salicylic Acid in Combating Cold Stress in Plants: A Review. *J Plant Growth Regul.* doi: 10.1007/s00344-020-10152-x
- Schulz E, Tohge T, Zuther E, Fernie AR, Hinch DK** (2016) Flavonoids are determinants of freezing tolerance and cold acclimation in *Arabidopsis thaliana*. *Sci Rep* **6**: 34027
- Scott IM, Clarke SM, Wood JE, Mur LAJ** (2004) Salicylate Accumulation Inhibits Growth at Chilling Temperature in *Arabidopsis*. *Plant Physiol* **135**: 1040 LP-1049
- Shan X, Zhang Y, Peng W, Wang Z, Xie D** (2009) Molecular mechanism for jasmonate-induction of anthocyanin accumulation in *Arabidopsis*. *J Exp Bot* **60**: 3849–3860
- Shi Y, Manley JL** (2007) A complex signaling pathway regulates SRp38 phosphorylation and pre-mRNA splicing in response to heat shock. *Mol Cell* **28**: 79–90
- Shin C, Feng Y, Manley JL** (2004) Dephosphorylated SRp38 acts as a splicing repressor in response to heat shock. *Nature* **427**: 553–558
- Shukla RR, Dominski Z, Zwierzynski T, Kole R** (1990) Inactivation of splicing factors in HeLa cells subjected to heat shock. *J Biol Chem* **265**: 20377–20383
- Tang K, Zhao L, Ren Y, Yang S, Zhu J-K, Zhao C** (2020) The transcription factor ICE1 functions in cold stress response by binding to the promoters of CBF and COR genes. *J Integr Plant Biol* **62**: 258–263
- Theocharis A, Clément C, Barka EA** (2012) Physiological and molecular changes in plants grown at low temperatures. *Planta* **235**: 1091–1105
- Thomashow MF** (1999) PLANT COLD ACCLIMATION: Freezing Tolerance Genes and Regulatory Mechanisms. *Annu Rev Plant Physiol Plant Mol Biol* **50**: 571–599
- Venegas-Molina J, Proietti S, Pollier J, Orozco-Freire W, Ramirez-Villacis D, Leon-Reyes A** (2020) Induced tolerance to abiotic and biotic stresses of broccoli and *Arabidopsis* after treatment with elicitor molecules. *Sci Rep* **10**: 10319
- Verhage L, Severing EI, Bucher J, Lammers M, Busscher-Lange J, Bonnema G, Rodenburg N, Proveniers MCG, Angenent GC, Immink RGH** (2017) Splicing-related genes are alternatively spliced upon changes in ambient temperatures in plants. *PLoS One* **12**: e0172950
- Wang Y, Bao Z, Zhu Y, Hua J** (2009) Analysis of temperature modulation of plant defense against biotrophic microbes. *Mol Plant Microbe Interact* **22**: 498–506

- Wang A, Hu J, Gao C, Chen G, Wang B, Lin C, Song L, Ding Y, Zhou G** (2019) Genome-wide analysis of long non-coding RNAs unveils the regulatory roles in the heat tolerance of Chinese cabbage (*Brassica rapa ssp.chinensis*). *Sci Rep* **9**: 5002
- Winkel-Shirley B** (2002) Biosynthesis of flavonoids and effects of stress. *Curr Opin Plant Biol* **5**: 218–223
- Xiang D, Hu X, Zhang Y, Yin K** (2008) Over-Expression of ICE1 Gene in Transgenic Rice Improves Cold Tolerance. *Rice Sci* **15**: 173–178
- Xu S, Zhang Z, Jing B, Gannon P, Ding J, Xu F, Li X, Zhang Y** (2011) Transportin-SR is required for proper splicing of resistance genes and plant immunity. *PLoS Genet* **7**: e1002159
- Yang DH, Kwak KJ, Kim MK, Park SJ, Yang K-Y, Kang H** (2014) Expression of Arabidopsis glycine-rich RNA-binding protein AtGRP2 or AtGRP7 improves grain yield of rice (*Oryza sativa*) under drought stress conditions. *Plant Sci* **214**: 106–112
- Zhan X, Qian B, Cao F, Wu W, Yang L, Guan Q, Gu X, Wang P, Okusolubo TA, Dunn SL, et al** (2015) An Arabidopsis PWI and RRM motif-containing protein is critical for pre-mRNA splicing and ABA responses. *Nat Commun* **6**: 8139
- Zhang X-N, Shi Y, Powers JJ, Gowda NB, Zhang C, Ibrahim HMM, Ball HB, Chen SL, Lu H, Mount SM** (2017) Transcriptome analyses reveal SR45 to be a neutral splicing regulator and a suppressor of innate immunity in *Arabidopsis thaliana*. *BMC Genomics* **18**: 772
- Zhao C, Zhang Z, Xie S, Si T, Li Y, Zhu J-K** (2016) Mutational Evidence for the Critical Role of CBF Transcription Factors in Cold Acclimation in *Arabidopsis*. *Plant Physiol* **171**: 2744–2759

Conclusions and Perspectives

3.1 The NSR-ASCO complex, a novel player in the plant response to environment

Throughout this work, we showed that the splicing factors NSRs together with the lncRNA ASCO modulate the plant response to a varied range of stresses. Indeed, the phenotypic and molecular analyses of NSRs and ASCO depleted plants suggest these actors play a role during the response to both biotic and abiotic cues, which respectively activate distinct signaling pathways (Figure 20). When plants perceive adverse external conditions, one of their first molecular response consists of changes in their cellular level of calcium ion, the adjustment of membrane fluidity and the production of reactive oxygen species (ROS) (Gilroy et al., 2016; Choudhury et al., 2017). This ROS production is mainly allowed by NADPH oxidases (NOXs), major integrators of stresses (Wang et al., 2016b). After sensing the external stress via specific receptors, the signal is transduced via the activation of protein kinases or phosphatases, resulting in expression changes in downstream target genes. These transcriptome changes end up modulating a myriad of intracellular aspects, including the biosynthesis of phytohormones that control plant growth and defense (Sheikh et al., 2016; Akimoto-Tomiyama et al., 2018). Hence, we can wonder at which of these steps the NSR-ASCO complex intervenes and how it contributes to plant resilience to stresses. Interestingly, 6 NADP-binding genes (AT1G07440, AT1G20020, AT2G29290, AT2G29300, AT2G29310, and AT2G29340) were found to experience AS in RNAi-ASCO lines. The AS events identified in AT2G29290 were one of the most significant events described in ASCO suppressed lines and were validated by RT-PCR. This event adds a premature stop codon in the mRNA sequence of AT2G29290, leading to the formation of a truncated protein (Rigo et al., 2020). Therefore, one can imagine that such AS changes in these NADP-related genes could participate in the control of ROS cellular content. Thus, the quantitation of ROS molecules such as H₂O₂ or the measurement of total antioxidants in ASCO and NSR deregulated plants would shed light on the role of the NSR-ASCO complex in ROS homeostasis (Venkidasamy et al., 2020).

One of the major factor impacting ROS metabolism is the phytohormone balance, including auxin, ABA, ethylene, SA and JA (Bouchez et al., 2007; Zhang et al., 2009; Maruta

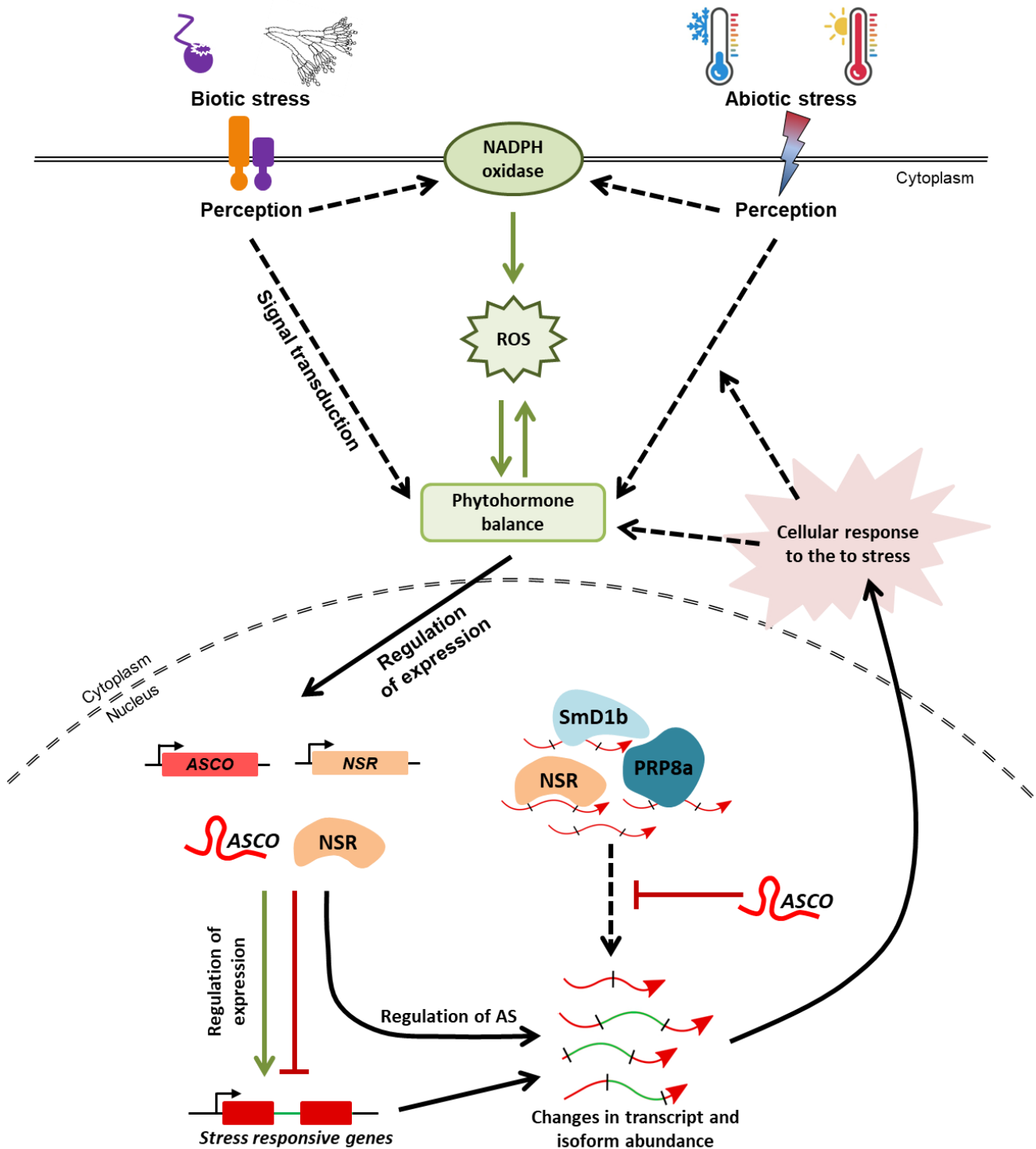


Figure 20. Integration of the NSR-ASCO complex in the plant response to stresses.

Plant cells perceive external stresses via specific receptors or modification of their integrity. Stress perception leads to the activation of distinct signaling pathways. The transduction of the signal provokes changes in ROS homeostasis and phytohormone balance of the plant. These changes further modulate the expression of NSR SFs and ASCO lncRNA, impacting the expression of a large subset of stress-responsive genes. Together with the core spliceosomal components PRP8a and SmD1b, NSRs modulate the splicing of specific transcripts. Their action on AS can be disturbed by their binding to ASCO. Finally, these changes in the transcriptome converge to the modification of cell features, allowing the proper establishment of plant resilience to the stress.

et al., 2011; Krishnamurthy and Rathinasabapathi, 2013; Han et al., 2013). Besides their impact on ROS homeostasis, phytohormones govern a plethora of cellular aspects, including the transcriptome (Ku et al., 2018). NSRs and ASCO were shown to regulate plant sensitivity to hormones such as auxin. Thus, the measurement of hormone contents in ASCO and NSRs deregulated lines subjected to distinct stresses would pinpoint which hormonal signalling pathways are impacted in these lines. Based on these results, crosses between ASCO / NSRs mutated lines and available mutants impaired in hormone signaling and/or biosynthesis could be performed, followed by the analysis of their phenotype. Taken altogether, these findings would permit to precise the position of the NSR-ASCO complex among specific signaling pathways and elucidate its biological role in the plant.

3.2 ASCO, a lncRNA interacting with the splicing machinery

ASCO is one of the few lncRNAs that were shown to modulate AS in plants. In Bardou et al. (2014), *in vitro* assays demonstrated that ASCO modulates the binding of AS targets to an NSR-containing complex, likely through target displacement. Hence, this lncRNA was proposed to act as an NSR competitor for binding to their AS targets. Here, our results show that ASCO also binds to the core spliceosomal proteins PRP8a and Smd1b (Rigo et al., 2020). Like for NSRs, ASCO can hijack PRP8a by altering its binding to pre-mRNA targets. Nevertheless, the exact molecular mechanism allowing this competition is still unknown. How does this hijacking occur and what are the features that are required for this process?

Each ASCO–SF interaction was demonstrated individually through directed RIP assays (Bardou et al., 2014; Rigo et al., 2020). But other techniques could be used in particular to analyze more deeply the interactions between these various SFs and decipher the way they regulate splicing. One could use coimmunoprecipitation (coIP), the most straightforward technique to study protein-protein interactions *in vivo* (Lee et al., 2007). Similarly, bimolecular fluorescence complementation (BiFC) analysis enables direct visualization of protein interactions in living cells (Kerppola et al., 2008). These experiments would provide clues about putative interactions between NSRs and the core spliceosomal proteins PRP8a and Smd1b, and their integration into larger RNP complexes. As NSRs modulate AS mainly in response to specific stimuli such as auxin, these methods would also be performed on plants subjected to various treatments (auxin, flg22, heat stress...) to investigate if these interactions undergo dynamic changes upon stress.

Another question that remains unanswered is the specificity of ASCO binding to SFs. Is ASCO sequence and/or structure directly recognized by its protein partners? A recent study described the importance of a U1-recognition site in lncRNAs which allows their tethering to chromatin by U1 snRNP (Yin et al., 2020). Hence, ASCO may display a similar motif that allows its binding to its protein partners. To investigate this hypothesis, different methods could be used including the individual-nucleotide resolution UV cross-linking and immunoprecipitation (iCLIP) assay. This method allows to identify protein–RNA crosslink sites on a genome-wide scale, allowing the identification of protein binding sites within RNA molecules (König et al., 2010; Meyer et al., 2017). This technique would also permit the identification of the RNA sequences interacting with NSRs, PRP8a or Smd1b genome-wide, and also characterize their potential relation with ASCO internal sequences. These may serve to further explore sequence specificities and complementarities between the lncRNA ASCO and the pre-mRNA targets of its protein partners.

Another technique that could be used to investigate ASCO-SF interactions is the trimolecular fluorescence complementation (TriFC) assay (Seo and Chua, 2019). This system combines conventional BiFC assay with the MS2 system that uses the phage MS2 coat protein (MCP) and its binding RNA sequence (MS2 sequence) to tag a specific lncRNA. ASCO protein partner and MCP would be tagged with YFP fragments, whereas the ASCO lncRNA would be tagged with 6xMS2 sequence, leading to its binding to MCP. Thus, if ASCO interacts with its protein partner, the 2 YFP fragments will be brought together leading to YFP activation. The DNA constructs encoding these fusion RNA and proteins would be infiltrated into tobacco leaves with *Agrobacterium* suspensions, and observed by confocal microscopy (Seo and Chua, 2019). This system would allow *in vivo* visualization of ASCO-protein interaction by transient expression in tobacco leaves.

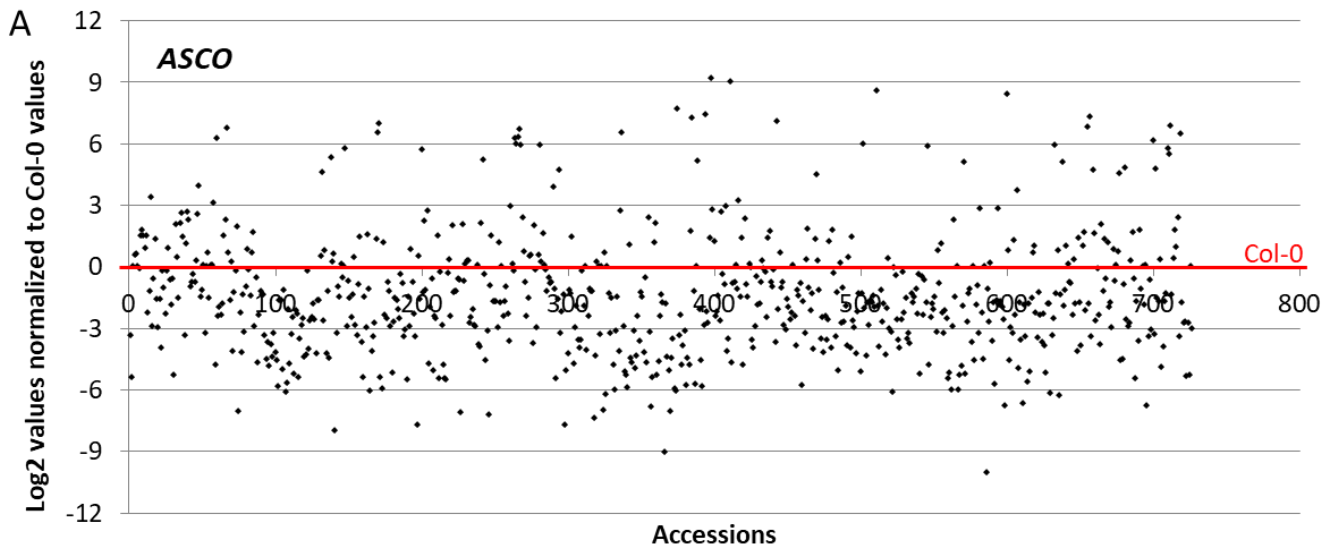
Based on RNAfold web analysis, ASCO was suggested to display a highly conserved stem-loop structure in the middle of its transcript (Romero-Barrios, 2016). Hence, the specificities in ASCO binding to proteins could also be driven by its structural features. In order to identify the potential secondary structures of ASCO and their associated protein interactions, the protein interaction profile sequencing (PIP-seq) assay could be used. This technique compares protein-depleted RNA samples treated with single- or double-strand-specific ribonucleases to infer RNA secondary structures. Further comparison with samples treated with the same nucleases in the presence of interacting proteins allows the identification of protected protein-bound sequences within the RNA molecules (Anderson et al., 2016; Kramer & Gregory, 2019). As ASCO and NSRs mainly intervene during the plant response to stresses, this technique could also be applied on stress-subjected plants in

comparison to control grown plants, in order to reveal stress-specific patterns of ASCO features.

3.3 The study of ASCO conservation, a key to understanding its role?

For now, the role of the lncRNA ASCO was only described in *A. thaliana*. Many studies demonstrated that species evolution and diversification is strongly influenced by non-coding RNAs. In chicken, the domestication traits that govern body morphology or behavior are often associated with lncRNA encoding genes and depend on specific single-nucleotide polymorphisms (SNPs) in these genes (Wang et al., 2017). Consistently, in plants, the comparison of SNPs associated with fruit development in two tomato cultivars also correspond to non-coding genomic regions (Scarano et al., 2017). Hence, investigating the conservation of ASCO sequence in other *Arabidopsis* ecotypes or species would be a powerful way to decipher which elements are necessary for its function. A preliminary search for ASCO homologs identified 9 additional copies of ASCO in *A. thaliana*. Moreover, ASCO related sequences were also found in other Brassicaceae species, including *A. halleri* and *A. lyrata*, and the more distant species *Capsella rubella* and *Capsella grandiflora* (Rigo et al., 2020). The thorough comparison of their sequences and putative secondary structures would provide additional data about conserved ASCO features, suggesting their importance in ASCO function.

Besides looking at the conservation of their sequence, the analysis of lncRNA expression variation among various species also provides evidence on their role and function. Thus, looking for ecotypes or species with deregulated ASCO expression levels would provide additional clues to understand how this lncRNA modulates the transcriptome. Preliminary studies using transcriptomic data from the 1001 Genome database demonstrate that ASCO expression is highly variable among *Arabidopsis* ecotypes (Figure 21A) (Kawakatsu et al., 2016; <http://signal.salk.edu/1001.php>; Rigo et al., unpublished results). Indeed, some ecotypes display no detectable expression whereas others express ASCO 500 times more than the Columbia-0 ecotype (Figures 21B and 21C). The phenotypic analysis of these “natural” ASCO null mutants or “natural” ASCO overexpressing ecotypes would help to understand to what extent this lncRNA participates in the acclimation of *Arabidopsis* to their local environment. In the end, the study of lncRNAs can also shed light on how species adapt to the adverse environmental conditions they face.



B

Accession number	Accession name	Normalized ASCO levels	Country
10010	Sij-4	116,47	Uzbekistan
7067	Ct-1	128,06	Italy
9594	IP-Vdm-0	153,50	Spain
9942	Agu-1	157,20	Spain
9606	Aitba-1	171,19	Morocco
9583	IP-Sne-0	209,50	Spain
9868	Moe-0	345,11	Spain
9759	Anz-0	389,34	Iran
9626	Kolyv-3	520,28	Russia
9610	Lesno-4	584,60	Russia

C

Accession number	Accession name	Normalized ASCO levels	Country
159	MAR2-3	0	France
9515	IP-Ala-0	0	Spain
9526	IP-Cab-3	0	Spain
9531	IP-Cdc-3	0	Spain
9597	IP-Vig-1	0	Spain
9827	Bos-0	0	Spain
9840	Dar-0	0	Spain
9851	Hue-3	0,00096	Spain
9574	IP-Rel-0	0,00187	Spain
6744	CSHL-5	0,00399	USA

Figure 21. ASCO exhibits highly variable expression among *Arabidopsis* ecotypes.

A. ASCO expression levels among accessions from the 1001 genomes database. Each accession value was normalized to Col-0 level, indicated by a red line.

B, C. Top 10 *Arabidopsis thaliana* accessions exhibiting respectively the highest (B) or lowest (C) ASCO levels. Expression levels are normalized to Col-0 values. The country of origin is indicated for each accession.

Data was obtained from Kawakatsu et al., 2016.

3.4 LncRNAs as a model for RNA therapeutics?

Here, we provided some hints on the way of action of a plant lncRNA involved in the modulation of AS. The complexity of lncRNA ways of action pinpoints their versatile roles in eukaryotic cells. The tremendous number of recently discovered eukaryotic lncRNAs illustrates the growing interest in the study of this class of non-coding RNAs. Moreover, their major role during many human diseases including viral infections exacerbates the need to investigate how lncRNAs function in the cell (Ginn et al., 2020). For example, lncRNAs were shown to play a role during the infection by Severe acute respiratory syndrome coronavirus 2 (SARS-CoV-2), a recently identified coronavirus that causes the respiratory disease known as coronavirus disease 2019 (COVID-19). Indeed, a subset of lncRNAs modulates gene expression during cytokine storms and antiviral responses caused by severe SARS-CoV-2 infection of the lung (Morenikeji et al., 2021; Mukherjee et al., 2021). Moreover, SARS-CoV-2 encodes various non-structural proteins that are required for its replication, including NSP16. Interestingly, this viral protein binds to the mRNA recognition domains of the U1 and U2 RNA components of the spliceosome, suppressing global mRNA splicing in SARS-CoV-2-infected human cells (Banerjee et al., 2020). As a large subset of lncRNAs bind to the U1 snRNP as well, the investigation of their role in this virus-induced splicing defects would provide exciting tracks for counteracting the virus progression in cells. Thus, lncRNAs may appear as putative pharmacological targets or potential drug candidates in viral diseases (Chen et al., 2021).

RNA therapeutics are a class of medications based on the use of antisense RNAs, RNA interference or coding mRNAs (Dammes and Peer, 2020). One of the most recent examples of RNA therapeutics are the mRNA vaccines that have been developed for combating COVID-19 (Polack et al., 2020). Nevertheless, the extensive use of RNAi interference has shown that this conserved mechanism is a powerful tool to modulate transcript abundance in both animals and plants (Zeng et al., 2019). Hence, further understanding of RNA-mediated mechanisms will increase the use and success rate of RNA therapeutics. Since non-coding RNAs exert their roles as RNA molecules in the cells, the investigation of their associated molecular mechanisms offers new ways to regulate cellular processes.

References

- Akimoto-Tomiyama C, Tanabe S, Kajiwara H, Minami E, Ochiai H** (2018) Loss of chloroplast-localized protein phosphatase 2Cs in *Arabidopsis thaliana* leads to enhancement of plant immunity and resistance to *Xanthomonas campestris* pv. *campestris* infection. *Mol Plant Pathol* **19**: 1184–1195
- Anderson SJ, Willmann MR, Gregory BD** (2016) Protein Interaction Profile Sequencing (PIP-seq) in Plants. *Curr Protoc Plant Biol* **1**: 163–183
- Ariel F, Jegu T, Latrasse D, Romero-Barrios N, Christ A, Benhamed M, Crespi M** (2014) Noncoding transcription by alternative rna polymerases dynamically regulates an auxin-driven chromatin loop. *Mol Cell* **55**: 383–396
- Ariel F, Romero-Barrios N, Jégú T, Benhamed M, Crespi M** (2015) Battles and hijacks: Noncoding transcription in plants. *Trends Plant Sci* **20**: 362–371
- Ariel F, Crespi M** (2017) Alternative splicing: The lord of the rings. *Nat Plants* **3**: 1–2
- Ariel F, Lucero L, Christ A, Mammarella MF, Jegu T, Veluchamy A, Mariappan K, Latrasse D, Blein T, Liu C, et al** (2020) R-Loop Mediated trans Action of the APOLO Long Noncoding RNA. *Mol Cell* **77**: 1055–1065.e4
- Asad S, Fang Y, Wycoff KL, Hirsch AM** (1994) Isolation and characterization of cDNA and genomic clones of MsENOD40; transcripts are detected in meristematic cells of alfalfa. *Protoplasma* **183**: 10–23
- Banerjee AK, Blanco MR, Bruce EA, Honson DD, Chen LM, Chow A, Bhat P, Ollikainen N, Quinodoz SA, Loney C, et al** (2020) SARS-CoV-2 Disrupts Splicing, Translation, and Protein Trafficking to Suppress Host Defenses. *Cell* **183**: 1325–1339.e21
- Barbosa-Morais NL, Irimia M, Pan Q, Xiong HY, Gueroussov S, Lee LJ, Slobodeniuc V, Kutter C, Watt S, Çolak R, et al** (2012) The evolutionary landscape of alternative splicing in vertebrate species. *Science (80-)* **338**: 1587–1593
- Bardou F, Ariel F, Simpson CG, Romero-Barrios N, Laporte P, Balzergue S, Brown JWS, Crespi M** (2014) Long Noncoding RNA Modulates Alternative Splicing Regulators in *Arabidopsis*. *Dev Cell* **30**: 166–176
- Barta A, Kalyna M, Lorković ZJ** (2008) Plant SR proteins and their functions. *Curr Top Microbiol Immunol* **326**: 83–102
- Bartels C, Klatt C, Lührmann R, Fabrizio P** (2002) The ribosomal translocase homologue Snu114p is involved in unwinding U4/U6 RNA during activation of the spliceosome. *EMBO Rep* **3**: 875–880
- Bazin J, Baerenfaller K, Gosai SJ, Gregory BD, Crespi M, Bailey-Serres J** (2017) Global analysis of ribosome-associated noncoding RNAs unveils new modes of translational regulation. *Proc Natl Acad Sci U S A* **114**: E10018–E10027
- Bedre R, Irigoyen S, Schaker PDC, Monteiro-Vitorello CB, Da Silva JA, Mandadi KK** (2019) Genome-wide alternative splicing landscapes modulated by biotrophic sugarcane smut pathogen. *Sci Rep* **9**: 1–12

- Beltran M, Puig I, Peña C, García JM, Álvarez AB, Peña R, Bonilla F, De Herreros AG** (2008) A natural antisense transcript regulates Zeb2/Sip1 gene expression during Snail1-induced epithelial-mesenchymal transition. *Genes Dev* **22**: 756–769
- Ben Amor B, Wirth S, Merchan F, Laporte P, D'Aubenton-Carafa Y, Hirsch J, Maizel A, Mallory A, Lucas A, Deragon JM, et al** (2009) Novel long non-protein coding RNAs involved in Arabidopsis differentiation and stress responses. *Genome Res* **19**: 57–69
- Berget SM, Moore C, Sharp PA** (1977) Spliced segments at the 5' terminus of adenovirus 2 late mRNA. *Proc Natl Acad Sci U S A* **74**: 3171–3175
- Bernard D, Prasanth K V., Tripathi V, Colasse S, Nakamura T, Xuan Z, Zhang MQ, Sedel F, Jourdren L, Culpier F, et al** (2010) A long nuclear-retained non-coding RNA regulates synaptogenesis by modulating gene expression. *EMBO J* **29**: 3082–3093
- Bernstein HD, Zopf D, Freymann DM, Walter P** (1993) Functional substitution of the signal recognition particle 54-kDa subunit by its Escherichia coli homolog. *Proc. Natl. Acad. Sci. U. S. A. Proc Natl Acad Sci U S A*, pp 5229–5233
- Bhatia G, Goyal N, Sharma S, Upadhyay SK, Singh K** (2017) Present Scenario of Long Non-Coding RNAs in Plants. *Non-coding RNA*. doi: 10.3390/ncrna3020016
- Bjellqvist B, Basse B, Olsen E, Celis JE** (1994) Reference points for comparisons of two-dimensional maps of proteins from different human cell types defined in a pH scale where isoelectric points correlate with polypeptide compositions. *Electrophoresis* **15**: 529–539
- Bouchez O, Huard C, Lorrain S, Roby D, Balagué C** (2007) Ethylene is one of the key elements for cell death and defense response control in the Arabidopsis lesion mimic mutant vad1. *Plant Physiol* **145**: 465–477
- Bourgeois CF, Lejeune F, Stévenin J** (2004) Broad Specificity of SR (Serine{plus 45 degree rule}Arginine) Proteins in the Regulation of Alternative Splicing of Pre-Messenger RNA. *Prog Nucleic Acid Res Mol Biol* **78**: 37–88
- Brosnan CA, Voinnet O** (2009) The long and the short of noncoding RNAs. *Curr Opin Cell Biol* **21**: 416–425
- Calixto CPG, Guo W, James AB, Tzioutziou NA, Entizne JC, Panter PE, Knight H, Nimmo HG, Zhang R, Brown JWS** (2018) Rapid and dynamic alternative splicing impacts the arabidopsis cold response transcriptome[CC-BY]. *Plant Cell* **30**: 1424–1444
- Calixto CPG, Tzioutziou NA, James AB, Hornyik C, Guo W, Zhang R, Nimmo HG, Brown JWS** (2019) Cold-dependent expression and alternative splicing of arabidopsis long non-coding RNAs. *Front Plant Sci*. doi: 10.3389/fpls.2019.00235
- Campalans A, Kondorosi A, Crespi M** (2004) Enod40, a short open reading frame-containing mRNA, induces cytoplasmic localization of a nuclear RNA binding protein in *Medicago truncatula*. *Plant Cell* **16**: 1047–1059
- Carlevaro-Fita J, Johnson R** (2019) Global Positioning System: Understanding Long Noncoding RNAs through Subcellular Localization. *Mol Cell* **73**: 869–883
- Carlevaro-Fita J, Lanzós A, Feuerbach L, Hong C, Mas-Ponte D, Pedersen JS, Abascal F, Amin SB, Bader GD, Barenboim J, et al** (2020) Cancer LncRNA Census reveals evidence for deep functional conservation of long noncoding RNAs in tumorigenesis. *Commun Biol* **3**: 1–16

- Carvalho RF, Carvalho SD, Duque P** (2010) The Plant-Specific SR45 protein negatively regulates glucose and ABA signaling during early seedling development in arabidopsis. *Plant Physiol* **154**: 772–783
- Chan SP, Cheng SC** (2005) The Prp19-associated complex is required for specifying interactions of U5 and U6 with pre-mRNA during spliceosome activation. *J Biol Chem* **280**: 31190–31199
- Charng YY, Liu HC, Liu NY, Hsu FC, Ko SS** (2006) Arabidopsis Hsa32, a novel heat shock protein, is essential for acquired thermotolerance during long recovery after acclimation. *Plant Physiol* **140**: 1297–1305
- Charng YY, Liu HC, Liu NY, Chi WT, Wang CN, Chang SH, Wang TT** (2007) A heat-inducible transcription factor, HsfA2, is required for extension of acquired thermotolerance in Arabidopsis. *Plant Physiol* **143**: 251–262
- Charon C, Sousa C, Crespi M, Kondorosi A** (1999) Alteration of enod40 expression modifies *Medicago truncatula* root nodule development induced by *Sinorhizobium meliloti*. *Plant Cell* **11**: 1953–1965
- Chaudhary S, Khokhar W, Jabre I, Reddy ASN, Byrne LJ, Wilson CM, Syed NH** (2019) Alternative splicing and protein diversity: Plants versus animals. *Front Plant Sci* **10**: 708
- Chen LL** (2016) The biogenesis and emerging roles of circular RNAs. *Nat Rev Mol Cell Biol* **17**: 205–211
- Chen L, Zhu QH, Kaufmann K** (2020) Long non-coding RNAs in plants: emerging modulators of gene activity in development and stress responses. *Planta* **252**: 92
- Chen Y, Li Z, Chen X, Zhang S** (2021) Long non-coding RNAs: From disease code to drug role. *Acta Pharm Sin B* **11**: 340–354
- Choudhury FK, Rivero RM, Blumwald E, Mittler R** (2017) Reactive oxygen species, abiotic stress and stress combination. *Plant J* **90**: 856–867
- Chow LT, Gelinas RE, Broker TR, Roberts RJ** (1977) An amazing sequence arrangement at the 5' ends of adenovirus 2 messenger RNA. *Cell* **12**: 1–8
- Clark MB, Johnston RL, Inostroza-Ponta M, Fox AH, Fortini E, Moscato P, Dinger ME, Mattick JS** (2012) Genome-wide analysis of long noncoding RNA stability. *Genome Res* **22**: 885–898
- Compaan B, Yang WC, Bisseling T, Franssen H** (2001) ENOD40 expression in the pericycle precedes cortical cell division in rhizobium-legume interaction and the highly conserved internal region of the gene does not encode a peptide. *Plant Soil*. Springer, pp 1–8
- Conn VM, Hugouvieux V, Nayak A, Conos SA, Capovilla G, Cildir G, Jourdain A, Tergaonkar V, Schmid M, Zubieta C, et al** (2017) A circRNA from SEPALLATA3 regulates splicing of its cognate mRNA through R-loop formation. *Nat Plants*. doi: 10.1038/nplants.2017.53
- Cooper DR, Carter G, Li P, Patel R, Watson JE, Patel NA** (2014) Long non-coding RNA NEAT1 associates with SRp40 to temporally regulate PPAR γ 2 splicing during adipogenesis in 3T3-L1 cells. *Genes (Basel)* **5**: 1050–1063
- Crespi MD, Jurkevitch E, Poiret M, D'Aubenton-Carafa Y, Petrovics G, Kondorosi E, Kondorosi A** (1994) Enod40, a gene expressed during nodule organogenesis, codes for a non-translatable RNA involved in plant growth. *EMBO J* **13**: 5099–5112

- Dammes N, Peer D** (2020) Paving the Road for RNA Therapeutics. *Trends Pharmacol Sci* **41**: 755–775
- Deng P, Liu S, Nie X, Weining S, Wu L** (2018) Conservation analysis of long non-coding RNAs in plants. *Sci China Life Sci* **61**: 190–198
- Derrien T, Johnson R, Bussotti G, Tanzer A, Djebali S, Tilgner H, Guernec G, Martin D, Merkel A, Knowles DG, et al** (2012) The GENCODE v7 catalog of human long noncoding RNAs: Analysis of their gene structure, evolution, and expression. *Genome Res* **22**: 1775–1789
- Deshpande S, Shuttleworth J, Yang J, Taramonli S, England M** (2019) PLIT: An alignment-free computational tool for identification of long non-coding RNAs in plant transcriptomic datasets. *Comput Biol Med* **105**: 169–181
- Diederichs S** (2014) The four dimensions of noncoding RNA conservation. *Trends Genet* **30**: 121–123
- Ding J, Lu Q, Ouyang Y, Mao H, Zhang P, Yao J, Xu C, Li X, Xiao J, Zhang Q** (2012) A long noncoding RNA regulates photoperiod-sensitive male sterility, an essential component of hybrid rice. *Proc Natl Acad Sci U S A* **109**: 2654–2659
- Djebali S, Davis CA, Merkel A, Dobin A, Lassmann T, Mortazavi A, Tanzer A, Lagarde J, Lin W, Schlesinger F, et al** (2012) Landscape of transcription in human cells. *Nature* **489**: 101–108
- Duque P** (2011) A role for SR proteins in plant stress responses. *Plant Signal Behav* **6**: 49–54
- Eddy SR** (2012) The C-value paradox, junk DNA and ENCODE. *Curr Biol*. doi: 10.1016/j.cub.2012.10.002
- Elvira-Matelot E, Bardou F, Ariel F, Jauvion V, Bouteiller N, Le Masson I, Cao J, Crespi MD, Vaucheret H** (2015) The nuclear ribonucleoprotein SmD1 interplays with splicing, RNA quality control, and posttranscriptional gene silencing in arabidopsisopen. *Plant Cell* **28**: 426–438
- Fabbri M, Girnita L, Varani G, Calin GA** (2019) Decrypting noncoding RNA interactions, structures, and functional networks. *Genome Res* **29**: 1377–1388
- Fabrizio P, Dannenberg J, Dube P, Kastner B, Stark H, Urlaub H, Lührmann R** (2009) The Evolutionarily Conserved Core Design of the Catalytic Activation Step of the Yeast Spliceosome. *Mol Cell* **36**: 593–608
- Fan Y, Yang J, Mathioni SM, Yu J, Shen J, Yang X, Wang L, Zhang Q, Cai Z, Xu C, et al** (2016) PMS1T, producing Phased small-interfering RNAs, regulates photoperiod-sensitive male sterility in rice. *Proc Natl Acad Sci U S A* **113**: 15144–15149
- Fang Y, Xie K, Xiong L** (2014) Conserved miR164-targeted NAC genes negatively regulate drought resistance in rice. *J Exp Bot* **65**: 2119–2135
- Fang J, Zhang F, Wang H, Wang W, Zhao F, Li Z, Sun C, Chen F, Xu F, Chang S, et al** (2019) Efc locus shortens rice maturity duration without yield penalty. *Proc Natl Acad Sci U S A* **116**: 18717–18722
- Fanucchi S, Fok ET, Dalla E, Shibayama Y, Börner K, Chang EY, Stoychev S, Imakaev M, Grimm D, Wang KC, et al** (2019) Immune genes are primed for robust transcription by proximal long noncoding RNAs located in nuclear compartments. *Nat Genet* **51**: 138–150

- Fickett JW** (1982) Recognition of protein coding regions in DNA sequences. *Nucleic Acids Res* **10**: 5303–5318
- Flynn RA, Chang HY** (2012) Active chromatin and noncoding RNAs: An intimate relationship. *Curr Opin Genet Dev* **22**: 172–178
- Fonouni-Farde C, Ariel F, Crespi M** (2021) Plant Long Noncoding RNAs: New Players in the Field of Post-Transcriptional Regulations. *Non-Coding RNA* **7**: 12
- Franco-Zorrilla JM, Valli A, Todesco M, Mateos I, Puga MI, Rubio-Somoza I, Leyva A, Weigel D, García JA, Paz-Ares J** (2007) Target mimicry provides a new mechanism for regulation of microRNA activity. *Nat Genet* **39**: 1033–1037
- Gao R, Liu P, Irwanto N, Loh DR, Wong SM** (2016) Upregulation of LINC-AP2 is negatively correlated with AP2 gene expression with Turnip crinkle virus infection in *Arabidopsis thaliana*. *Plant Cell Rep* **35**: 2257–2267
- Gibilisco L, Zhou Q, Mahajan S, Bachtrog D** (2016) Alternative Splicing within and between *Drosophila* Species, Sexes, Tissues, and Developmental Stages. *PLoS Genet*. doi: 10.1371/journal.pgen.1006464
- Gilroy S, Białasek M, Suzuki N, Górecka M, Devireddy AR, Karpiński S, Mittler R** (2016) ROS, calcium, and electric signals: Key mediators of rapid systemic signaling in plants. *Plant Physiol* **171**: 1606–1615
- Ginn L, La Montagna M, Wu Q, Shi L** (2020) Diverse roles of long non-coding RNAs in viral diseases. *Rev Med Virol*. doi: 10.1002/rmv.2198
- Goff LA, Rinn JL** (2015) Linking RNA biology to lncRNAs. *Genome Res* **25**: 1456–1465
- Golisz A, Sikorski PJ, Kruszka K, Kufel J** (2013) *Arabidopsis thaliana* LSM proteins function in mRNA splicing and degradation. *Nucleic Acids Res* **41**: 6232–6249
- Gonzalez I, Munita R, Agirre E, Dittmer TA, Gysling K, Misteli T, Luco RF** (2015) A lncRNA regulates alternative splicing via establishment of a splicing-specific chromatin signature. *Nat Struct Mol Biol* **22**: 370–376
- Graveley BR, Hertel KJ, Maniatis T** (1999) SR proteins are “locators” of the RNA splicing machinery. *Curr Biol*. doi: 10.1016/s0960-9822(99)80032-3
- Graveley BR** (2000) Sorting out the complexity of SR protein functions. *RNA* **6**: 1197–1211
- Guttman M, Amit I, Garber M, French C, Lin MF, Feldser D, Huarte M, Zuk O, Carey BW, Cassady JP, et al** (2009) Chromatin signature reveals over a thousand highly conserved large non-coding RNAs in mammals. *Nature* **458**: 223–227
- Han Y, Chaouch S, Mhamdi A, Queval G, Zechmann B, Noctor G** (2013) Functional analysis of *Arabidopsis* mutants points to novel roles for glutathione in coupling H₂O₂ to activation of salicylic acid accumulation and signaling. *Antioxidants Redox Signal* **18**: 2106–2121
- Hawkes EJ, Hennelly SP, Novikova I V., Irwin JA, Dean C, Sanbonmatsu KY** (2016) COOLAIR Antisense RNAs Form Evolutionarily Conserved Elaborate Secondary Structures. *Cell Rep* **16**: 3087–3096

- He X, Pool M, Darcy KM, Lim SB, Auersperg N, Coon JS, Beck WT** (2007) Knockdown of polypyrimidine tract-binding protein suppresses ovarian tumor cell growth and invasiveness in vitro. *Oncogene* **26**: 4961–4968
- He RZ, Jiang J, Luo DX** (2020) The functions of N6-methyladenosine modification in lncRNAs. *Genes Dis* **7**: 598–605
- Helder S, Blythe AJ, Bond CS, Mackay JP** (2016) Determinants of affinity and specificity in RNA-binding proteins. *Curr Opin Struct Biol* **38**: 83–91
- Herold N, Will CL, Wolf E, Kastner B, Urlaub H, Lührmann R** (2009) Conservation of the Protein Composition and Electron Microscopy Structure of *Drosophila melanogaster* and Human Spliceosomal Complexes. *Mol Cell Biol* **29**: 281–301
- Hisanaga T, Okahashi K, Yamaoka S, Kajiwara T, Nishihama R, Shimamura M, Yamato KT, Bowman JL, Kohchi T, Nakajima K** (2019) A cis-acting bidirectional transcription switch controls sexual dimorphism in the liverwort. *EMBO J*. doi: 10.15252/embj.2018100240
- Houseley J, Rubbi L, Grunstein M, Tollervey D, Vogelauer M** (2008) A ncRNA Modulates Histone Modification and mRNA Induction in the Yeast GAL Gene Cluster. *Mol Cell* **32**: 685–695
- Huarte M** (2015) The emerging role of lncRNAs in cancer. *Nat Med* **21**: 1253–1261
- Hutchinson JN, Ensminger AW, Clemson CM, Lynch CR, Lawrence JB, Chess A** (2007) A screen for nuclear transcripts identifies two linked noncoding RNAs associated with SC35 splicing domains. *BMC Genomics*. doi: 10.1186/1471-2164-8-39
- Ibrahim HMM, Kusch S, Didelon M, Raffaele S** (2021) Genome-wide alternative splicing profiling in the fungal plant pathogen *Sclerotinia sclerotiorum* during the colonization of diverse host families. *Mol Plant Pathol* **22**: 31–47
- Iñiguez LP, Hernández G** (2017) The Evolutionary Relationship between Alternative Splicing and Gene Duplication. *Front Genet* **08**: 14
- Islam MR, Feng B, Chen T, Tao L, Fu G** (2018) Role of Abscisic Acid in Thermal Acclimation of Plants. *J Plant Biol* **61**: 255–264
- Izawa T** (2021) What is going on with the hormonal control of flowering in plants? *Plant J* **105**: 431–445
- Jen CH, Michalopoulos I, Westhead DR, Meyer P** (2005) Natural antisense transcripts with coding capacity in *Arabidopsis* may have a regulatory role that is not linked to double-stranded RNA degradation. *Genome Biol* **6**: R51
- Jha UC, Nayyar H, Jha R, Khurshid M, Zhou M, Mantri N, Siddique KHM** (2020) Long non-coding RNAs: Emerging players regulating plant abiotic stress response and adaptation. *BMC Plant Biol*. doi: 10.1186/s12870-020-02595-x
- Ji Q, Zhang L, Liu X, Zhou L, Wang W, Han Z, Sui H, Tang Y, Wang Y, Liu N, et al** (2014) Long non-coding RNA MALAT1 promotes tumour growth and metastasis in colorectal cancer through binding to SFPQ and releasing oncogene PTBP2 from SFPQ/PTBP2 complex. *Br J Cancer* **111**: 736–748
- Jiang K, Patel NA, Watson JE, Apostolatos H, Kleiman E, Hanson O, Hagiwara M, Cooper DR** (2009) Akt2 regulation of Cdc2-like kinases (Clk/Sty), serine/arginine-rich (SR) protein

- phosphorylation, and insulin-induced alternative splicing of PKC β III messenger ribonucleic acid. *Endocrinology* **150**: 2087–2097
- Jones AM** (2016) A new look at stress: Abscisic acid patterns and dynamics at high-resolution. *New Phytol* **210**: 38–44
- Kang YJ, Yang DC, Kong L, Hou M, Meng YQ, Wei L, Gao G** (2017) CPC2: A fast and accurate coding potential calculator based on sequence intrinsic features. *Nucleic Acids Res* **45**: W12–W16
- Kanno T, Venhuizen P, Wu MT, Chiou P, Chang CL, Kalyna M, Matzke AJM, Matzke M** (2020) A collection of pre-mRNA splicing mutants in *Arabidopsis thaliana*. *G3 Genes, Genomes, Genet* **10**: 1983–1996
- Karakulah G, Unver T** (2017) Barley long non-coding RNAs and their tissue-specific co-expression pattern with coding-transcripts. *bioRxiv* 229559
- Karner H, Webb CH, Carmona S, Liu Y, Lin B, Erhard M, Chan D, Baldi P, Spitale RC, Sun S** (2020) Functional Conservation of LncRNA JPX Despite Sequence and Structural Divergence. *J Mol Biol* **432**: 283–300
- Kawakatsu T, Huang S, Shan C, Jupe F, Sasaki E, Schmitz RJJ, Urich MAA, Castanon R, Nery JRR, Barragan C, He Y, et al** (2016) Epigenomic Diversity in a Global Collection of *Arabidopsis thaliana* Accessions. *Cell* **166**: 492–505
- Kelemen O, Convertini P, Zhang Z, Wen Y, Shen M, Falaleeva M, Stamm S** (2013) Function of alternative splicing. *Gene* **514**: 1–30
- Kerppola TK** (2008) Bimolecular fluorescence complementation (BiFC) analysis as a probe of protein interactions in living cells. *Annu Rev Biophys* **37**: 465–487
- Khorkova O, Myers AJ, Hsiao J, Wahlestedt C** (2014) Natural antisense transcripts. *Hum Mol Genet*. doi: 10.1093/hmg/ddu207
- Kim JS, Jung HJ, Lee HJ, Kim KA, Goh CH, Woo Y, Oh SH, Han YS, Kang H** (2008) Glycine-rich RNA-binding protein7 affects abiotic stress responses by regulating stomata opening and closing in *Arabidopsis thaliana*. *Plant J* **55**: 455–466
- Kim DH, Doyle MR, Sung S, Amasino RM** (2009) Vernalization: Winter and the timing of flowering in plants. *Annu Rev Cell Dev Biol* **25**: 277–299
- Kim DH, Sung S** (2017) Vernalization-Triggered Intragenic Chromatin Loop Formation by Long Noncoding RNAs. *Dev Cell* **40**: 302–312.e4
- Kim DH, Xi Y, Sung S** (2017) Modular function of long noncoding RNA, COLDAIR, in the vernalization response. *PLoS Genet*. doi: 10.1371/journal.pgen.1006939
- Kim DH** (2020) Current understanding of flowering pathways in plants: focusing on the vernalization pathway in *Arabidopsis* and several vegetable crop plants. *Hortic Environ Biotechnol* **61**: 209–227
- Kindgren P, Ard R, Ivanov M, Marquardt S** (2018) Transcriptional read-through of the long non-coding RNA SVALKKA governs plant cold acclimation. *Nat Commun* **9**: 1–11

- Koncz C, deJong F, Villacorta N, Szakonyi D, Koncz Z** (2012) The spliceosome-activating complex: Molecular mechanisms underlying the function of a pleiotropic regulator. *Front Plant Sci.* doi: 10.3389/fpls.2012.00009
- Kong L, Zhang Y, Ye ZQ, Liu XQ, Zhao SQ, Wei L, Gao G** (2007) CPC: Assess the protein-coding potential of transcripts using sequence features and support vector machine. *Nucleic Acids Res.* doi: 10.1093/nar/gkm391
- König J, Zarnack K, Rot G, Curk T, Kayikci M, Zupan B, Turner DJ, Luscombe NM, Ule J** (2010) ICLIP reveals the function of hnRNP particles in splicing at individual nucleotide resolution. *Nat Struct Mol Biol* **17**: 909–915
- Kopelman NM, Lancet D, Yanai I** (2005) Alternative splicing and gene duplication are inversely correlated evolutionary mechanisms. *Nat Genet* **37**: 588–589
- Kramer MC, Gregory BD** (2019) Using Protein Interaction Profile Sequencing (PIP-seq) to Identify RNA Secondary Structure and RNA–Protein Interaction Sites of Long Noncoding RNAs in Plants. *Methods Mol. Biol. Humana Press Inc.*, pp 343–361
- Krchňáková Z, Thakur PK, Krausová M, Bieberstein N, Haberman N, Müller-McNicoll M, Staněk D** (2019) Splicing of long non-coding RNAs primarily depends on polypyrimidine tract and 5' splice-site sequences due to weak interactions with SR proteins. *Nucleic Acids Res* **47**: 911–928
- Krishnamurthy A, Rathinasabapathi B** (2013) Oxidative stress tolerance in plants: Novel interplay between auxin and reactive oxygen species signaling. *Plant Signal Behav.* doi: 10.4161/psb.25761
- Ku YS, Sintaha M, Cheung MY, Lam HM** (2018) Plant hormone signaling crosstalks between biotic and abiotic stress responses. *Int J Mol Sci.* doi: 10.3390/ijms19103206
- Kulichová K, Kumar V, Steinbachová L, Klodová B, Timofejeva L, Juříček M, Honys D, Hafidh SS** (2020) PRP8A and PRP8B spliceosome subunits act coordinately to control pollen tube attraction in *Arabidopsis thaliana*. *Development.* doi: 10.1242/dev.186742
- Kung JTY, Colognori D, Lee JT** (2013) Long noncoding RNAs: Past, present, and future. *Genetics* **193**: 651–669
- Kwenda S, Birch PRJ, Moleleki LN** (2016) Genome-wide identification of potato long intergenic noncoding RNAs responsive to *Pectobacterium carotovorum* subspecies *brasiliense* infection. *BMC Genomics.* doi: 10.1186/s12864-016-2967-9
- Laloum T, Martín G, Duque P** (2018) Alternative Splicing Control of Abiotic Stress Responses. *Trends Plant Sci* **23**: 140–150
- Lamesch P, Berardini TZ, Li D, Swarbreck D, Wilks C, Sasidharan R, Muller R, Dreher K, Alexander DL, Garcia-Hernandez M, et al** (2012) The Arabidopsis Information Resource (TAIR): Improved gene annotation and new tools. *Nucleic Acids Res.* doi: 10.1093/nar/gkr1090
- Lämke J, Bäurle I** (2017) Epigenetic and chromatin-based mechanisms in environmental stress adaptation and stress memory in plants. *Genome Biol* **18**: 1–11
- Lee C** (2007) Coimmunoprecipitation Assay. *Methods Mol. Biol. Methods Mol Biol*, pp 401–406
- Lee H, Zhang Z, Krause HM** (2019) Long Noncoding RNAs and Repetitive Elements: Junk or Intimate Evolutionary Partners? *Trends Genet* **35**: 892–902

- Leviatan N, Alkan N, Leshkowitz D, Fluhr R** (2013) Genome-Wide Survey of Cold Stress Regulated Alternative Splicing in *Arabidopsis thaliana* with Tiling Microarray. *PLoS One*. doi: 10.1371/journal.pone.0066511
- Lewis BP, Green RE, Brenner SE** (2003) Evidence for the widespread coupling of alternative splicing and nonsense-mediated mRNA decay in humans. *Proc Natl Acad Sci U S A* **100**: 189–192
- Li A, Zhang J, Zhou Z** (2014a) PLEK: A tool for predicting long non-coding RNAs and messenger RNAs based on an improved k-mer scheme. *BMC Bioinformatics*. doi: 10.1186/1471-2105-15-311
- Li L, Eichten SR, Shimizu R, Petsch K, Yeh CT, Wu W, Chetoor AM, Givan SA, Cole RA, Fowler JE, et al** (2014b) Genome-wide discovery and characterization of maize long non-coding RNAs. *Genome Biol*. doi: 10.1186/gb-2014-15-2-r40
- Li S, Liu J, Liu Z, Li X, Wu F, He Y** (2014c) HEAT-INDUCED TAS1 TARGET1 mediates thermotolerance via heat stress transcription factor A1a-directed pathways in *Arabidopsis*. *Plant Cell* **26**: 1764–1780
- Li S, Yamada M, Han X, Ohler U, Benfey PN** (2016) High-Resolution Expression Map of the *Arabidopsis* Root Reveals Alternative Splicing and lincRNA Regulation. *Dev Cell* **39**: 508–522
- Li RQ, Ren Y, Liu W, Pan W, Xu FJ, Yang M** (2017a) MicroRNA-mediated silence of onco-lincRNA MALAT1 in different ESCC cells via ligand-functionalized hydroxyl-rich nanovectors. *Nanoscale* **9**: 2521–2530
- Li S, Yu X, Lei N, Cheng Z, Zhao P, He Y, Wang W, Peng M** (2017b) Genome-wide identification and functional prediction of cold and/or drought-responsive lincRNAs in cassava. *Sci Rep* **7**: 1–17
- Li S, Wang Y, Zhao Y, Zhao X, Chen X, Gong Z** (2020) Global Co-transcriptional Splicing in *Arabidopsis* and the Correlation with Splicing Regulation in Mature RNAs. *Mol Plant* **13**: 266–277
- Lin MF, Jungreis I, Kellis M** (2011) PhyloCSF: A comparative genomics method to distinguish protein coding and non-coding regions. *Bioinformatics*. doi: 10.1093/bioinformatics/btr209
- Lin Y, Schmidt BF, Bruchez MP, McManus CJ** (2018) Structural analyses of NEAT1 lincRNAs suggest long-range RNA interactions that may contribute to paraspeckle architecture. *Nucleic Acids Res* **46**: 3742–3752
- Ling Y, Alshareef S, Butt H, Lozano-Juste J, Li L, Galal AA, Moustafa A, Momin AA, Tashkandi M, Richardson DN, et al** (2017) Pre-mRNA splicing repression triggers abiotic stress signaling in plants. *Plant J* **89**: 291–309
- Ling Y, Serrano N, Gao G, Atia M, Mokhtar M, Woo YH, Bazin J, Veluchamy A, Benhamed M, Crespi M, et al** (2018) Thermopriming triggers splicing memory in *Arabidopsis*. *J Exp Bot* **69**: 2659–2675
- Ling Z, Brockmüller T, Baldwin IT, Xu S** (2019) Evolution of alternative splicing in eudicots. *Front Plant Sci* **10**: 707
- Liu J, Jung C, Xu J, Wang H, Deng S, Bernad L, Arenas-Huertero C, Chua NH** (2012) Genome-wide analysis uncovers regulation of long intergenic noncoding RNAs in *Arabidopsis*. *Plant Cell* **24**: 4333–4345
- Liu J, Sun N, Liu M, Liu J, Du B, Wang X, Qi X** (2013) An autoregulatory loop controlling *Arabidopsis* HsfA2 expression: Role of heat shock-induced alternative splicing. *Plant Physiol* **162**: 512–521

- Liu J, Wang H, Chua NH** (2015) Long noncoding RNA transcriptome of plants. *Plant Biotechnol J* **13**: 319–328
- Liu SJ, Nowakowski TJ, Pollen AA, Lui JH, Horlbeck MA, Attenello FJ, He D, Weissman JS, Kriegstein AR, Diaz AA, et al** (2016) Single-cell analysis of long non-coding RNAs in the developing human neocortex. *Genome Biol.* doi: 10.1186/s13059-016-0932-1
- Long JC, Caceres JF** (2009) The SR protein family of splicing factors: Master regulators of gene expression. *Biochem J* **417**: 15–27
- Lucero L, Bazin J, Rodriguez Melo J, Ibañez F, Crespi MD, Ariel F** (2020) Evolution of the small family of alternative splicing modulators nuclear speckle RNA-binding proteins in plants. *Genes* (Basel). doi: 10.3390/genes11020207
- Luco RF, Allo M, Schor IE, Kornblihtt AR, Misteli T** (2011) Epigenetics in alternative pre-mRNA splicing. *Cell* **144**: 16–26
- Ma XY, Wang JH, Wang JL, Ma CX, Wang XC, Liu FS** (2015) Malat1 as an evolutionarily conserved lncRNA, plays a positive role in regulating proliferation and maintaining undifferentiated status of early-stage hematopoietic cells. *BMC Genomics.* doi: 10.1186/s12864-015-1881-x
- Ma J, Bai X, Luo W, Feng Y, Shao X, Bai Q, Sun S, Long Q, Wan D** (2019) Genome-Wide Identification of Long Noncoding RNAs and Their Responses to Salt Stress in Two Closely Related Poplars. *Front Genet.* doi: 10.3389/fgene.2019.00777
- Maeder C, Kutach AK, Guthrie C** (2009) ATP-dependent unwinding of U4/U6 snRNAs by the Brr2 helicase requires the C terminus of Prp8. *Nat Struct Mol Biol* **16**: 42–48
- Malakar P, Shilo A, Mogilevsky A, Stein I, Pikarsky E, Nevo Y, Benyamini H, Elgavish S, Zong X, Prasanth K V., et al** (2017) Long noncoding RNA MALAT1 promotes hepatocellular carcinoma development by SRSF1 upregulation and mTOR activation. *Cancer Res* **77**: 1155–1167
- Mandadi KK, Scholthof KBG** (2015) Genome-wide analysis of alternative splicing landscapes modulated during plant-virus interactions in brachypodium distachyon. *Plant Cell* **27**: 71–85
- Margueron R, Reinberg D** (2011) The Polycomb complex PRC2 and its mark in life. *Nature* **469**: 343–349
- Maris C, Dominguez C, Allain FHT** (2005) The RNA recognition motif, a plastic RNA-binding platform to regulate post-transcriptional gene expression. *FEBS J* **272**: 2118–2131
- Marquardt S, Raitskin O, Wu Z, Liu F, Sun Q, Dean C** (2014) Functional Consequences of Splicing of the Antisense Transcript COOLAIR on FLC Transcription. *Mol Cell* **54**: 156–165
- Marquez Y, Brown JWS, Simpson C, Barta A, Kalyna M** (2012) Transcriptome survey reveals increased complexity of the alternative splicing landscape in Arabidopsis. *Genome Res* **22**: 1184–1195
- Martín G, Márquez Y, Mantica F, Duque P, Irimia M** (2021) Alternative splicing landscapes in Arabidopsis thaliana across tissues and stress conditions highlight major functional differences with animals. *Genome Biol* **22**: 35
- Maruta T, Inoue T, Tamoi M, Yabuta Y, Yoshimura K, Ishikawa T, Shigeoka S** (2011) Arabidopsis NADPH oxidases, AtrbohD and AtrbohF, are essential for jasmonic acid-induced expression of genes regulated by MYC2 transcription factor. *Plant Sci* **180**: 655–660

- Medina J, Catalá R, Salinas J** (2011) The CBFs: Three arabidopsis transcription factors to cold acclimate. *Plant Sci* **180**: 3–11
- Meissner M, Dechat T, Gerner C, Grimm R, Foisner R, Sauermann G** (2000) Differential nuclear localization and nuclear matrix association of the splicing factors PSF and PTB. *J Cell Biochem* **76**: 559–566
- Melé M, Mattioli K, Mallard W, Shechner DM, Gerhardinger C, Rinn JL** (2017) Chromatin environment, transcriptional regulation, and splicing distinguish lincRNAs and mRNAs. *Genome Res* **27**: 27–37
- Merkin J, Russell C, Chen P, Burge CB** (2012) Evolutionary dynamics of gene and isoform regulation in mammalian tissues. *Science* (80-) **338**: 1593–1599
- Meyer K, Koester T, Staiger D** (2015) Pre-mRNA splicing in plants: In vivo functions of RNA-binding proteins implicated in the splicing process. *Biomolecules* **5**: 1717–1740
- Meyer K, Köster T, Nolte C, Weinholdt C, Lewinski M, Grosse I, Staiger D** (2017) Adaptation of iCLIP to plants determines the binding landscape of the clock-regulated RNA-binding protein AtGRP7. *Genome Biol* **18**: 1–22
- Mittler R, Finka A, Goloubinoff P** (2012) How do plants feel the heat? *Trends Biochem Sci* **37**: 118–125
- Morenikeji OB, Bernard K, Strutton E, Wallace M, Thomas BN** (2021) Evolutionarily Conserved Long Non-coding RNA Regulates Gene Expression in Cytokine Storm During COVID-19. *Front Bioeng Biotechnol* **8**: 582953
- Mukherjee S, Banerjee B, Karasik D, Frenkel-Morgenstern M** (2021) mRNA-lncRNA Co-expression Network Analysis Reveals the Role of lncRNAs in Immune Dysfunction during Severe SARS-CoV-2 Infection. *Viruses*. doi: 10.3390/v13030402
- Muthusamy M, Uma S, Suthanthiram B, Saraswathi MS, Chandrasekar A** (2019) Genome-wide identification of novel, long non-coding RNAs responsive to *Mycosphaerella eumusae* and *Pratylenchus coffeae* infections and their differential expression patterns in disease-resistant and sensitive banana cultivars. *Plant Biotechnol Rep* **13**: 73–83
- Ohno S** (1972) So much “junk” DNA in our genome. *Brookhaven Symp Biol* **23**: 366–370
- Olthof AM, White AK, Lee MF, Chakroun A, Abdel Aleem AK, Rousseau J, Magnani C, Campeau PM, Kanadia RN** (2020) The minor and major spliceosome interact to regulate alternative splicing around minor introns. *bioRxiv* 2020.05.18.101246
- Pan Q, Shai O, Lee LJ, Frey BJ, Blencowe BJ** (2008) Deep surveying of alternative splicing complexity in the human transcriptome by high-throughput sequencing. *Nat Genet* **40**: 1413–1415
- Pang J, Zhang X, Ma X, Zhao J** (2019) Spatio-temporal transcriptional dynamics of maize long non-coding RNAs responsive to drought stress. *Genes (Basel)*. doi: 10.3390/genes10020138
- Patel AA, Steitz JA** (2003) Splicing double: Insights from the second spliceosome. *Nat Rev Mol Cell Biol* **4**: 960–970
- Pintacuda G, Young AN, Cerase A** (2017) Function by structure: Spotlights on xist long non-coding RNA. *Front Mol Biosci* **4**: 90

- Pisignano G, Ladomery M** (2021) Epigenetic Regulation of Alternative Splicing: How LncRNAs Tailor the Message. *Non-Coding RNA* **7**: 21
- Polack FP, Thomas SJ, Kitchin N, Absalon J, Gurtman A, Lockhart S, Perez JL, Pérez Marc G, Moreira ED, Zerbini C, et al** (2020) Safety and Efficacy of the BNT162b2 mRNA Covid-19 Vaccine. *N Engl J Med* **383**: 2603–2615
- Punzo P, Grillo S, Batelli G** (2020) Alternative splicing in plant abiotic stress responses. *Biochem Soc Trans* **48**: 2117–2126
- Wang XQD, Crutchley JL, Dostie J** (2011) Shaping the Genome with Non-Coding RNAs. *Curr Genomics* **12**: 307–321
- Qin T, Zhao H, Cui P, Albeshar N, Xiong L** (2017) A nucleus-localized long non-coding rna enhances drought and salt stress tolerance. *Plant Physiol* **175**: 1321–1336
- Rai MI, Alam M, Lightfoot DA, Gurha P, Afzal AJ** (2019) Classification and experimental identification of plant long non-coding RNAs. *Genomics* **111**: 997–1005
- Ranwez V, Serra A, Pot D, Chantret N** (2017) Domestication reduces alternative splicing expression variations in sorghum. *PLoS One*. doi: 10.1371/journal.pone.0183454
- Rappsilber J, Ryder U, Lamond AI, Mann M** (2002) Large-scale proteomic analysis of the human spliceosome. *Genome Res* **12**: 1231–1245
- Reeves MB, Davies AA, McSharry BP, Wilkinson GW, Sinclair JH** (2007) Complex I binding by a virally encoded RNA regulates mitochondria-induced cell death. *Science (80-)* **316**: 1345–1348
- Romero-Barrios N** (2016) Non-codings RNAs, regulators of gene expression in *Arabidopsis thaliana* root developmental plasticity. <http://www.theses.fr>
- Romero-Barrios N, Legascue MF, Benhamed M, Ariel F, Crespi M** (2018) Survey and summary Splicing regulation by long noncoding RNAs. *Nucleic Acids Res* **46**: 2169–2184
- Roulé T, Ariel F, Hartmann C, Gutierrez-Marcos J, Crespi M, Blein T** (2020) The lncRNA MARS modulates the epigenetic reprogramming of the marneral 1 cluster in response to ABA. *bioRxiv* 2020.08.10.236562
- Ru Y, Wang BB, Brendel V** (2008) Spliceosomal proteins in plants. *Curr Top Microbiol Immunol* **326**: 1–15
- Satyawan D, Kim MY, Lee SH** (2017) Stochastic alternative splicing is prevalent in mungbean (*Vigna radiata*). *Plant Biotechnol J* **15**: 174–182
- Scarano D, Rao R, Corrado G** (2017) In Silico identification and annotation of noncoding RNAs by RNA-seq and de Novo assembly of the transcriptome of Tomato Fruits. *PLoS One*. doi: 10.1371/journal.pone.0171504
- Schlackow M, Nojima T, Gomes T, Dhir A, Carmo-Fonseca M, Proudfoot NJ** (2017) Distinctive Patterns of Transcription and RNA Processing for Human lincRNAs. *Mol Cell* **65**: 25–38
- Schmitt AM, Chang HY** (2016) Long Noncoding RNAs in Cancer Pathways. *Cancer Cell* **29**: 452–463
- Schor IE, Rascovan N, Pelisch F, Alió M, Kornblihtt AR** (2009) Neuronal cell depolarization induces intragenic chromatin modifications affecting NCAM alternative splicing. *Proc Natl Acad Sci U S A* **106**: 4325–4330

- Szabo EX, Reichert P, Lehniger MK, Ohmer M, de Francisco Amorim M, Gowik U, Schmitz-Linneweber C, Laubinger S** (2020) Metabolic labeling of RNAs uncovers hidden features and dynamics of the arabidopsis transcriptome[CC-BY]. *Plant Cell* **32**: 871–887
- Talavera D, Vogel C, Orozco M, Teichmann SA, De La Cruz X** (2007) The (In)dependence of alternative splicing and gene duplication. *PLoS Comput Biol* **3**: 0375–0388
- Tani H, Mizutani R, Salam KA, Tano K, Ijiri K, Wakamatsu A, Isogai T, Suzuki Y, Akimitsu N** (2012) Genome-wide determination of RNA stability reveals hundreds of short-lived noncoding transcripts in mammals. *Genome Res* **22**: 947–956
- The ENCODE Project Consortium** (2012) An integrated encyclopedia of DNA elements in the human genome. *Nature* **489**: 57–74
- Thomas CA** (1971) The Genetic Organization of Chromosomes. *Annu Rev Genet* **5**: 237–256
- Tran VDT, Souiai O, Romero-Barríos N, Crespi M, Gautheret D** (2016) Detection of generic differential RNA processing events from RNA-seq data. *RNA Biol* **13**: 59–67
- Tripathi V, Ellis JD, Shen Z, Song DY, Pan Q, Watt AT, Freier SM, Bennett CF, Sharma A, Bubulya PA, et al** (2010) The nuclear-retained noncoding RNA MALAT1 regulates alternative splicing by modulating SR splicing factor phosphorylation. *Mol Cell* **39**: 925–938
- Tsoi LC, Iyer MK, Stuart PE, Swindell WR, Gudjonsson JE, Tejasvi T, Sarkar MK, Li B, Ding J, Voorhees JJ, et al** (2015) Analysis of long non-coding RNAs highlights tissue-specific expression patterns and epigenetic profiles in normal and psoriatic skin. *Genome Biol.* doi: 10.1186/s13059-014-0570-4
- Turunen JJ, Niemelä EH, Verma B, Frilander MJ** (2013) The significant other: Splicing by the minor spliceosome. *Wiley Interdiscip Rev RNA* **4**: 61–76
- Ulitsky I, Shkumatava A, Jan CH, Sive H, Bartel DP** (2011) Conserved function of lincRNAs in vertebrate embryonic development despite rapid sequence evolution. *Cell* **147**: 1537–1550
- Ulitsky I, Bartel DP** (2013) XLincRNAs: Genomics, evolution, and mechanisms. *Cell* **154**: 26
- Unver T, Tombuloglu H** (2020) Barley long non-coding RNAs (lncRNA) responsive to excess boron. *Genomics* **112**: 1947–1955
- Urquiaga MC de O, Thiebaut F, Hemerly AS, Ferreira PCG** (2021) From Trash to Luxury: The Potential Role of Plant LncRNA in DNA Methylation During Abiotic Stress. *Front Plant Sci.* doi: 10.3389/fpls.2020.603246
- Vendramin R, Verheyden Y, Ishikawa H, Goedert L, Nicolas E, Saraf K, Armaos A, Delli Ponti R, Izumikawa K, Mestdagh P, et al** (2018) SAMMSON fosters cancer cell fitness by concertedly enhancing mitochondrial and cytosolic translation. *Nat Struct Mol Biol* **25**: 1035–1046
- Venkidasamy B, Karthikeyan M, Ramalingam S** (2019) Methods/protocols for determination of oxidative stress in crop plants. *React. Oxyg. Nitrogen Sulfur Species Plants Prod. Metab. Signal. Def. Mech.* Taylor and Francis, pp 421–435
- Villamizar O, Chambers CB, Riberdy JM, Persons DA, Wilber A** (2016) Long noncoding RNA Saf and splicing factor 45 increase soluble Fas and resistance to apoptosis. *Oncotarget* **7**: 13810–13826

- Vishwakarma K, Upadhyay N, Kumar N, Yadav G, Singh J, Mishra RK, Kumar V, Verma R, Upadhyay RG, Pandey M, et al** (2017) Abscisic acid signaling and abiotic stress tolerance in plants: A review on current knowledge and future prospects. *Front Plant Sci* **8**: 161
- Wachter A, Rühl C, Stauffer E** (2012) The role of polypyrimidine tract-binding proteins and other hnRNP proteins in plant splicing regulation. *Front Plant Sci*. doi: 10.3389/fpls.2012.00081
- Waititu JK, Zhang C, Liu J, Wang H** (2020) Plant non-coding rnas: Origin, biogenesis, mode of action and their roles in abiotic stress. *Int J Mol Sci* **21**: 1–22
- Wang H, Chua NH, Wang XJ** (2006) Prediction of trans-antisense transcripts in *Arabidopsis thaliana*. *Genome Biol*. doi: 10.1186/gb-2006-7-10-r92
- Wang ET, Sandberg R, Luo S, Khrebtkova I, Zhang L, Mayr C, Kingsmore SF, Schroth GP, Burge CB** (2008) Alternative isoform regulation in human tissue transcriptomes. *Nature* **456**: 470–476
- Wang KC, Yang YW, Liu B, Sanyal A, Corces-Zimmerman R, Chen Y, Lajoie BR, Protacio A, Flynn RA, Gupta RA, et al** (2011) A long noncoding RNA maintains active chromatin to coordinate homeotic gene expression. *Nature* **472**: 120–126
- Wang L, Park HJ, Dasari S, Wang S, Kocher JP, Li W** (2013) CPAT: Coding-potential assessment tool using an alignment-free logistic regression model. *Nucleic Acids Res*. doi: 10.1093/nar/gkt006
- Wang H, Chung PJ, Liu J, Jang IC, Kean MJ, Xu J, Chua NH** (2014) Genome-wide identification of long noncoding natural antisense transcripts and their responses to light in *Arabidopsis*. *Genome Res* **24**: 444–453
- Wang J, Yu W, Yang Y, Li X, Chen T, Liu T, Ma N, Yang X, Liu R, Zhang B** (2015a) Genome-wide analysis of tomato long non-coding RNAs and identification as endogenous target mimic for microRNA in response to TYLCV infection. *Sci Rep*. doi: 10.1038/srep16946
- Wang Y, Liu J, Huang B, Xu Y-M, Li J, Huang L-F, Lin J, Zhang J, Min Q-H, Yang W-M, et al** (2015b) Mechanism of alternative splicing and its regulation. *Biomed Reports* **3**: 152–158
- Wang X, Sehgal L, Jain N, Khashab T, Mathur R, Samaniego F** (2016a) Lncrna malat1 promotes development of mantle cell lymphoma by associating with ezh2. *J Transl Med*. doi: 10.1186/s12967-016-1100-9
- Wang YJ, Wei XY, Jing XQ, Chang YL, Hu CH, Wang X, Chen KM** (2016b) The fundamental role of NOX family proteins in plant immunity and their regulation. *Int J Mol Sci*. doi: 10.3390/ijms17060805
- Wang Y-M, Xu H-B, Wang M-S, Otecko NO, Ye L-Q, Wu D-D, Zhang Y-P** (2017) Annotating long intergenic non-coding RNAs under artificial selection during chicken domestication. *BMC Evol Biol* **17**: 192
- Wierzbicki AT, Haag JR, Pikaard CS** (2008) Noncoding Transcription by RNA Polymerase Pol IVb/Pol V Mediates Transcriptional Silencing of Overlapping and Adjacent Genes. *Cell* **135**: 635–648
- Will CL, Lührmann R** (2011) Spliceosome structure and function. *Cold Spring Harb Perspect Biol* **3**: 1–2

- Wilusz JE, Freier SM, Spector DL** (2008) 3' End Processing of a Long Nuclear-Retained Noncoding RNA Yields a tRNA-like Cytoplasmic RNA. *Cell* **135**: 919–932
- Witten JT, Ule J** (2011) Understanding splicing regulation through RNA splicing maps. *Trends Genet* **27**: 89–97
- Wongsurawat T, Jenjaroenpun P, Kwoh CK, Kuznetsov V** (2012) Quantitative model of R-loop forming structures reveals a novel level of RNA-DNA interactome complexity. *Nucleic Acids Res.* doi: 10.1093/nar/gkr1075
- Wood EJ, Chin-Inmanu K, Jia H, Lipovich L** (2013) Sense-antisense gene pairs: Sequence, transcription, and structure are not conserved between human and mouse. *Front Genet.* doi: 10.3389/fgene.2013.00183
- Wu J, Okada T, Fukushima T, Tsudzuki T, Sugiura M, Yukawa Y** (2012) A novel hypoxic stress-responsive long non-coding RNA transcribed by RNA polymerase III in Arabidopsis. *RNA Biol* **9**: 302–313
- Xin M, Wang Y, Yao Y, Song N, Hu Z, Qin D, Xie C, Peng H, Ni Z, Sun Q** (2011) Identification and characterization of wheat long non-protein coding RNAs responsive to powdery mildew infection and heat stress by using microarray analysis and SBS sequencing. *BMC Plant Biol.* doi: 10.1186/1471-2229-11-61
- Xing Q, Zhang W, Liu M, Li L, Li X, Yan J** (2019) Genome-Wide Identification of Long Non-coding RNAs Responsive to *Lasiodiplodia theobromae* Infection in Grapevine. *Evol Bioinforma.* doi: 10.1177/1176934319841362
- Yan X, Ma L, Yang MF** (2020) Identification and characterization of long non-coding RNA (lncRNA) in the developing seeds of *Jatropha curcas*. *Sci Rep* **10**: 1–10
- Yap K, Mukhina S, Zhang G, Tan JSC, Ong HS, Makeyev E V.** (2018) A Short Tandem Repeat-Enriched RNA Assembles a Nuclear Compartment to Control Alternative Splicing and Promote Cell Survival. *Mol Cell* **72**: 525–540.e13
- Yeap WC, Namasivayam P, Ho CL** (2014) HnRNP-like proteins as post-transcriptional regulators. *Plant Sci* **227**: 90–100
- Yin Y, Lu JY, Zhang X, Shao W, Xu Y, Li P, Hong Y, Cui L, Shan G, Tian B, et al** (2020) U1 snRNP regulates chromatin retention of noncoding RNAs. *Nature* **580**: 147–150
- Yu K, Feng M, Yang G, Sun L, Qin Z, Cao J, Wen J, Li H, Zhou Y, Chen X, et al** (2020) Changes in alternative splicing in response to domestication and polyploidization in wheat. *Plant Physiol* **184**: 1955–1968
- Zampetaki A, Albrecht A, Steinhofel K** (2018) Long non-coding RNA structure and function: Is there a link? *Front Physiol.* doi: 10.3389/fphys.2018.01201
- Zaynab M, Fatima M, Sharif Y, Qasim M, Aslam MM, Afzal MZ, Sajjad N** (2021) Biotic stress response of lncRNAs in plants. *Long Noncoding RNAs Plants.* Elsevier, pp 279–291
- Zeng, Gupta, Jiang, Yang, Gong, Zhu** (2019) Cross-Kingdom Small RNAs Among Animals, Plants and Microbes. *Cells* **8**: 371
- Zhan X, Qian B, Cao F, Wu W, Yang L, Guan Q, Gu X, Wang P, Okusolubo TA, Dunn SL, et al** (2015) An Arabidopsis PWI and RRM motif-containing protein is critical for pre-mRNA splicing and ABA responses. *Nat Commun.* doi: 10.1038/ncomms9139

- Zhang X, Clarenz O, Cokus S, Bernatavichute Y V, Pellegrini M, Goodrich J, Jacobsen SE** (2007) Whole-Genome Analysis of Histone H3 Lysine 27 Trimethylation in Arabidopsis. *PLoS Biol* **5**: e129
- Zhang Y, Zhu H, Zhang Q, Li M, Yan M, Wang R, Wang L, Welti R, Zhang W, Wang X** (2009) Phospholipase D α 1 and phosphatidic acid regulate NADPH oxidase activity and production of reactive oxygen species in ABA-mediated stomatal closure in arabidopsis. *Plant Cell* **21**: 2357–2377
- Zhang B, Gunawardane L, Niazi F, Jahanbani F, Chen X, Valadkhan S** (2014) A Novel RNA Motif Mediates the Strict Nuclear Localization of a Long Noncoding RNA. *Mol Cell Biol* **34**: 2318–2329
- Zhang R, Calixto CPG, Marquez Y, Venhuizen P, Tzioutziou NA, Guo W, Spensley M, Entizne JC, Lewandowska D, Have S Ten, et al** (2017) A high quality Arabidopsis transcriptome for accurate transcript-level analysis of alternative splicing. *Nucleic Acids Res* **45**: 5061–5073
- Zhang P, Wu W, Chen Q, Chen M** (2019a) Non-Coding RNAs and their Integrated Networks. *J Integr Bioinform*. doi: 10.1515/jib-2019-0027
- Zhang X, Wang W, Zhu W, Dong J, Cheng Y, Yin Z, Shen F** (2019b) Mechanisms and functions of long non-coding RNAs at multiple regulatory levels. *Int J Mol Sci*. doi: 10.3390/ijms20225573
- Zhang X, Dong J, Deng F, Wang W, Cheng Y, Song L, Hu M, Shen J, Xu Q, Shen F** (2019c) The long non-coding RNA lncRNA973 is involved in cotton response to salt stress. *BMC Plant Biol* **19**: 459
- Zhang D, Chen MX, Zhu FY, Zhang J, Liu YG** (2020) Emerging Functions of Plant Serine/Arginine-Rich (SR) Proteins: Lessons from Animals. *CRC Crit Rev Plant Sci* **39**: 173–194
- Zhao C, Zhang Z, Xie S, Si T, Li Y, Zhu JK** (2016) Mutational evidence for the critical role of CBF transcription factors in cold acclimation in Arabidopsis. *Plant Physiol* **171**: 2744–2759
- Zheng Q, Rowley MJ, Böhmendorfer G, Sandhu D, Gregory BD, Wierzbicki AT** (2013) RNA polymerase v targets transcriptional silencing components to promoters of protein-coding genes. *Plant J* **73**: 179–189
- Zhu QH, Stephen S, Taylor J, Helliwell CA, Wang MB** (2014) Long noncoding RNAs responsive to Fusarium oxysporum infection in Arabidopsis thaliana. *New Phytol* **201**: 574–584
- Zhu FY, Chen MX, Ye NH, Shi L, Ma KL, Yang JF, Cao YY, Zhang Y, Yoshida T, Fernie AR, et al** (2017) Proteogenomic analysis reveals alternative splicing and translation as part of the abscisic acid response in Arabidopsis seedlings. *Plant J* **91**: 518–533
- Zou C, Wang Q, Lu C, Yang W, Zhang Y, Cheng H, Feng X, Prosper MA, Song G** (2016) Transcriptome analysis reveals long noncoding RNAs involved in fiber development in cotton (*Gossypium arboreum*). *Sci China Life Sci* **59**: 164–171

Résumé

Les plantes sont des organismes sessiles contraints de s'adapter en continu à leur environnement. Ces stress peuvent être de nature biotique (bactéries pathogènes, champignons, nématodes...) ou abiotique (froid/chaud, sel, métaux lourds...), et requièrent une réponse rapide de la plante afin de permettre sa survie. Cette plasticité développementale implique la modulation de l'expression des gènes exprimés au sein de leurs cellules.

Au cours de ces dernières années, l'usage intensif des techniques de séquençage à haut-débit a permis de mieux comprendre cette modulation du transcriptome, révélant par la même occasion l'existence de milliers d'ARNs non-codants (ncARNs), c'est-à-dire ne conduisant pas à des protéines. Ces ncARNs se divisent en différentes catégories, notamment selon leur taille : les petits ncARNs et les longs ncARNs (lncARNs) de plus de 200 nucléotides. De nombreuses études ont montrées que ces lncARNs participeraient à la régulation de divers processus développementaux chez les eucaryotes.

Chez les plantes, plusieurs lncARNs ont été décrits comme essentiels à la survie en réponse à des stress, que ce soit par exemple lors d'une infection par un agent pathogène ou face à des changements importants de température. Certains de ces lncARNs sont notamment capables de réguler le transcriptome via différents mécanismes, dont l'épissage alternatif (EA). Ils peuvent, dans ce cas, intervenir dans le remodelage de la chromatine, former des duplexes avec des séquences d'ADN ou d'ARN, ou encore interagir avec des facteurs d'épissage spécifiques afin d'altérer leur activité. Chez *Arabidopsis thaliana*, le lncARN ASCO (pour *ALTERNATIVE SPLICING COMPETITOR*) a été montré comme interagissant avec les facteurs d'épissage NSRs (NUCLEAR SPECKLE RNA-BINDING protéines). Cette interaction permettrait une modulation de l'EA conduisant à la régulation du développement racinaire. Au cours de cette thèse, nous avons cherché à préciser le rôle du complexe ASCO-NSR dans la régulation du développement de la plante, notamment en réponse à des stress.

Dans un premier temps, nous avons cherché à décrire l'impact de la suppression de l'expression des 2 gènes *NSRa* et *NSRb* au niveau du transcriptome de la plante, et à identifier les ARNs pré-messagers avec lesquels ils interagissent. Les gènes de réponse à l'auxine présentent une expression altérée chez le double mutant *nsra/b*, soutenant l'importance des NSRs dans la réponse à cette phytohormone. De même, nous avons démontré que les NSRs interagissent avec de nombreux ARNs pré-messagers en lien avec l'auxine et les réponses de défense. De plus, le double mutant *nsra/b* présente une sensibilité accrue à deux

pathogènes différents, *Pseudomonas syringae* et *Botrytis cinerea*, suggérant que les NSRs sont des acteurs clés dans la mise en place de l'immunité chez *Arabidopsis thaliana*.

Dans un second temps, l'impact de la dérégulation de l'expression d'ASCO a été étudié en utilisant des plantes sur-exprimant ou n'exprimant plus ASCO. Ainsi, nous avons pu montrer que la modulation du niveau d'expression d'ASCO mène à la dérégulation de l'expression et de l'épissage de nombreux gènes, dont un grand nombre lié à l'immunité de la plante. À la suite d'un traitement par la flagelline, un peptide qui mime l'infection par une bactérie, les lignées n'exprimant plus ASCO ont montré une racine primaire plus petite comparée à celle de plantes sauvages, signe d'une plus grande sensibilité à ce peptide. De plus, ces mêmes lignées présentent une dérégulation de l'expression des gènes répondant à la flagelline. Ainsi, ASCO semble jouer un rôle dans la réponse à la flagelline chez la plante.

D'autre part, afin de mieux caractériser les mécanismes moléculaires par lesquels ASCO module l'EA, nous avons cherché à identifier les protéines interagissant avec ce lncARN. Nous avons montré que celui-ci est capable d'interagir avec les composants de la machinerie d'épissage PRP8a et SmD1b. De plus, ASCO serait capable, comme avec les NSRs, de détourner l'action de PRP8a et d'empêcher son interaction avec certains transcrits cibles, conduisant ainsi à une modulation de leur épissage.

Enfin, nous avons découvert un lien entre ASCO et la réponse aux changements de température chez la plante. En effet, le transcriptome de plantes n'exprimant plus ASCO est comparable à celui de plantes placées à 4°C. D'autre part, plus de 50% des gènes dont l'expression est régulée par ASCO sont également régulés au niveau transcriptionnel par le froid, dont des acteurs clés de la réponse aux basses températures. Enfin, quand les lignées n'exprimant plus ASCO sont placées à 4°C, elles présentent une accumulation plus importante d'anthocyanes au sein de leurs feuilles, des pigments impliqués dans l'acclimatation au froid. Ainsi, ASCO jouerait aussi un rôle dans la mise en place de la réponse aux basses températures.

L'ensemble de ces données suggèrent que le long ARN non codant ASCO pourrait agir comme intégrateur de multiples stress chez *Arabidopsis thaliana*. De par son interaction avec les NSRs mais aussi avec les protéines de la machinerie d'épissage, PRP8a et SmD1b, ASCO serait capable de moduler le transcriptome de la plante, notamment par le contrôle de l'EA de transcrits cibles spécifiques. Ainsi, les résultats présentés dans cette thèse ont permis de proposer de nouveaux rôles biologiques pour les complexes lncARN-facteur d'épissage, et de montrer leur importance dans la réponse des plantes à divers stress.

Titre : Rôle du complexe ribonucléoprotéique NSR-ASCO dans la régulation du développement des plantes

Mots clés : développement des plantes, ARN non-codant, épissage alternatif

Résumé : Au cours des dernières années, l'usage intensif de technologies de séquençage à haut débit a permis la découverte de milliers de longs ARNs non-codants (lncARNs) chez les eucaryotes, posant la question de leur rôle. Beaucoup d'entre eux ont déjà été caractérisés comme des régulateurs de processus cellulaires et moléculaires clés. Des études ont notamment montré que les lncARNs peuvent réguler le transcriptome via différents mécanismes, dont l'épissage alternatif (EA). Ils peuvent, dans ce cas, intervenir dans le remodelage de la chromatine, former des duplexes avec des séquences d'ADN ou d'ARN, ou encore interagir avec des facteurs d'épissage spécifiques afin d'altérer leur activité. Chez *Arabidopsis thaliana*, le lncARN appelé *ALTERNATIVE SPLICING COMPETITOR* (ASCO) interagit avec les facteurs d'épissage NUCLEAR SPECKLE RNA-BINDING (NSRs), menant à une modulation de l'EA au cours du développement racinaire. Dans cette étude, nous avons cherché à caractériser le rôle du complexe ASCO-NSR au sein de la plante. Nous avons démontré que les NSRs interagissent avec de nombreux ARNs pré-messagers en lien

avec l'auxine et les réponses de défense. De plus, les NSRs semblent être des acteurs clés dans la mise en place de l'immunité. L'impact de la dérégulation de l'expression d'ASCO au niveau développemental et moléculaire a également été étudié, révélant son implication dans la réponse à la flagelline chez la plante. En outre, ASCO peut interagir avec les composants de la machinerie d'épissage PRP8a et SmD1b. ASCO serait donc capable, comme pour les NSRs, de détourner l'action de PRP8a en empêchant l'interaction avec ses transcrits cibles, modulant ainsi leur épissage. Enfin, nous avons découvert un lien entre ASCO et la perception de la température chez la plante. Ces données suggèrent qu'ASCO pourrait agir comme intégrateur de multiples stress chez *Arabidopsis thaliana*. Ainsi, l'ensemble de ces travaux suggère de nouveaux rôles biologiques pour les complexes lncARN-facteur d'épissage, décrivant les mécanismes impliqués et leur intégration au cours du développement de la plante.

Title : Role of the NSR-ASCO ribonucleoprotein complex in plant development

Keywords : plant development, non-coding RNA, alternative splicing

Abstract : In recent years, the extensive use of high-throughput technologies led to the discovery of thousands of long non-coding RNAs (lncRNAs) in eukaryotes, questioning their roles. Many of them have already emerged as key regulators of a plethora of key cellular and molecular processes. In particular, lncRNAs were shown to impact the transcriptome content via different mechanisms, including alternative splicing (AS). In order to modulate AS, lncRNAs can either act as chromatin remodelers, form duplexes with DNA or RNA sequences, or interact with specific splicing factors to alter their activity. The plant lncRNA named *ALTERNATIVE SPLICING COMPETITOR* (ASCO) interacts *in vivo* with the NUCLEAR SPECKLE RNA-BINDING PROTEINS (NSRs) splicing factors, leading to AS modulation during root development in *Arabidopsis thaliana*. In this study, we aimed to characterize the role of the ASCO-NSR complex within plant development. We demonstrated that NSRs bind a large subset of pre-messenger RNAs involved in auxin pathway and

defense responses. Consistently, NSRs appear to be crucial for the establishment of proper immune responses. Furthermore, the impact of deregulation of ASCO expression was studied at both phenotypical and molecular levels, revealing its involvement in the plant response to flagellin and in the regulation of AS for key defense genes, respectively. Additionally, ASCO was shown to bind to the core spliceosomal proteins PRP8a and SmD1b. As for NSRs, ASCO can hijack PRP8a by altering its binding to pre-mRNA targets. Finally, an unsuspected link between ASCO and temperature acclimation was uncovered, suggesting that this lncRNA can act as a potential integrator of multiple stresses in the plant. Therefore, this work sheds light over new biological roles for lncRNA-splicing factor complexes in plants, describing non-coding RNA-mediated splicing regulatory mechanisms and their integration in plant development and stress responses.

Maison du doctorat de l'Université Paris-Saclay

2^{ème} étage aile ouest, Ecole normale supérieure Paris-Saclay

4 avenue des Sciences,

91190 Gif sur Yvette, France